Vol.: 50(3)
September, 2026
ISSN: 0250-4758
Online ISSN: 0973-970X

IJVP-2026

INDIAN JOURNAL OF VETERINARY PATHOLOGY

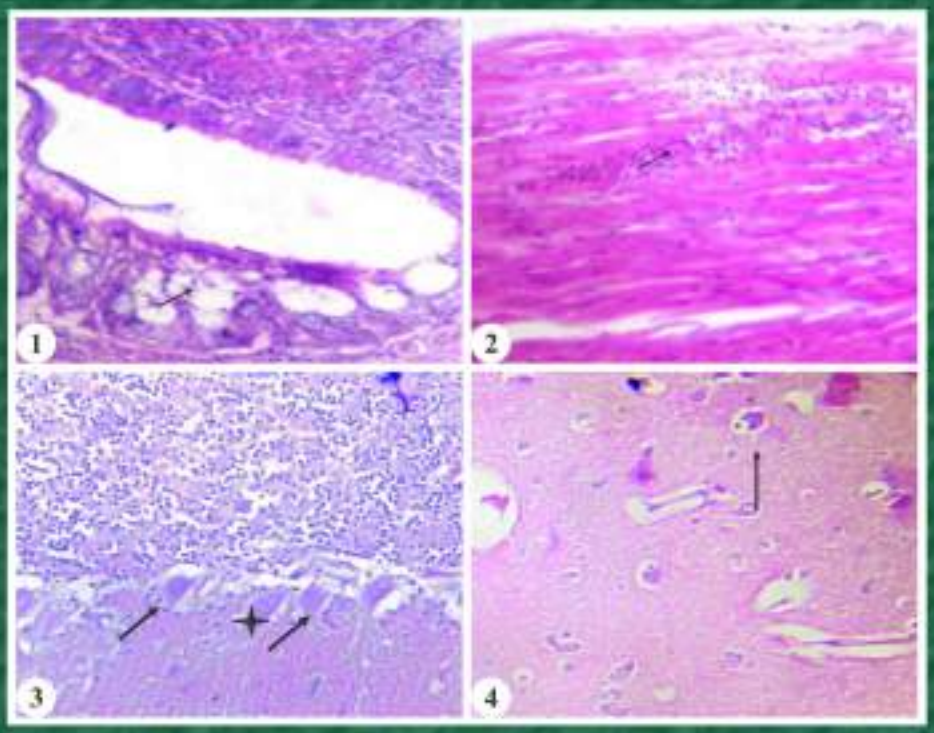

INDIAN ASSOCIATION OF VETERINARY PATHOLOGISTS
(Registered under article 21 of Societies Act 1860)

Visit us at: **www.iavp.org**
Journal available at: **www.indianjournals.com**

Vol. 50 (3)
September, 2026
ISSN: 0250-4758

INDIAN JOURNAL OF VETERINARY PATHOLOGY

Department of Veterinary Pathology, College of Veterinary Science,
Sri Venkateswara Veterinary University, Tirupati-517502, Andhra Pradesh
Mobile: +91-9441185383; E-mail: 7aakumar@gmail.com

INDIAN JOURNAL OF VETERINARY PATHOLOGY

Membership Fee and Subscription of Journal

● Individual life membership	Rs. 4,000/- (India)	US$ 600/- (Foreign)
● Individual life membership for the non-Indian citizens of the SAARC countries and other than North America, Europe and Australia	US$ 200/-	
● Individual Annual Membership (for foreign only)	US$ 60/- (with free online access; no hard copy of journal)	
● Library, Institutions, etc. (Annual)	Rs. 12,000/- (India)	US$ 400/- (Foreign)
● Individual Patron of IAVP	Rs. 1,00,000/- (Life member - paid patron for 5 years)	
● Govt./Non-Govt./Corporate/ Institution Patrons	Rs. 5,00,000/ (for 5 years)	

Advertisement Tariff

	Black and White	Full Colour
● Regular full page	Rs. 4,000	Rs. 6,000
● Regular half page	Rs. 2,000	Rs. 3,000
● Inside front & back cover page	–	Rs. 10,000
● Back cover page	–	Rs. 15,000

Note:

- Those submitting advertisement for two/four/six issues of the IJVP will be extended 15%/20%/25% discounts, respectively, on the above rates.
- The membership fee must be paid through Cash/Online/Crossed cheque or DD in favour of Treasurer "Indian Association of Veterinary Pathologists" payable at SBI, CARI Branch, Bareilly.

Contents

INDIAN JOURNAL OF VETERINARY PATHOLOGY

INDIAN ASSOCIATION OF VETERINARY PATHOLOGISTS
(Estd. 1974)

Cover Page Photo: Photomicrographs showing glyphosate-induced toxicity in birds: Hypertrophy of bronchiolar epithelium in lungs (Left top), focal cellular infiltration in myocardium (Right top), degeneration of Purkinje cells with pyknosis and karyolysis in cerebellum (Left bottom) and perinuclear vacuolation and neuronophagia in cerebrum (Right bottom).

Indian J. Vet. Pathol., 50(3) : 193-203, 2026: DOI: https://doi.org/10.56093/4fwwcv57

REVIEW ARTICLE

Prognostic biomarkers of cancer in animals: A systemic approach

Nithyashree S., Ravikumar P., Kavitha Rani B.*, Manjunatha S.S., Sunil Chandra U. and Prashanth Suresh Bagalakote

Department of Veterinary Pathology, Veterinary College, Karnataka Veterinary Animal and Fisheries Sciences University, Shivamogga - 577 204

***Address of correspondence**

Dr. Kavitha Rani B.; E-mail: hodvppvcs@gmail.com

Received: 15.4.26; Accepted: 7.6.26

ABSTRACT

Cancer is a condition characterized by uncontrolled cell proliferation, tissue invasion and metastasis. Animal cancers, which are on rise in the recent past, resemble human cancers and serve as valuable models for comparative research in cancer biology and drug development. Biomarkers are defined as measurable molecules indicating biological processes, disease or treatment response to cancer. Historical evolution of biomarkers spans from simple protein markers like alpha-fetoprotein (AFP) to advanced microRNAs and circulating tumour cells (CTCs). Ideal biomarkers must be tumor-specific, detectable in minimally invasive samples, correlate with tumor burden and enable high-throughput testing. Important proliferation markers of cancer include Ki-67, which is higher in malignant tumors, PCNA (Proliferating Cell Nuclear Antigen) which correlates with tumor grade and invasion, AgNORs (Argyrophilic Nucleolar Organizer Regions) which distinguish tumors as benign/malignant and telomerase which is 95% tumor-specific. Tumor suppressors like p53 and adhesion molecules like E-cadherin predict aggressiveness of tumors. Serum markers like AFP, TK1 (Thymidine Kinase-1), VEGF (Vascular Endothelial Growth Factor) aid in diagnosis and prognosis of hemangiosarcoma, osteosarcoma and prostate cancers. Tumor biomarker detection includes immunological methods, cytogenetic analysis and genetic analysis. Tumour biomarkers are beneficial in early detection of cancer, assessing prognosis, therapy response and monitoring relapse across species.

Keywords: Biomarkers, Detection, Diagnostics, Tumours

INTRODUCTION

Cancer remains a major cause of death in both humans and animals, particularly companion animals, despite notable advances in diagnostic and therapeutic methods in recent years. It encompasses a group of disorders characterized by uncontrolled cell proliferation, tissue invasion, and sometimes metastasis. Cancer is the second leading cause of mortality in humans and the first leading cause in dogs and cats. Globally, about 13% of annual deaths are attributed to cancer, with 70% occurring in low and middle income countries. Spontaneous tumors in domestic animals—especially in dogs, whose cancers often resemble those found in humans—provide valuable models for comparative research and for gaining insights into cancer biology and drug development. The age-related cancer incidence per 100,000 individuals per year is estimated to be about 381 in dogs and 264 in cats, compared with approximately 105 in humans[1].

BIOMARKER

According to the Working Group of the U.S. National Institutes of Health (NIH) and the Biomarkers Consortium, a biomarker is any characteristic that can be objectively measured and used to indicate normal biological activity, disease-related processes, or the body's response to a therapeutic intervention. The National Cancer Institute (NCI) further defines biomarkers as biological molecules present in blood, other bodily fluids, or tissues that signal normal or abnormal processes or the presence of a disease. They can also help assess how effectively the body responds to treatment and are sometimes referred to as molecular markers or signature molecules. The World Health Organization (WHO) defines a biomarker as any measurable substance, structure, or process within the body or its products that influences or predicts the occurrence or outcome of a disease[2].

How to cite this article : Nithyashree S., Ravikumar P., Kavitha Rani B., Manjunatha S.S., Sunil Chandra U. and Bagalakote, P.S. 2026. Prognostic biomarkers of cancer in animals: A systemic approach. Indian J. Vet. Pathol., 50(3) : 193-203.

HISTORY

Early cancer biomarkers were mainly protein-based, such as alpha-fetoprotein (AFP) and prostate-specific antigen (PSA), which were among the first to be developed for clinical use. With technological progress, biomarker research expanded to include circulating tumor DNA (ctDNA) like mutated EGFR, various forms of RNA (especially miRNA), genes released during cell division, peptides, proteins, lipids, metabolites, circulating tumor cells (CTCs), and extracellular vesicles such as exosomes. Cell-free DNA (cfDNA) was first reported in

1948, and later studies showed that tumor-specific genetic changes—such as mutations, methylation abnormalities, and chromosomal variations—could be detected in cfDNA, enabling non-invasive cancer diagnosis. In the 1970s and 1980s, interest in non-invasive biomarkers grew. The first clinically useful biomarker discovered through antibody-based methods was carcino-embryonic antigen (CEA) in 1965. By the late 1970s and 1980s, several other markers, including PSA, AFP, and cancer antigens like CA19-9, CA72-4, CA125, and CA15-3, were introduced. The development of monoclonal antibodies and immunoassays significantly advanced biomarker detection. Genetic discoveries followed, including BRCA1 and BRCA2 in the 1990s, which were useful as key to assessing hereditary cancer risk. From the late 1990s onward, genomic technologies such as microarrays, high-throughput sequencing, and proteomics broadened biomarker research. Major initiatives like the Human Genome Project (HGP) and The Cancer Genome Atlas (TCGA) provided deeper insights into cancer-related genetic alterations. Liquid biopsy emerged as a promising non-invasive approach for detecting ctDNA and monitoring disease. Recent progress includes single-cell sequencing to study tumor heterogeneity, immune biomarkers like PD-L1 for immunotherapy, and the use of artificial intelligence (AI) and machine learning (ML) to analyze large datasets[3].

CHARACTERSTICS OF IDEAL BIOMARKERS

An optimal tumor marker should:

1. be produced specifically by premalignant or malignant cells early in disease development;
2. appear at detectable levels in all individuals with a particular cancer;
3. show organ-specific expression;
4. be measurable in easily obtained, minimally invasive samples;
5. correlate with tumor size, behavior, or disease progression;
6. have a short half-life so that changes in tumor burden or treatment response are quickly reflected; and
7. have a reliable, standardized, and validated quantitative test[4].

CLASSIFICATION OF TUMOUR BIOMARKERS

Prognostic biomarkers are identified by characteristics that differentiate benign from malignant tumors. They may also be selected according to the degree of tumor differentiation, which can guide clinical decisions regarding treatment strategies. For instance, human papilloma virus (HPV) - associated oral tumors generally have a more favorable prognosis and longer survival outcomes, as they typically present in a relatively well-differentiated state[5].

Predictive biomarkers, also known as response markers, are used specifically to evaluate the effectiveness of a particular therapeutic agent. These biomarkers enable clinicians to tailor chemotherapy by selecting drugs most likely to be effective for an individual patient. For example, Herceptin® is effective only in breast cancer cases that exhibit Her2/Neu over expression, while tamoxifen is more suitable for other types of breast cancer. Consequently, Her-2/Neu serves as a predictive biomarker for certain breast cancer treatments [6]. Similarly, targeted therapies such as erlotinib and gefitinib are effective only in lung cancer patients harboring specific mutations in the epidermal growth factor receptor (EGFR) gene[7].

Diagnostic biomarkers may be detected at any point during cancer development[8,9]. Human papilloma virus (HPV) is a known diagnostic biomarker for cancers of the uterus and cervix since it is found in over 90% of tumour lesions. The identification of HPV as a diagnostic biomarker has been pivotal in advancing cervical cancer screening programs and in the development of preventive vaccines[10] (Table 1).

CANINE CANCERS AND THEIR BIOMARKERS

Canine cancer patients serve as valuable models for

Table 1. Methods of detection of tumor markers[11]

Cytogenetic analysis	• Spectral karyotyping • Comparative genomic hybridization • Fluorescent in-situ hybridization
Genetic analysis	• Sequencing (automated) • Reverse transcription • Gel electrophoresis • DNA micro-array analysis
Proteomics	• Surface-enhanced laser desorption / Ionization
Immunological	• Immunohistochemistry • Radio Immuno Assay • Enzyme-linked Immuno Sorbent Assay • Flow cytometry

human cancer research because many canine tumors closely resemble human cancers in histopathology, biological behavior, and treatment response. Apart from their significance in human cancer research, studying cancers in dogs is crucial for improving canine health and welfare. This emphasizes the importance of exploring the biological mechanisms underlying canine cancers and using comparative research approaches to identify therapeutic targets that can benefit dogs[12].

Canine mammary gland tumors (CMGTs) are the most frequently occurring neoplasms in intact female dogs and rank as the second leading cause of tumor-related death after skin cancers. Roughly half of all CMGTs are diagnosed as malignant based on histopathology, showing aggressive behavior with tendencies for metastasis and recurrence[13].Spontaneously arising canine mammary tumors have been examined more extensively than any other canine neoplasm worldwide and are considered the most common, accounting for about 52% of tumors in female dogs[14].

Ki-67

Ki-67 is one of the most extensively investigated biomarkers of cell proliferation and apoptosis in canine tumors and has been identified in a wide range of neoplastic types. In mammary tumors, it is the most commonly applied prognostic marker. Ki-67 is a non-histone nuclear protein present only in the nucleus during interphase and throughout mitosis. During mitosis, it relocates to the surface of the chromosomes. Its expression begins in the G1 phase, increases through the S and G2 phases, reaches its peak in the M phase, and then declines rapidly after cell division. It is absent in quiescent (G0) cells. Ki-67 can be measured both as a serum and tissue marker using various molecular techniques. Relying solely on the mitotic index from routine hematoxylin and eosin staining is less accurate than assessing Ki-67 via immunohistochemistry (IHC), because the mitotic index reflects only the cells in mitosis, whereas Ki-67 is expressed during multiple stages of the cell cycle. Moreover, Ki-67 can be assessed in cytology samples obtained by fine-needle aspiration, making it valuable for early detection of mammary tumors. Ki-67 can be detected by both serum ELISA testing and tissue immunohistochemistry (IHC). Increased Ki-67 expression is strongly associated with aggressive tumor behavior, including metastasis, larger tumor size, inflammation, ulceration, local tissue invasion, and lymph-node involvement. Dogs with high Ki-67 expression have shorter survival times and poorer overall prognosis. Older dogs generally exhibit lower Ki-67 expression than younger dogs, likely due to decreased cellular proliferative activity with aging[15].

Proliferating Cell Nuclear Antigen (PCNA)

PCNA is an indicator used to assess the proliferation index (PI). It functions as an accessory protein for DNA polymerase δ and is present in the nuclei of cells during the DNA synthesis phase of the cell cycle. PCNA participates in DNA repair, regulation of the cell cycle, chromatin organization, and RNA transcription. Its levels rise in late G1, peak during the S phase, and remain elevated through G2 and M phases because of its long half-life. It plays a key role in ensuring continuous cell-cycle progression and acts on both the leading and lagging DNA strands. In human oncology, PCNA is considered a useful proliferation marker, but only when interpreted alongside other breast cancer biomarkers such as ER, PR, Ki-67, or HER-2. One drawback is that PCNA is not exclusively linked to proliferation, as it is also involved in DNA repair. In veterinary medicine, PCNA is commonly measured in mammary tumors. Positive nuclear immunostaining for PCNA is associated with tumor size, histological type, level of differentiation, nuclear grade, mitotic activity, overall malignancy grade, and involvement of lymph nodes. Much like Ki-67, PCNA expression is higher in more aggressive tumors - those that are larger, ulcerated, of higher histologic grade, or associated with lymph-node metastasis. Elevated PCNA expression is linked with poorer prognosis and reduced survival. However, cytokines such as TGF, EGF, and PDGF may stimulate PCNA expression without initiating DNA synthesis, and its involvement in DNA repair also complicates interpretation. For this reason, PCNA is best evaluated in combination with additional biomarkers—especially Ki-67, whose expression is more strictly tied to cell-cycle activity[15].

A retrospective analysis examined the expression of proliferating cell nuclear antigen (PCNA) in canine round cell tumors. Forty cases – involving transmissible venereal tumors (TVT), canine cutaneous histiocytomas (CCH), and mast cell tumors (MCT) - were assessed using immunohistochemistry. Most samples showed moderate to strong PCNA staining. The proportions of PCNA-positive cells were 42.1% in TVT, 57.1% in CCH, and 57.1% in MCT. A statistically significant correlation ($P < 0.05$) was found between mitotic counts and PCNA expression in TVT and CCH. PCNA levels in TVT varied from 17.4% to 56.3%, indicating differing growth rates within this tumor type. Overall, the findings suggest that PCNA immunohistochemistry can serve as a useful supplementary method for evaluating the biological behavior of canine round cell tumors[16].

Argyrophilic Nucleolar Organizer Regions (AgNORs)

AgNOR is a molecular marker widely used to evaluate the rate of cellular proliferation in various types of tumors[17]. Nucleolar organizer regions (NORs) are DNA loops located within the nucleoli that contain genes encoding ribosomal RNA (rRNA), which are transcribed by RNA polymerase I[18]. These regions are

associated with specific argyrophilic proteins known as NOR-associated proteins (NORAPs). In rapidly proliferating tumor cells, these proteins accumulate as a result of active transcription and can be visualized as distinct black dots using silver staining on routine histopathological sections; these structures are referred to as argyrophilic nucleolar organizer regions (AgNORs)[19]. The number of AgNORs observed during interphase in continuously dividing cells correlates closely with the rate of cell proliferation[20]. Counting mitotic figures in hematoxylin and eosin–stained sections, along with AgNOR enumeration, represents a simple, cost-effective, and practical approach for assessing cellular proliferation. Both the mitotic index and AgNOR count reflect tumor proliferative activity[21].

Telomerase Activity

Recent research has focused on telomerase and its role in canine oncology, exploring whether telomerase is universally expressed in canine tumors and could serve as a promising target for therapy. Canine telomeres are composed of large, heterogeneous repeats ranging from 3 to 23 kbp. Telomere shortening has been observed *in vitro* in aging canine fibroblast cultures, and telomeric instability has also been documented *in vivo*. Telomerase activity is primarily restricted to tumor tissues, with little or no activity detected in normal somatic tissues such as lung, brain, liver, muscle, and heart. Exceptions include lens epithelial cells (both normal and cataractous) and testicular tissues, consistent with the high proliferative capacity of germ cells. Overall, the pattern of telomerase expression in canine somatic tissues closely resembles that in humans, underscoring that telomerase is not only one of the most widely expressed tumor markers in humans but also the most extensively recognized tumor marker in canines[12].

p53 Tumour Suppressor Gene

p53, often referred to as the "guardian of the genome," plays a critical role in sensing DNA damage and inducing apoptosis in cells that are irreparably damaged. In humans, its involvement in carcinogenesis is well documented: p53 is mutated or lost in roughly half of all tumors, and in cases where it remains intact, its activity is frequently suppressed. In breast cancer specifically, p53 mutations occur in about 30% of cases and are typically linked to more aggressive disease, including triple-negative subtypes. Moreover, elevated p53 expression is associated with poorer prognosis and reduced overall survival[22].p53 is a key biomarker involved in neoplastic transformation, regulation of cell proliferation, and apoptotic pathways. This protein plays a central role in cell-cycle control and programmed cell death and functions as a tumor suppressor. Alterations in the p53 gene are considered among the most frequent genetic changes observed in human breast cancer (HBC) and canine mammary tumors (CMT), and these mutations are linked to tumor progression. Mutant p53 can also promote the expression of p21, a cyclin-dependent kinase inhibitor; however, p21 expression may also be induced through p53-independent mechanisms. Increased p53 expression is generally linked to unfavourable overall survival[15].

A study aimed to examine the involvement of the p53 tumor suppressor gene in canine mammary tumors. Mutations in exons 5 and 7 were assessed in 15 mammary tumor tissue samples using PCR–single strand conformational polymorphism (PCR-SSCP) analysis followed by direct DNA sequencing. PCR-SSCP analysis detected abnormally migrating bands indicative of mutations in the amplified exon 5 (codons 117–175) of the p53 tumor suppressor gene in 3 (20%) cases of spontaneous canine mammary tumors. PCR-SSCP screening of the p53 gene region spanning amplified exon 5 (from codon 165) through exon 7 (up to codon 241) showed identical banding patterns across all 15 samples, indicating no detectable mutations in this segment[23].

BRCA-1 and BRCA-2

Among the various genetic alterations implicated in mammary tumorigenesis, mutations in the BRCA1 and BRCA2 genes play a particularly significant role in both human and canine mammary gland tumors. The BRCA1 gene, located on human chromosome 17q21, is widely expressed in mammalian tissues and encodes a nuclear phosphoprotein involved in regulating the cell cycle of mammary epithelial cells. Loss of BRCA1 expression leads to impaired DNA repair, disruption of normal cell-cycle control, increased apoptosis, and enhanced tumor development, confirming its function as a tumor suppressor gene. In human medicine, numerous genetic mutations have been identified in breast cancer cases. Germline mutations in BRCA1 and BRCA2 are inherited and confer a markedly elevated lifetime risk of developing human breast cancer, estimated at 56–84%[24]. Approximately 5–10% of all breast cancers in women are attributed to mutations in these two genes. In veterinary oncology, the hereditary basis of canine mammary tumors (CMT) remains under investigation, although certain dog breeds appear to be predisposed to the disease[15]. In one study analyzing mutations across ten breast cancer–related genes in CMT using iPLEX genotyping of 63 single-nucleotide polymorphisms, only BRCA1 and BRCA2 showed a significant association with tumor development[25]. Reduced nuclear expression of BRCA1 was particularly linked to malignant tumors, a finding consistent with earlier reports[26]. No significant difference in BRCA2 expression was observed between benign and malignant tumors in that study[25].

Cadherins

Cadherins are calcium-dependent transmembrane glycoproteins that mediate cell–cell adhesion and play

a crucial role in preserving normal tissue architecture. The cadherin family includes E-, P-, and N-cadherins. P-cadherin, also known as placental cadherin, is typically expressed in myoepithelial cells, and its overexpression in high-grade tumors is associated with increased tumor aggressiveness and an unfavorable prognosis. However, E-cadherin (epithelial cadherin) is the most extensively studied member of this family due to its central role in epithelial cell adhesion. Loss of E-cadherin is a hallmark of epithelial–mesenchymal transition (EMT), a process that facilitates tumor cell dissemination by enhancing migration and invasiveness. In veterinary oncology, since most canine mammary tumors originate from epithelial cells, decreased E-cadherin expression is associated with increased tumor progression, higher malignancy, metastatic aggressiveness, and shorter survival times. E-cadherin functions in conjunction with catenins, particularly β-catenin, which binds to its cytoplasmic domain and promotes the formation of adherens junctions. Disruption of this complex leads to weakened cell adhesion. During neoplastic transformation, β-catenin degradation is impaired, resulting in its accumulation within the cytoplasm and nucleus of tumor cells. Elevated β-catenin expression is associated with tumor progression, metastasis, and poor prognosis. Under normal conditions, circulating β-catenin levels are typically assessed alongside E-cadherin. In both human and veterinary patients, low E-cadherin expression—most commonly evaluated by immunohistochemistry in tumor tissues—is correlated with an unfavorable prognosis. However, its prognostic value is enhanced when interpreted in combination with other biomarkers, such as Ki-67. Despite its significance, E-cadherin is not among the most routinely assessed biomarkers in canine mammary tumors[15]. E-cadherin, in particular, is known to influence tumor progression and metastasis, as its loss is frequently linked to a more invasive and poorly differentiated phenotype in various carcinomas, including pancreatic cancer. On the other hand, N-cadherin (neural cadherin) is associated with increased cancer invasiveness. Recent research has shown that elevated N-cadherin expression in breast cancer is connected to greater invasiveness, driven by interactions between cancer cells and stromal cells mediated by N-cadherin[27].

Vimentin

Intermediate filaments (IFs), such as vimentin, perform roles that differ from those of microfilaments and microtubules. Early studies demonstrated that vimentin contributes to cellular integrity by providing structural stability and enhancing resistance to mechanical stress[28]. The structural and physiological roles of IFs are closely linked[29]. IFs participate in wound healing processes by regulating fibroblast proliferation, TGFβ1–Slug signaling, collagen deposition, and epithelial–mesenchymal transition (EMT). In addition, they influence cell proliferation[30], adhesion[31], migration and invasion[28,32] and act as positive regulators of cellular stemness[33]. Numerous studies have demonstrated that vimentin expression patterns differ significantly between normal and malignant epithelial tissues in the prostate, gastrointestinal tract, breast, central nervous system, and lung. Although the transcriptional and translational mechanisms regulating vimentin during cancer progression are varied[34,35], its overexpression is consistently linked to a more invasive and metastatic phenotype across these malignancies[28].

EGFR (Epidermal growth factor receptor)

Epidermal growth factor receptor (EGFR) is a transmembrane receptor tyrosine kinase that belongs to the human epidermal growth factor receptor (HER) family. This receptor family includes EGFR (HER-1/ErbB-1), HER-2/ErbB-2, HER-3/ErbB-3, and HER-4/ErbB-4, all of which are typically localized to the cell membrane. EGFR signaling enhances angiogenesis and metastatic potential and has been associated with unfavourable clinical outcomes in patients with breast cancer. Elevated EGFR expression, most often assessed by immunohistochemistry in tumor tissues, correlates with larger tumor size, presence of tumor necrosis, increased mitotic activity, higher histological grade, and more advanced clinical stage. Additionally, a relationship between EGFR expression and the age of affected dogs has been reported. Positive correlations have also been identified between EGFR and CD31 expression, as well as between EGFR and cyclooxygenase-2 (COX-2) levels. EGFR contributes to angiogenesis by regulating the production and release of pro-angiogenic factors such as vascular endothelial growth factor (VEGF)[15].

Androgen Receptors

The androgen receptor (AR) is a key steroid hormone receptor essential for male sexual differentiation, development, and the maintenance of secondary male characteristics, as well as the initiation and regulation of spermatogenesis[36]. Functioning as a ligand-dependent transcription factor, AR is activated upon binding to the androgenic hormone's testosterone or dihydrotestosterone[37]. Both normal prostate tissue and prostate cancer (PCa) rely on androgens for growth, and proper prostate development requires a functional androgen receptor (AR). Testosterone, the main circulating androgen in males, is primarily synthesized by Leydig cells in the testes[38]. Within the prostate, testosterone is converted by the enzyme 5α-reductase into 5α-dihydrotestosterone (DHT), which binds to AR and stimulates the growth of male urogenital tissues. AR serves as the principal mediator of androgen signaling in the prostate. Activation of AR by DHT is essential for full

prostate development, as individuals lacking functional 5α-reductase exhibit only rudimentary prostate tissue or complete absence of the prostate[39]. Prostate cancer is likewise initially androgen-dependent and requires functional AR signaling; tumors typically undergo temporary regression following castration. AR expression persists in both androgen-dependent (AD) and androgen-independent (AI) PCa and is maintained throughout disease progression to hormone-refractory stages[40,41]. Consequently, PCa treatment strategies primarily aim to inhibit androgen signaling, with androgen ablation leading to atrophy of the prostate epithelium. First-line therapy commonly involves androgen deprivation therapy (ADT), achieved by suppressing androgen production through surgical or chemical castration and/or administration of anti-androgens such as bicalutamide or enzalutamide (MDV3100). Despite initial responsiveness, many cases progress to an advanced androgen-independent state that is resistant to existing treatments, termed castration-resistant prostate cancer (CRPC), which arises due to reactivation of AR signalling[42].

Cycloxygenase - 2

Cycloxygenase (COX) is an enzyme of the myeloperoxidase family that catalyzes the conversion of arachidonic acid into prostanoids. These products—including prostaglandins, prostacyclin, and thromboxane—are biologically active molecules that regulate a wide range of physiological functions in both humans and animals[43]. Over expression of COX-2 induces a phenotypic shift from benign to malignant cells, a process associated with dysregulated growth and proliferation, enhanced resistance to apoptosis and immune surveillance, stimulation of angiogenesis, and increased invasive capacity[44]. Research on COX-2 expression in animal populations across different countries has shown that the enzyme is frequently overexpressed in a variety of canine epithelial tumors. These include mammary gland adenocarcinomas and carcinomas, ovarian and prostate tumors, transitional cell (urothelial) carcinoma (TCC), colorectal and small intestinal tumors, squamous cell carcinoma (SCC) of the skin and oral cavity, osteosarcoma, and melanoma[45,46,47,48]. In contrast, COX-2 is either minimally expressed or absent in canine lymphoma, sarcoma, fibrosarcoma, glioma, and mastocytoma[49].Studies on small groups of feline patients indicate that, in contrast to dogs, COX-2 is expressed less frequently and at lower levels in cats[50].

Alpha Fetoprotein

Alpha-fetoprotein (AFP) is produced in large amounts primarily by the liver during embryonic development and represents one of the predominant proteins in fetal circulation. After birth, AFP expression is transcriptionally suppressed, resulting in very low serum concentrations in adult animals. AFP has been reported to exert immunosuppressive effects and to promote angiogenesis, thereby supporting neovascularization in both fetal and neoplastic tissues. Because AFP is predominantly synthesized by the liver, veterinary research has mainly investigated its potential role as a biomarker for canine hepatic tumors. In dogs, serum AFP concentrations are markedly elevated at birth (approximately 14,080 ± 5,944 μg/ml) and progressively decline during growth, reaching values between 0.014 and 0.069 μg/ml in adulthood. Increased AFP concentrations are observed in dogs with lymphomas and mast cell tumors. Although elevated serum AFP levels may indicate an increased likelihood of neoplastic disease, no definitive serum cut-off value has been established in dogs to determine diagnostic sensitivity and specificity. A significant reduction in serum AFP levels has been observed following surgical resection of affected liver lobes[51]. A study evaluated Serum alpha-fetoprotein (AFP) levels before and after surgical excision of tumor masses in four dogs diagnosed with hepatocellular carcinoma (HCC), and assessed AFP expression in tumor tissues by immunohistochemistry. In three dogs, preoperative serum AFP concentrations were 10–20 times higher than those observed in healthy dogs and returned to normal levels within one to two months following surgery. Correspondingly, AFP immunoreactivity was detected in the tumor tissues of these cases. In contrast, one dog exhibited low serum AFP levels and showed no AFP expression within the tumor tissue[52.]

CEA (Carcino Embryonic Antigen)

Carcinoembryonic antigen (CEA) is a membrane-associated glycoprotein primarily produced in specific regions of the gastrointestinal tract, where it functions in cell adhesion. Under normal physiological conditions, circulating CEA levels are very low. However, certain tumor cells can overproduce CEA and express it across their entire cell surface as a result of loss of cellular polarity. Because these cells no longer adhere to the basal lamina, CEA is released into the blood stream, leading to elevated serum concentrations in patients with particular malignancies. CEA tumor marker is used to detect and monitor malignancies, including mammary gland tumors, in both humans and animals. Its molecular weight is typically around 180–200 kDa, though this can vary across species and protein isoforms[51]. CEA is mainly produced in the fetal gut and liver during embryonic development. In adults, its expression is minimal under normal conditions but can be produced by epithelial tissues. In pathological states, such as mammary gland tumors, tumor cells themselves can synthesize CEA, which is important for its diagnostic relevance[53]. CEA has no significant physiological role in healthy individuals. Elevated levels are associated with malignancies,

serving as a marker of tumor activity and indicating the presence of cancer, including mammary gland tumors in animals[54]. CEA was initially identified in human colon cancer and named for its detection in embryonic tissues. Its recognition as a tumor marker led to its use across multiple cancer types, including veterinary mammary tumors[55]. In dogs, reference serum CEA levels in healthy individuals are 0.12–0.23 ng/ml for radioimmunoassay[56].

Thymidine kinase (TK-1)

TK1 is an enzyme primarily synthesized in proliferating cells during the S phase of the cell cycle. While various tissues can produce TK1, its expression is markedly elevated in fast-dividing cells, including tumor cells. In hemangiosarcoma, cancer cells contribute significantly to circulating TK1 levels. The enzyme's synthesis is closely linked to DNA replication, and higher blood levels reflect increased cellular proliferation[57]. Under normal conditions, TK1 plays a vital role in DNA replication by phosphorylating thymidine, which is then incorporated into the growing DNA strand, supporting cell division and tissue growth. In cancer, TK1 levels rise substantially, reflecting abnormal cell proliferation, making it a sensitive marker for cancer detection and monitoring[58].TK1's role as a cancer biomarker is a relatively recent discovery. Elevated TK1 activity in the blood was linked to cancer cell proliferation, establishing its potential for diagnosing and monitoring malignancies, including hemangiosarcoma[59]. TK1 levels can be measured using techniques such as ELISA, spectrophotometry, radioimmunoassay (RIA), HPLC, and mass spectrometry. ELISA is commonly used due to its accuracy and practicality. These assays utilize antibodies specific to TK1, enabling precise quantification in biological samples[57]. Measuring TK1 in the bloodstream is crucial in veterinary oncology, particularly for hemangiosarcoma. Elevated TK1 reflects increased cell proliferation, aiding in early cancer detection, evaluating tumor burden, and monitoring treatment response. In hemangiosarcoma, TK1 helps to differentiate malignant from benign masses, which may be challenging by other diagnostic methods. TK1 is also included in specialized panels, such as the "TK canine cancer panel," to confirm cancer presence, assess therapy effectiveness, and verify remission[60]. For example, a study on canine malignant lymphoma showed that normal dogs had serum TK activity of 0–7 U/L, whereas dogs with lymphoma had levels ranging from 8.9 to 470 U/L—1.3 to 67 times higher than healthy dogs. These findings demonstrate that TK1 activity is significantly increased in dogs with malignancies, reinforcing its utility as a diagnostic biomarker[61].

VEGF (Vascular endothelial growth factor)

Vascular endothelial growth factor (VEGF) is one of the most widely used biomarkers in human medicine due to its central role in angiogenesis. VEGFs are encoded by four genes: VEGF-A, VEGF-B, VEGF-C, and VEGF-D. While VEGF-A and VEGF-B primarily regulate angiogenesis, VEGF-C and VEGF-D are involved in lymphangiogenesis. In normal tissues, VEGF regulates the formation, structure, and function of blood vessels. It promotes endothelial cell proliferation and migration, increases microvascular permeability—facilitating tumor cell escape and metastasis—prevents regression of newly formed vessels, stimulates endothelial invasion for new vessel formation, and inhibits apoptosis. Elevated VEGF levels are associated with tumor progression and metastasis, while reduced VEGF expression suppresses tumor growth. In canine mammary tumours (CMT), higher serum VEGF levels correlate with advanced clinical stage, poorer prognosis, and decreased survival, particularly in aggressive, infiltrative tumors or those with histological necrosis. VEGF is therefore considered a marker of tumor progression and metastatic potential. Both in human and veterinary medicine, VEGF serves as a reliable biomarker in tissue and serum and is particularly valuable for early detection of human and canine breast cancers. Its diagnostic sensitivity is further enhanced when combined with CA 15-3 measurements[15].

Canine Prostate-Specific Esterase (CPSE)

Canine prostate cancer, similar to human cases, primarily affects older male dogs and is often diagnosed at an advanced stage, frequently after metastasis, which complicates treatment. Unlike humans, where prostate-specific antigen (PSA) is a standard biomarker, dogs lack a single well-established marker, though canine prostate-specific esterase (CPSE) has shown promise and remains under investigation. Serum CPSE has emerged as a reliable and specific biomarker for various prostatic disorders in dogs, including benign prostatic hyperplasia (BPH), bacterial prostatitis, and prostatic carcinoma. Measuring CPSE in serum provides a new diagnostic and screening tool, useful for diagnosing BPH, proactively screening healthy dogs, and monitoring dogs during and after treatment. CPSE levels are stable regardless of circadian rhythms or trans-rectal palpation; however, sexual rest for at least 24 hours is recommended before measurement, as recent ejaculation can affect CPSE levels. CPSE shows diagnostic characteristics similar to human PSA, highlighting its potential for indicating prostate disorders[62].

Micro RNA

MicroRNAs (miRNAs) are small, non-coding RNA molecules present in cells that regulate gene expression by inhibiting mRNA translation. They are involved in many diseases, including cancer, due to their critical roles in cellular processes. In oncology, miRNAs can function as either tumor suppressors or oncogenes, making them promising targets for both diagnostic and

therapeutic applications. MicroRNAs are crucial for regulating gene expression and maintaining cellular homeostasis. In pathological conditions such as cancer, dysregulation of miRNAs can disrupt key processes like cell proliferation, apoptosis, and angiogenesis. Various techniques exist to measure miRNA levels in biological samples. Spectrophotometry can quantify miRNA concentrations, while reverse transcription-quantitative polymerase chain reaction (RT-qPCR) allows specific profiling. High-throughput analysis can be performed using microarrays, and ELISA can detect specific miRNAs in serum or plasma. In veterinary oncology, measuring miRNA levels in tumors, blood, or other biological fluids provides valuable diagnostic information. MicroRNAs can act as tumor-specific biomarkers, assisting in cancer detection, subtyping, and prognosis[62].

CTCs (Circulating tumor cells)

Circulating Tumor Cells (CTCs) play a key role in the formation of metastases. These cells originate from solid tumors and gain the ability to detach and enter the bloodstream. Because CTCs are extremely rare—approximately 1 CTC per 10^6–10^7 leukocytes—detection requires highly sensitive methods, often involving enrichment and isolation techniques. These approaches rely on identifying cell surface markers, exploiting physical or biological properties (such as size, density, or invasiveness), or using molecular methods like RT-PCR to detect CTC-specific RNA. Currently, the only FDA-approved method for identifying, isolating, and counting CTCs (approved in 2004) combines an enrichment step with specific antibody-based detection and high-resolution imaging. CTCs identified by this method are characterized by the phenotype $EpCAM^+$/CK^+/$DAPI^+$/$CD45^-$. Due to this approval, most human oncology studies use this technology[63]. In veterinary medicine, however, RT-PCR has been applied to detect CTC-specific mRNAs in canine blood[64].

Ct-DNA (Circulating tumour DNA)

In both human and veterinary medicine, circulating DNA, including circulating tumor DNA (ctDNA), offers valuable insights into disease processes. In humans, advanced technologies such as sequencing and digital PCR enable early cancer detection, detailed tumor characterization, prognostic evaluation, and treatment monitoring based on ctDNA levels. In canine oncology, the CNRS (French National Centre For Scientific Research). "Dog Genetics" team at the Institute of Genetics and Development in Rennes has developed ctDNA assays for histiocytic sarcoma and lymphoma. Their research identified tumor-specific mutations shared between canine and human histiocytic sarcomas, detectable in the plasma of affected dogs, providing a non-invasive diagnostic method. Notably, ctDNA was detectable in 92.3% of canine lymphoma cases at diagnosis and has been used to monitor treatment response and predict relapse in dogs with diffuse large B-cell lymphoma. These tests represent important tools for clinical oncology research and diagnostics. Circulating cell-free DNA (cfDNA) consists of short, double-stranded DNA fragments, usually 180–200 base pairs in length, present in blood and other biological fluids. cfDNA is released by cells from various organs through processes such as apoptosis, necrosis, and active secretion. While levels are low in healthy individuals, they rise in pathological conditions, including cancer. Under normal conditions, cfDNA is present at low levels and contributes to genetic material maintenance. In cancer, however, cfDNA can include ctDNA carrying tumor-specific genetic and epigenetic alterations that reflect tumor progression, treatment resistance, and malignancy. Techniques for cfDNA and ctDNA analysis include spectrophotometry, ELISA, HPLC, mass spectrometry, and RIA. These approaches allow for quantification and genetic profiling of ctDNA[62].

BOVINE CANCER BIOMARKER

Anti-Müllerian hormone (AMH) is a glycoprotein produced by sertoli cells in males and by granulosa cells of early-stage ovarian follicles in females. After puberty, AMH secretion decreases in several species, including men, bulls, and stallions. Consequently, AMH has mainly been investigated as a biomarker for granulosa cell tumors (GCT) and sertoli cell tumors (SCT) in humans and animals. In cows and mares, serum AMH concentrations accurately indicates the presence of GCT, with cut-off values of 0.36 ng/ml in cows and 4 ng/ml in mares, and sensitivities of 100% and 98%, respectively[51]. A study evaluated anti-Müllerian hormone (AMH) as a non-invasive biomarker for diagnosing granulosa-theca cell tumors (GTCTs) in cattle. It showed that AMH had the highest diagnostic value (AUC = 0.99). At a cutoff value of ≥0.36 ng/mL, AMH achieved 100% sensitivity, 99.1% specificity, and 99.2% diagnostic accuracy. These results indicated that plasma AMH concentration is a highly sensitive and reliable biomarker for the diagnosis of bovine GTCTs[65].

EQUINE CANCER BIOMARKER

A study evaluated whole-blood microRNAs (miRNAs) as long-term diagnostic and prognostic biomarkers for equine sarcoids. Based on clinical examination at 3 years of age and follow-up after 5–12 years, 77 horses were classified into regression, progression, newly affected, and tumor-free control groups. Expression of eight miRNAs was measured by RT-qPCR, and the effects of sex, breed, diagnosis, and prognosis were analyzed. Sex and breed significantly influenced miRNA expression. Eca-miR-127 distinguished sarcoid-affected horses from tumor-free controls, whereas no miRNA differentiated between sarcoid regression and progression. Expression

of eca-miR-125a-5p and eca-miR-432 differed in male horses that later developed sarcoids compared with male controls. Overall, the studied miRNAs were not predictive of sarcoid outcome but showed potential for identifying young, tumor-free male horses at risk of developing sarcoids. These findings emphasize the importance of sex- and breed-specific effects in equine miRNA biomarker studies[66].

POULTRY CANCER BIOMARKER

A study investigated the role of chicken telomerase reverse transcriptase (chTERT) in regulating the Wnt/β-catenin signaling pathway and its contribution to the tumorigenicity of avian leukosis virus subgroup J (ALV-J) in vivo. The reported plasma levels of β-catenin and c-Myc were markedly higher in chTERT-overexpressing, ALV-J-infected chickens compared with controls. ALV-J tumors exhibited enhanced Wnt/β-catenin pathway activity, increased c-Myc expression, reduced apoptosis, and higher viral replication relative to adjacent non-tumorous tissues, as confirmed by immunohistochemistry, western blotting, and RT-qPCR.These findings demonstrated that chTERT promotes ALV-J-induced tumorigenesis by activating the Wnt/β-catenin signaling pathway, providing insight into the molecular mechanisms underlying ALV-J-associated tumors[67].

CONCLUSION

Biomarkers play critical tools in modern veterinary oncology, providing valuable insights beyond what imaging and histopathology can offer. They aid in early and accurate diagnosis, helping into differentiate benign and malignant lesions and even identify the tumor origin. Real time monitoring using serum or liquid biomarkers allows better assessment of therapeutic effectiveness and early detection of relapse. While biomarkers enhance diagnostic precision, their high cost and limited availability can restrict routine use in general veterinary practice.

ACKNOWLEDGEMENT

We acknowledge the Dean, Veterinary College Shivamogga for the technical facilities.

Financial support & sponsorship: None

Conflicts of Interest: None

Use of Artificial Intelligence (AI)- Assisted Technology for manuscript preparation: The authors confirm that there was no use of AI- assisted technology for assisting in the writing of the manuscript and no images were manipulated using AI.

REFERENCES

1. Kumar P, Pawaiya RVS. 2010. Advances in Cancer Diagnostics. *Braz J Vet Pathol* **3**(2): 142-153.
2. Mishra A, Verma M. 2010. Cancer biomarkers: Are we ready for the prime time. *Cancers* **2**: 190-208.
3. Tenchov R, Sapra AK, Sasso J, Ralhan K, Tummala A, Azoulay N, Zhou QA. 2024. Biomarkers for Early Cancer Detection: A Landscape View of Recent Advancements, Spotlighting Pancreatic and Liver Cancers. *ACS Pharmacol Transl Sci* **7**: 586-613.
4. Bigbee W, Herberman RB. 2003. Holland-Frei Cancer Medicine. BC Decker Inc., Hamilton, Ontario, Canada, pp. 16-18.
5. Mishra A, Bharti AC, Varghese P, Saluja D, Das BC. **2006.** Differential expression andactivation of NF-kappaB family proteins during oral carcinogenesis: Role of high risk human-papillomavirus infection. *Int J Cancer 119*: 2840–2850.
6. Roses RE, Paulson EC, Sharma A, Schueller JE, Nisenbaum H, Weinstein S, Fox KR,Zhang PJ, Czerniecki BJ. 2009. HER-2/neu overexpression as a predictor for the transition from insitu to invasive breast cancer. *Cancer Epidemiol Biomarker Prev 18*: 1386–1389.
7. Sharma SV, Bell DW, Settleman J, Haber DA. 2007. Epidermal growth factor receptor mutationsin lung cancer. *Nat Rev Cancer7*: 169–181
8. Verma M, Manne U. 2006. Genetic and epigenetic biomarkers in cancer diagnosis and identifyinghigh risk populations. *Crit Rev Hematol Oncol 60*: 9–18.
9. Habis AH, Vernon SD, Lee DR, Verma M, Srivastava S, Unger U. 2004. Molecular quality ofexfoliated cervical cells: implications for molecular epidemiology and biomarker discovery. *Cancer Epidemiol Biomarkers Pre 13*: 492–496.
10. Schiffman M, Castle PE, Jeronimo J, Rodriguez AC, Wacholder S. 2007. Human papillomavirus and cervical cancer. *The Lancet* **370**: 890-907.
11. Sharma S. 2021. Tumor markers in clinical practice: General principles and guidelines. *Indian J Med Paediat Oncol* **30**: 1-8.
12. Argyle DJ, Nasir L. 2003. Telomerase: A Potential Diagnostic and Therapeutic Tool in Canine Oncology. *Vet Pathol* **40**: 1-7.
13. Fan Y, Ren X, Liu X, Shi D, Xu E, Wang S, Liu Y. 2021. Combined detection of CA15-3, CEA, and SF in serum and tissue of canine mammary gland tumor patients. *Sci Rep* **11**: 1-9.
14. Macewen EG, Withrow SJ. 1996. Soft tissue sarcomas. Small animal clinical oncology. 2nd edition, W.B. Saunders Company, Philadelphia, pp, 211-226.
15. Kaszak I, Ruszczak A, Kanafa S, Kacprzak K, Krol M, Jurka P. 2018. Current biomarkers of canine mammary tumors. *Acta Vet Scand* **60**: 1-13.
16. Tiwari KP, Bhaiyat MI, Chikweto A, Sharma R N, Younger CH, Pawaiya RS. 2016. Expression pattern of proliferating cell nuclear antigen (PCNA) in round cell tumors of dogs from Grenada, West Indies. *Indian J Vet Pathol* **40**(2): 144-147.
17. Crocker J, Nar P. 1987 Nucleolar organizer regions in lymphomas. *J. Pathol* **151**: 111-118.
18. Egan MJ, Crocker J. 1992 Review: Nucleolar organizer regions in pathology. *Brit J Cancer* **65**: 1-7.
19. Crocker J, Boldy D, Egan MJ. 1989. How should we count AgNORs? Proposals for a standardized approach. *J Pathol* **158**: 185-188.
20. Trere D. 2000. AgNOR staining and quantification. *Micron* **31**: 127-131.
21. Kumar P, Kumar R, Pawaiya RS, Puttaswamy MB. 2010. Diagnostic significance of mitotic index and AgNOR count in canine mammary tumours. *Braz Vet Pathol* **3**: 41-43.
22. Brunetti B, Bacci B, Angeli C, Benazzi C, Muscatello LV. 2020. p53, ER, and Ki67 Expression in Canine Mammary Carcinomas and Correlation With Pathological Variables and Prognosis. *Vet Pathol* **20**(10): 1-7.
23. Dhaygude VS, Joshi BP, Joshi CG, Prajapati KS. 2010. Mutational analysis of p53 tumour suppressor gene in canine mammary tumours using PCR-SSCP and sequencing. *Indian J Vet Pathol* **34**(2): 123-127.

24. Yoshikawa Y, Morimatsu M, Ochiai K, Ishiguro-Oonuma T, Wada S, Orino K, Watanabe K. 2015. Reduced canine BRCA2 expression levels in mammary gland tumors. *BMC Vet Res* **11**: 1-8.
25. Rivera P, Melin M, Biagi T, Fall T, Haggstrom J, Lindblad-Toh K, von Euler H. 2009. Mammary tumor development in dogs is associated with BRCA1 and BRCA2. *Cancer Res* **69**(22): 8770-8774.
26. Nieto A, Perez-Alenza MD, Del Castillo N, Tabanera E, Castano M, Pena L. 2003. BRCA1 Expression in canine mammary dysplasias and tumours: relationship with prognostic variables. *J Comp Path* **128**: 260-268.
27. Nakajima S, Doi R, Toyoda E, Tsuji S, Wada M, Koizumi M, Tulachan SS, Ito D, Kami K, Mori T, Kawaguchi Y, Fujimoto K, Hosotani R, Imamura M. 2004. N-Cadherin Expression and Epithelial-Mesenchymal Transition in Pancreatic Carcinoma. *Clin Cancer Res* **10**(12): 4125-4133.
28. Mogre S, Makani V, Pradhan S, Devre P, More S, Vaidya M, Dmello C. 2022. Biomarker Potential or Vimentin in Oral Cancers. *Life.* **12**(2): 1-11.
29. Herrmann H, Bär H, Kreplak L, Strelkov SV, Aebi U. 2007**.** Intermediate filaments: From cell architecture to nanomechanics. *Nat Rev Mol Cell Biol.* **8**: 562–573.
30. Cheng F, Shen Y, Mohanasundaram P, Lindström M, Ivaska J, Ny T, Eriksson JE. 2016**.** Vimentin coordinates fibroblast proliferation and keratinocyte differentiation in wound healing via TGF-β–Slug signaling. *Proc Natl Acad Sci USA* **113**: E4320.
31. Nieminen M, Henttinen T, Merinen M, Marttila–Ichihara F, Eriksson JE, Jalkanen S. 2006. Vimentin function in lymphocyte adhesion and transcellular migration. *Nat Cell Biol* **8**: 156–162.
32. Richardson AM, Havel LS, Koyen AE, Konen JM, Shupe J, Wiles WG, Martin WD, Grossniklaus HE, Sica G, Gilbert-Ross M, Marcus AI.2018.Vimentin Is Required for Lung Adenocarcinoma Metastasis via Heterotypic Tumor Cell–Cancer-Associated Fibroblast Interactions during Collective Invasion. *Clin Cancer Res* **24**(2): 420-432.
33. Peuhu E, Virtakoivu R, Mai A, Wärri A and Ivaska J. 2017. Epithelial vimentin plays a functional role in mammary gland development. *Development* **144**: 4103–4113.
34. Satelli A, Li S. 2011. Vimentin in cancer and its potential as a molecular target for cancer therapy. *Cell Mol Life Sci* **68**: 3033–3046.
35. Snider NT, Omary MB. 2014. Post-translational modifications of intermediate filament proteins: Mechanisms and functions. *Nat Rev Mol Cell Biol* **15**: 163–177.
36. Holdcraft RW, Braun RE. 2004. Androgen receptor function is required in Sertoli cells for the terminal differentiation of haploid spermatids. *Development* **131**: 459-67.
37. Eisermann K, Wang D, Jing Y, Pascal LE, Wang Z. 2013. Androgen receptor gene mutation, rearrangement, polymorphism. *Transl Androl Urol* **2**: 137–147
38. Debes JD, Tindall DJ. 2002. The role of androgens and the androgen receptor in prostate cancer. Cancer Lett **187**: 1-7.
39. Heinlein CA, Chang C. 2004. Androgen receptor in prostate cancer. *Endocr Rev* **25**: 276-308.
40. Knudsen KE, Penning TM. 2010. Partners in crime: deregulation of AR activity and androgen synthesis in prostate cancer. *Trends Endocrinol Metab* **21**: 315-24.
41. Yuan X, Balk SP. 2009. Mechanisms mediating androgen receptor reactivation after castration. *Urol Oncol* **27**: 36-41.
42. Waltering KK, Urbanucci A, Visakorpi T. 2012. Androgen receptor (AR) aberrations in castration-resistant prostate cancer. *Mol Cell Endocrinol* **360**: 38-43.
43. Chandrasekharan NV, Simmons DL. 2004. The cyclooxygenases. *Genome Biol* **5**: 241.
44. Rizzo MT. 2011. Cyclooxygenase-2 in oncogenesis. *Clin Chem Acta* **412**: 671–687.
45. Doré M. 2011. Cyclooxygenase-2 expression in animal cancers. *Vet Pathol* **48**: 254–265.
46. Doré M, Lanthier I, Sirois J. 2003. Cyclooxygenase-2 expression in canine mammary tumors. *Vet Pathol* **40**: 207–212.
47. Millanta F, Citi S, Della Santa D, Porciani M, Poli A. 2006. COX-2 expression in canine and feline invasive mammary carcinomas: correlation with clinicopathological features and prognostic molecular markers. *Breast Cancer Res Treat* **98**: 115–120.
48. Pestili de Almeida EM, Piché C, Sirois J, Doré M. 2001. Expression of cyclooxygenase-2 in naturally occurring squamous cell carcinomas in dogs. *J Histochem Cytochem* **49**: 867–875.
49. Mohammed SI, Khan KN, Sellers RS, Hayek MG, DeNicola DB, Wu L, Bonney PL, Knapp DW. 2004. Expression of cyclooxygenase-1 and 2 in naturally-occurring canine cancer. *Prostaglandins Leukot Essent Fatty Acids* **70**: 479–483.
50. Szweda M, Rychlik A, Babinska I, Pomianowski A. 2020. Cyclooxygenase-2 as a biomarker with diagnostic, therapeutic, prognostic, and predictive relevance in small animal oncology. *J Vet Res* **64**: 151-160.
51. Colombe P, Beguin J, Benchekroun G, Le Roux D. 2022. Blood biomarkers for canine cancer, from human to veterinary oncology. *Vet Comp Oncol* **20**(4): 767-777.
52. Kitao S, Yamada T, Ishikawa T, Madarame H, Furuichi M, Neo S, Kobayashi K. 2006. Alpha-fetoprotein in serum and tumor tissues in dogs with hepatocellular carcinoma. *J Vet Diagn Invest* **18**(3): 291-295.
53. Kawarai S, Hashizaki K, Kitao S, Nagano S, Madarame H, Neo S, Ishikawa T, Furuichi M, Hisasue M, Tsuchiya R, Tsujimoto H, Yamada T. 2006. Establishment and characterization of primary canine hepatocellular carcinoma cell lines producing alpha fetoprotein. *Vet Immunol Immunopathol* **113**: 30-36.
54. Yamada T, Kakinoki M, Totsuka K, Ashida Y, Nishizono K, Tsuchiya R, Kobayashi K. 1995. Purification of canine alphafetoprotein and alpha- fetoprotein values in dogs. *Vet Immunol Immunopathol* **47**: 25-33.
55. Yamada T, Fujita M, Kitao S,Ashida Y, Nishizono K, Tsuchiya R, Shida T, Kobayashi K. 1999. Serum alpha-fetoprotein values in dogs with various hepatic diseases. *J Vet Med Sci* **61**(6): 657-659.
56. Yeganeh-Amirkande S, Assmar M, Mansour-Ghanaei F Mozafari-Noor A. 2015. The frequency of CA15-3, CA125, CA19-9 in patients with hepatitis B and C. *Zahedan J Res Med Sci* **17**(5): 959.
57. Von Euler H, Eriksson S. 2011. Comparative aspects of the proliferation markerthymidine kinase 1 in human and canine tumour diseases. *Vet Comp Oncol* **9**: 1–15.
58. Welin M, Kosinska U, Mikkelsen N-E, Carnrot C, Zhu C, Wang L, Eriksson S,Munch-Petersen B, Eklund H. 2004. Structures of thymidine kinase 1 of human andmycoplasmic origin. *Proc Natl Acad Sci U S A* **101**: 17970–17975.
59. Bitter EE, Townsend MH, Erickson R, Allen C, O'Neill KL. 2020. Thymidine kinase1 through the ages: a comprehensive review. *Cell Biosci* **10**: 138.
60. Saellström S, Sharif H, Jagarlamudi KK, Rönnberg H, Wang L, Eriksson S. 2022.Serum TK1 protein and C-reactive protein correlate to treatment response and predict survivalin dogs with hematologic malignancies. *Res Vet Sci* **145**: 213–221.
61. Kayar A, Dokuzeylul B, Iskefli O, Bayrakal A, Saka SU, Yildirim F, Gurel A. 2018.Clinical features, haematologic parameters, blood serum biochemistry results and thymidinekinase activ-

ity of dogs affected by malignant lymphoma in Turkey
62. Knutsen HT. 2023. Minireview: Biomarkers in Veterinary Oncology- with the focus on Blood Biomarkers. **1**: 1-57.
63. Maly V, Maly O, Kolostova K, Bobek V. 2019. Circulating tumor cells in diagnosis and treatment of lung cancer. *In Vivo* **33**(4): 1027- 1037.
64. Mostert B, Sleijfer S, Foekens JA, Gratama JW. 2009. Circulating tumor cells (CTCs): detection methods and their clinical relevance in breast cancer. *Cancer Treat Rev* **35**(5): 463-474
65. Ali HE, Kitahara G, Nibe K, Yamaguchi R, Horii Y, Zaabel S, Osawa T. 2013. Plasma anti-Müllerian hormone as a biomarker for bovine granulosa-theca cell tumors: Comparison with immunoreactive inhibin and ovarian steroid concentrations. *Theriogenology* **80**(8): 950-949.
66. Cosandey J, Hamza E, Gerber V, Ramseyer A, Leeb T, Jagannathan, Blaszcyk K, Unger L. 2021. Diagnostic and prognostic potential of eight whole blood microRNAs for equine sarcoid disease. *Plos One* **16**(12): 1-17.
67. Xiang Y, Liang C, Li Q. 2022. Chicken telomerase reverse transcriptase promotes the tumorigenicity of avian leukosis virus subgroup J by regulating the Wnt/β-catenin signaling pathway. *Vet Res* **53**(100): 1-22.

Indian J. Vet. Pathol., 50(3) : 204-213, 2026: DOI: https://doi.org/10.56093/dhhmrt16

MINI REVIEW ARTICLE

Gasterointestinal cooperiasis: A mini review on an incidence of unusual malady of *Cooperia pectinata* (Ransom, 1907) in a calf from Tamil Nadu

N. Babu Prasath*, J. Selvaraj, M. Saravanan[1], R. Velusamy[2] and A. Latchumikanthan[2]
Department of Veterinary Pathology, Veterinary College and Research Institute, Orathanadu, Tamil Nadu Veterinary and Animal Sciences University, Thanjavur, Tamil Nadu, India
[1]Department of Veterinary Medicine
[2]Department of Veterinary Parasitology

***Address of correspondence**
Dr. N. Babu Prasath; E-mail: vetdrprasad@gmail.com
ORCID Id: 000-0002-8219-9265

Received: 17.2.26; Accepted: 13.3.26

ABSTRACT

A review on cooperiasis in cattle caused by *Cooperia pectinata* was described based on the authentic episode of the malady in a calf. A four-month-old Jersey cross-bred calf was presented for necropsy with the clinical history of inappetence, anaemia, diarrhea, weakness and death. Systematic post-mortem examination was conducted. Externally, carcass was thin with blanched mucous membranes. Internally, edematous fluid accumulated in pericardial sac, thoracic and abdominal cavities. Proximal small intestine revealed scattered nodules. Lumen of the distal abomasum and duodenum contained pale viscous contents and numerous pale yellowish-brown, hairy nematodes. Histologically, small intestine revealed acute catarrhal enteritis. Mucosal villi were blunt, fused and showed scattered areas of epithelial necrosis. Muco-serosal nodules revealed necrotic cell debris, throngs of neutrophils, eosinophils and few macrophages encircling the dead and degenerating nematodes. Nodules were thought to be hypobiosis of parasitic larval (L4&L5) stages. Muco-serosal nodules upholds the penetrating nature of the parasite and explained the host cell-mediated immune response. Morphologically, the parasites were identified as *Cooperia pectinata*. Adult male was identified with its morphology of spicules, structure and arrangement of bursal rays. Adult female was identified with its morphology of vagina and ovijector. The penetrating nature of the *C. pectinata* was responsible of intestinal pathology which in turn caused acute malady characterized by anaemia, diarrhea, loss of body weight gain, emaciation and death. The paper elaborates the pathology and pathogenesis of *C. pectinata* in cattle and records the incidence in southern India *at-long-last* documented evidence after 1940 from Madras state.

Keywords: Calf, *Cooperia pectinata*, Enteritis, Morphology, Pathology, Review

INTRODUCTION

Gastrointestinal nematodiasis is an economically significant parasitism in ruminants[1]. Among them, trichostrongylidae parasites are weighty and genus *Cooperia* spp. is reported to cause substantial reduction in production in domestic ruminants[2,3]. Among 19 valid species of *Cooperia* in ruminants, four species such as *C. oncophora*, *C. pectinata*, *C. punctata* and *C. spatulata* are reported to occur in cattle[4,5]. All four are lumen dwelling nematodes of small intestine. These parasites have pre-parasitic, free-living (L1-L3) and parasitic larval stages (L4-L5) and mature adult stage in its life cycle[6]. *C. pectinata* and *C. punctata* are found to be more pathogenic as its developmental larval stages penetrates deeper into the intestinal mucosa and cause destruction of mucosal epithelial cells, formation of muco-serosal nodules and catarrhal enteritis[7,8]. Species of *Cooperia* are differentiated by its morphology of spicules in male and vulva of females[5,9]. Advances in molecular diagnostic techniques are though unambiguous, traditional morphological features are equivalently prompt in identifying species of *Cooperia* in ruminants as a host-specific parasite[4,5]. *C. pectinata* are found to occur in tropical and subtropical countries[10]. Though the occurrence is rare in India, prevalence is documented by copromorphology from Northern India[1,11,12] howbeit, it is hardly ever reported in Southern India more specifically from Tamil Nadu[13]. Hence, this paper documents the first descriptive report on occurrence, morphology and pathology of *Cooperia pectinata* in a calf from Southern India (District Thanjavur, Tamil Nadu). Further, the paper reviews the morphology, incidence, pathology and treatment of *C. pectinata* in cattle based on the earlier documents and discusses them in context to the present report in calves.

How to cite this article : Prasath, N.B., Selvaraj, J., Saravanan, M., Velusamy, R. and Latchumikanthan, A. 2026. Gasterointestinal cooperiasis: A mini review on an incidence of unusual malady of *Cooperia pectinata* (Ransom, 1907) in a calf from Tamil Nadu. . Indian J. Vet. Pathol., 50(3) : 204-213.

MATERIALS AND METHODS

A four-month-old Jersey cross-bred calf was presented to Veterinary Clinical Complex, Veterinary College and Research Institute (VCRI), Orathanadu, Thanjavur, Tamil Nadu, India with the history of weakness, inappetence and hypothermia. Animal had cream-like diarrhea since one week. Animal was dull and showed pale conjunctiva indicating anaemia on clinical examination. First-line of treatment was initiated for anaemia and diarrhea. Animal collapsed and died on the immediate next day in spite of treatment regimen. The carcass was presented to the Department of Veterinary Pathology, VCRI, Orathanadu for necropsy. Systematic postmortem examination was carried out. Representative tissue samples were collected in 10% neutral buffered formalin for histopathology. Tissues were processed as per standard paraffin embedding technique and tissue sections of 3-5 µm thickness were prepared using manual rotatory microtome (Leica) and were subjected to Haematoxylin-Eosin (H&E) staining protocol[14]. The duplicate sections were subjected to Alcian blue-PAS staining[15]. Blood smears were prepared from peripheral blood and heart blood for cytological examination. Blood smears were air-dried and stained with Leishman-Giemsa cocktail stain. Worms collected from abomasum and small intestine were preserved in normal saline for morphological identification. Worms were cleared in lactophenol and morphological parameters were studied under zoom stereomicroscope (Nikon) and measured with a calibrated micrometer eyepiece (10x).

RESULTS

Externally, carcass was thin (Fig. 1a) and visible mucous membranes were pale (Fig. 1b). Internally, subcutaneous adipose tissue was meagre. Prescapular lymph nodes were slightly enlarged (Fig. 1b). Pericardial sac contained about 50 ml pale-yellowish, thin and clear transudate (Fig. 2a). Epicardial fat was gelatinized. Epicardial vessels were accentuated and engorged with blood. Both the lungs were pale, slightly enlarged and edematous. Liver was slightly enlarged with swollen hepatic lymph nodes. Gall bladder was distended with about 200 ml greenish, thin bile. Abomasal serosa was severely congested (Fig. 2b) and mucosa was slightly congested and on the surface of it showed few brownish, tiny, thread-like live round worms (5-14 mm length). Mesentery was severely congested at its attached border. Mesenteric lymph nodes were slightly enlarged and oedematous (Fig. 2c). The serosa of the small intestine revealed many cream-coloured nodules of 5-10 mm diameter scattered in duodenum and proximal jejunum (Fig. 3a&b). Small intestinal lumen contained grayish

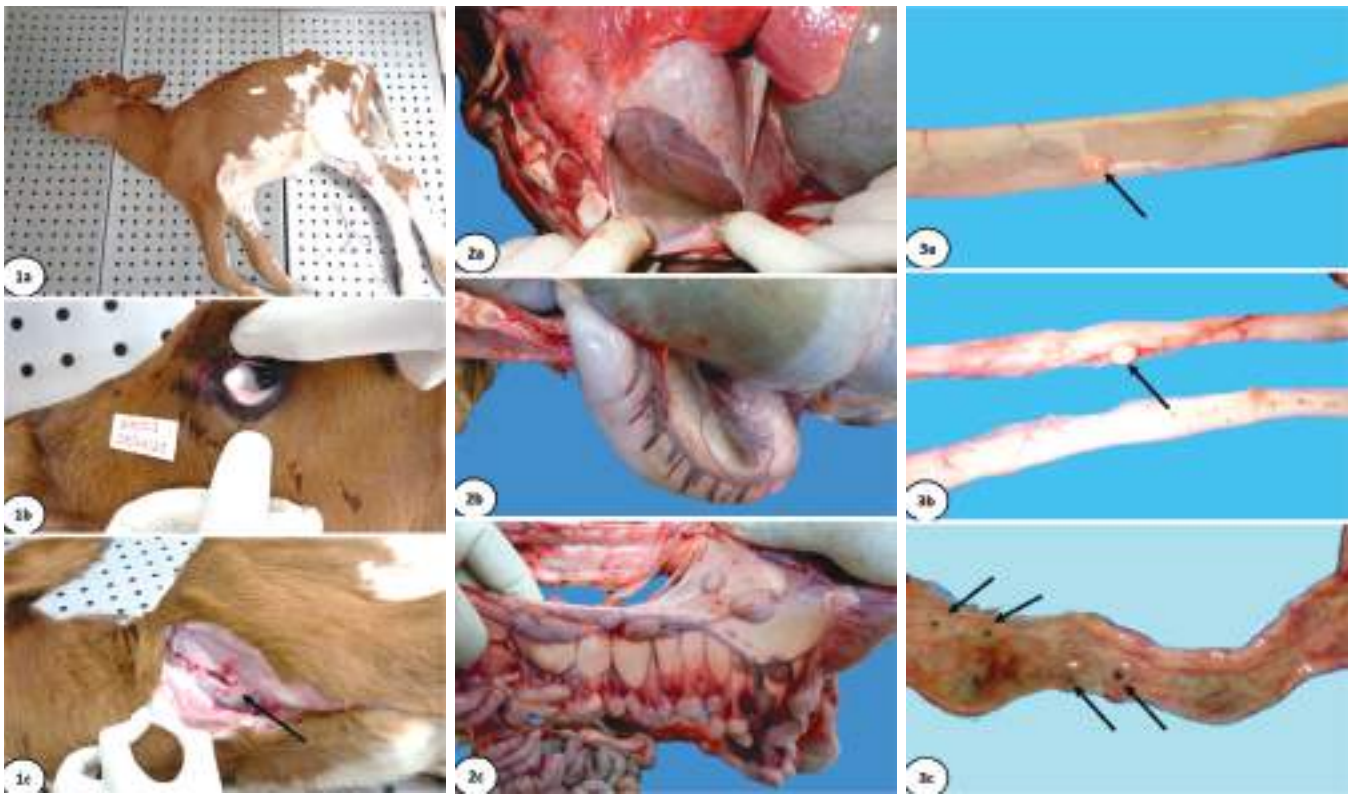

Fig. 1a-c. Thin emaciated carcass – Jersey-cross calf; Pale conjunctiva; Enlarged prescapular lymph node; **Fig. 2 a-c.** Hydropericaridum; congestion of serosa of abomasum; Enlarged mesenteric lymph nodes; **Fig. 3 a-c.** Grayish-white coloured nodule in the serosa of duodenum (3a) and jejunum (3b); Blackish-brown nodules in the mucosa of the small intestine (3c).

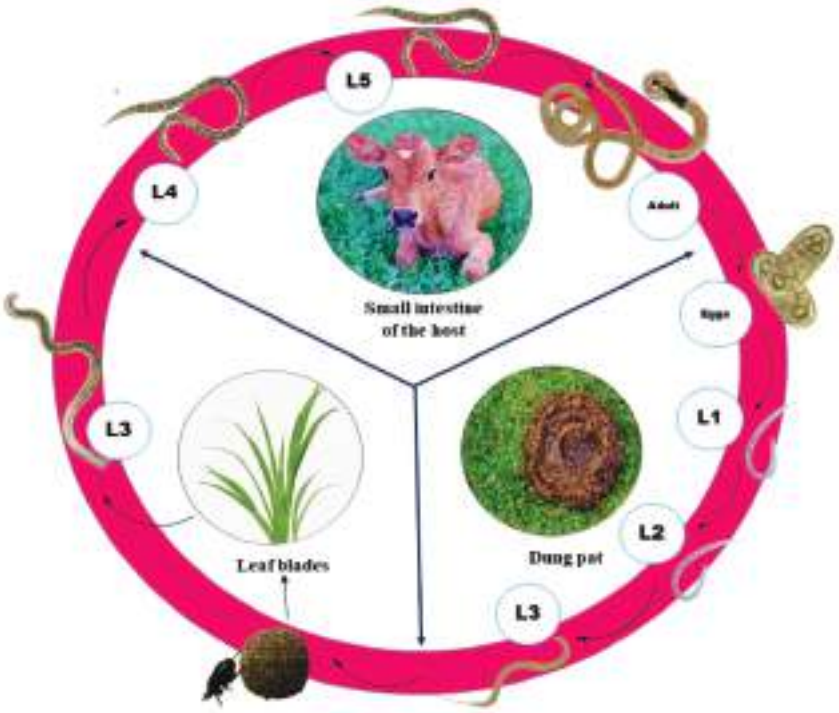

Life cycle of *Cooperia pectinata*. Adult female lays fertilized eggs in intestine which are excreted in dung. Egg hatch into L1 and transform by two moults into L2 and infective L3 in dung pat. Dung beetles disseminate eggs/infective L3 to distant places. L3 is double-sheathed infective stage, it moves to leaf blades and hibernate until ingested by cattle. Once it reaches in small intestine L3 exsheaths and moult to transform into L4 and L5. L5 matures into adult dimorphic *Cooperia pectinata* as male and female worms. Occasionally, under unfavourable environment inside the host, L4/L5 undergoes hypobiosis. Host cell-mediated immune response either disintegrate the hypobiotic larva or else it develop into adult worm once favourable conditions exist in intestine

white pasty contents smearing the mucosal surface. Mucosa was slightly congested. Mucosa of duodenum, jejunum and ileum showed multiple blackish brown slightly firm nodules of 1-5 mm diameter (Fig. 3c). Luminal surface showed multiple, brownish, tiny, thread-like live round worms (5-14 mm length). Skeletal muscles were pale and slightly dry. Meningeal vessels were slightly congested.

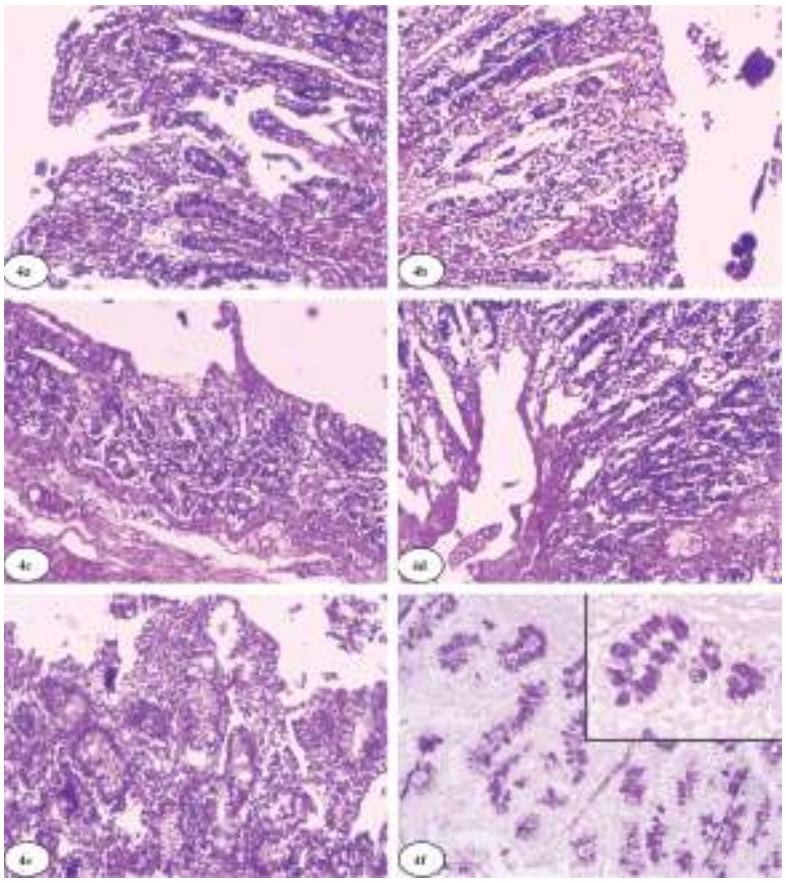

Fig. 4a&b. Widening of villi with inflammatory cell infiltration – Small intestine H&E x100; **Fig. 4c&d.** Atrophy and fusion of mucosal villi – Small intestine H&E x100; **Fig. 4e.** Goblet cell hyperplasia – Small intestine H&E x100; **Fig. 4f.** Goblet cell hyperplasia – Small intestine PAS stain x100 (inset – 400x).

Microscopically, duodenum and jejunum revealed multiple cut-sections of nematodes within the lumen. Mucosa showed subacute enteritis characterized by widening of villi with infiltration of neutrophils, eosinophils, lymphocytes and a few plasma cells (Fig. 4a&b). Mucosa also showed blunting (Fig. 4c), fusion and atrophy of villi (Fig. 4d). The small intestinal mucosa showed increased goblet cell activity (Fig. 4e). Hyperplasia of goblet cells in the mucosa under combined alcian blue-PAS technique revealed magenta coloured glycoproteins (Fig. 4f) suggestive of neural mucins. Nodular portions of serosa showed necrotic debris with cut section of nematode (Fig. 5a). Nodular portions of mucosa revealed throngs of eosinophils and a few neutrophils surrounding the nematode. Necrotic debris composed of dead cells, neutrophils, lymphocytes, plasma cells, globular leucocytes, macrophages and scattered eosinophils surrounding the disintegrated nematode section (Fig. 5b). Microscopically, the cut-section of nematode within the intestinal lumen showed cuticle with struts and around ten large cuticular

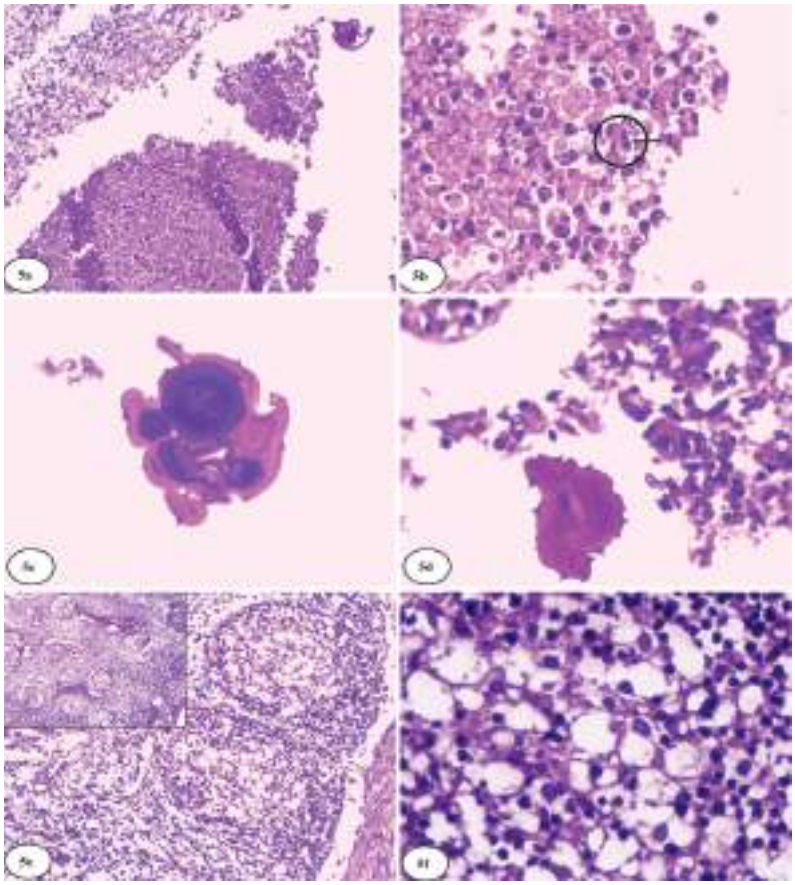

Fig. 5a. Necrosis with cut section of nematode – Serosal nodule – Small intestine H&E x100; **Fig. 5b.** Necrotic debris with throng of inflammatory cells around disintegrated nematode – Serosal nodule – Small intestine H&E x400; **Fig. 5c.** Cut-section of nematode within the intestinal lumen showing cuticle with struts and internal oesophagus H&E x400; **Fig. 5d.** Cuticular ridges showing prominent ten ridges H&E x400; **Fig. 5e.** Moderate lymphoid depletion and lymphocytolysis in prescapular and mesenteric lymph nodes H&E x100 (Inset H&E x40); **Fig. 5f.** Lymphocytolysis in mesenteric lymph node H&E x400.

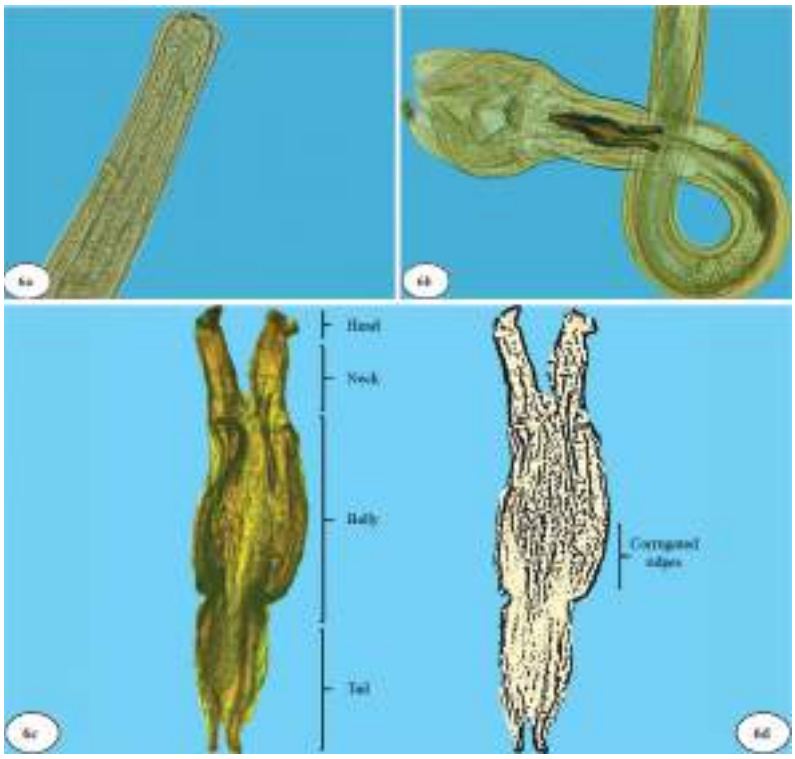

Fig. 6a. Cephalic end of male *Cooperia pectinata* x1000; **Fig. 6b.** Tail end of male *Cooperia pectinata* x1000; **Fig. 6c.** (Right): Bukly spicule of male *Cooperia pectinata* x1000; **Fig. 6d.** (Left): Sketch of edited original picture to show spicule of male *Cooperia pectinata* with well-demarcated corrugated ridges in the belly portion x1000.

ridges and internal oesophagus (Fig. 5c). Cuticular ridges were obvious in H&E section showing prominent five dorsal, five ventral and inconspicuous lateral ridges (Fig. 5d). Mesenteric lymph nodes revealed moderate lymphocytolysis whereas severe lymphoid depletion was observed in the peripheral lymph nodes (Fig. 5e&f) and hepatic lymph nodes. Liver revealed moderate vacuolar degeneration of hepatocytes.

Nematodes collected from abomasum and duodenum were identified based on the following morphological features. Head had cephalic inconspicuous cuticular swelling (Fig. 6a). Body had longitudinal cuticular striations (ridges). Male worms appeared coiled and had well-developed copulatory bursa with two lateral expansions (Fig. 6b). Copulatory bursa was symmetrical and composed of paired spicules, bursal rays and genital cone. Spicules were two, large, ornate, thick, sclerotized, stout and pigmented brown with wing-like expansion (ventral flange) at the middle having sweeping curves. It measured 340-350 μm. Spicules had short anterior head, a barrel neck, bulky belly, and a thin tail (Fig. 6c). Belly of the spicules had well-demarcated corrugated ridges (Fig. 6d). The tail was longer and occupied one-third of the total spicule length. Each spicule had a clear, thin membrane clenched to its tip. Bursal rays composed of ventral, lateral and dorsal rays. Lateral and ventral rays followed the pattern of the genus *Cooperia* spp. Anterio-ventral and posterio-ventral rays were obviously placed lateral to the bursal lobe whereas, anterio-lateral, medio-lateral and posterio-lateral rays pointed distally. The tip of the anterio-lateral rays was slightly bent and curved laterally. Dorsal rays were lyre-shaped and measured 180-190 μm. These dorsal rays were double-branched fork-like and its bifurcation was less than half of its total length. Genital cone was butterfly-

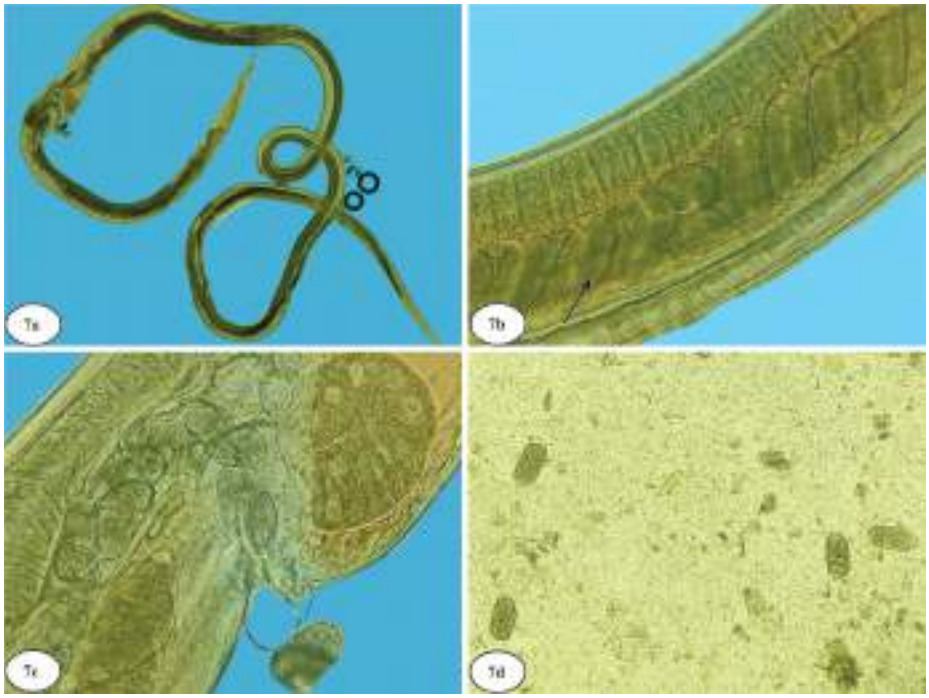

Fig. 7a. Coiled entire female, *Cooperia pectinata* x100; **Fig. 7b.** Uterus with parallelly arranged eggs of female *Cooperia pectinata* x1000; **Fig. 7c.** Vulva and ovijector of adult *female Cooperia pectinata* x1000; **Fig. 7d.** Eggs of *Cooperia pectinata* x1000

shaped situated in the middle of the bursa, a region behind the spicule. The adult females (Fig. 7a) measured 8.68-12.54 mm long and its widest part measured 200-250 mm just behind the vulva. Vagina was made of heavily cuticularized walls and vulva. Vulva had a transverse slit with prominent distinctive cuticular lips and ovijector (Fig. 7c). Ovijector was a well-developed vesicular-like structure which was distinct and stood out sharply from its main body wall. The tail end was narrow with pointed tip. Eggs were thin-shelled, cylindrical with rounded edges and parallel walls (Fig. 7d). Eggs had divided multiple yolks. These morphological features were consistent with *Cooperia pectinata*.

Cytological examination of blood smear revealed hypochromasia of erythrocytes, numerous Howell-Jolly bodies and stray *Anaplasma* spp.

DISCUSSION

Genus *Cooperia*

Nematodes of Tricho-strongylidae are gastrointestinal parasitic roundworms notably important in veterinary science. The family trichostrongylidae enclose the nematodes of genus *Trichostrongylus* spp., *Haemonchus* spp., *Ostertagia* spp., *Nematodirus* spp., *Cooperia* spp., *Mecistocirrus* spp. and *Hyostrongylus* spp. The genus *Trichostrongylus*, *Haemonchus*, *Ostertagia* reside in abomasum whereas genus *Cooperia* and *Nematodirus* reside in the anterior part of the small intestine (duodenum and jejunum). Among all, the genus *Haemonchus contortus* was found to be a highly pathogenic blood sucking nematode with high morbidity and mortality due to severe anaemia in ruminants[16].

The genus *Cooperia* contains thirty-four accepted species[4] of which, 19 valid species are of veterinary importance that parasitize gastro-intestine of both domestic and wild ruminants[5]. Four species such as *C. oncophora*, *C. pectinata*, *C punctata* and *C. spatulata* are found to parasitize cattle[4].

Cooperia spp. are gastro-intestinal lumen-dwelling parasites of ruminants, recovered from abomasum and small intestine but frequently from upper third of small intestine to be more precise. *Cooperia pectinata* and *C. punctata* are reported to be pathogenic whereas *C. oncophora* and *C. spatulata* are non-pathogenic[17]. The reason

Table 1. Average measurement of L4 and L5 of *Cooperia pectinata* (Anderson, 1986)

Sl. No.	Measurement parameters	L4		L5	
		Male	Female	Male	Female
1.	Total length (mm)	3.1-4.1	3.8-6.0	4.0-5.8	8.4-9.0
2.	Length of oesophagus (μm)	320-380	340-390	410	420
3.	Distance between excretory pore to anterior end (μm)	280-360	300-380	390	
4.	Distance between vulval opening to tail (μm)	-	610-970	-	1110
5.	Length of spicules (μm)	170-190	-	240-283	-
6.	Distance between anus to tail (μm)	-	120-170	-	180

thereof, former being the nematodes which burrow into the intestinal mucosa, but latter remain on the mucosal surface[2]. Nematodiasis by *C. pectinata* and *C. punctata* caused decreased feed intake and enteritis and an out-turn, decreased live weight gain, growth rate and mortalities when slew of *Cooperia* parasitized in younger animals such as calves[3,17].

Distribution

Cooperia spp. are distributed world-wide and its abundance is influenced by climatic conditions particularly rainfall and temperature. *C. oncophora* is abundant in temperate countries like Europe and Australia whereas *C. pectinata*, *C. punctata* and *C. spatulata* are prevalent in tropical and subtropical regions of the world[4]. Although it was not new, the occurrence of *Cooperia* spp. was rarely reported from Northern India and particularly scarce from southern India. In the distant past, the occurrence of *C. pectinata* and *C. punctata* from cattle in Madras was reported by Rao during the year 1940[13]. This was thought to be the first documented evidence on cooperiasis in ruminants. Later in the same decade down-the-road, these parasites were found to be the commonest trichostrongylid nematodes of cattle in the Kumaon hills of Uttarakhand (previously in Uttar Pradesh)[18]. Thereafter, the incidence of *Cooperia* spp. in animals was occasionally documented from India. It was found to be 17.77% in Tho-Tho indigenous cattle and cross-bred cattle of Nagaland[11,19]. The prevalence of *Cooperia* spp. was reported by coproculture in cattle (10.54%) and buffalo (0.92%) from Guwahati, Assam[12]. The fragmentary evidences on occurrence of *Cooperia* spp. in India elicits deficient reporting. More recently, sampling survey in the Sirmaur district of Himachal Pradesh of Northern India revealed 30%, 35%, 60% and 40% prevalence of *Cooperia* spp. in cattle, buffalo, goat and sheep, respectively by copromicroscopy of fecal samples[1]. Following the pause later 1940, the present reports records the occurrence of *C. pectinata* in calves in Thanjavur district, Tamil Nadu. This report registers the first descriptive evidence on morphology and pathology of *Cooperia pectinata* in calves.

Definitive host

The *C. pectinata* was found to hanger-on both domestic and wild ruminants. *Cooperia pectinata* are monoxenous parasite and even so, it was reported from cattle[13,20], sheep[18,20] and red deer[10].

Life cycle

Cooperia spp. are dimorphic parasite with direct life cycle having free-living pre-parasitic larval phases[5]. The mature female nematode in the small intestinal lumen lays thin-shelled eggs containing 16 cells yolk mass and voided in the host faeces or dung[5,21]. Under optimal conditions, first stage larva (L1) hatch out in the dung pat. Molting continues through second stage (L2) larva into infective third stage (L3) larva. Third stage larva was protected by two layers of cuticle (retention of cuticular sheath of second stage larva) and ardently climb up to grass blades to be taken up by the definitive host of ruminants[22]. The egg to L3 occurs in dung on pasture and its rate of development was temperature-dependent and approximately takes 1- to 6-weeks duration[23]. L3 larva survives for up to one year until swallowed by a definitive host. Contaminated dung remaining on the surface of pastures serve as reservoir for parasitic larva (Fincher and Stewart, 1979). It was proved that *Cooperia* larva travelled up to the maximum of 25 cm from dung pat[24]. The dung beetles were found to abet the dissemination of eggs or larva faraway by forming fecal balls which were rolled away from the dung pat[24].

Once in the gastro-intestinal tract, L3 larva exsheaths and undergoes further two molts as L4 and L5 to become mature adult of male and female worms[25,26]. The average measurement of L4 and L5 have been described earlier by Anderson (1986)[6] (Table 1). On an average, L4 male measures 3.1-4.1 mm and female measures 3.8-6.0 mm of total length whereas L5 male measures 4.0-5.8 mm and female measures 8.4-9.0 mm of total length[27]. The cycle continues when the fertilized female starts to lays eggs. Nevertheless, under adverse conditions, a deviation in life cycle occurs where L4 or L5 undergoes developmental arrest (hypobiosis) in the intestinal mucosa for up to several months[25,26]. The statement was in agreement with the present study where scattered mucosal and serosal nodules were noticed in the small intestine and histologically each nodule revealed inflammatory reaction around the cut section of the early adult nematode, probably L5. Larval migration in to the deep intestinal tissue observed in the present study was in accord with the findings of[25] who reported the *Cooperia* larva in the lamina propria of the intestine. After slumber, L5 develop into adult male and or female in the lumen of the gastro-intestinal tract.

Morphology and identification of *C. pectinata*

Adult parasite is identified by its morphological features of the male and female worms. Albeit a traditional diagnostic technique, it was found to be worthwhile for prompt identification from the former times as compared to recent newer advanced techniques. It was proposed that the most precise approach for morphological identification and species differentiation of adult worms of Trichostrongylidae immediate after necropsy were a) the morphology and morphometry of the spicule, b) arrangements of dorsal rays, c) morphology of genital cone and d) cephalic vesicle and e) the synlophe morphology (cuticular ridges)[4,28]. Infrequently, the shape of the dorsal rays of bursa have also been used[5,29]. Among pathogenic *Cooperia* spp., *C. pectinata* has been found to have larger and bulky spicule[4,5]. The spicule measured

about 220-390 µm which was comparatively larger than spicule of *C. punctata* (125-214 µm). Spicule of *C. pectinata* was differentiated by the presence of prominent corrugated ventral flange in the middle third (bulky belly)[4,20]. Adult male was 5.10 mm whereas adult female was 5.74 mm in length after an average measurement of 10 largest specimens in *in vitro* studies from calves[30]. Previously, Herlich (1965)[27] registered that the average measurement (length) of C. *pectinata* recovered from calves were 7.22 mm and 9.48 mm for male and female, respectively. These statements suggested that *C. pectinata* was quite larger when compared to *C. punctata*[4]. Previous workers[5,20,31] have documented that the cephalic vesicle at the anterior end of *Cooperia pectinata* was inconspicuous (with minimal expansion) when compared with broad (cephalic vesicle) of *C. punctate*. The same was convincible in the present study. Morphology of genital cone and dorsal rays observed in the present case was in accordance with Albrechtova and co-workers (2024)[5].

Female worms are not used to differentiate species, yet morphology of female genitalia unquestionably enable to identify the genus of Trichostrongylidae and trivial details support to confirm the species of *Cooperia*[32]. Adult female of *C. pectinata* is distinguished based on the anatomy of the vagina. The vagina is skeletal with transversely elongated vulva and ovijector. Vulva is composed of two heavily cuticularized walls situated just within the vaginal opening[9] and distinct posterior lip which stand out sharply from the main body[20]. The prominent and projecting vesicular posterior lip is labeled as ovijector[5,30]. Eggs of *C. pectinata* are ovoid to ellipsoid with nearly alike poles and straight and parallel sides. Eggs are thin-shelled surrounding the light brown cellular mass[1,21]. The average width is 34-36 µm and the length is 75-79 µm[1,33]. Eggs with the character of parallelism specific for genus *Cooperia* spp. observed in the present study was analogous with the above earlier illustration. Shorb (1938)[33] documented that the *C. pectinata* egg measured 72.7 (67-80) µm in length, 34.5 (31-38) µm width and had shell thickness of 1.4 µm.

Furthermore, *Cooperia* spp. was identified with supplementary features particularly the distribution and arrangement of longitudinal ridges present in the cuticle[34]. *Cooperia* spp. composed of 10 large ridges and four small ridges. Cuticular ridges were distributed as five large dorsal ridges, five large ventral ridges and short and small, a pair of lateral ridges on each side. *C. pectinata* was found to have closed pattern of cuticular ridge arrangement at the cervical region exhibiting small lateral ridges anterior to the level of excretory pore and cervical papilla[6,20]. The distribution of struts and cuticular ridge arrangement observed in the present investigation by histo-morphology of nematodes in intestine was in parallel with the above earlier description. The cuticular longitudinal ridge parameter also served as a supporting characteristic alongside the male spicule and female vulval traits of C. pectinata. The male and female morphology featured in the present study assured that the Trichostrongylidae worm was *Cooperia pectinata* keeping unwavering faith with the above earlier documented evidences.

Pathology

It was suggested that *C. pectinata* resides both in abomasum and small intestine, but latter being the most common predilection site[7]. Adults penetrate and induce substantial damages in the mucosa. Massive worm load caused severe catarrhal enteritis which hampered growth rate and appetite in calves[25]. Histopathological observation of the present study coincides with the earlier reports[2,8,17,25]. The adult nematodes within the lumen and deep into the mucosa produces the tissue alterations. Alteration in the mucosal barrier causes protein-losing enteropathy and catarrhal enteritis characterized by mucosal thickening, hyperplasia of goblet cells, broadening and fusion of mucosal villi, denudation of mucosal epithelial cells are found to be consistent feature of Cooperiasis[8,25] and were in parallel with the present report in a calf. Vascular congestion, marked infiltration of eosinophils, neutrophils, lymphocytes and plasma cells, appearance of globular leucocytes in the mucosa authenticate the cellular immune response of the host[8]. Depletion of lymphocytes and lymphocytolysis of lymph nodes and goblet cell hyperplasia of the small intestine observed in the present investigation testament the cellular and innate immune reaction towards the worm. The statement was in accordance with Stromberg and co-workers (2011)[2] who reported mesenteric lymphadenomegaly in *Cooperia punctata* infected calves.

Pathology induced by *C. pectinata* was found to be alarming in cattle especially in calves by two ways 1) it penetrates the mucosal epithelium of small intestine and 2) influence phosphorus kinetics and reduce phosphorus absorption and retention. Penetration into the intestinal epithelium disturbs the mucosal barrier by inducing defect in epithelial integrity, damage to the epithelial cells, mucosal irritation due to the movement and secretory products of parasite and provoke immune mediated damage to intestinal stromal cells[4,8,35]. These above reactions cause severe catarrhal enteritis, promote gastrointestinal fluid loss with subsequent malabsorption of micronutrients and resulted in loss of weight gain. Disturbance in phosphorus uptake leads to hypophosphatemia. Emaciation with extreme wasting of skeletal musculature, diarrhoea, hypoproteinaemia, subcutaneous oedema (mostly submandibular), anaemia and death are the tandem effects and outcome of *C. pectinata* infection in ruminants[2,3,35,36]. The above mechanism was plausible with the present investigation

regarding the clinico-pathological changes observed in a calf infected with *C. pectinata*. Pale conjunctival mucous membrane, hypochromasia of erythrocytes and appearance of Howell-Jolly bodies in peripheral blood smear in the present study supports that the animal suffered with anaemia. Besides, hydropericardium, goblet cell hyperplasia of proximal small intestine corroborated with protein-losing enteropathy (hypoproteinaemia), catarrhal enteritis and emaciation in the present investigation. To sum up, the proclivity of the *Cooperia pectinata* to the host was the reason for pathological changes observed in the current study. Altogether, *Cooperia pectinata* was the etiological agent responsible for the mortality in a calf in the present study .

Immunity

As was foreseeable, parasites avoid host defense to establish themselves in the intestine. It has been proposed that the Trichostrongylidae nematodes produce endogenous allergen, the aspartyl inhibitor (API-1). These allergens are presented to T-helper cell (CD4+) by antigen presenting cells followed by initiation of T-2 response by the host by releasing interleukins (IL) such as IL4, 5, 9, 13, 21, 33 and proliferation of plasma cells. The ILs activate mast cells and eosinophils to degrade the parasite[35]. Activation of plasma cells produce allergen-specific immunoglobulin E (IgE) which cause mast cell degranulation, activate eosinophils by binding with Fab (fragment antigen binding) region and immobilize and kill the parasite by binding with its Fc (Fragment crystallizable) region of IgE. Apart from the above, the damaged intestinal epithelial cells release IL33, which directly bind with ST2 receptors of eosinophils and mast cells to release major basic protein, free-radicals and vasoactive amines, respectively[35,37]. The amines facilitate recruitment of defense cells from vasculature and eliminate the parasite[8,35]. The appearance of tissue necrosis together with infiltration of eosinophils, neutrophils, lymphocytes, macrophages around the degraded nematode in the intestinal nodule substantiates the solid immune response to eliminate the nematode. Probably, the above elaborated mechanism postulated earlier was conceivable with the nodular lesions described in the present study.

Role of molecular diagnosis

Recent advances in molecular techniques showed keen interest to deepen the knowledge on species differentiation with irrefutable confirmation. In a recent study at Germany, *Cooperia* species has been subjected to genome sequence comparison. Partial sequence analysis of two mitochondrial genes, cytochrome oxidase 2 (*cox*2) and 12S rRNA and two nuclear genes, isotype 1 β tubulin and internal transcribed spacers (ITS-2) of four *Cooperia* species viz., *C. pectinata*, *C. punctata*, *C. spatulata* and *C. oncophora* have been studied. Multi-locus phylogenetic analysis conducted by keeping *Haemonchus contortus* as out group for all four *Cooperia* species infecting cattle revealed separate cluster of *C. pectinata* which was located at a more basal position where as *C. oncophora* occupied sister position to the cluster containing *C. punctata* and *C. spatulata*. Further *C. punctata* and *C. spatulata* did not cluster with each other[4]. The analysis concluded that species identified based on phylogenetic analysis revealed no differences on par with morphological differentiation. In contrary, phylogenetic analysis of *cox*2 gene and the ITS1-5, 8S-ITS2 of *Cooperia* species that were morphologically identified as *C. pectinata* in red deer and sika deer revealed the presence of distinct independent lineage forming a sister clade to *C. oncophora*. These above results indicated that the parasite does not belong to the *C. pectinata* parasitizing cattle and was therefore renamed as *Cooperia ventricosa*[5]. Even though, morphological similarities were observed with a few structural deviations, the molecular studies concluded that *Cooperia pectinata* was a monoxenous parasite typically found to occur in cattle[5]. Long ago, in 1981 a report of *C. pectinata* recorded from red deer in New Zealand[10] was probably the *C. ventricosa*[5]. What-so-ever, morphological features of *Cooperia* spp. are still found to be the standard rather traditional method with certainty to differentiate *Cooperia* species affecting cattle when molecular studies were unachievable. This study exemplar to be one in such circumstances.

Anthelmintic resistance

An extensive usage of macrocyclic lactone for the treatment and or to control gastro-intestinal nematodiasis contributed to drug resistance in recent years especially in ruminants[38]. Further, the repercussions of climate change and life cycle traits (pre-adult, adult, hypobiosis and the female fecundity) of the parasites added-up the resistance to thrive in the host[39]. The impact of these might change the parasitic disease pattern in the coming decades and hamper health, welfare and productive economy of ruminants. To avoid parasitic resilience, polyphenolic compounds have been used to establish effective control strategies[40]. Polyphenolic compounds such as quercetin, caffeic acid, rutin and coumarin have been used in combinations as bioactive (caffeic acid and coumarin) with non-bioactive (quercetin and rutin) molecules in the 8:2 ratio mixture. It has been proved that these combinations exhibited synergistic activity with ovicidal property and inhibition of exsheathment of L3 of *C. punctata*. It has been suggested that the hydroxylation of these above polyphenolic compounds resulted in cuticular damage and thereby exerted blockage of exsheathment of infective L3 larva[40]. More recently, von San-de Fernex *et al.,* (2023)[31] studied the anthelminthic activity of above two polyphenolic combinations against larval and adult stages of *Cooperia punctata* by *in vitro*

studies. It was postulated that dual combinations such as 1) coumarin:quercetin and 2) caffeic acid:rutin were found to affect motility of both infective larvae and adult worms. It was concluded that the above two polyphenolic combinations damaged the collagen and muscular layer of adult worms and caused muscular contraction, cuticular collapse, loss of turgor pressure and cellular damage[31]. Similar polyphenolic formulations could be used with different dilutions and could be combined with other regional herbs for effective control of sturdy parasites such as *C. pectinata* and other gastro-intestinal nematodes to avoid drug resistance.

CONCLUSIONS

The *Trichostrongylidae* nematode, *Cooperia pectinata* is a pathogenic parasite in cattle especially for calves. The parasitic larval stages are much more pathogenic as it penetrates deep into the mucosa forming muco-serosal nodules (hypobiosis) and destruction of mucosal epithelial cells. The change in the intestinal phosphorus kinetics and increased luminal plasma loss lead to diarrhea, hypoproteinaemia, anaemia, emaciation and death. The paper documents the first descriptive evidence on occurrence and pathology of *C. pectinata* in calves from southern India along with a detailed review on the genus *Cooperia*.

ACKNOWLEDGEMENTS

The authors thank the Dean, Veterinary College and Research Institute, Orathanadu, Thanjavur, Tamil Nadu and Tamil Nadu Veterinary and Animal Sciences University, Madhavaram Milk Colony, Chennai-51, Tamil Nadu, India for the facilities.

Financial support & sponsorship: None

Conflicts of Interest: None

Use of Artificial Intelligence (AI)-Assisted Technology for manuscript preparation: The authors confirm that there was no use of AI-assisted technology for assisting in the writing of the manuscript and no images were manipulated using AI.

REFERENCES

1. Sharma A, Sharma S, Kour S, Avatsingh AU, Perveen K, Alsulami JA, Singh N. 2023. Gastrointestinal nematodes and protozoa in small and large ruminants from rural agro-climatic regions of northern India. *Diversity* **15(11):** 1131.
2. Stromberg BE, Gasbarre LC, Waite A, Bechtol DT, Brown MS, Robinson NA, Olson EJ, Newcomb H. 2012. *Cooperia punctate*: Effect on cattle productivity? *Vet Parasitol* **183(3-4):** 284-291.
3. Hosseinnezhad H, Sharifdini M, Ashrafi K, Atrkar Roushan Z, Mirjalali H and Rahmati B. 2021. Trichostrongyloid nematodes in ruminants of northern Iran: prevalence and molecular analysis. *BMC Vet Res* **17(1):** 371.
4. Ramunke S, de Almeida Borges F, von Son-de Fernex E, von Samson-Himmelstjerna G, Krucken J. 2018. Molecular marker sequences of cattle *Cooperia* species identify *Cooperia spatulata* as a morphotype of *Cooperia punctata*. *PLoS One* **13(7):** e0200390.
5. Albrechtova M, Kasparova E, Langrova I, Hart V, Neuhaus B, Jankovska I, Petrtyl M, Magdalek J, Spakulova M. 2024. A revision of the trichostrongylid nematode Cooperia Ransom, 1907, from deer game: recent integrative research confirms the existence of the ancient host-specific species *Cooperia ventricosa* (Rudolphi, 1809). *Front Vet Sci* **11:**1346417.
6. Anderson IG. 1986. Observations on the life-cycle and larval morphogenesis of *Cooperia fuelleborni* (Nematoda: Trichostrongyloidea) parasitic in impala, *Aepyceros melampus*. *J Helminthol* **60(2):** 113-122.
7. Chollet JY, Jacquiet P, Cardinalem E, Ndamkou-Ndamkou C, Diop C, Thiam A, Dorchies P. 2000. *Cooperia pectinata* and *C. punctata*, parasites of the abomasum of cattle in Northern Cameroon (Central Africa). *Vet Parasitol* **88(1-2):** 135-138.
8. Rodrigues RR, Gennari SM, Guerra JL, Contieri MB, Abdalla AL, Vitti DM. 2004. Histopathological changes during experimental infections of calves with *Cooperia punctata*. *J Helminthol* **78(2):** 167-171.
9. Isenstein RS. 1971. Hybridization of two species of nematodes parasitic in ruminants, *Cooperia oncophora* (Railliet, 1898) Ransom, 1907, and *Cooperia pectinata* Ransom, 1907. *J Parasitol* **57(2):** 320-326.
10. McKenna PB, Charleston WAG, Hughes PL. 1981. *Cooperia pectinata* (Nematoda: Trichostrongylidae) in New Zealand. *N Z Vet J* **29(3):** 26-27.
11. Das M and Laha R. 2017. Parasitic infections of cattle in north Eastern region of India - An overview. *Arch Parasitol* **1(1):**107.
12. Das M and Deka DK. 2019. Prevalence of nematode larvae in cattle and buffalo of Guwahati, Assam. *IJHF* **32(1):** 144-151.
13. Rao MAN. 1940. On some worms of the genera Trichostrongylus Looss, 1905, and Cooperia Ransom, 1907, in south India. *Indian Vet J* **16:** 306-311.
14. Bancroft JD, Layton C. 2019. The hematoxylins and eosin. In: Suvarna SK, Layton C, Bancroft JD, eds, Bancroft's Theory and practice of histological techniques. China: Elsevier. 126-137.
15. Layton C, Bancroft JD. 2019. Carbohydrates. In: Suvarna SK, Layton C, Bancroft JD, eds, Bancroft's Theory and practice of histological techniques. China: Elsevier. 176-197.
16. Besier RB, Kahn LP, Sargison ND, Van Wyk JA. 2016. Diagnosis, treatment and management of *Haemonchus contortus* in small ruminants. *Adv Parasitol* **93:**181-238.
17. Coop RL, Sykes A, Angus K. 1979. The pathogenicity of daily intakes of *Cooperia oncophora* larvae in growing calves. *Vet Parasitol* **5:** 261-269.
18. Sarwar MM. 1945. ed. Incidence of some nematodes of domestic ruminants in the Punjab and United provinces with a note on the morphology of *Trichuris globulosa* (V. Linstow). Proceedings of the Indian Academy of Sciences; 1945; Nov 274-278; New Delhi: Springer India.
19. Chamuah JK and Borkotoky D. 2014. Comparative study of occurrence of gastrointestinal parasites in Tho-Tho and cross bred cattle of Nagaland. *Indian J Hill Farm* **27:** 52-53.
20. Lichtenfels JR. 1977. Differences in cuticular ridges among Cooperia spp. of North American ruminants with an illustrated key to species. Proceedings of the helminthological society of Washington; 44(2): 111-119.
21. Stewart TB. 1954. The life history of *Cooperia punctata*, a nematode parasitic in cattle. *J Parasitol* **40(3):** 321-327.
22. Kellerova P, Navratilova M, Nguyen LT, Dimunova D, Raisova Stuchlíkova L, Sterbova K, Skalova L, Matouskova P 2020. UDP-glycosyltransferases and albendazole metabolism in

the juvenile stages of *Haemonchus contortus*. *Front. Physiol* **11:** 594116.
23. Fiel CA, Fernandez AS, Rodriguez EM, Fuse LA, Steffan PE. 2012. Observations on the free-living stages of cattle gastrointestinal nematodes. *Vet Parasitol* **187:** 217-26.
24. Fincher GT, Stewart TB. 1979. Vertical migration by nematode larvae of cattle parasites through soil. Proceedings of Helminthological society of Washington; **46(1):** 43-46.
25. Armour J and Duncan M. 1987. Arrested larval development in cattle nematodes. *Parasitol Today* **3(6):** 171-176.
26. Vlaar LE, Bertran A, Rahimi M, Dong L, Kammenga JE, Helder J, Goverse A, Bouwmeester HJ. 2021. On the role of dauer in the adaptation of nematodes to a parasitic lifestyle. *Parasit Vect* **14:** 554.
27. Herlich H. 1965. The development of *Cooperia pectinata*, a nematode parasite of cattle. *Am J Vet Res* **26(114):** 1026-1031.
28. Gibbons LM. 1981. Revision of the African species of the genus Cooperia, Ransom, 1907 (nematode, trichostrongylidae). *Syst Parasitol* **2(4):** 219-252.
29. Durette-Desset MC. 1974. Keys to genera of the superfamily Trichostrongyloidea. No. 10. In: Anderson RC, Chabaud AG, Willmott S, eds, CIH Keys to the Nematode Parasites of Vertebrates. Farnham Royal, Bucks: Commonwealth Agricultural Bureaux. 1-85.
30. Leland Jr SE. 1967. The *in-vitro* development of *Cooperia pectinata*, a nematode parasite of cattle, from third-stage larvae to adults, including egg production. *J Parasitol* **53(3):** 630-633.
31. von Son-de Fernex E, Zuniga-Olivos E, Jiménez-García LF, Mendoza-de Gives P. 2023. Anthelmintic-Like Activity and ultrastructure changes produced by two polyphenolic combinations against *Cooperia punctata* adult worms and infective larvae. *Pathogens* **12:** 744
32. Gonzalez-GarduñoI R, Martínez FN, Arece-García J. 2014. Presence of *Cooperia curticei*, *C. punctata* and *Trichostrongylus colubriformis*, (Strongylida: Trichostrongylidae) in Tabasco, Mexico. *Rev Salud Anim* **36(3):** 159-163.
33. Shorb DA. 1939. Differentiation of eggs of various genera of nematodes parasitic in domestic ruminants in the United States. Tech Bull No. 694, United State Department of Agriculture; Washington D.C.,1-11.
34. Singh J. 2012. A study on the structure and distribution of ridges in the cuticle of *Haemonchus contortus* (Rudolphi, 1803) Cobb, 1898. *J Bio Innov* **1(6):** 264-275.
35. Bhat AH, Tak H, Malik IM, Ganai BA, Zehbi N. 2023. Trichostrongylosis: a zoonotic disease of small ruminants. *J Helminthol* **97:** e26.
36. Barker IK. 1975. Intestinal pathology associated with *Trichostrongylus colubriformis* infection in sheep: histology. *Parasitol* **70(2):** 165-171.
37. Frankena K. 1987. The interaction between *Cooperi*a spp. and *Ostertagia* spp. (Nematode: Trichostrongylidae) in cattle (dissertation). Marijkeweg, The Netherlands: The Agricultural University Wageningen.
38. Gasbarre LC, Smith LL, Lichtenfels JR, Pilitt PA. 2009. The identification of cattle nematode parasites resistant to multiple classes of anthelmintic in a commercial cattle population in the US. *Vet Parasitol* **166(3-4):** 281-285.
39. Verschave SH, Rose H, Morgan ER, Claerebout E, Vercruysse J, Charlier J. 2016. Modelling *Cooperia oncophora*: Quantification of key parameters in the parasitic phase. *Vet Parasitol* **223:** 111-114.
40. Escareno-Diaz S, Alonso-Diaz MA, Mendoza de Gives P, Castillo-Gallegos E, von Son-de Fernex E. 2019. Anthelmintic-like activity of polyphenolic compounds and their interactions against the cattle nematode *Cooperia punctata*. *Vet Parasitol* **274:** 108909.

Indian J. Vet. Pathol., 50(3) : 214-217, 2026: DOI: https://doi.org/10.56093/y5k9xp10

RESEARCH ARTICLE

Amyloidosis in lymphoid organs of buffaloes

T. Mounica*, P. Amaravathi, A. Anand Kumar and W. Deepti Swapna Latha[1]
Department of Veterinary Pathology, College of Veterinary Science, Sri Venkateswara Veterinary University, Tirupati, Andhra Pradesh
[1]Department of Veterinary Parasitology

***Address of correspondence**
Dr. T. Mounica; PG Scholar, E-mail: mounicatankasala@gmail.com
ORCID ID: 0009-0005-6465-3566

Received: 18.3.26; Accepted: 9.4.26

ABSTRACT

A total of 50 spleens and 250 lymph nodes collected from buffaloes were examined, in which amyloid deposition was identified in 3 spleens and 144 lymph nodes, included 30 prescapular, 38 prefemoral, 29 hepatic, 23 mesenteric and 24 bronchial lymph nodes. Cytological examination revealed the presence of amorphous, homogenous, extracellular material suggestive of amyloid along with associated cellular changes. Histopathological examination demonstrated eosinophilic, amorphous extracellular deposits within the lymphoid tissues, lead to partial distortion of the normal architecture of the affected organs. The findings of the present study indicated that increased occurrence of amyloidosis in the lymphoid organs of buffaloes and highlighting the significance of cytological and histopathological techniques in the detection of this condition.

Keywords: Amyloidosis, Buffaloes, Cytology, Histopathology, Lymphoid organs

INTRODUCTION

Amyloidosis is a pathological condition characterized by extracellular deposition of insoluble fibrillar proteins known as amyloid in various tissues and organs. These amyloid fibrils are composed of misfolded protein subunits arranged in a Beta-pleated sheet configuration, which accumulate in the extracellular spaces and disrupt normal tissue architecture and function[1,2]. Depending upon the distribution of amyloid deposits, the condition may occur as localized or systemic amyloidosis.

Amyloidosis was reported in a wide range of animal species viz., cattle, buffaloes, dogs, cats and birds, affecting organs such as the liver, spleen, kidneys and lymph nodes[2,3]. Deposition of amyloid within these organs may leading to compression and atrophy of adjacent cells and ultimately impair organ function. Lymphoid organs such as the spleen and lymph nodes play a critical role in immune responses and are frequently examined during pathological investigations. Amyloid deposition in these tissues may alter the normal lymphoid architecture and interfere with immunological functions[2]. Although amyloidosis was documented in several organs of animals, reports describing its occurrence in lymphoid tissues of buffaloes were limited.

Therefore, the present study was undertaken to investigate the occurrence of amyloidosis in the lymphoid organs of buffaloes through cytological and histopathological examination.

MATERIALS AND METHODS

A total of 50 spleens and 250 lymph nodes including prescapular, prefemoral, hepatic, mesenteric, bronchial lymph nodes were collected from buffaloes slaughtered in slaughterhouses in and around Tirupati and examined for the present study with approval obtained from the Institutional Animal Ethics Committee (IAEC) wide no: - 281/ go/ ReBi/ S/ 2000/ CPCSEA/ CVSc/ TPTY/ 047/ Veterinary Pathology/ 2025 dated: 02-08-2025.

How to cite this article : Mounica, T., Amaravathi, P., Kumar, A.A. and Latha, W.D.S. 2026. Amyloidosis in lymphoid organs of buffaloes. Indian J. Vet. Pathol., 50(3) : 214-217.

The impression smears were prepared from the collected spleens and lymph node samples using standard preparation techniques. The air-dried smears were stained with Wright's stain and Leishman's stain and examined under a light microscope[4].

Representative tissue samples of spleen and lymph nodes were fixed in 10% neutral buffered formalin, processed by routine paraffin embedding technique, and sections of approximately 4-5 microns thickness were prepared using a rotary microtome. The sections were stained with hematoxylin and eosin (H&E) for routine histopathological examination[4,5].

To confirm the presence of amyloid, selected tissue sections were subjected to Congo red and

crystal violet staining techniques. The stained sections were examined microscopically for characteristic staining reactions indicative of amyloid deposition[4,6].

RESULTS

Histopathological sections revealed amyloid deposition in 3 (6%) out of 50 spleens and 144 (57.6%) out of 250 lymph nodes examined. The overall occurrence of amyloidosis in the present study was 49% of lymphoid organs of buffaloes (Table.1).

Cytological smears of spleen and lymph nodes revealed the presence of amorphous, homogenous, extracellular material suggestive of amyloid. The material appeared as pale to eosinophilic, structureless deposits distributed among the cellular elements of the lymphoid tissue (Fig.1).

In the spleen, amyloid deposits were observed as extracellular, eosinophilic, amorphous and hyalinized deposits within the capsule (Fig.2), red pulp and were distributed around the sheathed arteries. In addition deposition of amyloid was also noted in the capsule and trabeculae, resulting in partial alteration of the normal splenic architecture.

Among the lymph nodes examined, amyloid deposition was recorded in 30 (60%) prescapular, 38 (76%) prefemoral, 29 (58%) hepatic, 23 (46%) mesenteric and 24 (48%) bronchial lymph nodes. Histologically, the deposits were observed in the hilus, around blood vessels (Fig.3), lymphatic vessels and, lymphoid follicles (Fig.4).

Table.1. Distribution of amyloid deposition in spleen and lymph nodes of buffaloes

	Lymphoid tissues	Number of organs examined	Number of positive cases	Percentage (%)
1.	Spleen	50	3	6.0
2.	Prescapular lymph node	50	30	60.0
3.	Prefemoral lymph node	50	38	76.0
4.	Hepatic lymph node	50	29	58.0
5.	Mesenteric lymph node	50	23	46.0
6.	Bronchial lymph node	50	24	48.0
	Total	**300**	**147**	**49.0**

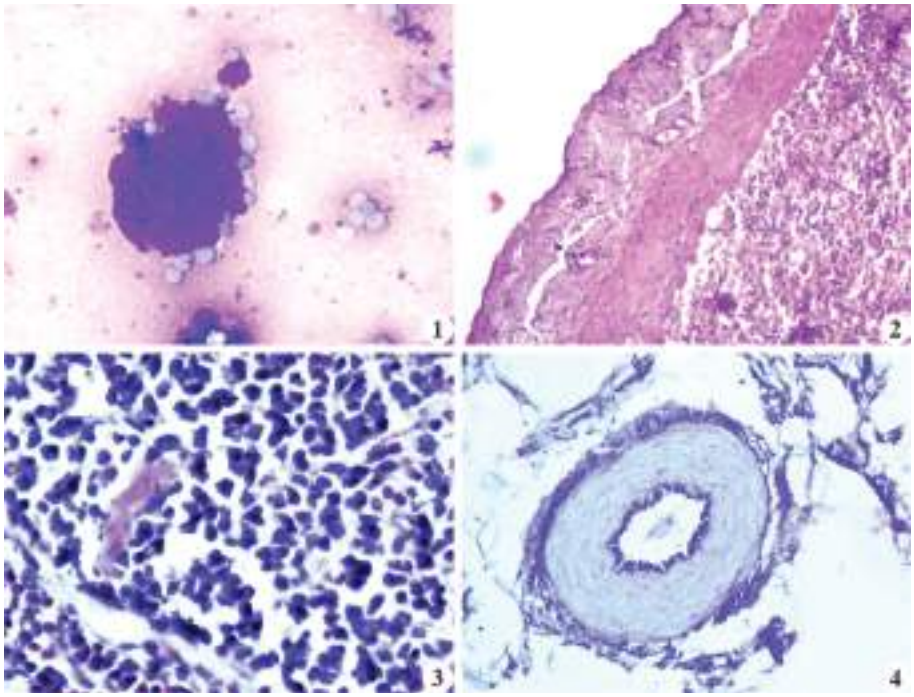

Amyloidosis in lymphoid organs in buffaloes. Fig.1. Amorphous, homogenous, extracellular material - Leishman's stain - spleen x400; **Fig.2.** Extracellular, eosinophilic, amorphous and hyalinized deposits within the capsule - H&E - spleen x100; **Fig.3.** Red coloured deposits of amyloid in the lymphoid follicles - Congo red stain - prescapular lymph node x400; **Fig.4.** Dark purple coloured deposits of amyloid in and around blood vessels - Crystal violet stain - prefemoral lymph node x100.

Follicular amyloidosis was predominantly noticed in the hepatic and mesenteric lymph nodes, where amyloid deposits were mainly localized within the lymphoid follicles.

The presence of amyloid was further confirmed by Congo red stain in which amyloid appeared as red colored deposits and in Crystal violet stain as dark purple colored deposits in the spleen and lymph nodes.

DISCUSSION

The prevalence was lower compared to the findings of[7] with nodular ('sago' spleen) type of splenic amyloidosis (5.3%) in cattle. A higher prevalence was documented in sheltered cats, where systemic amyloidosis with splenic involvement was recorded in 52-73% of animals, and in captive cheetahs where splenic amyloid was frequently encountered as a part of systemic disease[8]. Histopathologically, amyloid deposits appeared as homogenous eosinophilic extracellular material, which is considered a characteristic microscopic feature of amyloidosis[2,3]. In domestic ruminants such as cattle and sheep, splenic amyloidosis was described qualitatively as an occasional or nodular ('sago' spleen) lesion rather than a common finding[3]. It might be attributed to fewer chronic inflammatory conditions, reduced antigenic stimulation, or species variation in susceptibility to systemic amyloidosis[2]. Similar patterns of amyloid distribution in the spleen was reported in domestic animals, where deposits commonly occur in association with vascular and connective structures of the splenic parenchyma[2,3]. Amyloidosis in animals were reported in several organs including the liver, spleen, kidneys and lymph nodes, indicating that the disease frequently occurs as a systemic condition affecting multiple tissues[9]. In the liver, amyloid deposition was described in the space of Disse and along hepatic sinusoids, lead to compression and atrophy of hepatocytes[2]. Similarly, in the kidneys, amyloid deposits were commonly found in the glomeruli and interstitial tissues, which might result in renal dysfunction[3]. [10]described renal amyloidosis in cattle confirmed by Congo red staining, while[11]reported amyloid deposition associated with chronic inflammatory diseases in cattle. Continuous immune stimulation within lymph nodes during chronic infections, inflammatory diseases or immune-mediated conditions could therefore result in amyloid accumulation within lymphoid follicles and vascular walls[2,12]. Comparable localization of amyloid in lymphoid follicles and vascular structures of lymph nodes was described in animals affected with systemic amyloidosis[2,9]. Similar cytomorphological appearance of amyloid was described in cytological preparations of affected tissues, where it appeared as homogenous extracellular deposits[13]. Confirmation of amyloid deposition in the present study was achieved with special staining techniques. Congo red stain demonstrated red deposits, while crystal violet stain revealed dark purple deposits, which were considered characteristic reactions for amyloid material[4,6].The development of amyloidosis in animals is commonly associated with chronic inflammatory or infectious conditions that stimulate prolonged hepatic production of serum amyloid A protein, an acute-phase reactant. Persistent elevation of this protein leads to its misfolding and conversion into insoluble amyloid fibrils that accumulate in tissues such as the spleen, liver, kidney and lymph nodes[2,3,9].

CONCLUSION

The present study demonstrated the increased occurrence of amyloidosis in the lymphoid organs of buffaloes. Amyloid deposition was successfully detected through cytological and histopathological examination and confirmed by special staining techniques, highlighting the importance of these methods in the identification of amyloidosis in buffalo lymphoid tissues.

ACKNOWLEDGEMENT

The authors extend their gratitude to the Sri Venkateswara Veterinary University, Tirupati for providing the facilities necessary to conduct this study.

Financial support & sponsorship: Sri Venkateswara Veterinary University

Conflicts of Interest: None

Use of Artificial Intelligence (AI)-Assisted Technology for manuscript preparation: The authors confirm that there was no use of Al-assisted technology for assisting in the writing of the manuscript and no images were manipulated using AI.

REFERENCES

1. Sipe J D, Benson M D, Buxbaum J N, Ikeda S, Merlini G, Saraiva M J M and Westermark P. 2014. Nomenclature 2014: Amyloid fibril proteins and clinical classification of the amyloidosis. *Amyloid,* **21(4):** 221–224.
2. Zachary J F. Ed. 2017. Pathologic basis of veterinary disease. *Elsevier* Sixth edition Pp 261-266.
3. Maxie M G. Ed. 2016. Jubb, Kennedy and Palmer's pathology of domestic animals. *Elsevier* Sixth edition Vol. 1 Pp 29-33.
4. Bancroft J D and Gamble M. Eds. 2008. Theory and practice of histological techniques. *Churchill Livingstone/Elsevier* 6th ed Pp 309-311 and 335-337.
5. Luna L G. Ed. 1968. Manual of histologic Staining methods of the Armed Forces Institute of pathology. *McGraw-Hill* 3rd ed Pp 94-95 and 156-158.
6. Kiernan J A 2015. Histological and histochemical methods: Theory and practice. *Scion* 5th edition Pp 212-215.
7. Al-Sadi HI and Ridha AM 1994. Comparative pathology of the spleen and lymph nodes of apparently normal cattle, sheep and goats at the time of normal slaughter. *Small Rumin. Res* **14:** 167-174.

8. Papendick R E, Munson L, O'Brien T D and Johnson K H 1997. Systemic AA Amyloidosis in Captive Cheetahs (*Acinonyx jubatus*). *Vet Path* **34(6):** 549–556.
9. Erik G 2004. Protein folding pathology in domestic animals. *J. Zhejiang Univ. Sci. A* **5(10):** 1226–1238.
10. Seifi H A, Karimi K and Movasseghi A R 1997. Renal Amyloidosis in Cattle: A Case Report in Iran. *J. Vet Med, Series B* **44(1–10):** 631–633.
11. Elitok O M, Elitok B and Unver O 2008. Renal Amyloidosis in Cattle with Inflammatory Diseases. *J. Vet Intern Med* **22(2):** 450–455.
12. Woldemeskel M 2012. A Concise Review of Amyloidosis in Animals. *Vet. Med. Int* 1-11.
13. Kumar V, Abbas A K and Aster J C. Eds. 2015. Robbins and Cotran pathologic basis of disease. *Elsevier/Saunders* Ninth edition Pp 252-258.

Indian J. Vet. Pathol., 50(3) : 218-227, 2026: DOI: https://doi.org/10.56093/0ngak147

RESEARCH ARTICLE

Haemato-biochemical, cytological, histopathological and immuno-histochemical studies on canine mammary gland tumors

V. Sarachandra[1], A. Nasreen*[2], A. Anand Kumar, N. Dhanalakshmi[2], K. Rajesh[2] and M. Raghunath[2]
Department of Veterinary Pathology, College of Veterinary Science, Sri Venkateswara Veterinary University, Tirupati, Andhra Pradesh, India
[1]MVSc Scholar; [2]Department of Veterinary Clinical Complex

***Address of correspondence**
Dr. A. Nasreen; E-mail: nashreen7@gmail.com
ORCID Id: 0009-0001-3859-652X

Received: 6.3.26; Accepted: 7.3.26

ABSTRACT

The present study was carried out to investigate paraneoplastic syndromes along with histopathological and immunohistochemical characterization. A total of 55 tumors cases were evaluated and about 10 canine mammary tumor cases were recorded at Veterinary Clinical Complex, Tirupati, Andhra Pradesh over a period of 6 months (April 2025-September 2025). General clinical signs shown by these dogs were cancer anorexia, cachexia, inappetence, dullness, dehydration along with pigmented plaques in a few cases. Grossly, the tumor masses were predominantly cystic, nodular and solid, exhibiting a texture that ranged from soft to firm. Some of these masses were pedunculated, either solitary or affecting the entire chain of the mammary gland. Cytological analysis of mammary tumors revealed an acinar pattern of glandular epithelial cells alongside a limited number of myoepithelial cells exhibiting significant anaplasia. Hematological findings indicated the presence of anemia accompanied by neutrophilic leukocytosis, lymphocytosis, monocytosis and thrombocytopenia. Assessment of serum showed reduced levels of alanine amino transferase (ALT) and aspartate amino transferase (AST); elevated protein levels accompanied by increased gammaglobulin, along with hypoglycemia and hypocalcemia. The histopathological examination of the tumors identified simplex cystic papillary and mixed type carcinoma, tubulopapillary carcinoma, microacinar carcinoma, chondrosarcoma, fibrosarcoma, capillary hemangioma, as well as mixed mammary tumors including cystic chondrolipofibroma and hemangiochondrocystic fibrolipoma. Van Geison staining was performed for required set of tissues for differentiation of tissue origin. Immunohistochemistry was conducted with vimentin, cytokeratin for tissue differentiation, estrogen (ER) and progesterone receptor to confirm the presence or influence of hormones for tumor proliferation.

Keywords: Canine mammary tumors, Cytology, Haematology, Histopathology, Immunohistochemistry, Serum biochemistry

INTRODUCTION

The most common neoplasm in female dogs is mammary tumor. They get cancer on their own and have many biological, clinical, pathological, and molecular traits in common with human breast cancer. Additionally, breast cancer represents one of the leading causes of cancer-related in both species[1]. In humans, approximately 10 million deaths related to cancer are reported each year, along with 19.3 million new diagnoses, whereas in dogs, there are 4 million new cancer cases diagnosed annually[1]. Canine mammary tumors (CMT) pose a serious concern for veterinarians around the world because of their high frequency and low survival outcomes. Around 50% of these tumors are malignant, and due to their similarities with human breast cancer, they are often used as models for studying the disease. These tumors are most commonly found in older dogs, particularly those between 5 to 10 years old and are more prevalent in breeds like Labradors, Golden Retrievers and German Shepherds[2]. While these tumors are prevalent, early diagnosis is essential for formulating treatment plans and avoiding unnecessary surgeries for a better prognosis. Cytology plays a crucial role in the early detection of tumors, and it is also an inexpensive, straightforward, and less painful diagnostic method. Nevertheless, cytology has its limitations, including the challenge of obtaining enough samples and the need for greater expertise in diagnosis. Since histopathology is considered the gold standard for tumor diagnosis, histopathological confirmation is always necessary for precise tumor identification. Additionally, poorly differentiated tumors can be challenging to differentiate from other types, and immunohistochemistry is beneficial in distinguishing tumors as well as identifying their nature and origin in such cases. The recent remarkable progress in molecular medicine, genomics, proteomics, and translational research will facilitate the identification of biomarkers, potentially equipping veterinarians and

How to cite this article : Sarachandra, V., Nasreen, A. Kumar, A.A., Dhanalakshmi, N., Rajesh, K. and Raghunath, M. 2026. Haemato-biochemical, cytological, histopathological and immunohistochemical studies on canine mammary gland tumors. Indian J. Vet. Pathol., 50(3) : 218-227.

clinicians with the most effective strategies to address diseases through early diagnosis and the implementation of appropriate treatments. The objective of the present study is to record the paraneoplastic syndromes, analyze haemato-biochemical alterations, pathomorphology of canine mammary tumors and evaluating with few immunohistochemical biomarkers.

MATERIALS AND METHOD

The study was conducted on cases of canine mammary tumors in dogs presented to the Department of Veterinary Clinical Complex (VCC), College of Veterinary Science (C.V.Sc), Tirupati and pet clinics of local veterinary practitioners in and around Tirupati.

Haematology: Two millilitre whole blood samples were collected in EDTA for haematological parameters such as haemoglobin(Hb) via Sahli's method[23], total leucocyte count (TLC), total erythrocyte count (TEC) using the dilution method[9], differential leucocyte count (DLC), total platelet count following the Battlement method[9].

Biochemistry: Blood samples obtained from dogs, collected in clot activating vacutainers for separation of serum and analysis of alanine transaminase (ALT), aspartate amino transferase (AST), gamma-glutamyl transferase (GGT), serum blood urea nitrogen (BUN), serum creatinine, serum total protein, serum calcium, serum alkaline phosphatase (ALP), glucose, albumin and globulin were conducted using an auto span semiautomatic biochemical analyser along with commercial biochemical kits (ERBA and Biosystem kits)

Cytology: Fine needle aspiration cytology (FNAC) and impression smears of tumor tissue samples were obtained. Smears were stained with with Field's A and B stains for examination[26].

Histology: Tumor tissue samples obtained after surgical mastectomy were collected and fixed in 10% neutral buffered formalin (NBF) for histopathological examination using routine Hematoxylin & Eosin stain after obtaining 3-4µm thin paraffin sections.[3]

Special stains: van Gieson staining was conducted as required on tumor tissue sections to distinguish collagen fibres from the surrounding stroma[24].

Immunohistochemistry: Immunohistochemistry was performed on tumor tissue cut sections onto APES-coated slides and incubated overnight at 37°C. After deparaffinization and rehydration, sections were immersed in a preheated antigen retrieval solution and cooled. The slides were then rinsed in Tris Ethylene Diamine Tetra-acetic Acid (EDTA) buffer, peroxidase blocking solution, and power block solution included in kit. Primary antibodies (Vimentin, Cytokeratin, Estrogen receptor, Progesterone receptor) obtained from BioGenex Company in Bangalore, with 1:100 dilution were introduced, and the slides were kept at room temperature. Secondary antibody conjugated with poly Horseradish peroxidase obtained from BioGenex Company, were applied for 30 minutes and followed by tris EDTA buffer wash.The sections were then stained with DAB (Diamino benzidine), counterstaining with Harris hematoxylin and treated with lithium carbonate. The sections were air dried, mounted in Dibutylphthlate Polystyrene Xylene (DPX) and air dried again.

RESULTS

The present study has focused on the evaluation of different canine mammary tumors that were brought to the Veterinary Clinical Complex (TVCC), College of Veterinary Science, Sri Venkateswara Veterinary University, Tirupati, between April 2025 and December 2025 for assessing paraneoplastic syndrome using clinical signs, haemato-biochemistry and histological classification. The research encompassed thorough patient histories, which entailed gathering crucial information such as breed, age, body weight and specifics about the quantity and location of the impacted mammary glands. The analysis of the findings included investigating the frequency of mammary tumor occurrences in relation to several factors, such as their overall appearance, age, breed, glandular involvement, cytological traits, histopathological characteristics and immunohistochemical profiling.

Occurrence of CMTs: The breed most frequently affected was the Pomeranian, accounting for 50% (5 cases), followed by the Labrador Retriever at 30% (3 cases). The other breeds included German Shepherds (10%) and Spitz (10%), with only isolated cases reported.

The occurrence of canine mammary tumours (CMT) across different age groups is a significant factor to take into account when researching this condition in dogs. Age of affected dogs varied from 1 to 15 years. The highest occurrence of CMT was noted in the age range of 10-12 years (50%), followed by the 13-15 years group (30%) and the 7-9 years group (20%). In contrast, there were no reported cases of CMT in dogs younger than 6 years of age.

Dogs weighing between 10-15 kg had highest (40%) occurrence of CMT, followed by dogs weighing between 30-35 kg (20%) and 35-40 kg (20%), least occurrence in 5-10 kg (10%) and 20-25 kg (10%) each. In dogs bearing weight of 0-5 kg, 15-20 kg, 25-30 kg no cases recorded.

The most common site of occurrence was caudal abdominal followed by inguinal, cranial abdominal and cranial thoracic mammary glands. In few cases more than one mammary gland was affected, where whole side mastectomy was conducted to excise the tumor mass.

Clinical signs: General signs of cancer anorexia, cachexia, inappetence, dullness and dehydration were observed. Pigmented plaques of melanin deposition in skin appearing brown to black color were also noticed. Tumor masses were ulcerated and necrosed with foul smell emitting in few mammary tumors.

Haematology: Haematology revealed anaemia with neutrophilic leucocytosis, lymphocytosis, monocytosis and thrombocytopenia compared with normal reference values (Table 1).

Biochemistry: Serum evaluation revealed decreased levels of ALT, AST; hyperproteinemia with hypergammaglobulinemia, hypoglycemia and hypocalcemia compared with normal reference values (Table 2).

Cytology of CMTs: FNAC and impression of different mammary tumors revealed predominance of malignant tumors over benign tumors. Cytological examination of cells from benign tumors showed minimal variation in both shape and size, with nuclear characteristics remaining unchanged. The cells exhibited strong adhesion to one another and were found in clusters, indicating a high level of cohesion within the cellular mass. In contrast, smears from malignant tumors displayed signs of cellular anisocytosis (Fig.1a), pleomorphism, an increase in cell exfoliation, reduced cohesion among cells, hypercellularity, anisokaryosis (Fig.1b), an elevated nuclear to cytoplasmic ratio, nuclear moulding, a coarse chromatin pattern and presence of clumped chromatin (Fig.1c) with characteristic myoepithelial cells (Fig.1d) and mammary epithelial cells showing round to polyhedral shapes with single individual cells or clusters.

Histopathology of canine mammary tumors: In current study, a total of 10 cases of canine mammary tumors were recorded. The most frequently documented were malignant tumors, accounting for 7 cases (70%), while benign tumors were recorded in 3 cases (30%). These are classified according with WHO classification[4].

Among the malignant tumors, simple cystic-papillary carcinoma was common, which was grossly located on left inguinal, right caudal abdominal and cranial abdominal mammary gland in one case; left

Table 1. Haematological parameters of different canine mammary tumors

Mammary tumors	Hb (g/dL)	TEC (millions/µl)	PLT (Thousands/µl)	TLC (Thousands/µl)	DLC			
					N (%)	L (%)	E (%)	M (%)
Ma1	8.6	5.45	669	33.5	80	15	3	2
Ma2	11	5.2	165	16	76	22	1	1
Ma3	11.2	6.87	149	12	86	12	1	1
Ma4	13.6	6.45	50	13.19	67	18	4	11
Ma5	14.6	7.06	177	12.42	7	81	2	10
Ma6	9.6	5.1	179	8	81	17	1	1
Ma7	11.8	6.07	198	17.08	67	19	3	11
Ma8	12	7.01	197	9	89	8	2	1
Ma9	22.2	10.6	194	12.22	72	16	5	7
Ma10	9	5	90	14	59	39	1	1
MEAN±SE	12.36±1.25	6.48±0.52	206.8±53.64	14.74±2.26	68.4±7.42	24.7±6.77	2.3±0.45	4.8±1.50

Table 2. Biochemical parameters of different canine mammary tumors

Mammary tumors	ALT (U/L)	AST (U/L)	TP (g/dL)	Creatinine (mg/dL)	Alb (mg/dL)	Glob (mg/L)	Glucose (mg/dL)	Calcium (mg/dL)	GGT (U/L)	ALP (U/L)	BUN (mg/dL)
Ma1	16.72	33.33	5.1	0.57	2.88	2.22	23.77	4.97	4.35	40.42	28.8
Ma2	26.5	17.13	5.76	0.79	3.23	2.53	56.86	5.7	0.85	55	14.3
Ma3	17.91	34.64	7.12	0.68	4.04	3.08	50.81	4.28	0.69	35	15
Ma4	60	41.3	7.3	1.19	3.5	3.8	78.2	8.8	9	133	17
Ma5	32.09	46.95	6.66	0.68	3.76	2.9	40.17	4.37	1.46	43.5	13.2
Ma6	60.14	31.48	5.96	0.71	2.84	3.12	67.14	6.94	5.54	66	18
Ma7	22.1	26.52	6.44	1.22	1.84	4.6	62.67	10.2	3.4	55	14.2
Ma8	42	28	7.3	1.7	2.7	4.6	105	7.8	0.58	34	11
Ma9	7.01	20.1	8.26	0.68	2.92	5.34	64.83	4.24	1.2	55	18.4
Ma10	25.4	16.66	8.64	0.63	2.95	5.69	81.21	7.05	5.48	103	18
MEAN± SE	30.99± 5.67	29.61± 3.17	6.85± 0.35	0.88± 0.11	3.06± 0.19	3.79± 0.38	63.7± 21.3	6.43± 0.65	3.25± 0.89	61.99± 10.11	16.79± 1.53

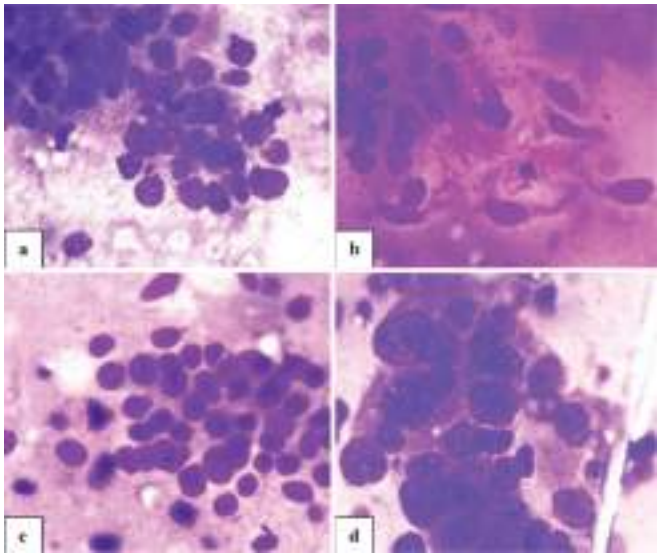

Fig.1. a. Round to polyhedral cells arranged in linear to cluster pattern with moderate amount of eosinophilic cytoplasm and round to oval nucleus with clumped chromatin. Field's stainx1000; **b**. Fusiform cells showing oval to spindle shaped nucleus with whispy borders and had clumped chromatin. Field's stainx1000; **c.** Mammary epithelial cells arranged in acinar pattern with prominent nucleoli and chromatin clumping. Field's stainx1000; **d.** Polyhedral cells with anisocytosis and anisokaryosis showing prominent nucleoli. Field's stainx1000.

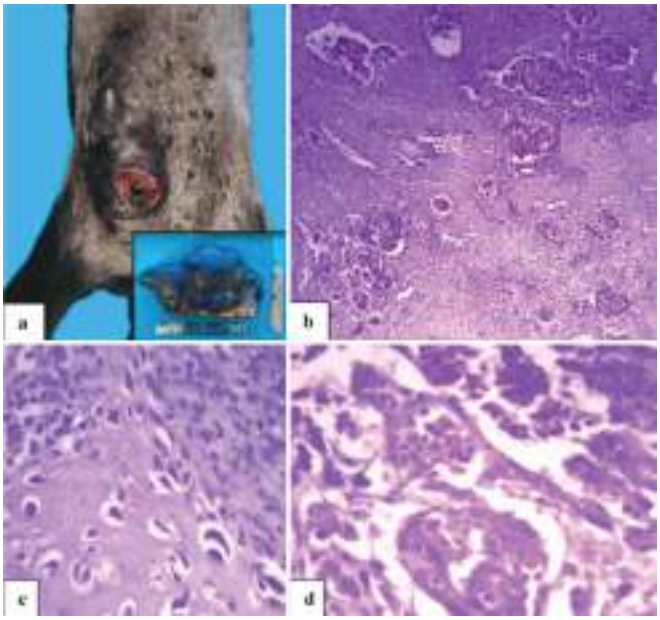

Fig.3. Chondrosarcoma with adenocarcinoma a. Ulcerated, hyperaemic and necrotic mass present on the right inguinal mammary gland; Inset: Hard mass of size 15cmx15cm after resection; **b.** Intermixed chondroid and glandular tissue. H&Ex40; **c.** Chondroid matrix showing cells with single to bi nucleus and cytoplasmic vacuolation H&Ex400; **d.** Carcinomatous cells with anisokaryosis and anisocytosis and few vacuolations. H&Ex400.

caudal abdominal and right inguinal mammary gland in other case. A white solid mass characterized by its pedunculated appearance few cystic structures and

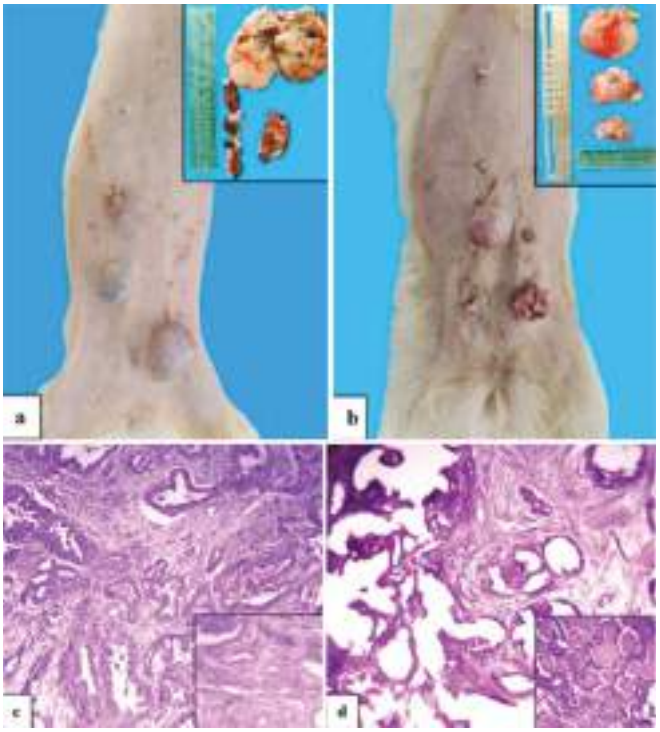

Fig.2. Simple cystic papillary carcinoma a. Solid masses on left inguinal, right caudal abdominal and cranial abdominal mammary gland. Inset: Cut section of mass with white solid and cystic areas; **b.** Solid multinodular masses left caudal abdominal and right inguinal mammary gland. Inset: White, solid, pedunculated mass with few cystic structures and nodular growth of varying sizes (7cm x 5cm; 5cm x 4cm); **c.** Glandular epithelium formed papillae that extended into dilated and cystic lamina. H&E x100; Inset: Tubules with proliferation of neoplastic epithelial cells with eosinophilic cytoplasm and nucleus appeared hypochromic with prominent nucleoli. H&E x400; **d.** Multiple cystic spaces along with projections into lumen. H&E x100. Inset: Glands dilated and cystic with few spaces filled with serous eosinophilic material H&E x10

nodular growth of varying sizes (7cm × 5cm; 5cm × 4cm) papillae that extended into dilated and cystic lamina (Fig.2 a). Many glands were dilated and cystic with few spaces filled with serous eosinophilic material (Fig.2b and 2c). Tubules were lined by multiple layers of columnar epithelial cells with eosinophilic cytoplasm and hypochromic nucleus with multiple nucleoli. Intertubular stroma had few congested blood vessels and infiltration of mononuclear cells.

A case of chondrosarcoma with adenocarcinoma was noted. It was located in right inguinal mammary gland with 15cm×15cm size, appeared ulcerated with hyperaemic and necrosed areas (Fig.3a). Histology revealed blending of chondroid tissue with glandular tissue. Neoplastic cells showed small round hyperchromatic nucleus with occasionally bi or multinucleate cells. The outline of nucleus was irregular with prominent nucleoli. Chondroid matrix was having cells with single to double nucleus, cytoplasmic vacuolation (Fig. 3b).

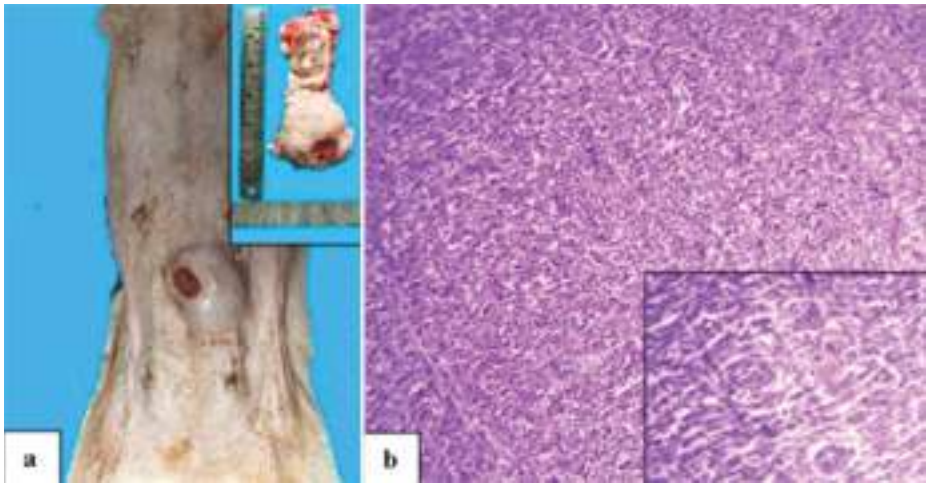

Fig.4. Capillary hemangioma a. Mass located in between caudal abdominal and inguinal mammary gland. Inset: Ulcerated solid hard mass with size of 8cm×6cm. **b.** Prominent neovascularization with compact arrangement of cells.H&Ex100. Inset: Capillaries are lined by endothelial cells which were elongated with oval nucleus and prominent nucleoli. H&Ex400

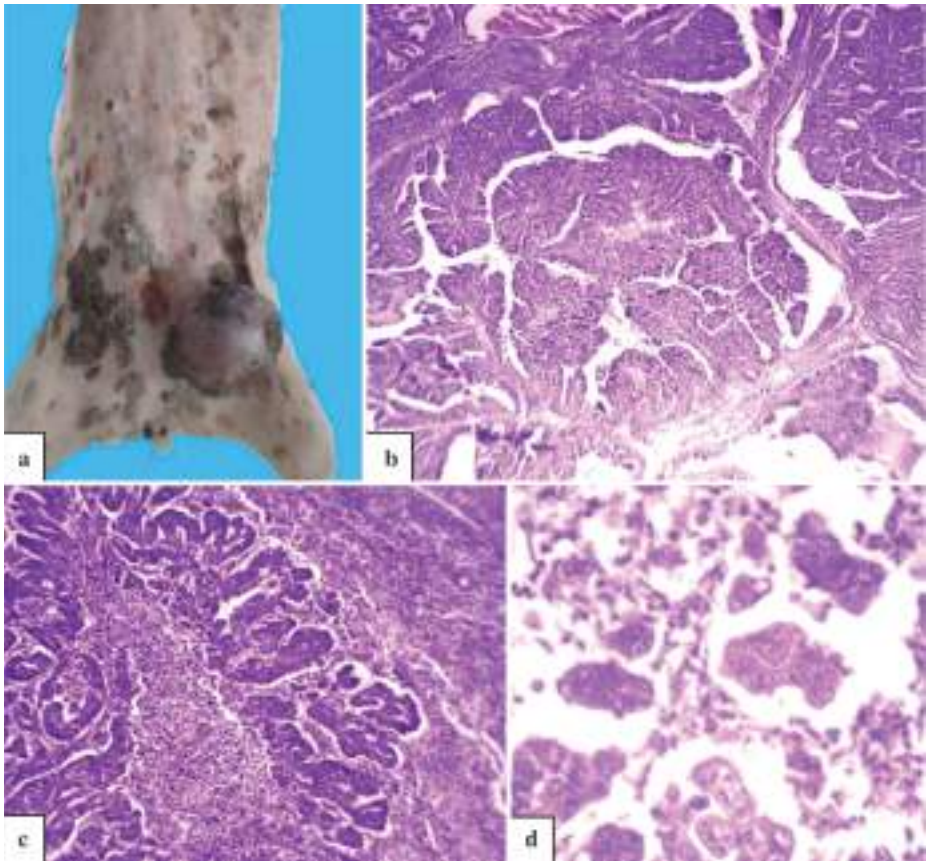

Fig.5. Simple tubulo-papillary carcinoma a. Mass located at cranial thoracic and left inguinal mammary gland. Inset: Simple tubulo-papillary carcinoma: Solid mass solid with few cystic spaces of sizes 10cm×8cm and a cystic mass of 11cm×12cm. **b.** Diffuse infiltration of glandular structures with several papillary projections into lumen.H&Ex40. **c.** Hyperplastic and hyperchromatic alveolar epithelial cells in single or multiple layers along the alveolar ducts exhibiting pleomorphism H&Ex100. **d.** Few giant cells with multiple nuclei and prominent nucleoli. H&Ex400.

The carcinomatous cells showed anisokaryosis and anisocytosis with few vacuolations in some glands (Fig. 3c and 3d).

Capillary hemangioma appeared ulcerated, solid hard mass and located in between left caudal abdominal and inguinal mammary gland with a size 8cm×6cm (Fig. 4a). Histopathology revealed section showing compactly arranged microvasculature formed by neovascularization. Infiltration of inflammatory cells in between the capillaries was noticed amidst congested blood vessels. The capillaries were lined by endothelial cells which were elongated with oval nucleus and prominent nucleoli (Fig.4b and 4c).

The simple tubulo-papillary carcinoma was found in the cranial thoracic and left inguinal mammary gland. Grossly, mass appeared solid with few cystic spaces with sizes 10cm×8cm and a cystic mass of 11cm×12cm (Fig.5a). Histology showed diffuse infiltration of glandular structures with several papillary projections into lumen (Fig. 5b). Neoplastic cells were oval to round shaped with scanty cytoplasm arranged in multiple layers with prominent nucleus and multiple nucleoli. Areas of cholesterol deposition with cleft formation was evident.

Microacinar type mammary tumor was in left side between caudal abdominal and inguinal mammary gland. Mass was 12cm×7cm, hard, solid, and pedunculated. On incision, mass was solid white with cystic area towards periphery filled with serous fluid surrounded by necrotic borders (Fig.6a). Histological examination revealed formation of multiple islands of neoplastic cell infiltration

separated by fibrous vascular bands (Fig.6b). The islands revealed formation of acini by epithelial cells. The cells showed pleomorphism with eosinophilic cytoplasm and round to oval nuclei (Fig.6c). Van Gieson staining of section showed positive staining for collagen (red) and glandular epithelium (yellow) (Fig. 6d).

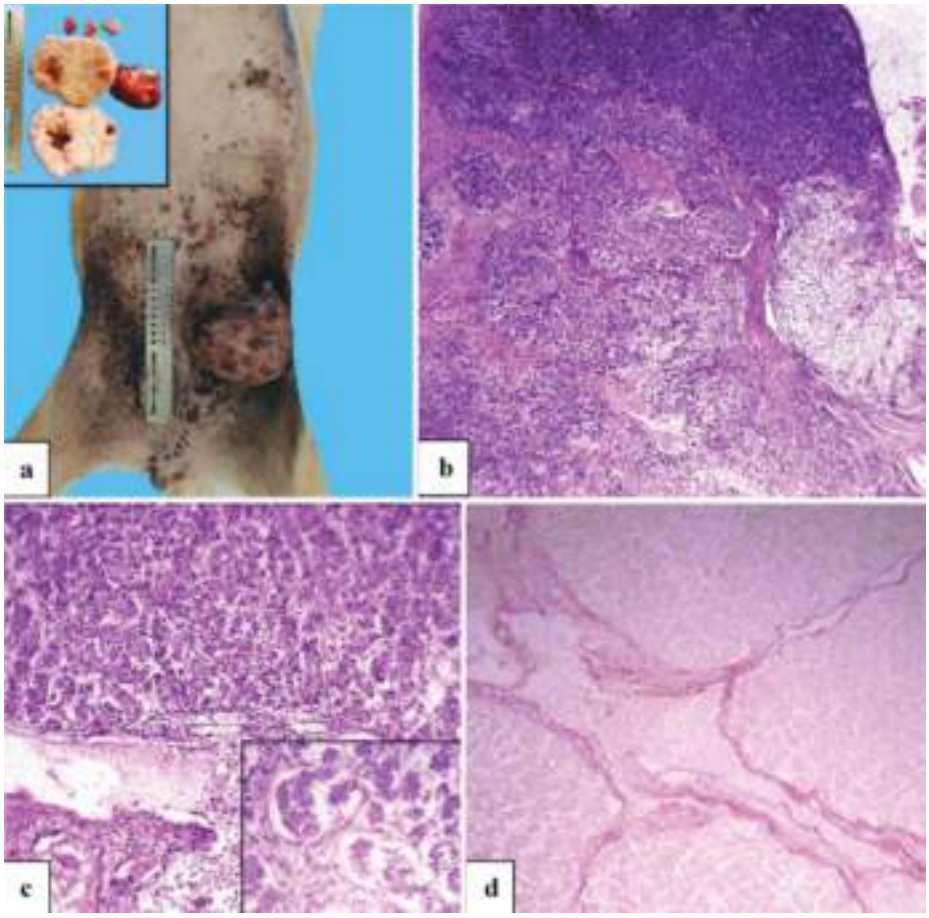

Fig.6. Microacinar adenocarcinoma a. Mass located on left side between caudal abdominal and inguinal mammary gland. Inset: Cut section showed solid white with cystic area towards periphery filled with serous fluid surrounded by necrotic borders. **b.** Multiple islands of neoplastic cells separated by fibrous vascular bands. H&Ex40. **c.** Acinar pattern with epithelial cells showing pleomorphism. H&Ex100. Inset: Few cells showing vacuolation with multiple nuclei and prominent nucleoli. **d.** Collagen stained red with glandular epithelium showing yellow stain. VanGiesonx100

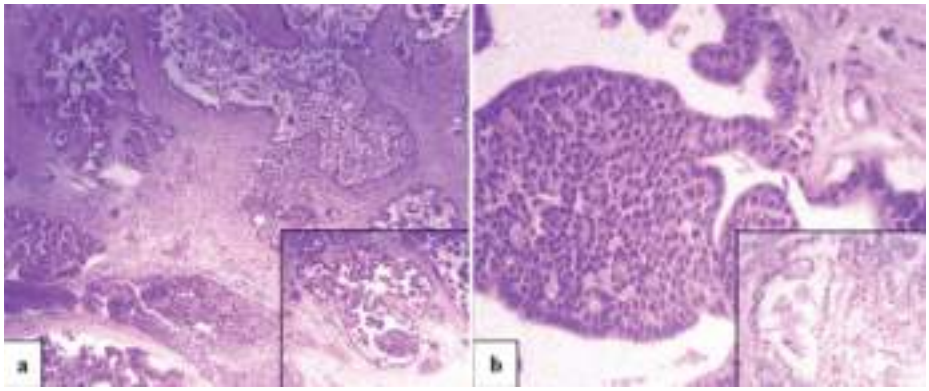

Fig.7. Mixed cystic-papillary carcinoma a. Papillary projections into lumen of glands surrounded by fibrous tissue. H&Ex40. Inset: Epithelial cells proliferation into long papillary projections. H&Ex100. **b.** Cells were proliferating from one pole of gland into lumen with round to elongated nucleus and eosinophilic cytoplasm. H&Ex400. Inset: Cells with foamy eosinophilic cytoplasm and round nucleus with prominent nucleoli and distinct borders. H&Ex400

In mixed cystic-papillary carcinoma, firm nodular mass was located on left cranial thoracic mammary gland. Histology revealed multiple glands with papillary projections into lumen with fibrous tissue proliferation in between the glands. Cystic spaces of glands with long papillary projections due to epithelial cell proliferation into spaces was noticed. Few areas showed glandular epithelial proliferation into solid structures (Fig.7a). The cells were proliferating from one pole of gland into lumen with round to elongated nucleus and eosinophilic cytoplasm. Few cystic spaces showed cells with foamy eosinophilic cytoplasm and round nucleus with prominent nucleoli and distinct borders characteristic of mammary foam cells (Fig.7b).

Fibrosarcoma of mammary gland was located at left caudal abdominal mammary gland with size of 11cm×5cm, which was hard solid with scarcely nodular appearance. Mass upon incision, showed viscous surface with greyish white areas and mild haemorrhagic areas (Fig. 8 a). Histopathology revealed high cellularity of fusiform shaped fibroblast cells proliferating into distinct interwoven pattern with varying size and shape. Fibroblasts showed spindle shape with small quantity of eosinophilic cytoplasm and whispy borders. Nucleus were oval to elongate which contained finely stippled chromatin and prominent nucleoli (Fig.8b).

Out of 10 tumor cases, two cases of mixed mammary tumors were recorded. Cystic chondro lipofibroma case with mass was located at caudal abdominal

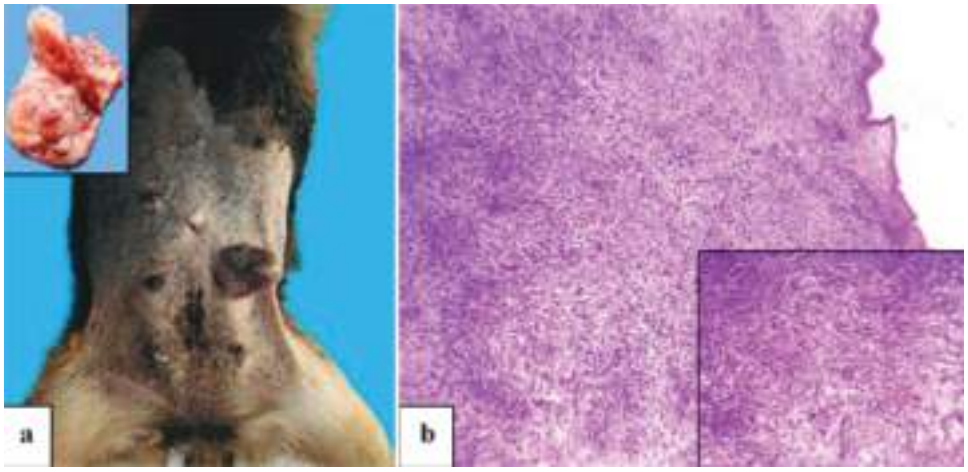

Fig.8. Fibrosarcoma a. Mass was located at left caudal abdominal mammary gland. Inset: Cut surface showing greyish white areas with mild haemorrhages. **b.** High cellularity of fusiform shaped fibroblast cells proliferating into distinct interwoven pattern. H&Ex40. Inset: Spindle shaped fibroblasts with small quantity of eosinophilic cytoplasm and whispy borders. H&Ex100

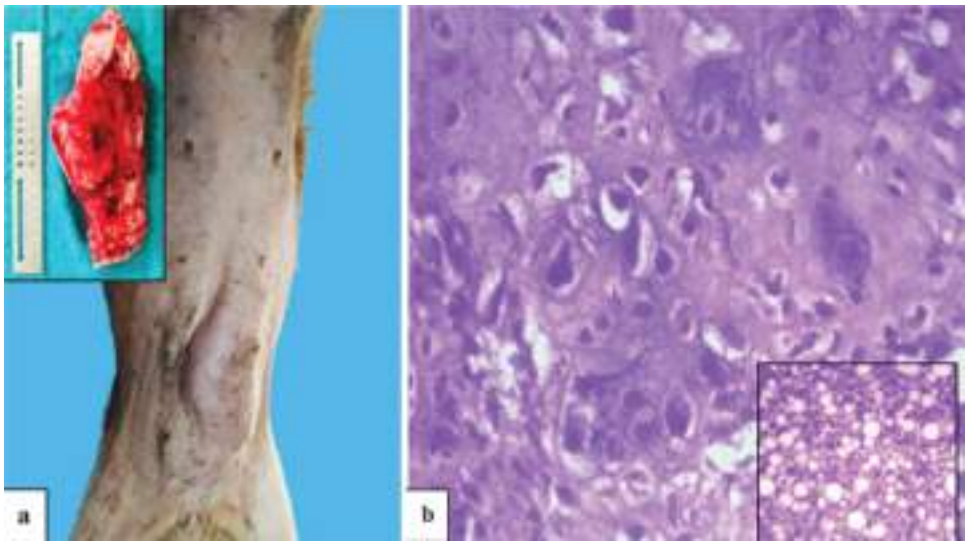

Fig.9. Cystic chondro lipofibroma a. Mass located at caudal abdominal mammary gland with hyperaemic areas. Inset: Solid hard mass measuring 15cm×9cm. **b.** Matrix of chondroid tissue, adipocytes with cystic spaces of glandular tissue and proliferation of glandular epithelium. H&Ex40. Inset: Adipocytes with large cytoplasmic vacuolation and nucleus pushed to periphery. H&Ex400

mammary gland with size measuring 15cm×9cm and appeared hard with fluctuation and hyperaemic areas (Fig.9a). Cut section of mass appeared cystic with mild grittiness and brown color slimy fluid. Histopathological examination of mass revealed multiple matrices of chondroid tissue, adipocytes with cystic spaces of glandular tissue and proliferation of glandular epithelium into multiple layers in few areas (Fig.9b). Adipocytes appeared with large cytoplasmic vacuolation and nucleus pushed to periphery. Some fibroblasts proliferated in between the adipocytes (Fig.9b).

Other tumor was cystic hemangio chondro fibrolipoma, mass was located in between caudal thoracic and cranial abdominal mammary gland (Fig.10a) with soft fluctuating and mild firm consistency with size of 13cm×10cm. On cut section mass showed solid white areas with focal haemorrhagic areas and surface appeared viscous nature with blood tinge (Fig.10b). Histopathology revealed solid infiltration with high cellularity and few areas showing numerous blood pockets with fibrous tissue proliferation around it (Fig.10c). Fusiform shaped fibroblasts proliferated with adipocytes which had large vacuoles with nucleus pushed to periphery (Fig.10d). Blood pockets were characterised numerous spaces filled with erythrocytes and lined by endothelial cells. Chondroid matrix was evident in few areas with bluish stroma having cells with multiple nucleus and vacuolated space around nucleus (Fig.10e). Special staining of tissue section with Van Gieson stain revealed positive for collagen staining red, muscle and glandular epithelium with erythrocytes staining yellow (Fig.10f).

Immunohistochemistry: In this study, a panel of four monoclonal antibodies was used to demonstrate various tissue markers in sequential paraffin-embedded tissue sections from clinical cases of CMTs. The mammary gland tumor showed positive reaction to the vimentin marker by staining cytoplasm of the neoplastic mesenchymal cells appearing brown color (Fig.11a and 11b).

The papillary projections of mammary gland epithelium in tubular papillary type tumor showed strong positive reaction with brown precipitate in the epithelial surfaces with cytokeratin (Fig.11c). The cystic papillary type of mammary tumor showed strong positive reaction to the cytokeratin marker staining the cytoplasm of the neoplastic epithelium (Figs.11d). The mixed mammary tumor showed

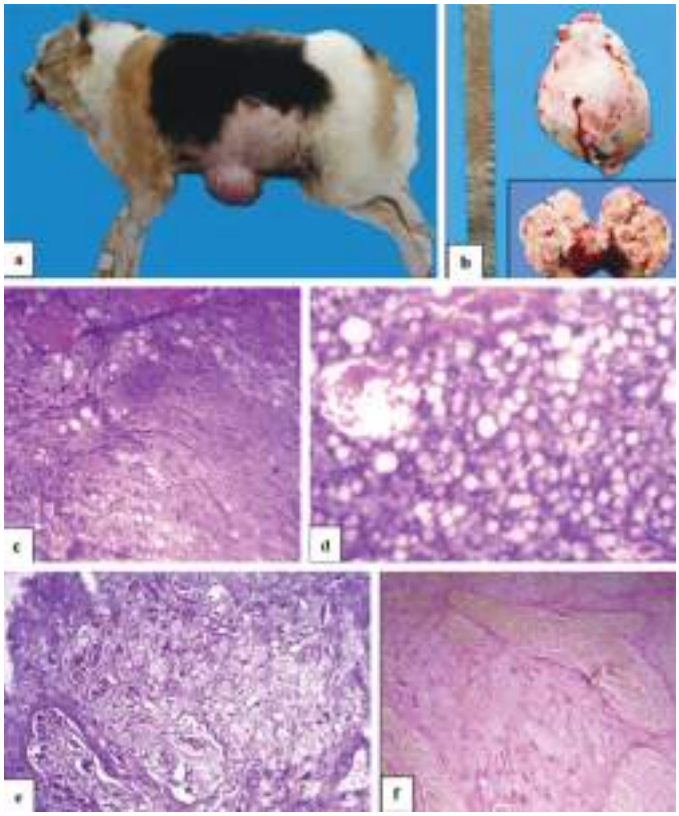

Fig.10. Cystic hemangio chondro fibrolipoma a. Mass located in between caudal thoracic and cranial abdominal mammary gland. **b.** Soft fluctuating mass with mild firm consistency and of 13cm×10cm size. Inset: Cut section showing solid white areas with focal haemorrhagic. **c.** Solid infiltration with high cellularity and few areas showing numerous blood pockets along with fibrous tissue proliferation. H&Ex40. **c.** Spindle shaped fibroblasts proliferation in between adipocytes. H&Ex100. **d.** Adipocytes having large vacuoles with nucleus pushed to periphery. H&Ex400. **e.** Chondroid matrix evident in few areas of bluish stroma having cells with multiple nucleus and vacuolated space around nucleus. H&Ex100. **f.** Positive staining for collagen appeared red; muscle and glandular epithelium along with erythrocytes staining yellow. VanGiesonx100

strong immunopositive reaction to the cytokeratin marker staining the epithelial cells cytoplasm.

ER and PR expressions revealed papillary adenoma of mammary gland showing mild positive immunostaining for both estrogen (Fig. 11e) and progesterone receptors as nucleus of glandular epithelium have taken brown color (Fig. 11f).

DISCUSSION

Based on the findings of the current study and those of previous researchers, it can be concluded that pet owners tend to prefer specific breeds such as Labrador, German Shepherd, and Pomeranian, among others, influenced by the popularity of these breeds in their respective regions. Consequently, the population of these breeds varies across different geographical areas, reflecting the breed-specific occurrence of various disorders, including

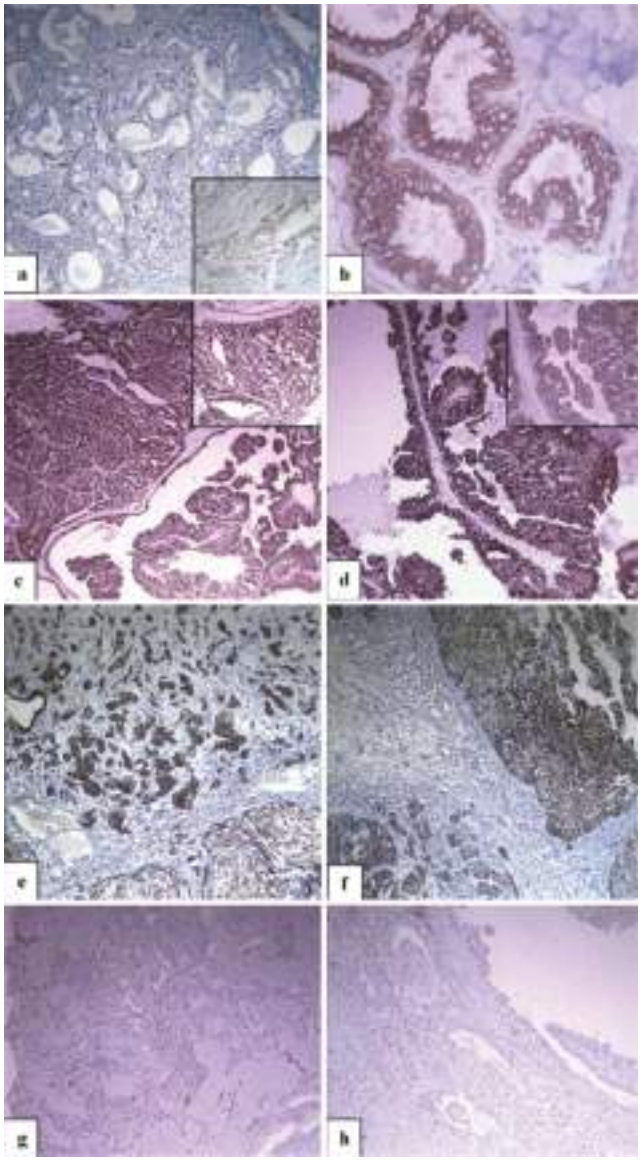

Fig.11. Immunohistochemistry. a. Vimentin: Strong positive reactivity of cells with marker in cytoplasm. IHCx100. Inset: Strong positive reactivity of mesenchymal cells with marker in cytoplasm. IHCx400; **b. Cytokeratin:** Epithelial cells showed strong positivity in the cytoplasm as a brown precipitate. IHCx400;. **c. Cytokeratin:** Papillary projections of mammary gland epithelium in tubular papillary type showed strong positive reaction with brown precipitate in the epithelial surfaces. IHCx40. Inset: Epithelial cells of papillary projections showing high positivity to marker in cytoplasm. IHCx10; **d. Cytokeratin:** Cystic papillary type showed strong positive reaction to the cytokeratin marker staining the cytoplasm of the neoplastic epithelium. IHCx100. Inset: Cystic papillary type showed strong positive reaction to the cytokeratin marker staining the cytoplasm of the neoplastic epithelium. IHCx400; **e. Cytokeratin:** Mixed mammary tumor showed strong immunopositive reaction to the marker staining the cytoplasm of glandular epithelial cells. IHCx40; **f. Cytokeratin:** Mixed mammary tumor showed strong immunopositive reaction to the marker staining the epithelial cells cytoplasm. IHCx40; **g. Estrogen receptor:** Papillary adenoma of mammary gland showed moderate positive nuclear immunostaining. IHCx100; **h. Progesterone receptor:** Papillary adenoma of mammary gland showed moderate focal positive immunostaining. IHCx100.

mammary tumors. While the precise reasons for the natural predispositions observed in certain breeds remain unclear, the inheritance of abnormal genes or oncogenes in purebred dogs can be partially attributed to the selective breeding of specific genetic traits over time to achieve the desired morphological characteristics of a breed[5].

The age-related incidence of canine mammary tumors (CMT) can also be explained by hormonal fluctuations, particularly the exposure to progesterone and estrogen[6]. Dogs that are spayed before their first heat cycle have a significantly lower risk of developing mammary cancers compared to intact (unspayed) females[6]. With each heat cycle a dog experiences, the risk of CMT decreases further[6]. The results of the current study indicated a rising frequency of mammary tumors from the cranial to the caudal region majorly involving the caudal and followed by inguinal mammary gland. In several previous studies, the majority of CMT cases were reported in two pairs (inguinal and caudal abdominal). This may be attributed to the fact that these areas contain the largest glands with a greater amount of mammary tissue, making them more vulnerable to various physiological changes that could result in neoplasms[6].

Clinical signs were cancer anorexia and cachexia along with pigmented plaques which are observed by several researchers[7]. Haematology reported anaemia with neutrophilic leucocytosis, lymphocytosis, monocytosis and thrombocytopenia due to lack of erythropoietin, release of cytokines which suppress megakaryopoiesis, necrosis and inflammation[8,9]. Serum evaluation revealed decreased levels of ALT, AST; hyperproteinemia with hypergammaglobulinemia, hypoglycemia and hypocalcemia due to severe damage of liver leading to increase due to antigenic stimulation leading to production of gammaglobulins or decrease in production of proteins and deviated gluconeogenesis[7,10-12].

Cytology is a fast and cost-effective method for diagnosing tumors. This technique aids in the early detection of mammary gland tumors in dogs. Cytological classification and prognostic methods are well established in human breast cancers, achieving a correct cytological diagnosis rate exceeding 90% when compared to diagnoses in veterinary medicine[13]. Cytological examination is utilized to distinguish between benign and malignant tumors, which can be regarded as adequate for the cytological diagnosis of benign and malignant tumors[7,13].

Histopathologically 70% malignant and 30% benign were reported, revealing simplex cystic papillary is most common, followed by mixed type carcinoma, tubulopapillary carcinoma, microacinar, chondrosarcoma, fibrosarcoma, capillary hemangioma and mixed mammary tumors such as cystic chondro lipofibroma and hemangio chondro cystic fibrolipoma[14-19]. The participation of multiple mammary glands in dogs is relatively common, as noted in this study and others[20].

Immunohistochemical analyses of papillary type tumors demonstrated moderate positive reactivity for vimentin and strong positive reactivity with cytokeratin, as evidenced by the staining of the cytoplasm in neoplastic epithelial cells. The vimentin marker also exhibited positive immunostaining in the cytoplasm of mammary gland epithelial cells, indicating positive reactivity. Estrogen Receptor (ER) and Progesterone Receptor (PR) play crucial roles in the normal development and functioning of the mammary gland. However, their involvement in the development and progression of mammary gland tumors has recently captured the attention of the scientific community, aiming to unravel the complex behavioral patterns of this neoplasm[21]. Additionally, estrogen and progesterone receptors showed positive staining in the immunohistochemical examination[13,21].

Paraneoplastic syndrome reported during this study were mainly anaemia, neutrophilic leucocytosis, lymphocytosis, monocytosis and thrombocytopenia along with hypoproteinemia, hypoalbuminemia, hypoglycemia, hypocalcemia, inflated levels of AST, ALT and elevated levels of ALP and BUN in some cases[7,10,11].

CONCLUSION

Mammary cancer ranks among the most commonly diagnosed malignant tumors in canines, and it is the most prevalent tumor found in non-spayed female dogs[1]. CMT is a significant health issue in dogs and because of its traits, such as size similarities, swift growth, and comparable clinical stages to human breast cancer, it is regarded as a compelling option for comparative studies.[6] Our research concludes that paraneoplastic syndrome can be used as an early indicator for early diagnosis of canine mammary tumors. Haematology and serum biochemistry give information regarding the status of the condition and prognosis. Histopathology add the best tool for the diagnosis of different canine mammary tumors. Immunohistochemistry is a potent method for classifying the CMTs[22]. The findings of this study indicate that canine mammary tumors can be utilized as models for research comparable to human breast cancers, promoting further studies in the fields of medicine, pharmacology, and molecular pathways.

Financial support & sponsorship: None

Conflicts of Interest: None

Use of Artificial Intelligence (AI)-Assisted Technology for manuscript preparation: The authors confirm that

there was no use of AI-assisted technology for assisting in the writing of the manuscript and no images were manipulated using AI.

REFERENCES

1. Vazquez E, Lipovka Y, Cervantes-Arias A, Garibay-Escobar A, Haby MM, Queiroga FL, Velazquez C. 2023. Canine Mammary Cancer: State of the Art and Future Perspectives. *Animals: an open access journal from MDPI*. **13**(19): 3147.
2. Prakash G, Kumar K, Kumar S, Sharma RK, Tiwary R, Mutkule AG, Anand A. 2024. Clinicopathological analysis and immunohistochemical profiling of HER-2, PCNA and CK in spontaneous canine mammary tumour. (2024). *Indian J Vet Pathol* **48**(4): 335-341.
3. Bancroft DJ and Cook CH. 1994. Fundamentals of normal histology and histopathology. Manual of histopathological techniques and their diagnostic application, 2nd edition, Chur chill Livingstone, Edinburgh.
4. Goldschmidt M, Peña L, Rasotto R, Zappulli V. 2011. Classification and Grading of Canine Mammary Tumors. *Vet Pathol* **48**(1):117–131.
5. Sorenmo K. 2003. Canine mammary gland tumors. *The Veterinary clinics of North America. Small animal practice*, **33**(3): 573–596.
6. Zatloukal J, Lorenzová J, Tichý F, Nečas A, Kecová H, Kohout P. 2005. Breed and Age as Risk Factors for Canine Mammary Tumours. *Acta Vet Brno*. **74**: 103-109.
7. Finora K. 2003. Common Paraneoplastic Syndromes. *Clinical Techniques in Small Animal Practice* **18**(2):123-126
8. Godse SD. 2001. Study of canine mammary tumors with special reference to some elemental profiles. An M.V.Sc. thesis submitted to konkan krishi vidyapeeth, Dapoli.
9. Kumar Pradeep, Parashar MC. 2020. Clinical evaluation of haemato-biochemical alteration with different therapeutic approaches to canine mammary tumours. *J. Chem. Res. Adv.* **01**(01): 22-25.
10. Alvarez L, Whittemore J. 2009. Liver Enzyme Elevations in Dogs: Physiology and Pathophysiology. *Compendium* (Yardley, PA) **31**(9):408-414.
11. Holowaychuk MK. 2013. Hypocalcemia of Critical Illness in Dogs and Cats. *Veterinary Clinics of North America: Small Animal Practice* **43**(6):1299–1317.
12. Duda Naila CB, Stella de FV, Juliana PM, Natália CA, Luciane CV, Luciana OO, Luciana S, Félix HDG. 2017. Paraneoplastic Hematological, Biochemical, and Hemostatic Abnormalities in Female Dogs with Mammary Neoplasms. *Pesq Vet Brasil* **37**(5): 479–484
13. Chavan CA, Kaore MP, Bhandarkar AG, Dhakate MS, Kurkure N. 2016. Cytological, histological and immunohistochemical evaluation of canine mammary tumors. *Indian J Vet Pathol* **40:** 139-143.
14. Misdorp W, Else RW, Hellmen E, Lipscomb TP. 2001. Histological classification of mammary tumors of the dog and cat. In: WHO International Histological Classification of Tumors of Domestic Animals, Second Series, vol VII, Washington DC, Armed Forces Institute of Pathology, American Registry of Pathology.2
15. Shekhar CS, Sakthivelan SM, Vijaysarthi SK, Suguna R, Mahesh MJK. 2004. Osteochondrosarcoma in the mammary gland of dog. *Indian J Vet Pathol* **28** (1): 73-74.
16. Reddy GBM, Kumar R, Kumar P, Sharma AK, Singh ND. 2009. Canine skin tumours: Occurrence and histopathology. *Indian J Vet Pathol* **33(**2):200-203.
17. Sorenmo KU, Kristiansen VM, Cofone MA, Shofer FS, Breen AM, Langeland M, Goldschmidt MH. 2009. Canine mammary gland tumours; a histological continuum from benign to malignant; clinical and histopathological evidence. *Vet Comp Oncol* **7**(3): 162–172.
18. Goldschmidt M, Peña L, Rasotto R, Zappulli V. 2011. Classification and grading of canine mammary tumors. *Vet Pathol* **48**(1):117-31.
19. Jain V, Raghunath M, Gupta K, Sood NK. 2011. Pathology of canine mammary neoplasms. *Indian J Vet Pathol* **35** (1): 89-90.
20. Al-Mansour MA, Kubba MAG, Al-Azreg SA, Dribika SA. 2018. Comparative histopathology and immunohistochemistry of human and canine mammary tumors. *Open Vet J* **8**(3): 243-249
21. Kumbhani TR, Fefar DT, Trangadia BJ, Bhadaniya AR, Kalaria VA, Javia BB. 2022. Cytological, Histopathological and Immunohistochemical study of canine mammary gland tumors. *Indian J Vet Pathol* **46**(3): 224-229.
22. Niyas N, Sajitha IS, Prasanna KS, Devi SS, Nair SS, Anseena AK, Afsal S. 2024. Histopathological and immunophenotypical classification of canine mammary tumours. *J Vet Anim Sci* **55**(1):122-128.
23. Coles EH. 1986. Veterinary Clinical Pathology. 4th edn, W S Saundere, Publ. Philadelphia: 241-288.
24. Luna LG. 1968. In: Manual of Histological staining methods of the Armed Forces Institute of Pathology. New York: Mcgraw-Hill Book Co. 3rd Edn. pp:76-77.
25. Hassan SMH, Zaghlol NF, El-Shamy SA, Latteef DK. 2015. Hematological and Biochemical Abnormalities of Canine Mammary Gland Tumors Correlated to Their Histopathological Types and Serum Biomarkers. *Assiut Vet. Med. J.* **61**(145): 178–200.
26. Moody AH, Fleck SL. 1985. Versatile Field's stain. *J. Clinic. Pathol*. **38**(7): 842–843. https://doi.org/10.1136/jcp.38.7.842.

Indian J. Vet. Pathol., 50(3) : 228-235, 2026: DOI: https://doi.org/10.56093/bncv8821

RESEARCH ARTICLE

Wound healing potential of a gel formulation of porcine cholecyst extracellular matrix in a rat full-thickness excision model

Chandramohanan Purnima[1]*, Kanakarajan V. Pratheesh, Reshmi Raj[2], Manjula P. Mony and T.V. Anilkumar
Division of Experimental Pathology, Biomedical Technology Wing, Sree Chitra Tirunal Institute for Medical Sciences and Technology, Poojappura 695012, India
[1]School of Biology, Indian Institute of Science Education and Research-Thiruvananthapuram, Maruthamala PO, Vithura, Thirunvananthapuram-695551
[2]Research Scientist, Health Economics and Finance Research Group, Research Institute of Medical and Health Sciences, University of Sharjah, Sharjah, UAE e-mail: rnair@sharjah.ac.ae

***Address of correspondence**
Dr. Chandramohanan Purnima; E-mail: purnimac@iisertvm.ac.in
ORCID Id: 0000-0003-1006-2814

Received: 13.2.26; Accepted: 5.7.26

ABSTRACT

Collagen-rich extracellular matrices (ECMs) recovered from mammalian organs and tissue have found clinical uses in several formats like thin sheets, powder, ointments, gels, *etc.;* either as a standalone tissue engineering scaffold or in combination with other biomaterials and pharmaceuticals for many regenerative medical applications. Out of these, gel formulations of 'advanced wound care products' made of animal-derived ECMs have high utility because of structural adaptability, biocompatibility, and tunable physicochemical properties. This study demostrated the wound healing potential of a porcine cholecystic extracellular matrix gel formulation in rat full-thickness skin-excision wound model by gross and histomorphological studies.

Keywords: Extracellular matrix, Full-thickness skin excision wound, Wound healing

How to cite this article : Purnima, C., Pratheesh, K.V., Raj, R., Mony, M.P. and Anilkumar, T.V. 2026. Wound healing potential of a gel formulation of porcine cholecyst extracellular matrix in a rat full-thickness excision model. Indian J. Vet. Pathol., 50(3) : 228-235.

INTRODUCTION

Tissue engineering scaffolds (TES) fabricated out of animal-derived extracellular matrix (ECM) recovered from appropriately decellularized mammalian organs/tissues can be used as 'advanced wound care' products[1]. They contain ECM constituents (e.g.: collagen, laminin, glycosaminoglycan, fibronectin, *etc.*) with variable purity. Indeed, collagen-rich ECMs have found clinical uses in several formats like thin sheets, powder, gels *etc*, either as a standalone product or in combination with other biomaterials and pharmaceuticals[2]. Despite several limitations in clinical utility due to shape/form/presentation, the ECM sheets are widely used as surgical grafts for wound healing applications. On the other hand, for topical wound healing applications, gel formulation is preferred over sheet forms[3].

Our laboratory has developed several sheet formulations using ECM of porcine gall bladder (cholecyst) with potential clinical applications[4,5,6,7]. Preparation of powder[8] and gel formulations[9] were also attempted from porcine cholecystic extracellular matrix (CECM). The original gel formulation of CECM was intended for surface modification of polymeric hernial repair graft which mitigated the nature of tissue reaction around intramuscular implants, but was not suitable for topical wound healing application because of its high viscosity and storage modulus[9].

This study evaluated the wound healing potential of a modified CECM-hydrogel with a softer consistency in a rat full-thickness skin-excision wound model.

MATERIALS AND METHODS

Preparation of the gel

The CECM hydrogel was prepared by the original method[8] involving solubilisation (using, pepsin-HCl), followed by neutralisation (using, 0.1 N NaOH and 10x PBS), functionalization [using, 1-ethyl 3-(3-dimethyl aminopropyl) carbodiimide, 2 mM and N hydroxysuccinimide acrylate, 4 mM] and gelling [using, poly(ethylene glycol) diacrylate, M_n-700, 2 mg/ml]. The acrylate modified CECM pre-gel solution and the gelling agent PEGDA were mixed in the ratio of 1:0.08 (w/w). The consistency of the original viscous CECM hydrogel was reduced by the addition of PBS solution.

Wound healing study in rats

Animal experiments were conducted on 36 sub adult (4-6 weeks of age) male Sprague Dawley rats of 150-200 mg bodyweight, with the statutory permission of the Institutional

Animal Ethics committee (SCT/IAEC-366/JULY/2020/106) under the direct supervision of a veterinarian. Essentially, rats were housed in individually ventilated cages (temperature 22 ± 3°C; humidity 30 – 70%; 12 h day/ light cycle) with *ad libitum* access to feed and water. Animals were anaesthetized using Ketamine (80-100 mg/Kg, Indian Immunologicals Limited, India) and Xylazine (10 mg/Kg, Neon Laboratories Limited, India) in combination intraperitoneally. The surgical site, on the dorsum was shaved with an electrical hair trimmer in caudo-cephalo direction and painted with Betadine Surgical Scrub 7.5% (G. S. Pharmbutor Private Limited, India) for sterilization. Loss of pedal reflex was checked to ensure that the animals were in a surgical plane of anaesthesia. In the dorsal region, about 1 cm posterior to the transverse line connecting lower angle of scapula was considered as the cranial border of wound. Full-thickness dorsal skin excision wounds of 2.5 cm x 1.5 cm dimension craniocaudally were created in each animal using a scalpel blade (scalpel size 15, BP handle 3). Underlying panniculus carnosus muscle was also removed. Immediately after surgery, rats were randomly allotted to three groups as described below. The wound areas were photographed by digital planimetry[10] and was recorded as initial wound area. The first group had only open wound (OW) which served as the control without any assistance for healing. The second group received CECM-gel formulation (CG) for assisted wound healing. The third group was treated with *Gencoll* (GC), a commercially available gel formulation (Cologenesis Healthcare Pvt Ltd, Salem, India) containing gentamycin, and used for assisted skin wound healing applications. The rats were observed and routine veterinary care was given daily. Rats were observed every day for any signs of infection or illness and the wounds were gently cleaned with hypertonic saline every day. The treatment with CG and GC was repeated for the first five days followed by once in every 5 days (10th day and the 15th day). Four rats were selected from each group and euthanized on three time points namely 10, 15 and 20 days, by carbon dioxide asphyxiation. Immediately after the death, digital planimetry was performed and recorded as final wound area. While recording wound area, presence of scab was considered as unhealed area.

Tissue samples of the wounds were collected in 10% neutral buffered formalin along with adjacent normal area for histomorphological evaluation.

Histomorphological evaluation

Skin tissues preserved in 10% neutral buffered formalin were processed through isopropanol and xylene and four-micron thin sections were routinely stained with haematoxylin and eosin (H&E) stains. All the histomorphological evaluations were performed by a veterinary pathologist and light microscopic images were captured using an Olympus BX51 (Olympus Corporation, Japan) mounted with a DP71 camera. The nature of wound healing was evaluated by assessing the progression through re-epithelialisation, inflammation, angiogenesis, and collagen remodelling.

Morphometry

In order to quantitatively evaluate extend of re-epithelialisation, morphometry was performed on the H&E sections using *Image-Pro®* software. For this, images were captured under low power and calibrated. The length between healthy well differentiated epithelium on either end of the neo-epithelium of the healing wound was considered as the total length of the wound. The length of the unbridged neo-epithelium was measured as the unhealed remaining wound length. Percentage of re-epithelialisation was calculated by the formula,

$$\text{Percentage of re-epithelilisation} = \frac{\text{length of re-epithelialised wound}}{\text{length of total wound}} \times 100$$

Statistical analysis

Statistical analysis was performed using *GraphPad Prism 6®*. Students t-test was performed on the planimetry data and the percentage of re-epithelialisation.

RESULTS

Gross pathology and planimetry

Grossly, all the wounds appeared to heal under a scab without any clinical complication. Gross images of the wounds on various time points and the planimetry data are presented in Fig 1 and 2 respectively. Wound healing was similar in all rats in the first 10 days. However, by day 15, wound closure in the CG group appeared better than OW and the GC groups as evidenced by planimetry data (Fig 2) and there was significant difference between CG and GC group. However, no significant difference was statistically apparent in the morphometry data collected on day 20 between the CG and the other groups. On day 20, all the rats in the CG group had 100% healing, while all rats of OW group and GC group had scabs.

Histomorphological Evaluation

Representative histomorphological appearances of the healing wounds are presented in Fig 3, and Fig 5 to Fig 9. Morphometry data on extend of re-epithelialisation is shown in Fig 4. The nature of the healing reaction was similar in all groups, with respect to re-epithelialisation, inflammation, angiogenesis, and collagen remodelling. Additionally, multifocal granulomas and foreign body giant cell reactions were present in the CG and GC groups (Fig 7 and Fig 9).

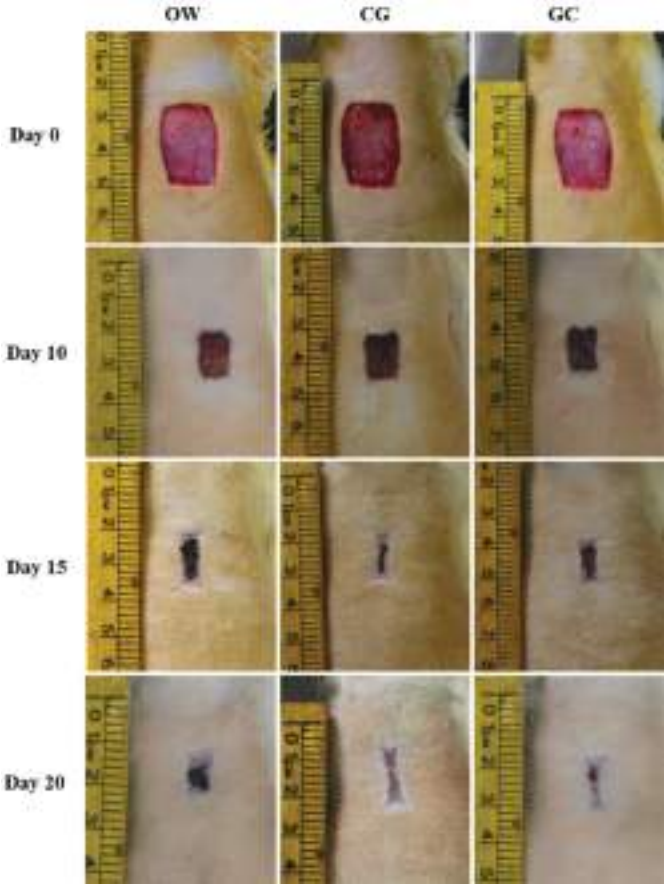

Fig 1. Gross photographs showing the morphology of wounds in rat untreated group (open wound, OW), wounds treated with the gel formulation containing porcine cholecyst extracellular matrix (CG) and *Gencoll* (GC, a commercially available gel formulation containing Gentamycin) on day 0, day 10, day 15, and day 20 after surgery. Note the complete closure of the wound and absence of scab on day 20 in the CG group.

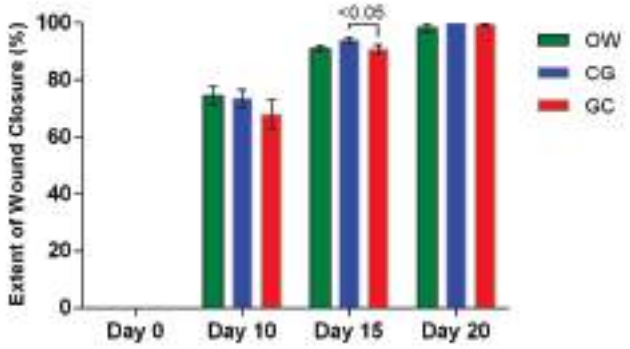

Fig 2. Bar diagram drawn from the planimetry values depicting the extend of wound closure in rats.

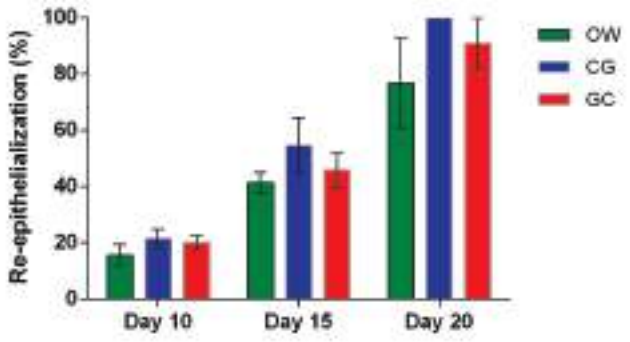

Fig 4. Bar diagram showing percentage of re-epithelialisation in rats with open wound (OW and those treated with cholecyst extracellular matrix gel (CG) and the *Gencoll* (GC). No significant difference between groups was seen, although the re-epithelialisation was complete in all animals of the CG group.

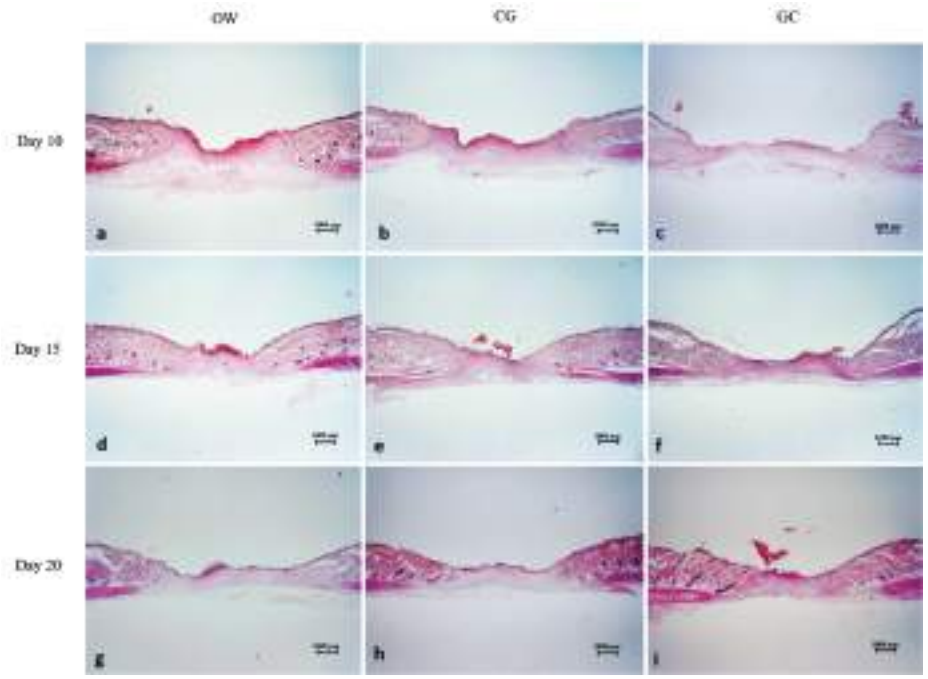

Fig 3. Representative light microscopic images of hematoxylin and eosin-stained sections showing the nature of re epithelialization at low magnification. Re-epithelialisation was complete in CG group by day 20.

However, the nature of the healing reactions progressively varied between groups. On day 10, prominent neo-epithelium characterized by hypertrophied epidermal cells was evident that appeared to migrate from the healthy wound edges towards the centre of the wound bed (Fig 5a to c). These relatively undifferentiated cells having occasional mitotic figures (Fig 5h and 5i), were situated a few cells behind the leading edges in both

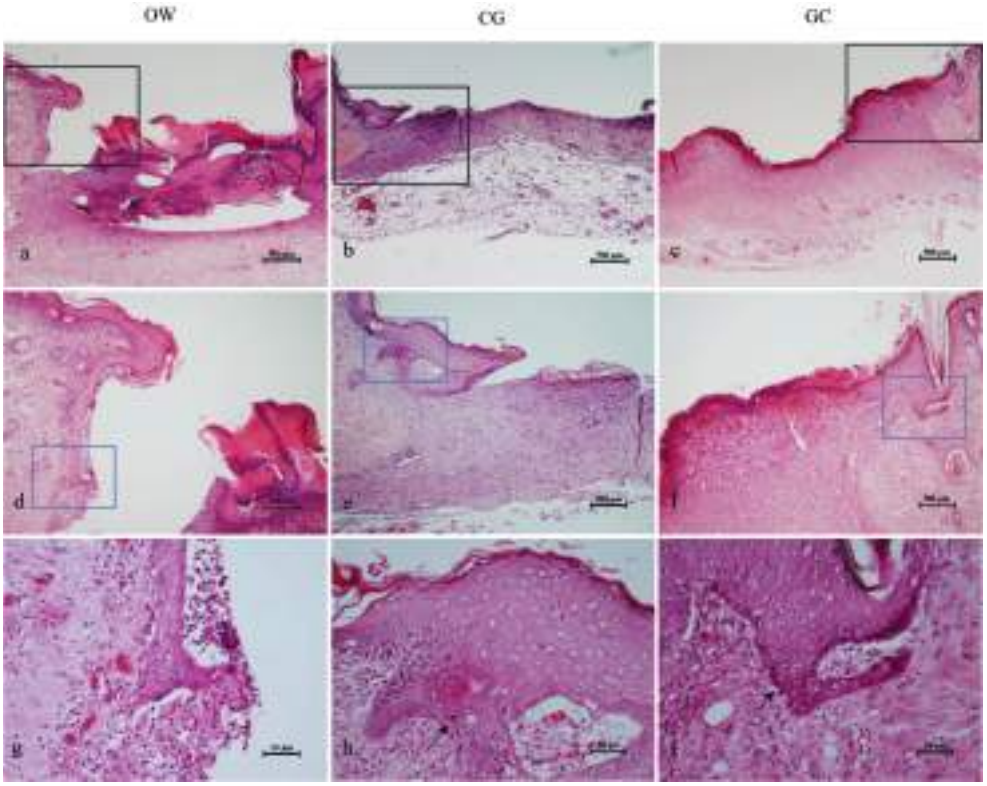

Fig.5. Light microscopic images of hematoxylin and eosin-stained sections showing extend of re-epithelialization on day 10. Occasional mitotic figures (arrow) were present, a few cells behind the tip of the leading edges in the CG (h) and the GC (i) groups, compared to the OW group (g). Mild to moderate inflammation, mostly mononuclear cells was seen in all sections. The marked rectangle represents the area enlarged in the corresponding photographs of the immediate lower row.

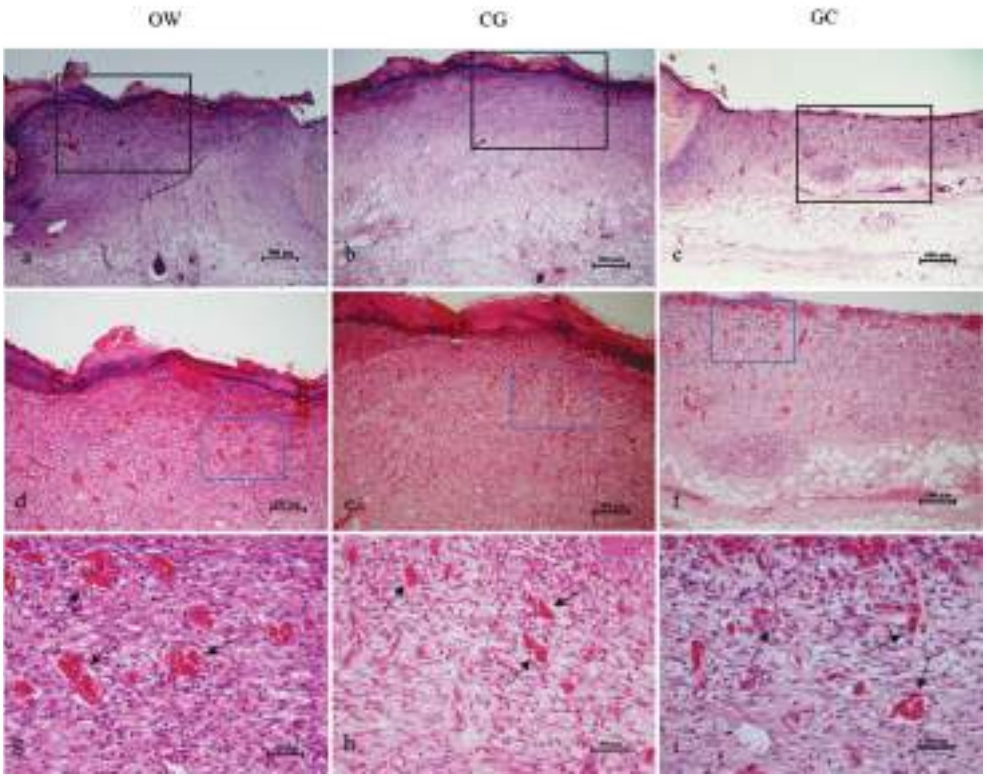

CG and GC groups. Scabs were present in many of the wounds. In the dermis, inflammatory cells (mostly mononuclear), sprouting thin-walled capillaries, and plump fibroblasts were present; as expected in a mild to moderate granulation tissue (Fig6). In addition, granulomas were present in CG and GC treated rats (Fig 7).

Between day 15 and day 20 day, the extent of re-epithelialisation was marked by a reduction of wound length and the epidermal height reduced, as epidermal cells matured and differentiated (Fig 9). Re-epithelialization was complete in all rats of the CG group by day 20, as evident from the quantitative morphometry data. Besides, functional differentiation evaluated by the degree of hyalinisation, keratinisation, as well as rete peg formation were also prominent in the CG group (Fig 9h). In the dermis, by day 15 and 20, granulation tissue were markedly reduced, and thin-walled capillaries were replaced by mature muscular blood vessels. The presence of plump fibroblasts was still evident in CG group (Fig 9k) even at day 20, contrasting sharply with OW and GC groups featuring mature fibrocytes and compact collagen (Fig 9g and 9i).

Fig.6. Light microscopic images of hematoxylin and eosin-stained sections showing granulation tissue on day 10 characterized by the presence of capillaries filled with RBCs in the lumen (g, h and i; arrow), fibroblasts and mononuclear inflammatory cells.

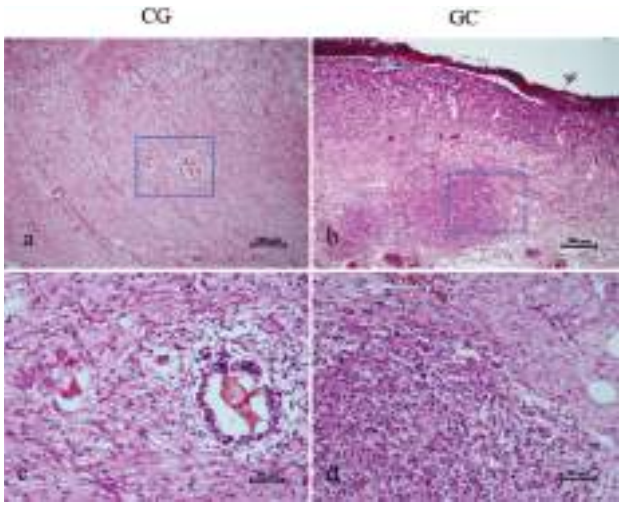

Histomorphological features of different groups at various time points are provided in tabular form (Table 1).

Morphometry

The extent of re-epithelialisation was more in the CG group than OW and GC groups. This was perceptible at day 15 (Fig 4), where CG group had 54.76% re-epithelialisation when compared to GC (45.88%) and OW (41.39%) groups. By day 20, re-epithelialisation was complete in all four animals of the CG group, three animals of the GC and two animals of the OW group.

Fig 7. Photomicrographs of hematoxylin and eosin-stained sections showing granuloma in CG and GC group on day 10. Multifocal granulomas comprising of mononuclear inflammatory cells were also clearly visible in the boxed areas of first row which are magnified in the second row.

Table 1. Table showing summary of important histopathological lesions

Time points	Histomorphological parameters	Open Wound	Cholecystic Extracellular Matrix gel	*GenColl*®
Day 10	Nature of re-epithelialisation	Prominent neo-epithelium characterized by hypertrophied epidermal cells was evident that appeared to migrate from the healthy wound edges towards the centre of the wound bed.	Prominent neo-epithelium characterized by hypertrophied epidermal cells was evident that appeared to migrate from the healthy wound edges towards the centre of the wound bed.	Prominent neo-epithelium characterized by hypertrophied epidermal cells was evident that appeared to migrate from the healthy wound edges towards the centre of the wound bed.
	Mitotic figures	Mitotic figures were not evident.	Occasional mitotic figures were found, a few cells behind the leading edges of proliferating epithelium.	Occasional mitotic figures were found, a few cells behind the leading edges of proliferating epithelium.
	Inflammation and granulation tissue formation	Presence of granulation tissue and mild to moderate inflammation (mostly mononuclear cells) was also observed.	Presence of granulation tissue and mild to moderate inflammation (mostly mononuclear cells) was also observed.	Presence of granulation tissue and mild to moderate inflammation (mostly mononuclear cells) was also observed.
	Presence of granulomas	Absent	Present	Present
Day 15	Granulation tissue	Persistence of unorganised granulation tissue.	Granulation tissue were markedly reduced, and thin-walled capillaries were replaced by mature muscular blood vessels.	Persistence of unorganised granulation tissue.
Day 20	Completion of re-epithelialisation	Incomplete re-epithelialisation	Complete re-epithelialisation	Incomplete re-epithelialisation
	Extend of functional differentiation of epithelial layers	Incomplete differentiation	Functional differentiation of epithelium was marked by degree of hyalinisation, keratinisation, as well as rete peg formation.	Incomplete differentiation
	Nature of fibroblast/ fibrocyte	Mature fibrocytes were abundant in dermis	Presence of plump fibroblasts was still evident in the dermis, rather than fibrocytes	Mature fibrocytes were abundant in dermis
	Collagen deposition	Compact mature collagen were present in the dermis.	less compact collagen deposition in dermis	Compact mature collagen were present in the dermis.
	Presence of foreign body giant cells	Not evident	Occassionaly, foreign body giant cells were present	Occassionaly, foreign body giant cells were present

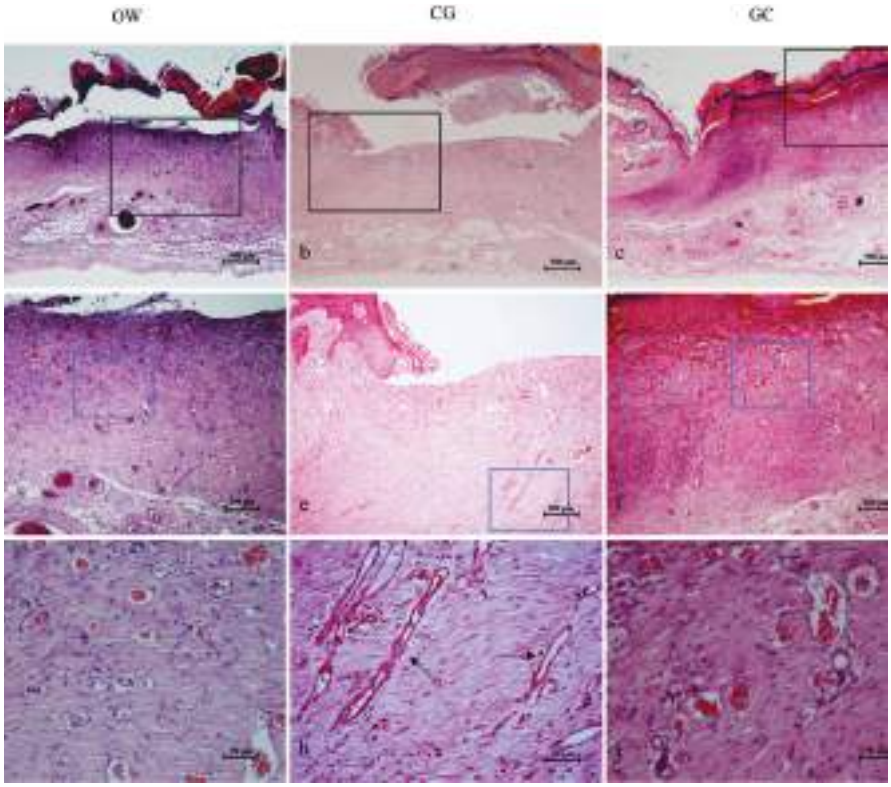

Fig. 8. Light microscopic images of hematoxylin and eosin-stained sections showing angiogenesis and collagen remodeling on day 15. There was regression of vascular channels and accumulation of fibroblasts in dermis of CG group (b,e and h). Note that in the CG group, there was matured blood vessels (arrow) seen perpendicular to the wound surface, probably primary branches of the main blood vessels beneath the panniculus carnosus muscle (e and h). However, in the OW and GC groups the neo-blood vessels are terminal branches in tufts as commonly seen in unorganized granulation tissue indicating a delayed healing reaction.

DISCUSSION

Healing of skin wounds happen through regeneration and/or repair depending on the extent/depth of the injury. Based on the depth of wounds, excision skin wounds can be classified into superficial, partial-thickness, or full-thickness[12]. Skin wounds involving only epithelium heal by regeneration and restoration of the pristine architecture; wounds involving dermis heal by a repair process involving variable degrees of inflammation, angiogenesis, collagen deposition and remodelling[11]. In this study, healing response of a full-thickness skin excision wound in a rat model assisted by the application

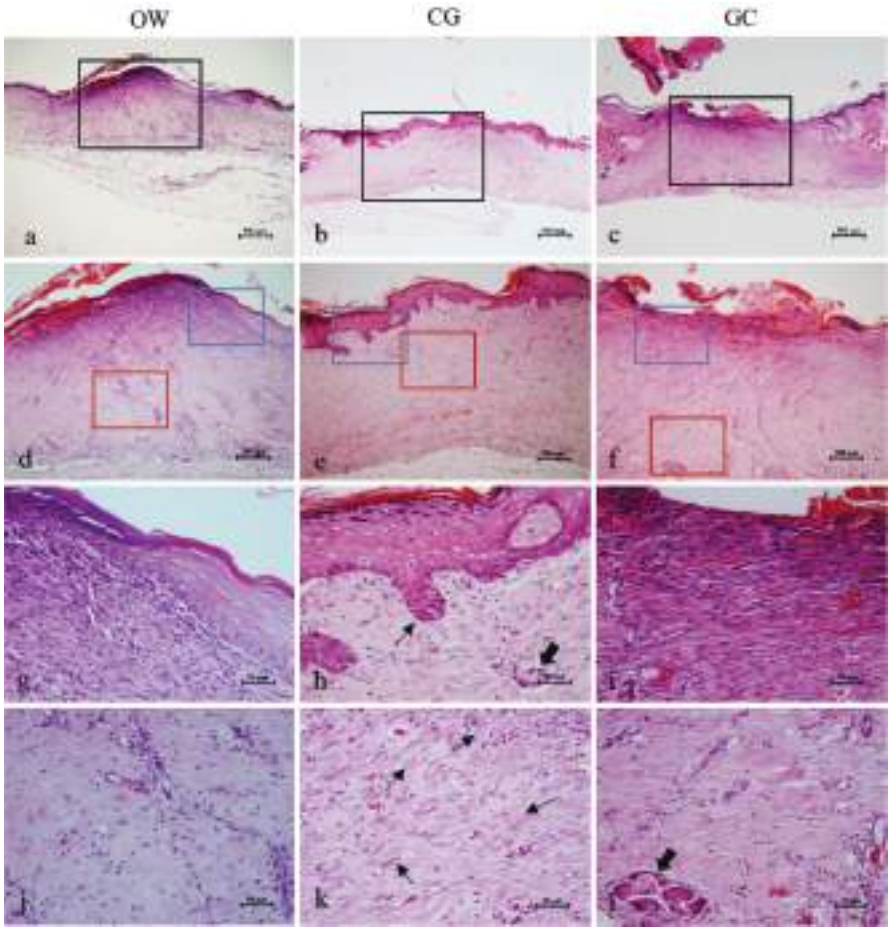

Fig. 9. Light microscopic images of hematoxylin and eosin-stained sections showing extend of wound closure and maturation of collagen by day 20. Complete re-epithelialisation was observed in the CG group (Fig b, e, h) with differentiation of epithelial layers visualised as hyalinisation and keratinisation of epidermis and restoration of rete pegs (Fig h, thin arrow). Relatively, number of plump fibroblasts (Fig k) was aboundant in CG group compared to the OW and the GC groups. In the OW and the GC groups, re-epithelialisation was not complete. Moreover, the inflammation, granulation tissue, angiogenesis and excess fibrosis (g and i) were persistent in the OW and GC groups. Occassionaly, foreign body giant cells were present in both the CG and the GC groups (Fig h and l; thick arrow). Blue and red boxed areas of the second row are magnified in the third and fourth rows respectively.

of a gel formulation of cholecyst extracellular matrix. The wound involved removal of the epidermis (epithelium), entire dermis down to subcutaneous tissue and the panniculus carnosus muscle. The removal of the panniculus carnosus muscle avoided healing by contraction[12]. The observations on the OW group facilitated the healing response of unassisted healing, whereas the GC group gave an option for comparison with nature of assisted healing with a predicate device.

Grossly, the nature of wound closure was similar in all groups up to 10 days. Faster wound closure in CG group was visibly observed by 15 days. By day 20, wound closure appeared to have completed amongst four rats in CG, while wounds still had scabs in GC and OW groups. However, by day 20 re-epithelialisation was complete in all four rats in CG, three and two rats GC and OW groups respectively. This could probably be due to the presence of scab observed during planimetry and absolute re-epithelialisation observed at histomorphometry. The morphometry data corroborated the histomorphological observation. Lack of significant difference in morphometric data of re-epithelialisation on day 20 could be because, the wounds of the CG might have healed much before day 20 and the wound in the OW and GC groups were only nearing completion of the healing process. This notion is supported by previous observations by similar experiments using different preparations of the CECM formulation[10, 13]. These reports suggest complete re-epithelialisation of rat excision wound by day 16 and day 18 respectively compared to OW which healed only by 21 or 24 days. Presumably, more interim assessments of the healing process between 16 to 19 days would have been more precise and cogent. However, extend of re-epithelialisation gives a strong indication of the better healing potential of the CG, even in comparison to the established commercial product GC.

Histomorphological evaluation showed infiltrating inflammatory cells in all samples collected on day10. Although there was a reduction in acute inflammation, infiltration of mononuclear cells (granuloma) and foreign body giant cell reaction persisted even on day 15 and day 20. The sprouting blood vessels were abundant in day 10 but regressed by day 15 especially in the CG group. This could probably be an indication of the faster healing potential of the CG compared to GC and unassisted healing in OW groups.

In this study, granulomas with foreign body giant cells, considered as histological markers of chronic inflammation in response to foreign materials[14], were observed in the wounds treated with CG and GC formulations. Considering that 20 days of duration is too short a period for complete degradation of CECM formulations[4,] the presence of foreign body reaction was not surprising. Further, gel components which did not degrade might have also stimulated the granulomas and the foreign body giant cell reactions. Remarkably, the foreign body giant cell reaction were not present in the OW group.

Collagen remodelling also had some qualitative difference between groups. Although plump fibroblasts and mature fibrocytes were present throughout the study points in all groups. It is known that the CECM can stimulate fibroblasts that synthesise Type III degradable collagen and less of Type I mature collagen[5], that contribute scar formation. In the present study the CG group had a lot of plump fibroblast still actively secreting collagen even at day 20 and the formation of thick bundles of collagen was relatively less. However, a detailed study for differentiating Type I collagen and Type III collagen was not attempted in this experiment. A quantitative evaluation for differentiating the proportion of the Type I collagen and the Type III collagen might have given a better indication of the scarring potential of CG.

The persistence of inflammation and granulation tissue at variable degrees also indicated the differential healing potential of the gel-assisted healing. A detailed histomorphological and morphometric evaluations deploying immunohistochemistry and molecular pathology tools are required for deciphering the nature of healing with respect to inflammation, angiogenesis and collagen remodeling[15]. Nevertheless, the overall preliminary results suggested that assisted healing with either of the gels healed the wounds faster compared to OW. The CG-treated rats probably had a better healing response than those treated with the predicate device, as evidenced by the extent of gross observations on wound closure and morphometry data on re-epithelialisation. Therefore, it is plausible to think that the CG formulation has better wound healing potential than GC, but further corroborative evidence is required to establish the notion.

In conclusion, CG promoted better healing than the GC or the OW groups. However, the present CG formulation may need further modifications before advocating its use as an effective wound healing gel for faster healing with minimal scarring.

ACKNOWLEDGMENTS

This work was supported by the Indian Council of Medical Research (ICMR), Project No.: 2020-6969 to Dr Purnima C. She wishes to thank Director, Sree Chitra Tirunal Institute for Medical sciences and Technology, Thiruvananthapuram 695012 for hosting the research project in the Division of Experimental Pathology.

Financial support & sponsorship: Yes

Conflicts of Interest: None

Use of Artificial Intelligence (AI)- Assisted Technology for manuscript preparation: The authors confirm that there was no use of AI- assisted technology for assisting in the writing of the manuscript and no images were manipulated using AI.

REFERENCES

1. Saldin LT, Cramer MC, Velankar SS, White LJ, Badylak SF. 2017. Extracellular matrix hydrogels from decellularized tissues: Structure and function. *ActaBiomater;*49:1-15.
2. Wosicka-Frąckowiak H, Poniedziałek K, Woźny S, Kuprianowicz M, Nyga M, Jadach B, Milanowski B. 2024. Collagen and Its Derivatives Serving Biomedical Purposes: A Review. *Polymers;*16(18):2668.
3. S.H. Aswathy, U. Narendrakumar, I. Manjubala. 2020.Commercial hydrogels for biomedical applications,Heliyon, Volume 6, Issue 4,,e03719,ISSN 2405-8440,https://doi.org/10.1016/j.heliyon.2020.e03719.
4. Anilkumar TV, Vineetha VP, Revi D, Muhamed J, Rajan A. 2014. Biomaterial properties of cholecyst-derived scaffold recovered by a non detergent/enzymatic method. J Biomed Mater Res B102:1506-1516.
5. Revi D, Geetha C, Thekkuveettil A, Anilkumar TV. Fibroblast loaded cholecyst-derived scaffold induces faster healing of full-thickness burn wound in rabbit. J Biomater Appl. 2016;30: 1036-1048.
6. Reshma S. Nair, Jimna Mohamed Ameer, Malcolm R. Alison, Thapasimuthu V. Anilkumar.2017. A gold nanoparticle coated porcine cholecyst-derived bioscaffold for cardiac tissue engineering, Colloids and Surfaces B: Biointerfaces157: 130-137.
7. Mony MP, Anilkumar TV. 2020. Controlled cross-linking of porcine cholecyst extracellular matrix for preparing tissue engineering scaffold. J Biomed Mater Res. 108B: 1057–1067.
8. Raj R, Sobhan PK, Pratheesh KV, Anilkumar TV. 2020. A cholecystic extra cellular matrix-based hybrid hydrogel for skeletal muscle tissue engineering. J Biomed Mater Res- Part A108:1922-1933.
9. Raj R, Shenoy SJ, Mony MP, Pratheesh KV, Nair RS, Geetha CS, Sobhan PK, Purnima, C, Anilkumar TV. 2021. Surface Modification of Polypropylene Mesh with a Porcine Cholecystic Extracellular Matrix Hydrogel for Mitigating Host Tissue Reaction. ACS Appl. Bio Mater4:3304-3319.
10. Pratheesh KV, Nair RS, Purnima C, Raj R, Mony MP, Geetha CS, Sobhan PK, Ramesan RM, Nair PD, Thomas LV, Anilkumar TV. 2025. An injectable hydrogel of porcine cholecyst extracellular matrix for accelerated wound healing. J Biomed Mater Res A.113(1):e37795.
11. Mark R. Ackermann, Chapter 3 – Inflammation and Healing, Editor(s): James F. Zachary, Pathologic Basis of Veterinary Disease (Sixth Edition),Mosby,2017,Pages 73-131.e19,ISBN 9780323357753
12. Seaton M, Hocking A, Gibran NS. 2015. Porcine models of cutaneous wound healing. ILAR J56(1):127-38.
13. Mony MP, Shenoy SJ, Raj R, Geetha CS, Pratheesh K V., Nair RS, Purnima C, Anilkumar TV. Gelatin-Modified Cholecyst-Derived Scaffold Promotes Angiogenesis and Faster Healing of Diabetic Wounds. ACS Appl Bio Mater. 2021;4:3320-3331.
14. Anderson JM, Rodriguez A, Chang DT. 2008. Foreign body reaction to biomaterials, Seminars in Immunology, 20 (Issue 2): 86-100,
15. Muhamed J, Revi D, Rajan A, Anilkumar TV. Comparative local immunogenic potential of scaffolds prepared from porcine cholecyst, jejunum, and urinary bladder in rat subcutaneous model. J Biomed Mater Res B ApplBiomater. 2015 Aug;103(6):1302-11. doi: 10.1002/jbm.b.33296. Epub 2014 Nov 5. PMID: 25370716.

Indian J. Vet. Pathol., 50(3) : 236-242, 2026: DOI: https://doi.org/10.56093/4xp5bc50

RESEARCH ARTICLE

Protective effect of ashwagandha *(Withania somnifera)* on glyphosate induced toxicity in body weight and selected organs of Kuroiler birds

K. Kalai* and S. Baruah
Department of Veterinary Pathology, College of Veterinary Sciences and A.H., R.K. Nagar, West, Tripura - 799 008

Address for Correspondence
K. Kalai, Associate Professor, E-mail: kanikakalai@gmail.com
ORCID Id: 0000-0002-8013-6498

Received: 4.3.26; Accepted: 3.4.26

ABSTRACT

The present study evaluated the toxic effects of glyphosate and the ameliorative potential of *Withania somnifera* (ashwagandha/ Indian ginseng) powder on growth performance and organ integrity in kuroiler birds. A total of 75 birds were observed over a period of three months for changes in body weight and pathological alterations in the lungs, brain, spleen, pancreas and gastrointestinal tract (proventriculus, gizzard and intestine). Orally glyphosate-exposed birds exhibited a significant reduction ($p<0.05$) in body weight gain compared to control and Ashwagandha-supplemented groups. The growth suppression was associated with marked gross and histopathological lesions in the examined organs, indicating systemic cellular stress and tissue damage. In contrast, birds co-administered with Ashwagandha showed significant improvement in body weight and reduced severity of pathological alterations. High-performance liquid chromatography (HPLC) analysis of liver, kidneys, brain and skeletal muscle samples did not detect residues of the parent glyphosate compound. This finding suggests possible rapid metabolism or elimination of glyphosate, or that tissue damage may be mediated by its metabolites rather than by persistence of the parent compound. The study demonstrates the systemic toxic potential of glyphosate exposure and highlights the protective efficacy of Ashwagandha as a natural ameliorative agent against herbicide-induced toxicity in poultry.

Key words: Ashwagandha, Glyphosate, Growth performance, Histopathology, HPLC, Kuroiler

INTRODUCTION

Glyphosate is one of the most widely used herbicides worldwide[1] and its extensive application in agriculture has raised concerns regarding its potential toxic effects on non-target organisms including birds[2]. Exposure to glyphosate through contaminated feed, drinking water or environmental residues may result in systemic toxicity mediated through oxidative stress, cellular degeneration and disruption of normal physiological functions. Free-range birds such as Kuroiler, a widely reared dual-purpose backyard poultry breed in India, are particularly vulnerable due to their scavenging nature and close interaction with the external environment. Such exposure poses a potential threat to growth performance, immune competence and organ integrity in poultry.

Ashwagandha (*Withania somnifera*) is widely regarded as the Indian ginseng. It is a well-known medicinal herb with strong antioxidant, anti-inflammatory and tissue-protective properties[3&4]. It has been traditionally used to improve reproductive health and enhance stress tolerance. The withanolides present in *W. somnifera* are known to inhibit lipid peroxidation by their antioxidant properties[5&6]. Being a highly valued drug in ayurveda, it was decided to explore the utility of ashwagandha in combating glyphosate induced toxicity in kuroiler birds. So, the present study was undertaken to evaluate the toxico-pathological effects of glyphosate and to assess the ameliorative potential of ashwagandha supplementation on growth performance and organ integrity in Kuroiler birds.

How to cite this article : Kalai, K. and Baruah, S. 2026. Protective effect of ashwagandha *(Withania somnifera)* on glyphosate induced toxicity in body weight and selected organs of Kuroiler birds. Indian J. Vet. Pathol., 50(3) : 236-242.

MATERIALS AND METHODS

Ethical Approval for Animal Studies

The experiment was conducted for a period of three months to determine the effects of chronic toxicity of glyphosate in Kuroiler chickens and its amelioration by ashwagandha. The study was carried out after obtaining prior approval from the Institutional Animal Ethics Committee (IAEC), College of Veterinary Science, Assam Agricultural University (AAU), Khanapara, Guwahati, Assam (Approval No. 770/ac/CPCSEA/FVSc/AAU/IAEC/17-18/559 dated 09.08.2017). All experimental procedures were performed in accordance with CPCSEA guidelines for the care and use of experimental animals.

Experimental design

A total of 75 kuroiler birds aged three months were selected for the study. Birds were maintained under standard management conditions and were provided with standard pellet feed and clean drinking water ad libitum. The birds were kept under constant observation throughout the experimental period. The birds were randomly divided into three groups, each consisting of 25 birds. Group I served as control and provided with standard pellet feed and clean drinking water. Group II was administered glyphosate (field grade glyphosate, HIJACK, 41% glyphosate SL; Insecticide India Ltd., Rajasthan) was used for induction of experimental toxicity orally at a dose rate of 27.8 mg/kg body weight daily for a period of three months. The dose was calculated based on a pilot study conducted for LD_{50} estimation as per OECD guideline 425[7, 8]. Group III was administered glyphosate along with ashwagandha powder (Baidyanath Ayurved Ltd.) supplementation at the rate of 0.5% of feed and was provided daily throughout the experimental period[9]. Body weight was measured in the electronic measuring device and recorded at weekly intervals.

Histopathology

Tissue samples from brain, spleen, heart, lungs, proventriculus, gizzard, intestine and pancreas were collected for histopathological examination. Collected samples were fixed in 10% neutral buffered formalin and processed by standard routine histopathological procedure. The paraffin embedded tissue sections were cut at 4–5 µm thickness and stained with Haematoxylin and Eosin (H&E) for microscopic examination[10]. Histopathological lesions were graded on a semi-quantitative scale of 0 to 3, where 0 = normal, 1 = mild, 2 = moderate and 3 = severe, based on the extent and severity of tissue alterations.

High profile liquid chromatography (HPLC)

Tissues from liver, kidneys, brain and muscle were collected in plastic pouch and transferred to laboratory in ice packs and stored in deepfreeze (at -20°C) for HPLC to detect the presence of glyphosate parent compounds[11]. The sample was processed and derivatized at the Department of Veterinary Pharmacology and Toxicology, CVS, AAU, Khanapara. HPLC was performed at Biotech Park, IIT, Guwahati. One gram of chicken tissue (liver, kidney, brain and muscle) was finely minced and transferred into a 250 mL volumetric flask. A mixture of water and methanol (4:1, v/v) was added and the contents were mixed using a circular tube rotator for 1 h. The homogenate was centrifuged at 4000 rpm for 15 min and the supernatant was collected. The supernatant was mixed with an equal volume of methanol, vortexed and centrifuged again at 4000 rpm for 30 min. The final supernatant was diluted fivefold with distilled water. For derivatization, 1 mL of the extract was taken in a 15 mL polypropylene tube. To this, 0.25 mL of 50 mM borate buffer (pH 9.5) and 0.3 mL of 2 g/L FMOC-Cl (Sigma aldrich) in acetonitrile were added and vortex mixed. The reaction mixture was kept overnight at room temperature. The reaction was terminated by adding 0.3 mL of 2% phosphoric acid. The final solution was filtered through a 0.2 µm syringe filter and analysed by HPLC. A UHPLC machine with fluorescent detector was used with a C18 reverse phase HPLC column (ACE 5 µm 4.6x 250 mm). Elution was done with a mobile phase consisting of 50 mM phosphate buffer (pH 2.5) and HPLC grade acetonitrile. Flow rate was fixed at 0.8 ml/min. Fluorescence detection set at emission wavelength 270 nm with excitation at 325 nm. The standard solution of glyphosate (Glyphosate, analytical grade, Sigma Aldrich, Bangalore) was prepared by dissolving 2 mg of glyphosate in 10 ml of HLC grade water in a graduated glass tube. Working standard solutions of 0.05, 1.0, 2.0, 4.0 and 8.0 mg/ml were prepared by diluting standard solution with appropriate volume of HPLC grade water. The glyphosate solutions were then derivatized with FMOC-Chloride overnight. Then filtered through 0.2 mm syringe filter and injected into UHPLC and standard curve was prepared as shown in the Fig. 1.

Statistical analysis

The data generated from the experiment were subjected to statistical analysis using GraphPad Prism software. Results were expressed as mean ± standard error (SE). The differences among groups were analysed by one-way analysis of variance (ANOVA)

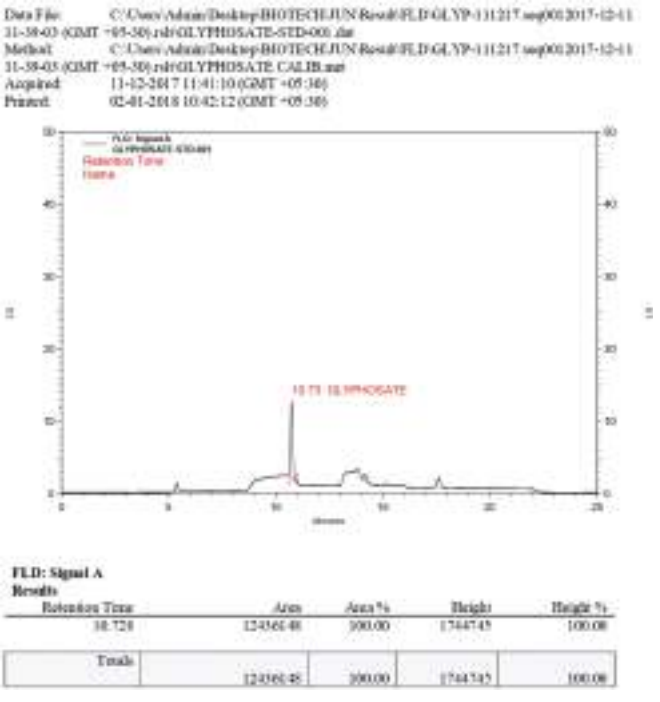

Fig. 1. Glyphosate standard curve.

and students t test. Values of P< 0.05 and P< 0.01 were considered statistically significant and highly significant respectively[12].

RESULT

The weekly mean body weights of birds are presented in Table 1 and Fig. 1. Body weight increased progressively in all groups during the experimental period; however, the control group consistently recorded higher mean body weight than the treated groups. The mean body weight in group II differed significantly (P< 0.05) and highly significantly (P< 0.01) from the 3rd to 10th week when compared to the groups I and III. During the 11th and 12th weeks, the mean body weight showed a highly significant difference (P< 0.01) among all three groups.

The macroscopical examination in Group II birds predominantly exhibited pulmonary congestion and haemorrhages (Fig. 3). Splenic involvement was characterized by splenomegaly, late-stage pallor and infarction (Fig. 4). Myocardial petechial haemorrhages (Fig. 5) and cerebral vascular congestion and swelling (Fig. 6) found in later stages of the experiment. In the gastrointestinal tract, a thin kaolin membrane adhered to the gizzard mucosa and moderate haemorrhages in the caecal tonsils (Fig. 7). In group III birds the gross lesions

Table 1. Body weight (mean ± SE).

Time of weighing (week)	Body weight (Kg)		
	Group I	Group II	Group III
1	1.05±0.02	1.07±0.02	1.04±0.02
2	1.34±0.01	1.24±0.01*	1.27±0.02
3	1.59±0.01	1.35±0.02**	1.53±0.01
4	1.76±0.02	1.50±0.02**	1.67±0.03
5	1.88±0.02	1.58±0.02**	1.83±0.02
6	2.10±0.03	1.68±0.02**	2.04±0.02
7	2.32±0.04	1.83±0.02**	2.26±0.03
8	2.48±0.05	1.97±0.03**	2.38±0.03
9	2.63±0.05	2.10±0.03**	2.48±0.03
10	2.71±0.06	2.21±0.02**	2.56±0.03
11	2.89±0.06	2.29±0.02**	2.68±0.04
12	3.12±0.06**	2.37±0.02**	2.76±0.04

*P < 0.05, **P < 0.01

Table 2. Comparative lesion scoring (Group II vs Group III).

Organ	Group II (Glyphosate)	Group III (Glyphosate+Ashwagandha)
Lungs	2.00 ± 0.12*	1.00 ± 0.08
Brain	1.50 ± 0.10*	1.00 ± 0.07
Spleen	1.75 ± 0.11*	1.00 ± 0.09
Pancreas	2.00 ± 0.13*	1.00 ± 0.08
Heart	1.00 ± 0.09*	0.50 ± 0.05
Proventriculus	2.00 ± 0.12*	1.00 ± 0.07
Gizzard	2.00 ± 0.11*	1.00 ± 0.08
Intestine	2.00 ± 0.14*	1.00 ± 0.09

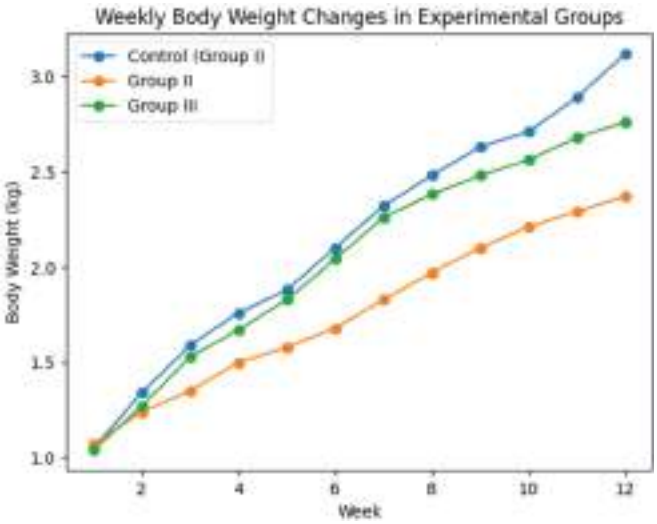

Fig. 2. Changes in body weight in experimental groups.

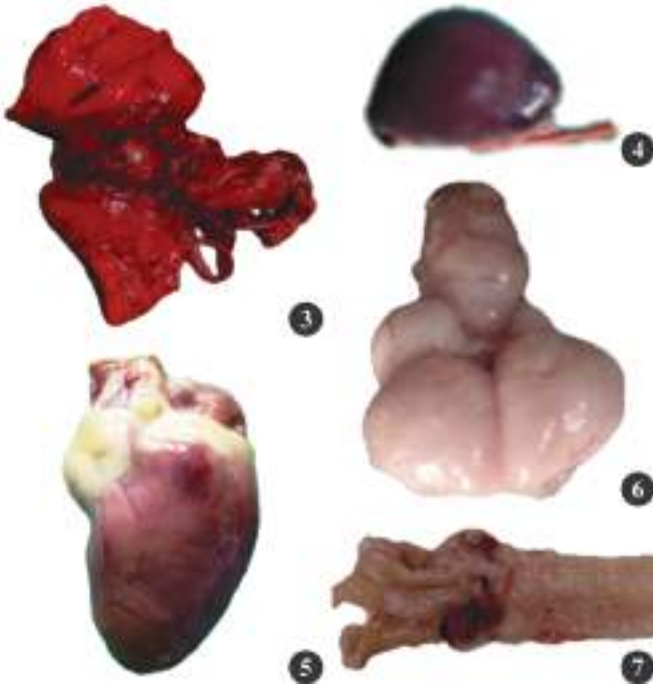

Fig. 3. Photograph showing congestion in lungs (group II); **Fig. 4.** Photograph showing swelling of cerebrum (group II); **Fig. 5.** Heart showing focal petechial haemorrhage in myocardium (group II); **Fig. 6.** Infarct in spleen (group II); **Fig. 7.** Photograph showing haemorrhage in cecal tonsil (group II).

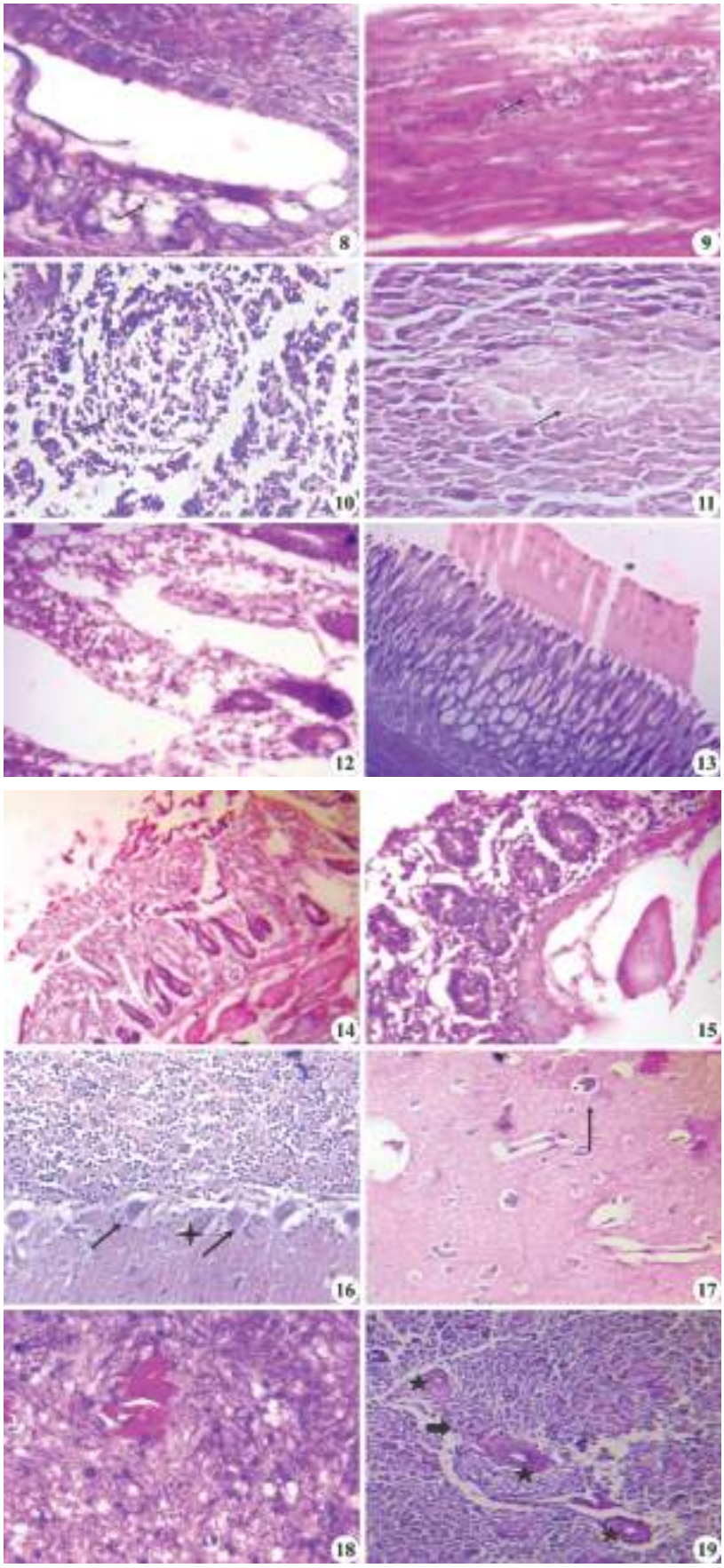

were not observed in all the organs.

Microscopical examination of lungs in group II revealed haemorrhage, congestion and emphysema, perivascular aggregation of mononuclear cells, bronchial lymphoid hyperplasia. (Fig. 8) Heart sections revealed focal myocardial inflammatory infiltration (Fig. 9). Depletion of lymphoid tissue observed in spleen (Fig. 10). Pancreatic islets appeared granular and degenerated (Fig. 11). Proventriculus showed cellular necrosis, haemorrhage and epithelial sloughing (Fig. 12). Gizzard exhibited decreased keratinoid layer and sloughing of koilin membrane (Fig. 13). Intestine showed desquamation of epithelium and necrotic debris and increased secretory cells in large intestine (Fig. 14 & 15). Brain sections showed congestion, vacuolation, neuronophagia and degeneration of Purkinje cells (Fig. 16-18). Spleen revealed formation of secondary lymphoid follicles and thickening of blood vessels in group III birds (Fig. 19). Histopathological lesion scores were significantly higher ($p < 0.05$) in glyphosate-treated birds (Group II) compared to the Ashwagandha-supplemented group (Group III) across all examined organs. The absence of lesions in Group III indicates a significant protective effect of Ashwagandha against glyphosate-induced tissue damage.

In the present study glyphosate parent compound was not detected in any of the

Fig. 8. Mild hypertrophy of bronchial epithelium in lungs (H&E stain 400X); **Fig. 9.** Focal cellular infiltration in myocardium (H&E stain 100X, group II); **Fig. 10.** Spleen (Group II) Depletion of lymphoid follicles (H&E stain 100X); **Fig. 11.** Pancreas (Group II) showing degeneration in Islets of Langerhans (H&E stain 400X); **Fig. 12.** Proventriculus showing necrotic secretory cells (H&E stain 400X); **Fig. 13.** Gizzard, less keratinoid material in gastric pit and sloughing of kaolin membrane (H&E stain 100X); **Fig. 14.** Intestine showing sloughing and desquamation (H&E stain 100X); **Fig. 15.** Large intestine increase in secretary cells (H&E stain 100X); **Fig. 16.** Degeneration in Purkinje cells. Pyknosis of nucleus (star), Karyolysis (arrow) (Group II, H&E 400X); **Fig. 17.** Perinuclear vacuolation and nuronophagia in cerebrum (arrow) (Group II, H&E 400X); **Fig. 18.** Congestion in brain (Group II, H&E 400X); **Fig. 19.** Spleen (Group III) showing thickening of blood vessels and formation of secondary lymphoid follicles (H&E stain 100X).

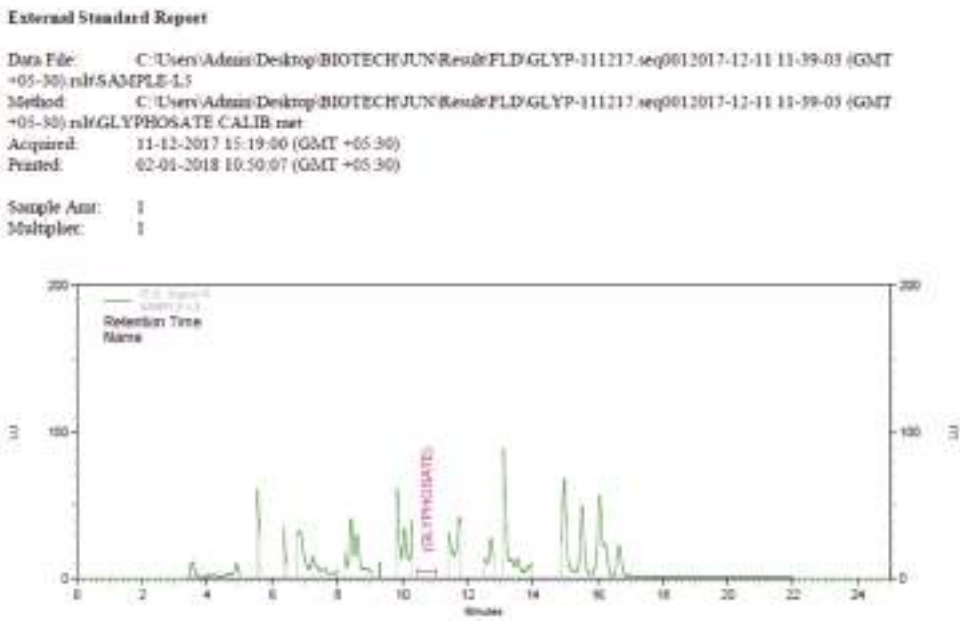

Fig. 20. UHPLC Curve in sample.

tested samples by UHPLC (Fig. 20)

DISCUSSION

The present study demonstrates that chronic exposure to glyphosate exerts significant adverse effects on growth performance and multiple organ systems in kuroiler birds. The marked reduction in body weight gain observed in Group II birds can be primarily attributed to the toxic impact of glyphosate on the gastrointestinal tract. This toxicity likely induces diarrhoeal conditions and compromises intestinal integrity resulting in impaired digestion and nutrient absorption. Such findings are consistent with earlier reports that identify reduced growth performance as a key indicator of systemic toxicity following chronic exposure[13, 14]. The architectural disruption in the spleen is indicative of an immunotoxic response[15]. Such alterations are often associated with oxidative stress–mediated damage and can impair normal immune function[16]. Similar findings reported in previous studies highlight that toxicants like glyphosate can induce lymphoid depletion and structural disorganization in immune organs, ultimately leading to immune dysregulation[17, 18]. Furthermore, the gastrointestinal alterations noted in the study may also be linked to glyphosate-induced disruption of the normal gut microbiota[19].

Glyphosate is known to affect microbial populations by inhibiting the shikimate pathway, which is present in many commensal bacteria. The pancreatic lesions are attributed to the affect in mRNA expression of some enzymes such as Interleukin 6 (IL) in pancreatic tissue[20]. This disruption can lead to intestinal dysbiosis, further exacerbating nutrient malabsorption and contributing to the overall decline in health status. Brain lesion observed in the present study, including congestion, cytoplasmic vacuolation and neuronophagia, suggest substantial neuronal injury. These changes may be mediated through excitotoxic mechanisms and the generation of reactive oxygen species leading to oxidative stress and mitochondrial dysfunction causing neuronal degeneration[21]. The ability of glyphosate and its metabolites to induce oxidative damage in neural tissues has been increasingly recognized, thereby supporting the observed histopathological findings[22]. An important aspect of glyphosate toxicokinetics is its rapid biotransformation into metabolites such as amino methyl phosphonic acid (AMPA), which are themselves biologically active and contribute to overall toxicity. Thus, the absence or low detection of the parent compound in tissues does not preclude toxic effects, as these may be mediated by its metabolites and associated co-formulants.

In contrast, birds in Group III supplemented with ashwagandha powder showed significant improvement in growth performance along with the absence of notable histopathological lesions. This indicates a protective and ameliorative role of the plant. The beneficial effects of Ashwagandha can be attributed to its well-documented adaptogenic, antioxidant and anabolic properties. These properties enhance the physiological resilience of the host, mitigate oxidative stress and help maintain cellular integrity under toxic conditions[23, 24].

CONCLUSION

Chronic glyphosate exposure induces significant systemic toxicity in kuroiler birds, as evidenced by impaired growth performance and multisystemic pathological alterations. The findings also highlight the need for comprehensive evaluation of the toxic contributions of glyphosate metabolites, as well as formulation adjuvants and surfactants, which may exacerbate overall toxicity. Dietary supplementation with ashwagandha powder demonstrated a pronounced protective effect by mitigating toxic insults, preserving tissue integrity and improving physiological performance. These results underscore its potential as a phytogenic adaptogen for alleviating herbicide-induced stress and enhancing productivity in poultry under conditions of agrochemical exposure. Further investigations are warranted to elucidate the precise molecular mechanisms underlying its protective actions and to establish optimal dosage regimens for effective field-level application.

ACKNOWLEDGEMENT

The authors gratefully acknowledge the financial support provided by the Authority of the College of Veterinary Science (CVS), Khanapara, Assam Agricultural University (AAU) for carrying out this research work. The authors are also thankful to the Dean and the Director of Post Graduate Studies (DPGS), HOD, Department of Pathology, College of Veterinary Science, Khanapara, for their administrative support and encouragement. The authors sincerely express their deep sense of gratitude to Dr. T. N. Upadhyay for his invaluable guidance and constant support. The authors further acknowledge the valuable suggestions and cooperation extended by Dr. D. C. Pathak, Dr. S. Sarma, and Dr. G. C. Roy during the course of the study.

Financial support & sponsorship: None

Conflicts of Interest: None

Use of Artificial Intelligence (AI)-Assisted Technology for manuscript preparation: The authors confirm that there was no use of AI-assisted technology for assisting in the writing of the manuscript and no images were manipulated using AI.

REFERENCES

1. Brookes G. 2025. Glyphosate use in agricultural products: Its contribution in global carbon di oxide emission. *GM Crops Food* 17(11): 2594217
2. Benbrook CM. 2024. Trends in glyphosate herbicide use and its implications in human and environmental health. *Environmental Sciences Europe* **36** (1): 45-60.
3. Pal A, Mahadeva N, Farhath K, Bawa AS. 2012. In-vitro studies on the antioxidant assay profiling of root of Withaniasomnifera. (Ashwagandha) Dunal. *Agriculturae Conspectus Scientificus* **77**: 95-101
4. Jediya H, Joshi M, Sharma SK. 2026. Effect of Phytobiotic Feed Additives- Garlic (Allium sativum), Ashwagandha (*Withaniasomnifera*) and Shatavari (Asparagus racemosus) as Alternatives to Antibiotic on Growth Performance and Economics in Broiler Chicken. *Agricultural Science Digest* **10**.18805/ag. D-6403.
5. Bhargavan D, Deepa B, Shetty H, Krishna AP. 2017. The protective effect of *Withaniasomnifera* against oxidative damage caused by ethanol in the testes of adult male rats. *International Journal of Basic & Clinical Pharmacology* **4**(6): 104–1108.
6. Kalaiselvan K, Sweatha V, Gayathri V, Kalaivani P, Siva R, Tamrakar S. 2025. Reproductive and developmental safety assessment of Ashwagandha (Withaniasomnifera) root extract in Wistar rats. *Front Pharmacol* **16**:1572025.
7. OECD. 2008. Test No. 425: Acute Oral Toxicity: Up-and-Down Procedure, OECD Guidelines for the Testing of Chemicals, Section 4. OECD Publishing, Paris.
8. Deora PS, Mishra CK, Mavani P, Asha R and Shrivastava B, Rajesh KN. 2010. Effective alternative methods of LD50 help to save number of experimental animals. *J. Chem. Pharm. Res* **2**(6):450-453
9. Bishnoi N. 2015. Studies on effect of Ashwagandha (*Withania somnifera*) on chlorpyrifos toxicity in broiler chicks. Department of Veterinary Pathology, Lala Lajpat Rai University of Veterinary and Animal Sciences, Hissar.
10. Luna LG. 1968. Manual of Histologic staining methods of the Armed Forces Institute of Pathology. 3rd Edition, McGrew-Hill, Toronto, London, Sydney.
11. Sharma OP, Pholphana N, Rangkadilok N, Parkian P, Satayavivad J. 2015. Development of simple and sensitive HPLC method and determination of Glyphosate residues in Soybean. *Nep Environ Sci* **3**: 21-26.
12. Snedecor GW, Cochron WG. 1994. Statistical Methods. 6th ed., Oxford and IBH Publishing Company, New Delhi.
13. Seralini GE, Mesnage R, Gress S, Defrage N, Malatesta M, Hennequin D, de Vendomois JS. 2014. Republished study: long term toxicity of a Roundup herbicide and a Roundup tolerant genetically modified maize. *Env Sci Europe* **26**:14.
14. Strilbyska OM, Tsiumpala SA, Kozachyshyn II, Strutynska T, Burdyliuk N, Lushchak VI, Lushchak O.2022. The effects of low-toxic herbicide Roundup and glyphosate on mitochondria. EXCLI J **21**:183-196.
15. Ishola OA, Ajao AA,AdewoyeSO. 2026. Histopathological Evidence of Liver and Spleen Alterations Following Sub-Chronic Glyphosate Exposure in Wistar Rats. *Direct Research Journal of Public Health and Environmental* **11**(1): 53-57.
16. Calmday OD, Oghosa AJ, Imafidon EO, Popoola SO, Innih S. 2026. Anatomical Investigation of Glyphosate-Induced Toxicity on the Spleen of Adult Wistar Rats. *Journal of Applied Sciences and Environmental Management* **29**(12): 3739-3746.
17. Turkmen R, Yildirim S, Kaya H. 2025. Immunotoxin and oxidative effects of glyphosate on splenic tissue in experimental rats. *Environmental Research* 240: 117389.
18. AdebayoIO, Ajao AA,AdewoyeSO. 2025. Histopathologicaland immunotoxin effects of sub-chronic glyphosate exposure in Wistar rats. *Journal of Environmental Toxicology and Public Health* **18**(2): 115–126.
19. Ignacio ADC, Guerra AMDR, de Souza-Silva TG, Carmo MAVD, Paula HAA.2024. Effects of glyphosate exposure on intestinal microbiota, metabolism and microstructure: a systematic review. *Food Funct* **15**(15):7757-7781.
20. Laptev GY, Tiurina DG, Yildirim EA, Filippova VA, Dubrovin AV, Duvrovina AS et al. 2025. Effects of Glyphosate, antibiotics and an anticoccidial drug on pancreatic gene expression and blood physiology in broilers. *J Zhejiang Uni Sci B* **26**(2): 185-199.
21. Mazuryk J, Klepacka K, Kutner W, Sharma PS. 2024. Gly-

phosate: Impact on the microbiota-gut-brain axis and the immune-nervous system, and clinical cases of multiorgan toxicity. *Ecotoxicol Environ Saf* 271:115965.
22. Chavez-Reyes J, Gutierrez-Reyes CD, Hernandez-Cuellar E, Marichal-Cancino BA. 2024. Neurotoxicity of glyphosate: focus on molecular mechanisms probably associated with alterations in cognition and behavior. *Environ Toxicol Pharmacol* **106**:104381.
23. Vasanthkumar P, Pangayarselvi B, Sasikumar P, Chandrasekaran D, Doraisamy KA, Purushothaman MR. 2015. Performance of broilers fed Ashwagandha *(Withania somnifera)* incorporated diets during summer season for alleviating heat stress. *Indian J Anim Res* **B-2646**: 1-3.
24. Mitra S, Munni YA, Dash R, Sultana A, Moon IS .2022. Unveiling the effect of *Withania somnifera* on neuronal cytoarchitecture and synaptogenesis: a combined in vitro and network pharmacology approach. *Phytother Res* **36**:2524-41.

Indian J. Vet. Pathol., 50(3) : 243-246, 2026: DOI: https://doi.org/10.56093/drh69m27

SHORT COMMUNICATION

Pathological and molecular studies on tropical theileriosis in a HF cross cow calf

Dhaygude V.S.*, Chandan H.U., Mote C.S., Surabhi Bhandekar, Dethe Prajakta, Payal Nirmal, Prashanth Pawar and Gokul Sonawane
Krantisinh Nana Patil College of Veterinary Science, Shirwal, Dist-Satara (MS), India
Maharashtra Animal and Fishery Sciences University, Nagpur

***Address of correspondence**
Dr. V.S. Dhaygude, Professor; E-mail: drvitthalp@gmail.com
ORCID Id: 0000-0002-2870-4822

Received: 3.2.26; Accepted: 2.6.26

ABSTRACT

Bovine tropical theileriosis (BTT), a tick borne lymphoproliferative disease of bovines, is caused by intracellular hemoprotozoan, *Theileria annulata*. It is one of the most economically significant disease of livestock in India. The blood sample from a month old HF cross cow calf with the history of high fever, anorexia and weakness was presented for hematological examination to Department of Veterinary Pathology, KNPCVS, Shirwal. The hematological analysis revealed anaemia as evident by decrease in Hb (6.5g/dl) and PCV (20.68%) values. The blood smear examination revealed piroplasms (annular rings/rods) of *Theileria* spp. in RBCs. The calf was died on same day and thorough necropsy was performed to note gross lesions. The carcass showed emaciation, pale/anaemic mucous membranes, swollen edematous prescapular lymphnodes, typical punched out ulcers in abomasum, multifocal epicardial ecchymotic hemorrhages along with paleness in myocardial muscles were salient gross findings. The microscopic examination of impression smear from lymphnode revealed typical Koch blue bodies in lymphocytes. The histopathological examination of affected tissues corroborated with gross findings. DNA was extracted from the blood sample and PCR targetting Tams 1 gene specific for *Theileria annulata* yielded expected product of 751 base pair confirming the tropical theileriosis.

Keywords: HF cross cow calf, Lesions, PCR, Tams 1 gene, *Theileria annulata*

How to cite this article : Dhaygude, V.S., Chandan, H.U., Mote, C.S., Bhandekar, S., Prajakta, D., Nirmal, P., Pawar, P. and Sonawane, G. 2026. Pathological and molecular studies on tropical theileriosis in a HF cross cow calfloes. Indian J. Vet. Pathol., 50(3) : 243-246.

INTRODUCTION

India with its tropical climate has widespread distribution of several vector borne diseases like theileriosis, anaplasmosis, babesiosis, trypanosomosis and ehrlichiosis. Theilerial species infecting bovines can be broadly divided into transforming Theilerial species (*T. annulata* and *T. parva*) and non-transforming species (*T. orientalis/ T. sergenti/T. buffalei complex*).

Theileria annulata responsible for tropical bovine theileriosis is the most economically important tick transmitted pathogen species[1]. Infection prevalence has been reported from several states across the country, including Andhra Pradesh, Telangana, Haryana, Punjab, Gujarat, Uttar Pradesh, Uttarakhand, West Bengal, Chhattisgarh, Maharashtra, Madhya Pradesh, Kerala, Odisha, Karnataka, and Tamil Nadu. Serological surveys indicated 30-60% cross bred cattle positive for *T. annulata* specific antibodies, all over India, except in Himalayan regions. In one of the most recent surveys in Maharashtra has reported 24.5 % cases positive for theileriosis by molecular methods in four different agro climatic zones[2].

T. orientalis which causes oriental theileriosis has also been reported in India[3]. In Kerala, examination of blood smears from 246 apparently healthy adult crossbred cattle (Jersey, Holstein Friesian, and Swiss Brown) demonstrated a 26.82% prevalence of *Theileria orientalis* infection[4]. The disease is characterized by carriers status and these animals play role in biomagnification of infection in population. East Coast fever has however not been reported in India due to the absence of its vector[5].

The disease primarily affects exotic, crossbred cattle and young indigenous calves. The sub-clinical form of the disease has been linked to reduced milk production in cattle, while the severe form leads to high mortality. Tropical theileriosis is especially severe in European cattle breeds, with a mortality rate ranging from 40% to 90%. In contrast, the mortality rate in indigenous cattle breeds from endemic regions can be as low as 3%. Numerous fatal clinical cases of bovine tropical theileriosis have been reported worldwide. A tentative diagnosis is made based on clinical signs and confirmatory diagnosis is achieved through microscopic examination of Giemsa-stained blood smears, lymph node fine needle aspirate smears, and the use of serological and molecular

techniques[6]. Although bovine tropical theileriosis caused by *Theileria annulata* is widely reported in adult and crossbred cattle in India, detailed reports describing the clinicopathological alterations and molecular confirmation of fatal infection in very young calves are limited. Therefore, the present study describes the hematological changes, gross and histopathological lesions, along with molecular confirmation of *Theileria annulata* infection in a one-month-old HF cross cow calf.

MATERIALS AND METHODS

The present investigation was conducted on a HF cross cow calf. The blood sample from a month old HF cross cow calf with the history of high fever over 104 °F, anorexia and weakness was presented for hematological examination to the Department of Veterinary Pathology, Krantisinh Nana Patil College of Veterinary Science, Shirwal.

Hematology

The complete blood count was performed by automated hematology analyzer (Abacus Jr. Vet.5, Diatron, Hungary) and blood sample was kept at -20°C for molecular studies. Giemsa stained blood smear was examined for the presence of parasites.

Necropsy and Histopathology

The animal died on the same day of hematological examination and a thorough post-mortem examination was performed to note gross lesions. Tissue samples of affected lymph nodes and other visceral organs were collected in 10% neutral buffered formalin for routine histopathological examination. Impression smear was prepared from affected lymph node and stained with Giemsa staining technique for cytological examination. The formalin fixed tissues were processed by paraffin embedding technique, blocks were prepared, sectioned at 5 µm and stained with hematoxylin and eosin (H&E) for histopathological examination[7].

DNA extraction & PCR

DNA was extracted from affected blood sample by using phenol chloroform method[8]. Micro tubes containing the extracted DNA were stored at -20 °C until further use. The PCR was prepared in a 50µl reaction mixture, which included 25µl of PCR Master Mix, 3µl of each primer (F:5′-CCGTTAATGCTGCAAATGAGGAGG-3′, R: 5′-GAGGCGAAGACTGCAAGGGGAG-3′ from Eurofins Genomics India Pvt. Ltd., Bengaluru)[9] and 5 µl of DNA template. The volume was then adjusted to 50 µl with nuclease-free water. PCR amplification was performed in an automatic thermocycler (Applied biosystems), starting with an initial denaturation step at 95°C for 5 minutes. This was followed by 30 cycles of denaturation at 94°C for 45 seconds, annealing at 57°C for 1 minute, and elongation at 72°C for 1 minute. A final extension step was carried out at 72°C for 10 minutes. The amplified products were visualized by electrophoresis in a 1.5% agarose gel stained with ethidium bromide.

RESULTS

Hematological Examination

The hematological examination of blood sample from the HFX calf affected with theileriosis revealed decreased Hb (6.5g/dl), PCV (20.68%) and total erythrocyte count ($3.6 \times 10^6/\mu l$) and severely hypochromic RBCs on microscopic examination confirming anaemia. The MCV value was 36.93 fl and MCHC 31.43 gm/dl. The values for total leucocyte and platelet count were $2.75 \times 10^3/\mu l$ and $260 \times 10^3/\mu l$ respectively. Thin blood smears were prepared, fixed with absolute methanol and stained with Giemsa stain. The differential leukocytes count revealed 30% neutrophils and 70% lymphocytes. The microscopic examination blood smear showed mostly annular ring shaped piroplasms of Theileria spp. in the erythrocytes (Fig. 1). However few rod and ring shaped piroplasms were also evident.

Necropsy and histopathological findings

The calf was died on the same day of confirmation of theileriosis in the laboratory. The necropsy examination revealed pale/anaemic mucous membranes, diffusely and severely swollen edematous & hemorrhagic prescapular lymphnodes (Fig. 2). Impression smear from affected lymphnode stained with Giemsa stain showed presence of typical Koch Blue Bodies in cytoplasm of many lymphocytes (Fig. 3). Enlarged and congested spleen, typical multifocal generalized punched out ulcers in abomasum (Fig. 4), multifocal hemorrhages and ulcers in urinary bladder, mildly pale/anaemic kidneys with focal hemorrhages, multifocal epicardial ecchymotic hemorrhages along with paleness in myocardial muscles (Fig. 5), diffusely edematous lungs and swollen pale liver with flat whitish foci as salient gross findings. Histopathologically, lymph node revealed lymphocytic proliferation and degenerative changes in the germinal centre along with infiltration of plasma cells and macrophages in cortex and paracortex region (Fig. 6). Heart muscle showed degeneration of cardiac myofibers along with mild infiltration of lymphocytes between muscle fibres (Fig. 7). Multifocal areas of mild tubular degeneration and necrosis, focal mild hemorrhages along with mild interstitial lymphocytic infiltration were evident in both the kidneys. The lung parenchyma revealed presence of pinkish edematous fluid in alveolar spaces along with congestion of alveolar capillaries and focal hemorrhages. The histopathological changes in other organs corroborated with gross lesions.

Molecular confirmation

For molecular confirmation of involvement of *T. annulata*, the PCR targeting *Tams 1* gene specific for

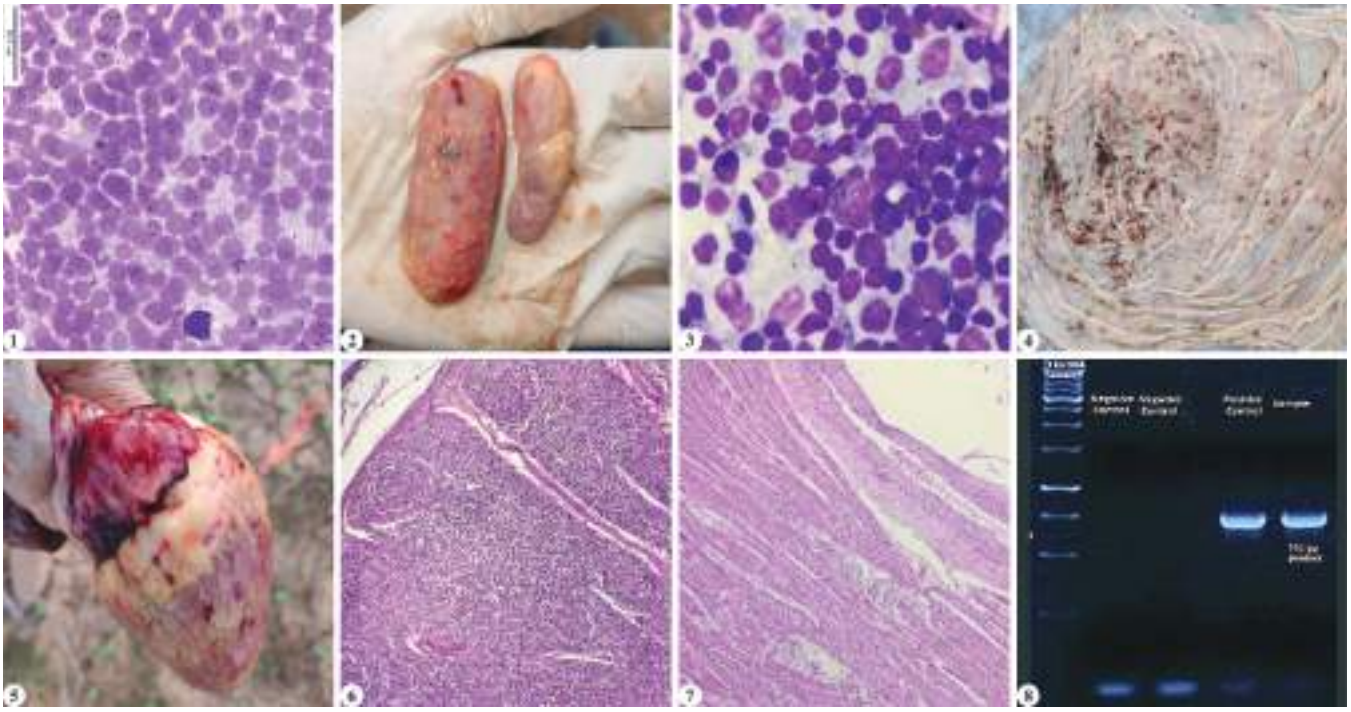

Fig. 1. Giemsa stained thin blood film showing intra-erythrocytic annular ring shaped piroplasms of *Theileria* spp. x1000; **Fig. 2.** Enlarged, edematous prescapular lymphnodes; **Fig. 3.** Lymhnode impression showing Koch's blue bodies in lymphocytes. x1000; **Fig. 4.** Typical punched out ulcers in abomasum; **Fig. 5.** Multifocal epicardial ecchymoitic hemorrhages along with paleness in myocardial muscles; **Fig. 6.** Lymphnode showing lymphoid hyperplasia in cortex and pericotex region. H&E x100; **Fig. 7.** Degeneration of cardiac myofibers along with mild infiltration of lymphocytes. H&E x100; **Fig. 8.** PCR targetting Tams 1 gene specific for *Theileria annulata* showing positive amplification to yield product of 751bp.

Theileria annulata was performed on the DNA sample extracted from blood sample of affected animal. The PCR yielded expected product of 751 base pair (Fig. 8) confirming the tropical theileriosis.

DISCUSSION

Seven species of Theileria are known to infect cattle, of these *T. parva* and *T. annulata* are considered the most pathogenic and economically significant. The other five species are less pathogenic, and some of them may confuse the epidemiology of theileriosis. Various criteria and methods have been used to identify these parasites. Identification of Theileria species based solely on morphological characteristics of piroplasms and schizonts in blood or lymphoid tissues can be challenging, as these stages often show considerable overlap among species. Moreover, mixed infections with different Theileria species may further complicate microscopic identification. Therefore, molecular diagnostic methods are considered more reliable for accurate species confirmation.

The anemia observed in the present case may be attributed to multiple pathogenic mechanisms associated with *Theileria annulata* infection. The parasite invades and multiplies within erythrocytes, leading to direct damage and destruction of infected red blood cells. In addition, immune-mediated erythrophagocytosis by macrophages contributes to the removal of parasitized erythrocytes from circulation. The reticuloendothelial system, particularly in the spleen and liver, actively clears infected erythrocytes, further reducing the circulating red cell population. Activation of complement pathways and increased oxidative stress may also promote erythrocyte membrane damage and hemolysis, thereby exacerbating the anemia observed in infected animals[10].

The major gross lesions observed during necropsy included enlargement, edema, and hemorrhages in the lymph nodes and spleen, punched-out ulcers in the abomasal mucosa, and multifocal ecchymotic hemorrhages on the epicardium. These lesions are consistent with the systemic nature of tropical theileriosis. Histopathologically, the lymph nodes and spleen showed marked proliferation of lymphoid cells within the hematopoietic regions, reflecting intense stimulation of the lymphoid system. This change occurs because Theileria annulata primarily infects and transforms lymphoid cells, leading to uncontrolled proliferation of infected leukocytes and resulting lymphoid hyperplasia. In addition to lymphoid tissues, infiltration of lymphocytes and macrophages was observed in the intermyseal spaces of the heart and in the interstitial tissue of the kidneys. These inflammatory changes may result from

the systemic dissemination of infected leukocytes and the host immune response against parasitized cells. Increased activity of reticular cells in lymphoid organs has also been suggested to represent a protective response aimed at limiting the spread of infection. Similar pathological alterations involving the spleen, epicardium, myocardium, and kidneys have been documented in earlier studies[11] of tropical theileriosis, supporting the observations recorded in the present case.

PCR targeting the *Tams-1* gene specific for *Theileria annulata* yielded an expected amplicon of 751 bp, confirming the presence of tropical theileriosis in the affected calf. The *Tams-1* gene encodes an immunodominant merozoite surface protein and is widely used as a reliable molecular marker for the detection of *Theileria annulata*. Similar molecular confirmation based on the Tams-1 gene has been reported by previous studies[12].

Theileriosis is a economically important disease. There were reports on theileriosis with blood smear examination and molecular studies, but the reports on necropsy findings in young calves were sparse in this region, hence the findings of current study adds to the knowledge on clinical findings, gross and microscopic lesions and etiology of bovine tropical theileriosis.

Financial support & sponsorship: None

Conflicts of Interest: None

Use of Artificial Intelligence (AI) Assisted technology for manuscript preparation: The authors confirm that there was no use of AI – Assisted Technology for assisting in the writing of the manuscript and no images were manipulated using AI.

REFERENCES

1. Bhatnagar CS, Bhardawaj B, Sharma DK & Meena SK. 2015. Incidence of haemoprotozoan diseases in cattle in Southern Rajasthan, India. *Int. J. Curr. Microbiol. App. Sci*. **4(3)**: 509-514.
2. Kolte SW, Larcombe SD, Jadhao SG, Magar SP, Warthi G, Kurkure NV & Shiels BR. 2017. PCR diagnosis of tick-borne pathogens in Maharashtra state, India indicates fitness cost associated with carrier infections is greater for crossbreed than native cattle breeds. *Plos one* **12(3)**: e0174595.
3. Brahma J, Baishya BC, Phukan A, Mahato G, Deka DK & Goswami S. 2018. Prevalence of Theileria orientalis in cross-bred cattle of Kamrup district of Assam. *International Journal of Chemical Studie* **6**: 1791-94.
4. Kariyappa PR, Ravindran R, Nimisha M, Amrutha BM, Kurbet PS, Kumar KGA & Dinesh CN. 2017. Prevalence of bovine babesiosis and theileriosis in Kerala, India. *Int. J. Curr. Microbiol. Appl. Sci.* **6(8)**: 2310-2314.
5. Singla LD & Kaur P. 2022. A comprehensive review on bovine tropical theileriosis under Indian scenario. *Indian J. Vet. Med. Vol*. **42(2)**: 1-12.
6. Azhahianambi P, Madhanmohan M, Madan N, Kumaran D, Priyadharshini MLM, Bharathi R & Manoharan S. 2021. Successful treatment of severe form of bovine tropical theileriosis in dairy cattle and genotyping of *Theileria annulata* isolates of Tamil Nadu, India. *Veterinary Parasitology: Regional Studies and Reports* **26**: 100628.
7. Luna LG. 1968. Manual of histologic staining methods of the Armed Forces Institute of Pathology. 3rd Edition, Mc-Graw-Hill, New York.
8. Sambrook J, Fritsch EF and Maniatis T. 1989. Molecular Cloning: *A Laboratory Manual*. Cold Spring Harbor Press, New York.
9. Kundave VR, Nehra AK, Ram H, Kumari A, Shahzad M, Vinay TS & Tiwari AK. 2021. Genetic diversity in the Tams 1 gene of *Theileria annulata* (Duschunkowsky and Luhs, 1904) infecting cattle. *Acta tropica* **224**: 106121.
10. Agrawal V, Das G, Singla LD, Shukla S, Maharana BR, Jayraw AK & Jatav GP. 2023. Bovine cerebral theileriosis: first molecular report in cross bred cattle calf in India. *Journal of Parasitic Diseases* **47(1):** 113-117.
11. Gill BS, Bhattacharyulu Y & Kaur D. 1977. Symptoms and pathology of experimental bovine tropical theileriosis (*Theileria annulata* infection). *Annales de parasitologie humaine et compare.* **52(6)**: 597-608.
12. Rajendran C, Ray DD & Bansal GC. 2008. Expression of gene encoding immunodominant merozoite surface protein of Theileria annulata in *Escherichia coli*. *Indian J Biotechnol* **7**: 200-203.

Indian J. Vet. Pathol., 50(3) : 247-250, 2026: DOI: https://doi.org/10.56093/ywbnw583

SHORT COMMUNICATION

Clinicopathological evaluation of cutaneous fibroma in horses

Kaushal Kumar, Vishal K. Sinha*, Deepak Kumar, Imran Ali, Ramesh Tiwary[1] and Prashant Kumar[2]
Department of Veterinary Pathology, Bihar Veterinary College, Bihar Animal Sciences University, Patna, Bihar, India
[1]Department of Veterinary Surgery and Radiology
[2]Veterinary Officer, Bihar Police Academy, Rajgir, Nalanda, Bihar, India

***Address of correspondence**
Dr. Vishal K. Sinha; E-mail: vishalbvc17@gmail.com
ORCID Id: 0009-0008-8765-1485

Received: 22.3.26; Accepted: 21.4.26

ABSTRACT

Cutaneous fibroma is a benign neoplasm of fibrous connective tissue that is occasionally encountered in horses often presenting as nodular growths on various body regions. The present study was conducted over a period of one year to evaluate the prevalence, haematological, biochemical and histopathological characteristics of cutaneous fibroma in horses maintained at the Bihar Police Academy, Rajgir. A total of 32 horses were examined, out of which 6 cases were diagnosed with fibroma, indicating a prevalence of 18.75%. The affected horses included both sexes with ages ranging from 16 to 18 years suggesting a higher occurrence in older animals. Clinically, the lesions were observed as solitary or multiple nodular, ulcerated and proliferative masses predominantly located on the lateral body wall involving the paralumbar (flank) and gluteal (rump) regions. The nodular masses were surgically excised under aseptic conditions and the excised tissues were subsequently submitted for histopathological examination. Haematological evaluation revealed mild anaemia, leucocytosis and neutrophilia, indicative of chronic inflammatory response while biochemical analysis showed slight elevation in liver enzymes (ALT and AST) along with increased total protein and globulin levels. Histopathological examination confirmed the diagnosis of fibroma, characterized by dense interlacing bundles of well-differentiated fibroblasts and collagen fibres with minimal cellular atypia and low mitotic activity. These findings indicate that cutaneous fibroma, although benign can occur with appreciable frequency in aged horses and may be associated with mild systemic alterations. This study emphasizes the importance of surgical excision followed by histopathological confirmation for accurate diagnosis and effective management of cutaneous fibroma in horses.

Keywords: Cutaneous Fibroma, Horse, Surgical excision

INTRODUCTION

Cutaneous fibroma is a benign mesenchymal neoplasm arising from fibroblasts of the dermis and subcutis and is characterized by slow-growing, well-circumscribed nodular masses in various animal species including horses[1,2]. In equines, fibromas are relatively uncommon compared to other skin tumours such as sarcoids, papillomas and squamous cell carcinoma; however, they remain an important differential diagnosis for nodular cutaneous lesions[3,4]. These tumours are generally non-invasive and non-metastatic but may cause discomfort, ulceration or interference with movement depending on their size and anatomical location[5].

In horses, cutaneous neoplasms are frequently encountered in regions subjected to repeated trauma, friction or environmental exposure. Fibromas have been reported on the head, neck, trunk and limbs, with occasional occurrence over the flank and gluteal regions[6,7]. Although the exact etiology remains unclear, chronic irritation, wound healing disturbances and fibroblastic proliferation have been suggested as contributing factors[8,9]. Unlike equine sarcoids, fibromas are not typically associated with papillomavirus infection and exhibit a more uniform and benign biological behaviour[2].

Clinically, fibromas present as solitary or multiple firm nodular masses that may be pedunculated or sessile and occasionally ulcerated due to trauma or secondary infection[3,10]. Larger lesions may undergo surface necrosis and become prone to contamination leading to chronic inflammatory changes. Such lesions are often mistaken for sarcoids or exuberant granulation tissue, necessitating confirmatory diagnosis through histopathological examination[4,5].

How to cite this article : Kumar, K., Sinha, V.K., Kumar, D., Ali, I., Tiwary, R. and Kumar, P. 2026. Clinicopathological evaluation of cutaneous fibroma in horses. Indian J. Vet. Pathol., 50(3) : 247-250.

Haematological and biochemical alterations in affected horses are usually mild but may reflect chronic inflammation, secondary infection or stress responses associated with long-standing lesions[6]. Histopathologically, fibromas are characterized by dense interwoven bundles of well-differentiated fibroblasts embedded in abundant collagen matrix with minimal cellular atypia and low mitotic activity, confirming their benign nature[1,2].

Although fibromas are considered sporadic in occurrence, studies documenting their prevalence and clinicopathological features in organized equine populations are limited, particularly in India. Institutional settings such as mounted police units provide a unique opportunity to evaluate such conditions due to uniform management and prolonged exposure of animals to similar environmental factors.

Therefore, the present study was undertaken to investigate the prevalence, anatomical distribution, age and sex predisposition along with haematological, biochemical and histopathological characteristics of cutaneous fibroma in horses maintained at the Bihar Police Academy, Rajgir. The findings aim to contribute to better understanding, accurate diagnosis and differentiation of fibroma from other cutaneous lesions in equine clinical practice.

MATERIALS AND METHODS

The present study was conducted on thoroughbred and Kathiawari horses maintained at the Bihar Police Academy, Rajgir (Nalanda), Bihar, over a period of one year to investigate the occurrence and clinicopathological characteristics of cutaneous fibroma. A total of 32 horses of different ages and sexes were examined under uniform management conditions. Out of these, 6 horses were selected for the study based on the presence of nodular cutaneous growths which were subsequently confirmed as fibroma upon histopathological examination.

The affected horses were presented with a history of slow-growing nodular masses on different parts of the body, particularly over the left lateral body wall involving the paralumbar (flank) and gluteal (rump) regions. The duration of growth as reported by caretakers ranged from 2 months to 10 months. In some cases, the lesions showed ulceration, surface necrosis and occasional bleeding likely due to repeated trauma or friction. No significant systemic clinical signs such as anorexia or depression were consistently observed.

On clinical examination, horses were generally alert and in fair body condition. The nodular lesions were firm, well-circumscribed, sessile or pedunculated, varying in size from approximately 3 cm to 10 cm in diameter. Some lesions exhibited ulceration and serosanguinous exudation. Vital parameters including rectal temperature, pulse rate and respiration rate were within normal physiological limits in most cases.

For diagnostic evaluation, haematological and biochemical analyses were carried out following standard procedures. Blood samples were collected aseptically from the jugular vein into EDTA and plain vacutainers. Haematological parameters evaluated included haemoglobin (Hb), packed cell volume (PCV), total erythrocyte count (TEC), total leukocyte count (TLC) and differential leukocyte count (DLC). Biochemical parameters included alanine aminotransferase (ALT), aspartate aminotransferase (AST), alkaline phosphatase (ALP), total protein, albumin, globulin, blood urea nitrogen (BUN) and creatinine which were estimated using an automatic biochemical analyser.

For confirmatory diagnosis, the nodular masses were surgically excised under sedation and local anaesthesia. Horses were sedated using xylazine (1.1 mg/kg body weight, i.v.) and local infiltration of 2% lignocaine hydrochloride was administered around the lesion. The surgical site was prepared aseptically and a careful incision was made to excise the mass completely. Haemostasis was achieved by ligation of bleeding vessels and the wound was closed using appropriate suture materials.

The excised tissue samples were immediately fixed in 10% neutral buffered formalin and submitted to the Department of Veterinary Pathology, Bihar Veterinary College, BASU, Patna for further evaluation. Gross examination of the masses was carried out to assess size, shape, colour, consistency and presence of ulceration. For histopathology, tissues were processed by routine paraffin embedding technique, sectioned at 4–5 μm thickness and stained with Haematoxylin and Eosin (H&E) for microscopic examination.

Postoperative management included administration of broad-spectrum antibiotics (Ceftriaxone @ 20–25 mg/kg, i.m.) for 5 days and non-steroidal anti-inflammatory drugs (meloxicam @ 0.2 mg/kg, i.m.) for 3 days. The surgical site was dressed regularly with antiseptic solution, and sutures were removed after 10–14 days.

All procedures were carried out in accordance with standard animal welfare practices.

RESULTS AND DISCUSSION

All affected horses recovered uneventfully following surgical excision of the nodular masses. The animals resumed normal feeding and activity within 4–8 days post-surgery. The surgical wounds healed satisfactorily and sutures were removed between 10–14 days without any complications. On follow-up examination after two months, no recurrence of the lesions was observed, indicating a favourable prognosis and effectiveness of complete surgical excision in the management of fibroma.

Grossly, the lesions were observed as nodular, ulcerated cutaneous masses located predominantly on the lateral body wall, including the paralumbar (flank) and gluteal (rump) regions (Fig. 1–5). The growths varied from solitary to multiple, with some appearing as small discrete nodules while others formed

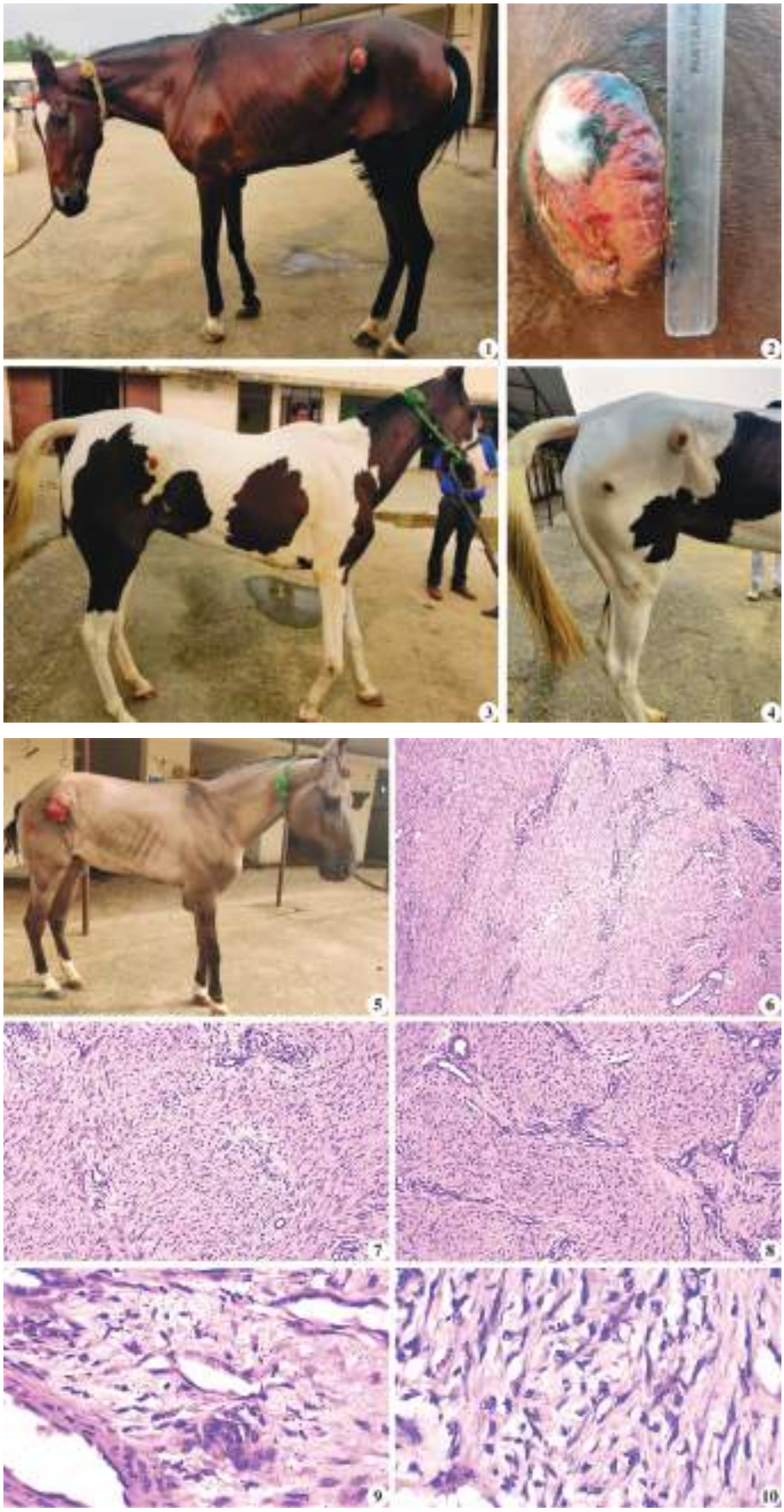

large proliferative masses (Fig. 1, 3–5). Close examination revealed ulcerated surfaces with areas of haemorrhage and necrosis, likely due to repeated trauma (Fig. 2, 4, 5). The excised masses were well-circumscribed, firm to hard in consistency and varied from 3 cm to 10 cm in diameter. On cut section, the masses appeared whitish to grayish-white with a homogeneous fibrous texture. The distribution of lesions, predominantly over the flank and gluteal regions, suggests a possible association with mechanical irritation or pressure in these areas.

Histopathologically,the tumour sections at low magnification (H&E, x4) revealed dense interlacing bundles of collagen fibres with spindle-shaped fibroblasts (Fig. 6). At higher

Fig. 1. Gross appearance of a nodular, ulcerated cutaneous mass located on the left paralumbar (flank) region of a horse; **Fig. 2.** Close-up view of ulcerated nodular growth (~9 – 10cm) on the left flank of a horse; **Fig. 3.** Lateral view of a horse showing a solitary nodular lesion on the right paralumbar (flank) region; **Fig. 4.** Clinical photograph showing multiple ulcerated nodular lesions on the left gluteal (rump) region of a horse; **Fig. 5.** Clinical photograph showing a large ulcerated nodular mass on the left gluteal (rump) region of a horse; **Fig. 6.** Histological section of cutaneous fibroma (H&E, x4) showing dense interlacing bundles of collagen fibers with spindle-shaped fibroblasts; **Fig. 7.** Histological section of cutaneous fibroma (H&E, x10) revealing well-differentiated fibroblasts with elongated nuclei embedded in dense collagenous stroma; **Fig. 8.** Histological section of cutaneous fibroma (H&E, x10) showing spindle-shaped fibroblasts arranged in a criss-cross pattern with abundant collagen deposition; **Fig. 9.** Histological section of cutaneous fibroma (H&E, x40) showing spindle-shaped fibroblasts embedded in collagen fibres along with occasional giant tumour cells; **Fig. 10.** Histological section of cutaneous fibroma (H&E, x40) exhibiting mild nuclear pleomorphism and occasional multinucleated giant cells embedded in dense collagen fibres.

magnification (H&E, x10), the lesion showed well-differentiated fibroblasts with elongated nuclei embedded in a dense collagenous stroma (Fig. 7), with areas demonstrating a criss-cross (interlacing) arrangement of fibroblasts and abundant collagen deposition (Fig. 8). On further magnification (H&E, x40), the fibroblasts were seen embedded within collagen fibres along with occasional giant tumour cells (Fig. 9) and exhibited mild nuclear pleomorphism with occasional multinucleated giant cells (Fig. 10). Overall, the fibroblasts were spindle-shaped with minimal cellular atypia and low mitotic activity. The overlying epidermis was intact in some areas while in ulcerated lesions it was disrupted and replaced by necrotic debris. Mild lymphoplasmacytic infiltration was observed in the stroma, indicating a chronic inflammatory response. Based on these features, the lesions were diagnosed as cutaneous fibroma.

Cutaneous fibroma is considered a benign tumour of fibroblastic origin and is reported less frequently in horses compared to sarcoids and other cutaneous neoplasms[1,7]. In the present study, 6 out of 32 horses (18.75%) were affected, indicating a moderate occurrence within the studied population. The affected animals were predominantly older (16–18 years and above) which is in agreement with previous reports suggesting a higher incidence of fibrous tumours in aged animals due to prolonged exposure to environmental and mechanical factors[9,11].

The histopathological features observed in the present study, including well-differentiated fibroblasts, abundant collagen deposition and minimal atypia are in accordance with previous descriptions of fibroma in equines[1,7]. The absence of cellular pleomorphism, high mitotic activity and invasive growth pattern differentiates fibroma from malignant fibrosarcoma and other aggressive mesenchymal tumours. Furthermore, differentiation from equine sarcoid is essential, as sarcoids typically exhibit epidermal hyperplasia and fibroblastic proliferation associated with papillomavirus infection, which were not observed in the present cases[5,9].

The favourable clinical outcome, absence of recurrence and benign histological features confirm that cutaneous fibroma in horses has an excellent prognosis following complete surgical excision. The findings emphasize the importance of histopathological examination for definitive diagnosis, as clinical appearance alone may mimic other proliferative lesions.

CONCLUSION

Cutaneous fibroma in horses is a benign tumour predominantly affecting older animals, commonly observed in the paralumbar and gluteal regions. Although non-invasive, lesions may ulcerate due to trauma. Accurate diagnosis through histopathology is essential to differentiate it from other cutaneous tumours. Surgical excision provides an excellent prognosis with no recurrence. Early detection and proper management are important for maintaining animal welfare.

ACKNOWLEDGEMENTS

The authors express their gratitude to the Vice Chancellor and the Dean of Bihar Veterinary College, Bihar Animal Sciences University, Patna, for providing the necessary facilities to carry out this work.

Financial support & sponsorship: None

Conflicts of Interest: None

Use of Artificial Intelligence (AI)- Assisted Technology for manuscript preparation: The authors confirm that there was no use of AI- assisted technology for assisting in the writing of the manuscript and no images were manipulated using AI.

REFERENCES

1. Rich AF, Ricci E, Gates S, Hinnigan GJ and Owen KR. 2021. Intratendinous Fibroma of the Superficial Digital Flexor Tendon within the Carpal Sheath of a Horse. *Journal of Equine Veterinary Science* **105:** 103693.
2. Baker JL and Leyland AH. 1975. Histological survey of tumours of the horse, with particular reference to those ofthe skin. *Veterinary Record* **96(19):** 419-422. https://doi.org/10.1136/vr.96.19.419
3. Turek B, Górski K, Drewnowska O, Buczkowska R, Kozłowska N and Sapierzyński R. 2021. Ossifying Fibroma in the Nasal Cavity of a 2-Year-Old Horse. *Animals* ***11*****(2):** 317. https://doi.org/10.3390/ani11020317
4. Knottenbelt DC, Kane JP and Snalune KL. 2015. Tumours of the skin in horses. In book: Clinical Equine Oncology (pp. 544-584).
5. Yadollahi F, Azizi S and Tehrani A. 2023. Surgical Treatment and Relative Frequency of Skin Tumors in Domestic Equids: A Retrospective Study. *Iranian Journal of Veterinary Surgery* **18(1):** *84-92.*
6. Agrawal SA. 2005. Fibroma in a horse: A case report. *CAB Abstracts.*
7. Scott DW and Miller WH. 2011. Equine dermatology and cutaneous neoplasms. In: *Equine Dermatology.* 2nd edn. Elsevier.
8. Poore LA, Duncan N and Williams J. 2018. Unilateral subcutaneous fibroma in the distal femoral region of a 5-year-old Nooitgedacht mare. *J S Afr Vet Assoc* **89(0):** e1-e4.
9. Jaglan V, Singh P, Punia M, Saharan S and Gupta RP. 2018. Therapeutic Management and Histopathological Study of Sarcoid tumours in Equine. *Int. J. Curr. Microbiol. App. Sci.* **7(10):** 444-448. doi: https://doi.org/10.20546/ijcmas.2018.710.047
10. Valentine BA. 2006. Survey of Equine Cutaneous Neoplasia in the Pacific Northwest. *J. Vet. Diag. Invest.* **18(1):** 123-126. doi:10.1177/104063870601800121
11. Martens A, De Moor A, Demeulemeester J and Ducatelle R. 2000. Histopathological characteristics of equine sarcoids. *Vet. Dermatol.* **11(4):** 253-260.

Indian J. Vet. Pathol., 50(3) : 251-254, 2026: DOI: https://doi.org/10.56093/e3b1hr20

SHORT COMMUNICATION

Clinicopathological and histopathological studies on canine traumatic uroabdomen

J. Hari Chandana[1], A. Nasreen*[2], A. Anand Kumar, V. Vaikunta Rao*[2], and M. Raghunath[2]
Department of Veterinary Pathology, College of Veterinary Science, Sri Venkateswara Veterinary University, Tirupati, Andhra Pradesh, India
[1]MVSc Scholar
[2]Department of Veterinary Clinical Complex

***Address of correspondence**
Dr. A. Nasreen; E-mail: nashreen7@gmail.com
ORCID Id: 0009-0001-3859-652X

Received: 6.3.26; Accepted: 22.4.26

ABSTRACT

Uroabdomen is a critical condition resulting from leakage of urine into the peritoneal cavity, leading to hematological, biochemical, cytological and histopathological alterations. The present report describes a rare case of uroabdomen associated with traumatic herniation of the urinary bladder through the rectum in a three-month old male non-descript dog presented to Department of Veterinary Clinical Complex, Tirupati. Clinical examination revealed moderate abdominal distension, pallor of visible mucous membranes and a fluid-filled sac protruding through the rectal opening. Hematological evaluation showed severe anemia and neutrophilic leucocytosis with the left shift. Peritoneal fluid analysis revealed high total nucleated cell count (TNCC) with reactive mesothelial cells along with inflammatory cells. Biochemical analysis of peritoneal fluid revealed very high creatinine concentration compared to that in serum. Histopathological examination of the peritoneum revealed reactive changes characterized by vascular congestion, hemorrhage and marked neutrophilic infiltration. This case highlights the diagnostic significance and correlation of imaging with hematology, peritoneal fluid cytology, biochemical analysis, histopathology for definitive confirmation of uroabdomen.

Keywords: Creatinine, Dog, Peritoneal fluid cytology, Reactive peritonitis, Uroabdomen

INTRODUCTION

Uroabdomen also termed as uroperitoneum, is defined as the accumulation of urine within the peritoneal cavity following any rupture of urinary tract or leakage of urine. In dogs, the condition is most frequently associated with any blunt abdominal trauma, urethral obstruction or iatrogenic injury to the urinary bladder or urethra[1,2]. This leakage results in chemical irritation of the peritoneum and diffusion of urinary components into the systemic circulation, producing characteristic clinicopathological alterations in the animal.

Although diagnostic imaging techniques such as ultrasonography and contrast radiography are essential for identifying the site and cause of urinary tract disruption, laboratory evaluation of peritoneal fluid remains the most reliable method for confirming uroabdomen[3]. Cytological and biochemical evaluation of peritoneal fluid, particularly the comparison of creatinine concentrations between serum and effusion, plays an important role in diagnosis. Histopathological examination of the peritoneum further provides an insight into the tissue response to chemical peritonitis. The present case report describes a rare incidence of uroabdomen with bladder herniation through the rectum and emphasizes the importance of comprehensive pathological evaluation along with other diagnostic techniques.

Case history and clinical examination

A three-month-old male non-descript dog weighing 5 kg body weight was presented with abdominal distension and a history suggestive of trauma. Clinical examination revealed pale cutaneous mucous membranes, capillary refill time of less than two seconds and absence of peripheral lymphadenopathy. The animal exhibited an arched back posture due to abdominal discomfort (Fig. 1). Per rectal examination identified a fluid-filled sac protruding through the rectal opening.

How to cite this article: Chandana, J.H., Nasreen, A., Kumar, A.A., Rao, V.V. and Raghunath, M. 2026. Clinicopathological and histopathological studies on canine traumatic uroabdomen. Indian J. Vet. Pathol., 50(3) : 251-254.

Diagnostic imaging

Urethral catheterization followed by contrast radiography was performed to evaluate the urinary bladder for any bladder displacement, herniation or rupture in dogs[2,4]. The procedure confirmed herniation of the urinary bladder through the rectum (Fig.2). Ultrasonographic examination revealed anechoic

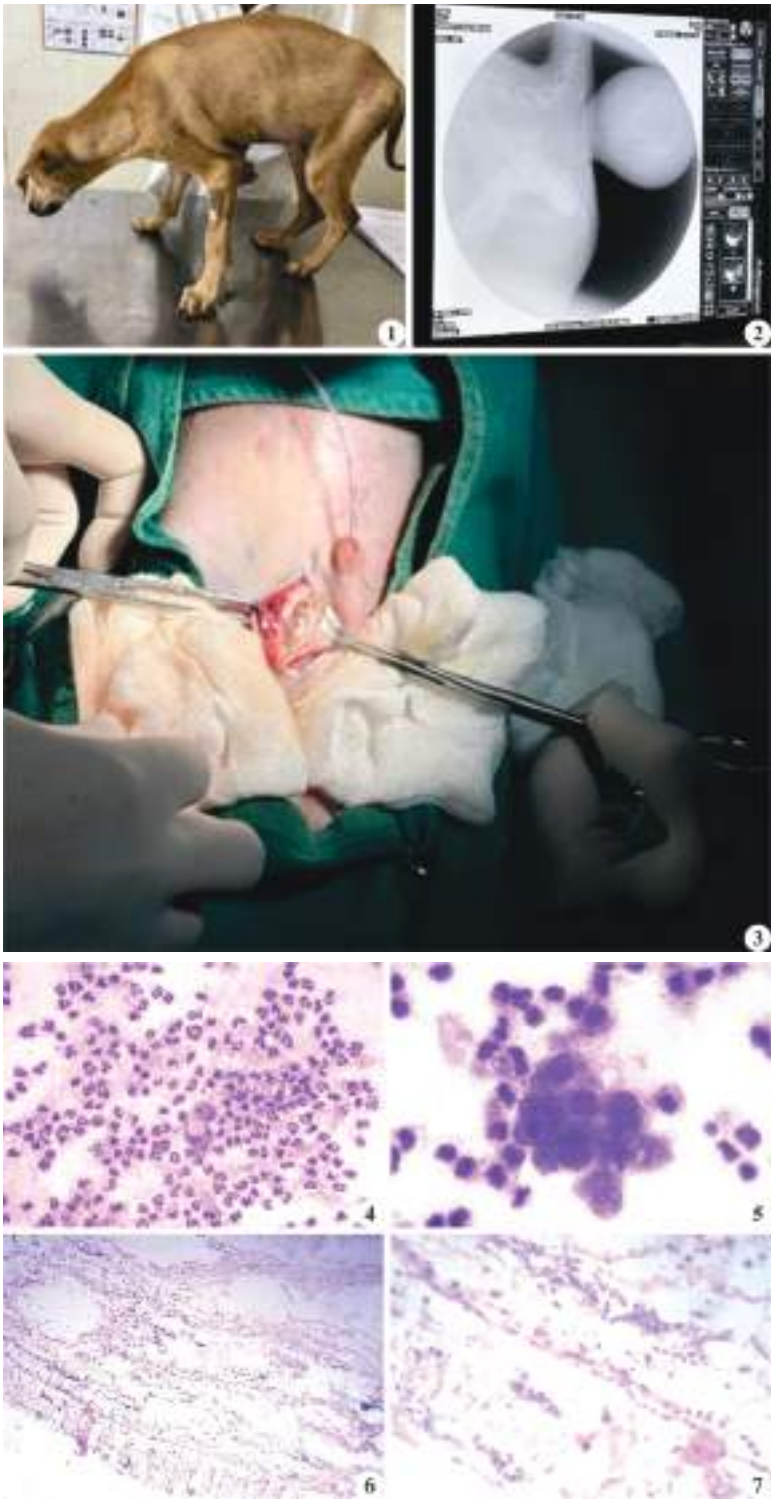

Fig.1. Arched back posture of dog due to abdominal discomfort and pain; **Fig.2**. Contrast radiography revealed abnormal positioning of the urinary bladder into rectum; **Fig.3**. Exploratory laparotomy revealed approximately 100 mL of fluid within the peritoneal cavity; **Fig.4**. Cytology showing many degenerated neutrophils (Field's stain, x100); **Fig.5**. Presence of reactive mesothelial cells within sheets and multinucleated (Field's stain, x1000); **Fig.6.** Peritoneum- Infiltration of numerous inflammatory cells in mesothelial and submesothelial connective tissue. (H&E, x100); **Fig.7.** Peritoneum-Presence of numerous degenerative neutrophils along with hemorrhage (H&E, x400)

to mildly hypoechoic free fluid within the abdominal cavity[5].

RESULTS AND DISCUSSION

Hematological analysis

Blood samples were collected in anticoagulant vials and analyzed for Hemoglobin concentration, Total erythrocyte count (TEC), Total leukocyte count (TLC) and Differential leukocyte count (DLC). The result revealed severe anemia with hemoglobin-5 g/dl and TEC-1.6× 10^6/µl. The TLC was slightly elevated at 14,500 cells/µl and DLC showed marked neutrophilia (84%) with band cells, indicating a left shift. Lymphocytes accounted for 15% of the total count. The analysis were performed using standard hematological techniques[5,6]. In the present case, severe anemia may be attributed to hemorrhage and the effects associated with peritoneal fluid accumulation. In addition to hemorrhage secondary to trauma, hemodilution due to fluid shifts into the peritoneal cavity and suppression of erythropoiesis secondary to systemic inflammatory response may contribute to anemia observed in uroabdomen[7,8]. Neutrophilic leukocytosis with left shift reflected an acute inflammatory response to chemical irritation.

Peritoneal fluid analysis

Exploratory laparotomy was performed for management of uroabdomen and peritoneal fluid, peritoneal tissues were collected intraoperatively[2,4]. Intraoperative collection of peritoneal effusions is recommended for accurate fluid analysis and minimization of contamination[3,7].

Through this procedure approximately 100ml of accumulated peritoneal fluid was removed (Fig.3) from which 2 ml sample was collected aseptically. Physical examination of fluid revealed moderate transparency and was devoid of any detectable odour. TNCC was determined using a hemocytometer following standard guidelines[3] which was 2,500 cells/µl, consistent with modified transudate.

Cytological Examination

For cytological evaluation, the fluid was centrifuged at 3000 rpm for 5 minutes and sediment was taken from which smears were prepared and stained with Field's stain following standard Romanowsky staining principles[3,9]. The smear revealed moderate

cellularity comprising reactive mesothelial cells, degenerated neutrophils, macrophages, lymphocytes and few nucleated erythrocytes. The reactive mesothelial cells were seen as clusters and the cells were characterized by polyhedral shape with basophilic vacuolated cytoplasm and round to oval nucleus (Fig. 4, Fig. 5). Peritoneal fluid cytology in these cases showed predominance of reactive mesothelial cells and non septic neutrophils. According to the previous researches[3,8], mesothelial hyperplasia and multinucleation are hallmarks of chronic or ongoing peritoneal irritation.

Biochemical Analysis

Comparative biochemical analysis of serum and effusions is a standard and reliable method for evaluation of abdominal effusions and confirmation of uroabdomen in dogs[7,9]. Serum and peritoneal fluid were analyzed (Table.1) for total protein which revealed hypoproteinemia (1.87 g/dl), albumin, creatinine, blood urea nitrogen (BUN), Alanine transaminase (ALT), Aspartate transferase (AST), alkaline phosphatase (ALP), cholesterol, triglycerides and lactate dehydrogenase (LDH) using a semi-automatic biochemical analyzer with commercially available diagnostic kits. LDH activity was markedly elevated in the peritoneal fluid (215.64 U/L) compared to serum (31.95 U/L). Consequently, biochemical evaluation remains the main aid of diagnosis. A peritoneal fluid-to-serum creatinine ratio > 2 is considered of having diagnostic importance[1,7]. Several authors have emphasized that creatinine is a more reliable marker than BUN because of its slower diffusion rate across the peritoneal membrane[1,3]. Elevated LDH activity in peritoneal fluid further supports tissue injury and inflammation[3,10].

Urine creatinine estimation was also performed for comparison (Table 2). Simultaneous evaluation of serum, peritoneal fluid and urine creatinine concentrations is recommended for accurate diagnosis of uroperitoneum. Creatinine levels were significantly higher in peritoneal fluid (6.12 mg/dl) than in serum (2.79 mg/dl), and was in markedly elevated concentration in urine (21.82 mg/dl), which is a characteristic finding, confirming uroabdomen. Experimental and clinical studies have demonstrated that urea and creatinine diffuse rapidly across the peritoneum, contributing to azotemia, electrolyte imbalance, metabolic acidosis and systemic toxemia in affected animals[10,11].

Histopathological Examination

A small peritoneal biopsy sample was collected for histopathological examination during exploratory laparotomy . Peritoneal biopsy obtained during laparotomy is an accepted method for assessing reactive and inflammatory changes associated with chemical peritonitis[8,9].Tissue being fixed in 10% neutral buffered formalin, routinely processed, embedded in paraffin, sectioned at 4–5 μm thickness and stained with hematoxylin and eosin for microscopic examination [12].

Histopathological examination revealed hemorrhage and congestion of blood vessels with infiltration of numerous inflammatory cells. The submesothelial connective tissue showed prominent neutrophilic infiltration along with interstitial edema consistent with reactive peritonitis secondary to urine leakage.

Table 1. Biochemical analysis of serum and peritoneal fluid

PARAMETER	SERUM	PERITONEAL FLUID	UNITS	INTERPRETATION
Albumin	1.66	1.43	g/dL	↓ Slightly lower in fluid
Creatinine	**2.79 ↑**	**6.12 ↑ ↑**	mg/dL	**Marked increase in fluid (>> serum)**
BUN	9.14	**61.82 ↑**	mg/dL	**Marked increase in fluid**
Cholesterol	**305.36 ↑**	**213.48 ↑**	mg/dL	Increased in both
Triglycerides	**476.29 ↑**	**360.57 ↑**	mg/dL	Markedly increased in both
Total Protein	1.87	1.50	g/dL	Lower in fluid - Hypoproteinemia
SGOT (AST)	31.43	23.28	IU/L	No significant change
SGPT (ALT)	27.71	28.57	IU/L	No significant change
LDH	**3495 ↑ ↑**	**215.64 ↑**	IU/L	Markedly elevated, higher in serum

Table 2. Biochemical analysis of BUN and Creatinine

PARAMETER	SERUM	PERITONEAL FLUID	URINE	UNITS	INTERPRETATION
BUN	9.14	**61.82 ↑**	**45.46 ↑**	mg/dL	Markedly increased in fluid and urine
Creatinine	**2.79 ↑**	**6.12 ↑ ↑**	**21.82 ↑ ↑**	mg/dL	Highest concentration in urine

(Fig. 6, Fig. 7). Histopathological changes observed in the peritoneum are characteristic of reactive chemical peritonitis. Studies have documented that prolonged exposure of mesothelium to urine results in cell activation, increased vascular permeability and recruitment of inflammatory leukocytes, which may progress to fibrosis if not promptly corrected[13,14]. Thus, histopathology not only confirms diagnosis but also provides insight into disease chronicity and severity.

CONCLUSION

Uroabdomen produces a distinct set of clinicopathological alterations resulting from diffusion of urine components across the peritoneal membrane[7]. The present case underscores the importance of an integrated diagnostic approach for confirmation of uroabdomen in dogs. While imaging identifies urinary tract disruption, definitive diagnosis requires laboratory confirmation through hematology, peritoneal fluid cytology and biochemical analysis, particularly creatinine estimation.

Histopathological evaluation of peritoneal tissue supports the diagnosis by demonstrating characteristic reactive inflammatory changes associated with chemical peritonitis which contributes to better understanding of the pathogenesis and tissue response in uroabdomen [8].

Early recognition and prompt intervention are crucial, as prolonged uroperitoneum can result in severe metabolic derangements and septic complications. Therefore, routine evaluation of abdominal effusions for creatinine, BUN and LDH, along with cytological examination are essential in veterinary clinical practice[2,3]. This case highlights the diagnostic value of correlating clinical, imaging, biochemical, cytological and histopathological findings for accurate diagnosis.

ACKNOWLEDGEMENT

The authors extend their gratitude to the Sri Venkateswara Veterinary University, Tirupati for providing the facilities necessary to conduct this study.

Conflicts of Interest: None

Use of Artificial Intelligence (AI)-Assisted Technology for manuscript preparation: The authors confirm that there was no use of Al-assisted technology for assisting in the writing of the manuscript and no images were manipulated using AI.

REFERENCES

1. Burrows C F and Bovee K C. 1974. Uroperitoneum in the dog. *J Am Vet Med Assoc* 165: 546–548.
2. Fossum T W. Ed. 2019. Small animal surgery. *Elsevier Fifth edition* Pp 368–375.
3. Valenciano A C and Cowell R L. 2020. Fluid analysis and interpretation. In: Cowell R L and Tyler R D. Eds. Diagnostic Cytology And Hematology Of The Dog And Cat. *Elsevier* Pp 273–312.
4. Tobias K M and Johnston S A. Eds. 2012. Veterinary surgery: small animal. *Elsevier* Pp 1860–1875.
5. Jain N C. Ed. 1986. Schalm's Veterinary Hematology. Lea & Febiger Fourth edition Pp 4–58.
6. Stockham S L and Scott M A. Eds. 2016. Fundamentals Of Veterinary Clinical Pathology. *Wiley-Blackwell Second edition* Pp 1–60.
7. Maxie M G. Ed. 2016. Jubb, Kennedy and Palmer's pathology of domestic animals. *Elsevier Sixth edition* Vol. 1 Pp 1–50.
8. Nyland T G and Mattoon J S. Eds. 2015. Small animal diagnostic ultrasound. *Elsevier Third edition* Pp 263–310.
9. Thrall M A, Weiser G, Allison R W and Campbell T W. Eds. 2012. Veterinary Hematology And Clinical Chemistry. *Wiley-Blackwell Second edition* Pp 3–60.
10. Kaneko J J, Harvey J W and Bruss M L. Eds. 2008. Clinical Biochemistry Of Domestic Animals. *Elsevier Sixth edition* Pp 117–145.
11. Prophet E B, Mills B, Arrington J B and Sobin L H. Eds. 1992. Laboratory methods in histotechnology. *American Registry of Pathology* Pp 25–78.
12. Bancroft J D and Gamble M. Eds. 2019. Theory and practice of histological techniques. *Elsevier Eighth edition* Pp 91–140.
13. Zachary J F. Ed. 2017. Pathologic basis of veterinary disease. *Elsevier Sixth edition* Pp 53–122.
14. Langston C. 2018. Urinary tract emergencies. In: Ettinger S J, Feldman E C and Côté E. Eds. Textbook of veterinary internal medicine. *Elsevier Eighth edition* Pp 2030–2045.

Indian J. Vet. Pathol., 50(3) : 255-258, 2026: DOI: https://doi.org/10.56093/9d6ys548

SHORT COMMUNICATION

Therapeutic management of *Muellerius capillaris* infection in Himalayan musk deer *(Moschus leucogaster)*

Karikalan M.*, Hira Ram, L.M.S. Nayal[1], Mahendran K., Bablu Kumar, P.S. Banerjee, A.M. Pawde and A.K. Sharma

ICAR-Indian Veterinary Research Institute, Izatnagar (U.P.), India

[1]In-charge, Musk Deer Farm, Central Council for Research in Ayurvedic Sciences (CCRAS), Bageshwar (Uttarakhand)

***Address of correspondence**

Dr. M. Karikalan; E-mail: karyvet11@gmail.com

ORCID Id: 0000-0002-2013-9179, 0000-0001-8272-5352

Received: 18.3.26; Accepted: 5.7.26

ABSTRACT

An investigation was conducted to determine the cause of mortality and ill health in a captive musk deer farm at the Musk Deer Research Centre, Bageshwar, Uttarakhand. Six musk deer died within a period of two months, and pathological findings confirmed verminous pneumonia due to nematode infestation. Faecal samples collected from eleven animals and examined using standard flotation and sedimentation techniques revealed infection with *Muellerius capillaris* in all animals, with mild infection in 7 and moderate and severe infection in two animals. All animals were initially treated with ivermectin (0.2 mg/kg body weight, subcutaneously), but follow-up examination on day 10 indicated persistence of infection in seven animals. Subsequently, fenbendazole (5 mg/kg body weight orally for 15 days) was administered to all animals. Post-treatment faecal examinations on days 10 and 30 confirmed complete clearance of lungworm infection and overall improvement in animal health. The poor response to ivermectin may be due to limited drug availability within nodular lung lesions, whereas prolonged fenbendazole treatment proved effective in eliminating persistent *M. capillaris* infection in captive musk deer.

Key words: Anthelmintic, Lung worm, *Muellerius capillaris*, Musk deer

INTRODUCTION

The Himalayan musk deer *(Moschus leucogaster)* is a small deer species found in the Himalayan forests of India, also locally known as the Kasturi Mrig and known for the musk gland present in males[1]. Due to illegal hunting for musk and habitat loss, its population has declined significantly. Therefore, it is listed under Endangered on the IUCN Red List and Schedule I of the Wildlife Protection Act, 1972, giving it the highest level of legal protection in India[2]. The Himalayan musk deer is susceptible to several infectious and parasitic diseases that can affect its survival. Parasitic bronchitis is one of the most important diseases affecting domestic and wild ruminants and widely prevalent in Himalayan belt of Jammu and Kashmir, Himachal Pradesh and Gharhwal hills of Uttarakhand[3]. The free ranging wild ruminants, usually share the grazing habitat of domestic ruminants (migratory flocks) very often in these areas and thus there is potential of cross-transmission of lungworm infections, besides gastrointestinal (GI) parasites.

The common etiological agents of the parasitic bronchitis in small ruminants include *Dictyocaulus filaria*, *Protostrongylus rufescens* and *Mullerius capillaris*[4]. Pathogenesis of these nematodes differs greatly because of variation in their predilection sites. *D. filaria* lives in the trachea and bronchi, whereas *P. rufescens* is found in the small bronchioles and *M. capillaris* inhabit the lung parenchyma of the host[4]. Epidemiology of disease depends usually on the pasture contamination by carrier animals and rainfall/precipitation appears to be the stimulant for both larvae and snail intermediate hosts. Clinical course of disease depends on severity of the infection, age and immunological status of the host[5]. The common clinical signs include coughing, unthriftiness, tenacious nasal discharge, respiratory distress and pneumonia[5]. However, pneumonia is rarely observed in *P. rufescens* and *M. capillaris* infected animals and these infections are almost unapparent being identified only at necropsy[6]. The present communication describes the impact and successful management of *M. capillaris* infection in musk deer maintained in captivity.

How to cite this article: Karikalan, M., Ram, H., Nayal, L.M.S., Mahendran, K., Kumar, B., Banerjee, P.S., Pawde, A.M. and Sharma, A.K. 2026. Therapeutic management of *Muellerius capillaris* infection in Himalayan musk deer *(Moschus leucogaster)*. Indian J. Vet. Pathol., 50(3) : 255-258.

MATERIALS AND METHODS

History

Musk Deer Research Centre, Mahroori in Bageshwar, Uttarakhand, is involved in breeding Himalayan musk deer for musk production, which has high medicinal value. The centre is located at about 7320 ft above mean sea level and is managed

under the Central Council for Research in Ayurvedic Sciences, an autonomous body of the Ministry of AYUSH, Government of India. The farm maintains musk deer in individual captive pens with adequate feed and water. During the monsoon season, mortality of six musk deer occurred within two months, and the cause was investigated. Systematic necropsy was performed and tissue samples from major organs (liver, lungs, kidney, spleen, heart, intestine, and brain) were fixed in 10% neutral buffered formalin for histopathological examination. Sections (4-5µm) were prepared using a microtome and stained with haematoxylin and eosin following standard procedures[7]. Heart blood and heart blood smears (heat fixed) were collected aseptically for bacteriological examination (culture isolation). Nasopharyngeal and oropharyngeal swabs, together with samples of the spleen, lymph nodes, intestine, and lung, were collected for genome detection of viruses by RT-PCR (PPRV and blue tongue virus). Stomach contents and tissue samples from the liver and kidney were collected for toxicological analysis.

Health examination of live animals and treatment

During the investigation, individual Himalayan musk deer were carefully captured and examined for general health status. Rectal temperature, respiration rate, and mucous membrane colour were recorded. Blood samples from six animals were collected for haematological and parasitological examination. Faecal samples from eleven animals were collected from the rectum to detect gastrointestinal parasites, and follow-up examinations were conducted after treatment with Ivermectin and Fenbendazole. Blood samples were analysed using Giemsa stain on thin blood smears. Faecal samples were examined using conventional parasitological methods, and lungworm larvae were recovered using the Baermann technique[8]. The number of larvae per gram (LPG) of faeces was calculated and larvae were identified morphologically using standard keys. Based on the findings, infected animals were treated with ivermectin (0.2 mg/kg, subcutaneously), followed by fenbendazole (5 mg/kg orally for 15 days). Treatment efficacy was assessed on days 10 and 30 after the final treatment.

RESULTS

The carcass of musk deer showed emaciation (Fig. 1), pale mucous membranes, and marked reduction in subcutaneous adipose tissue. The lungs exhibited multifocal dark red areas of consolidation involving all lobes of both lungs with serosanguinous fluid in

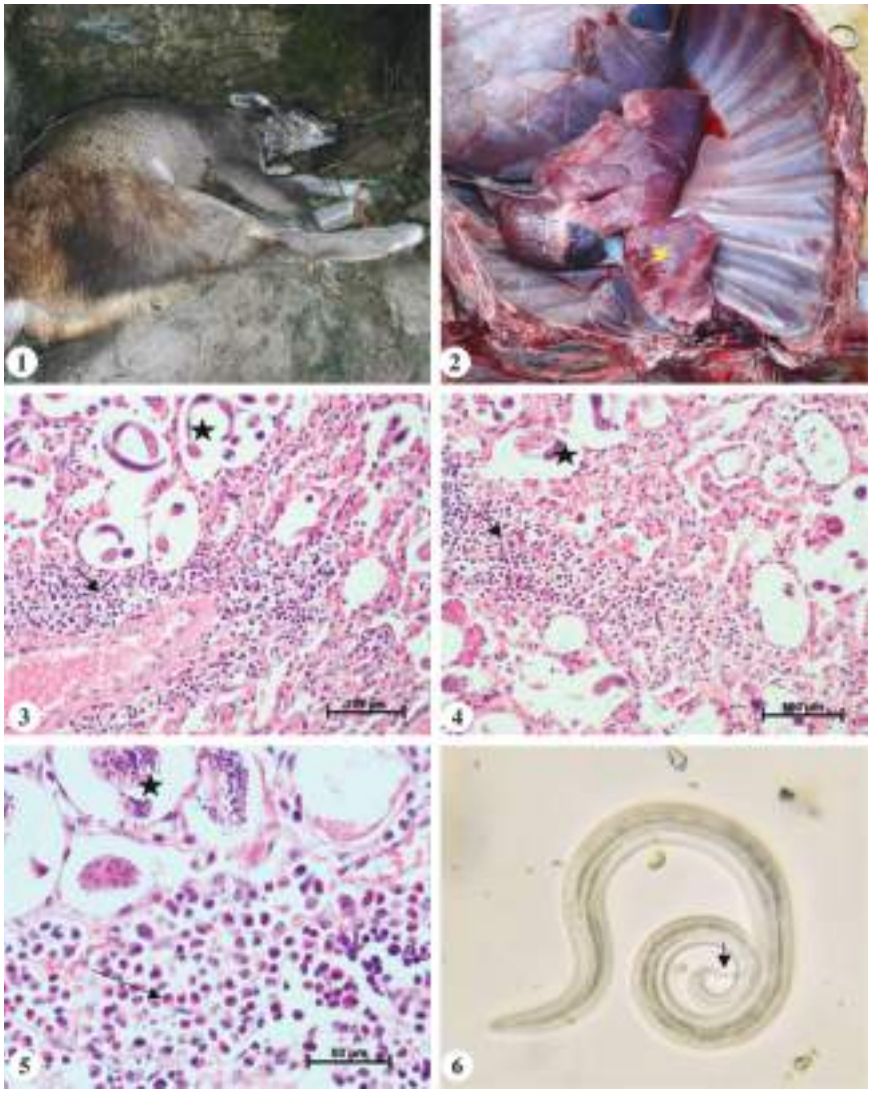

Fig. 1. Carcass of musk deer found dead in the enclosure of musk deer farm; **Fig. 2.** Left lung showing multifocal dark red areas of consolidation (arrow) with serosanguineous fluid in the thoracic cavity; **Fig. 3&4.** Lung showing highly engorged pulmonary vessels with numerous parasitic stages in the alveolar lumen (star) surrounded by severe infiltration of inflammatory cells (arrow). HE, x200; **Fig. 5.** Higher magnification of fig.4 showing the parasitic stages in the alveoli (star) surrounded by mixed population of inflammatory cells (arrow). HE, x400; **Fig. 6.** *Muellerius capillaris* larvae with undulating tail tip possessing a small, sharp dorsal spine in fecal examination (arrow).

Sl. No.	Identification No.	Larval count per gram of faecal pellets (LPG) before treatment	Larval count (LPG) after treatment		
			Ivermectin	Fenbendazole treatment for 15 days	
			Treatment after 10th dpt	10th dpt	30th dpt
1.	Musk deer 1	<10	<10	absent	absent
2.	Musk deer 2	<10	absent	absent	absent
3.	Musk deer 3	<10	absent	absent	absent
4.	Musk deer 4	10-50	<10	absent	absent
5.	Musk deer 5	<10	<10	absent	absent
6.	Musk deer 6	>50	10-50	absent	absent
7.	Musk deer 7	10-50	<10	absent	absent
8.	Musk deer 8	<10	absent	absent	absent
9.	Musk deer 9	<10	absent	absent	absent
10.	Musk deer 10	>50	10-50	absent	absent
11.	Musk deer 11	<10	<10	absent	absent

LPG <10- Mild, 10-50-Moderate, >50 Severe

the thoracic cavity. (Fig. 2). Histopathology revealed numerous parasite stages and desquamated epithelial cells in the alveoli, bronchi and bronchioles. These lesions were associated with moderate to severe infiltration of inflammatory cells, predominantly eosinophils, macrophages, and lymphocytes, along with highly engorged pulmonary blood vessels and oedema (Fig 3-5). Other organs did not reveal any significant histopathological changes. Bacteriological culture of heart blood on blood agar did not yield any growth of *Pasteurella* spp. Additionally, microscopic examination of Giemsa-stained heart blood smears did not reveal any bipolar organisms. Virological examination of the lung, spleen, lymph nodes, and intestinal samples by RT-PCR did not detect significant viral pathogens, including PPRV and BTV. Toxicological analyses of the stomach contents, liver, and kidney samples were negative for the presence of heavy metals, nitrate, nitrite, hydrogen cyanide (HCN), and commonly used insecticides.

All the live Himalayan musk deer examined had normal rectal temperature and respiratory rate while pale mucous membranes indicated possible anaemia. Haematological examination showed a mild decrease in haemoglobin, PCV, and RBC counts (9.0 ± 1.0 g/dL, 35.0 ± 4.2%, and 2.2 ± 0.6 × 10^6/μL). In contrast, the total white blood cell (WBC) count remained within the normal reference range. Microscopic examination of Giemsa-stained blood smears did not reveal any haemoparasites. No gastrointestinal parasites were detected by direct faecal examination. However, faecal examination using the Baermann technique revealed first-stage larvae of *Muellerius capillaris* (Fig. 6). Mild infection (<10 LPG) was observed in seven animals, moderate infection (10-50 LPG) in two animals, and heavy infection (>50 LPG) in two animals. After treatment with Ivermectin, lungworm infection persisted in seven animals at day 10 post-treatment. Subsequent treatment with Fenbendazole resulted in complete clearance of the parasite, as no larvae were detected on days 10 and 30 after the final treatment.

DISCUSSION

The Himalayan musk deer belongs to the family *Moschidae* and resembles true deer of the *Cervidae*, but lacks antlers. It is widely distributed across the Himalayan regions. They feed primarily on leaves, flowers, grasses, mosses, and lichens. The declining population of musk deer in India and other parts of the world has been attributed to infectious diseases and anthropogenic factors such as habitat loss, ecological degradation, and poaching[2]. As herbivores sharing grazing areas with domestic and wild ruminants, musk deer are exposed to various parasitic infections through contaminated pastures. Among these, Parasitic bronchitis (lungworm infection) is common in small ruminants of the Himalayan region[4]. The disease is mainly associated with *D. filaria,* while *P.* rufescens and *M. capillaris* are also reported in grazing animals. Lungworm infections have also been documented in wild ruminants such as spotted deer and blue sheep in Himalayan ecosystems[7,9].

In the present study, poor health in captive musk deer at the breeding farm was associated mainly with *M. capillaris* infection. Previous records from the same farm indicated mortality due to Fasciolosis and verminous pneumonia[6]. Persistent lungworm infection at the farm may be associated with the use of fodder collected from adjacent forest areas, which could serve as a source of infection. *Muellerius capillaris*, commonly known as the nodular lungworm, generally causes mild or subclinical disease. However, pathological findings frequently reveal diffuse broncho-interstitial pneumonia with minimal or absent characteristic pulmonary nodules,

indicating that significant pathological changes may occur even in the absence of overt clinical signs[10]. Control of lungworm infections in ruminants generally involves the use of anthelmintic drugs such as benzimidazoles, pro-benzimidazoles, and Ivermectin[11-13]. However, these drugs may not completely eliminate adult parasites and may only temporarily reduce the fecundity of small lungworms[14]. In the present study, ivermectin treatment showed limited efficacy against *M. capillaris*, which is consistent with earlier reports indicating incomplete effectiveness of this drug[13]. In contrast, treatment with fenbendazole for 15 days effectively eliminated adult parasites, and no larvae were detected in subsequent faecal examinations up to 30 days post-treatment. Since the parasite forms nodules in lung tissue that may later become fibrotic or calcified, a prolonged treatment regimen is often necessary. Therefore, the present findings support the use of fenbendazole for extended treatment in lungworm infections of domestic as well as wild ruminants.

ACKNOWLEDGEMENT

The authors are thankful to Director, ICAR-Indian Veterinary Research Institute, Izatnagar necessary facilities to perform this investigation.

Financial support & sponsorship: None

Conflicts of Interest: None

Use of Artificial Intelligence (AI)-Assisted Technology for manuscript preparation: The authors confirm that there was no use of AI-assisted technology for assisting in the writing of the manuscript and no images were manipulated using AI

REFERENCES

1. Shukla M, Joshi BD, Kumar VP, Thakur M, Mehta AK, Sathyakumar S and Goyal SP. 2019. Species dilemma of musk deer (*Moschus* spp.) in India: Molecular data on cytochrome c oxidase I suggests distinct genetic lineage in Uttarakhand compared to other *Moschus* species. *Anim Biotechnol* **30**: 193-201.
2. Ilyas O. 2015. Status, habitat use and conservation of Alpine musk deer (Moschus chrysogaster) in Uttarakhand Himalayas, India. *J Appl Anim Res* **43**: 83-91.
3. Pedersen AB, Jones KE, Nunn CL and Altizer SA. 2007. Infectious disease and mammalian extinction risk. *Conserv Biol* **21**: 1269-1279.
4. Sharma RL. 1994. Parasitic bronchitis in goats and the possible use of *Dictyocaulus filaria* vaccine for its control. *Vet Parasitol* **5**: 255-262.
5. Urquhart GM, Armour J, Duncan JL, Dunn AM and Jennings FW. 1996. *Veterinary Parasitology*. 2nd edn., Blackwell Science Ltd., London, pp. 301-309.
6. Singh KP, Chandra D, Nayal LMS and Chauhan RS. 2007. Hepatic fasciolosis and verminous pneumonia in captive musk deer (*Moschus chrysogaster*). *Indian J Anim Sci* **77**: 1258-1260.
7. Karikalan M, Ram H, Pathak S, Banerjee PS, Chandra MS, Pawde AM and Sharma AK. 2020. Pneumonia due to protostrongylid lung worms in wild Himalayan blue sheep (*Pseudois nayaur*). *Indian J Vet Pathol* **44**: 181-183.
8. Soulsby EJL. 1982. *Helminths, Arthropods and Protozoa of Domesticated Animals.* Baillière Tindall, London, pp. 521-531.
9. Ramaswami K and Arora BM. 1991. Prevalence of *Muellerius capillaris* in free-ranging spotted deer (*Cervus axis*) in India and its experimental cross-transmission to goats. *J. Wildl Dis* **27**: 102-104.
10. Kanwar NS, Paliwal OP and Ram K. 1998. Verminous pneumonia in goats. *J Vet Parasitol* **12**: 139.
11. Helle O. 1986. The efficacy of fenbendazole and albendazole against the lungworm *Muellerius capillaris* in goats. *Vet Parasitol* **22**: 293-301.
12. Cabaret J. 1991. Efficacy of netobimin against *Muellerius capillaris* and resistant strains of digestive tract strongyles in dairy goats. *Am J Vet Res* 52: 1313–1315.
13. McCraw BM and Menzies PI. 1986. Treatment of goats infected with the lungworm *Muellerius capillaris*. *Can Vet J 27*: 287–290.
14. Vadlejch J, Makovicky P, Cadkova Z and Langrova I. 2016. Efficacy and persistent activity of moxidectin against natural *Muellerius capillaris* infection in goats and pathological consequences of muelleriosis. *Vet Parasitol* **218**: 98-101.

Indian J. Vet. Pathol., 50(3) : 259-261, 2026: DOI: https://doi.org/10.56093/7k8p0449

CASE REPORT

A rare case of pulmonary adenocarcinoma in Pattanam sheep

K. Thilagavathi* and J. Selvaraj
Department of Veterinary Pathology, Veterinary College and Research Institute, Tamil Nadu Veterinary and Animal Sciences University, Orathanadu, Thanjavur District, Tamil Nadu - 614 625

***Address of correspondence**
Dr. K. Thilagavathi; E-mail: thilagapatho@gmail.com
ORCID Id: 0000-0002-1624-251X

Received: 27.3.26; Accepted: 5.5.26

ABSTRACT

A two-year-old female Pattanam sheep was submitted for necropsy to the Department of Veterinary pathology, Veterinary College and Research institute, Orathanadu. During necropsy, the gross lesions were observed and required tissue samples were collected for histopathology. Grossly, tracheal and bronchial lumen contained frothy exudate. Lungs were adhered to the pleura and showed dark red firm consolidated areas with grey or pale nodular areas. Histopathologically, lungs revealed multifocal adenomatous appearance of the parenchyma. Alveolar wall transformed into cuboidal epithelium as well as columnar epithelium which formed acinar and papillary pattern. Based on the gross lesions and histopathology, a very rare case of pulmonary adenocarcinoma in a Pattanam sheep is documented.

Keywords: Pulmonary adenocarcinoma, Pattanam Sheep

Respiratory infections are quite common and responsible for 30-40% of mortality in sheep of various ages[1]. Ovine pulmonary adenocarcinoma (OPA) is a contagious respiratory tumour of small ruminants, characterized by chronic weight loss and respiratory failure. Infection with the beta retrovirus Jaagsiekte sheep retrovirus (JSRV) is the cause of OPA[2]. The disease primarily affects both domestic and wild sheep, and does not occur in other livestock except goats, in which, the disease has been described in subclinical form. OPA was first described as a cause of respiratory distress in sheep in South Africa in 1865. In that time, the disease was called "jaagsiekte", the name that is derived from the Afrikaans and means "chasing sickness". This is because affected animals show difficulty to breathe as if they are being chased. Since then, OPA has distributed worldwide except in Australia, New Zealand and Iceland which have eradicated the disease[3]. Two- to four-year-old sheep are primarily affected[4]. It has been identified in a wide variety of breeds in many countries around the world including India. It is responsible for severe economic losses to the sheep industry in many sheep rearing countries and the subclinical form of the disease affects growth rate, carcass weight, and milk and wool production.

OPA is believed to be the most important disease that can affect international trade as determined by the Office International des Epizooties (OIE). In addition to its importance as a Veterinary study on cancer, it has similar pathological and epidemiological features to bronchoalveolar carcinoma in humans, and is considered a useful animal model of pulmonary carcinogenesis[1]. Neoplastic proliferation of type II pneumocytes and Clara cells, produce papillary to acinar tumoral pattern with infiltration of macrophages, lymphocytes and plasma cells[5]. The gross findings of naturally occurring OPA are heterogeneous, exhibiting variations in anatomical patterns or forms: classical, atypical and mixed. Classical forms exhibit extensive, consolidated, grey areas, primarily located in the cranioventral lung regions, and appear moist on section. Atypical forms are characterized by white, well-demarcated nodules that are dry at the cut surface. A wide variety of mixed forms may be observed in the same affected flock, and even nodules resembling atypical lesions have been noted in the same lung in which the classical lesion is present[4].

How to cite this article : Thilagavathi, K. and Selvaraj, J. 2026. A rare case of pulmonary adenocarcinoma in Pattanam sheep Indian J. Vet. Pathol., 50(3) : 259-261.

A two-year-old female Pattanam sheep from an organised farm was submitted to the Department of Veterinary pathology, Veterinary College and Research institute, Orathanadu for necropsy. The flock was composed of 200 sheep. During necropsy, required tissue samples were collected and fixed in 10% formalin. The tissues were processed, sectioned and stained with Hematoxylin and Eosin (H&E) stain.

Grossly, the tracheal and bronchial lumen contained frothy exudate. Cranial lobe of left lung was adhered with white fibrinous membrane (Fig. 1). Left lung cranial lobe showed dark red firm consolidated areas with grey or pale nodular areas and on sectioning the pale areas, showed white granular appearance with oozing of frothy exudate (Fig. 2). Histopathologically, the

pleura was thick with sero-fibrinous exudate. The lungs revealed multifocal adenomatous appearance of the parenchyma. Hyperplasia of type II pneumocytes on the alveolar wall into cuboidal epithelium as well as columnar epithelium forming acinar pattern (Fig. 3, 4 & 6). In some places, the proliferation of type II pneumocytes on the alveolar wall projected into the lumen forming papillary projections (Fig. 5). In many alveoli, the epithelium desquamated into the lumen. Scattered areas showed moderate lymphocyte and macrophage infiltrations (Fig. 6). The bronchial lymph node showed congestion in the cortex with lymphoid depletion. The spleen also showed mild lymphoid depletion. There were no metastases of tumour cells.

The frothy exudate in tracheal and bronchial lumen as well as fibrinous adhesion in lungs was in accordance with previous report[6]. Lungs with dark red firm consolidated areas with grey or pale nodular areas and on sectioning the pale areas, showed white granular appearance with oozing of frothy exudate which was in agreement with earlier works[1&6]. The lungs had multifocal adenomatous appearance with hyperplasia of type II pneumocytes into cuboidal epithelium as well as columnar epithelium forming acinar and papillary pattern. These findings were in strong agreement with earlier reports[3&7]. The transformation of alveolar epithelial lining into cuboidal and columnar cells are pathognomonic for ovine pulmonary adenocarcinoma[3]. The epithelium desquamated in the alveolar lumen was observed earlier also[6]. The infiltration of alveolar macrophages surrounding the neoplastic foci was a consistent histologic feature but very little is known about their pathogenic role in OPA. The excessive surfactant like protein produced in this tumour may represent a stimulus for accumulation of macrophages[6]. The bronchial lymph node congestion and lymphoid depletion was in accordance with earlier report[8] who also observed moderate plasmacytosis in the medullary areas. In the present study, there were no metastases of tumour cells. In contrast, extra-thoracic metastases were found in the liver, kidneys, skeletal muscles, digestive system, spleen, skin and adrenal glands while intrathoracic metastases occurred in chest wall, regional lymph nodes, diaphragm and heart were reported[9].

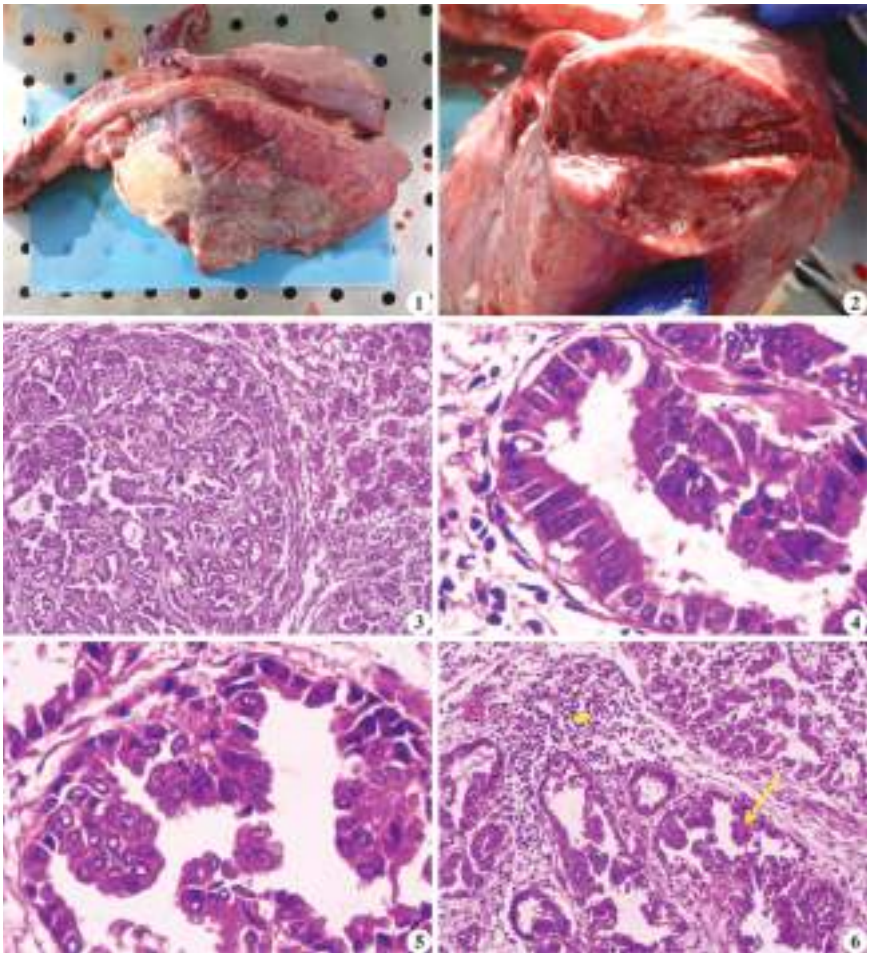

Fig.1. Lung showing fibrinous adhesion with grey nodules on the surface; **Fig. 2.** Lung on section showing granular appearance with frothy exudate; **Fig. 3.** Lung showing adenomatous appearance forming acinar pattern with papillary projections (H&E x 40); **Fig. 4.** Lung showing hyperplasia of alveolar type II pneumocytes into columnar cells (H&E x 400); **Fig. 5**. Lung showing proliferation of alveolar type II pneumocytes into cuboidal cells forming papillary projections. (H&E x 400); **Fig. 6.** Lung showing hyperplasia of alveolar type II pneumocytes into cuboidal cells forming acinar pattern with papillary projections (arrow). Around the alveoli interstitial tissue showing lymphocyte and macrophage infiltration (star) (H&E x 100)

The present case is documented as the very rare incidence of pulmonary adenocarcinoma in a Pattanam sheep.

Financial support & sponsorship: None

Conflicts of Interest: None

Use of Artificial Intelligence (AI) Assisted technology for manuscript preparation: The authors confirm that there was no use of AI – Assisted Technology for assisting in the writing of the manuscript and no images were manipulated using AI

REFERENCES

1. Sonawane GG, Tripathi BN, Kumar R and Kumar J. 2016. Diagnosis and prevalence of ovine pulmonary adenocarcinoma in lung tissues of naturally infected farm sheep. *Vet. World* **9(4):** 365-370.
2. Ortega J, Corpa JM, Castillo D and Murphy BG. 2023. Pathological spectrum of ovine pulmonary adenocarcinoma in small ruminants: A focus on the mixed form. *Animals* **13:** 2828.
3. Radad K and Khalil S. 2014. Natural ovine pulmonary adenocarcinoma in an Egyptian sheep farm. *Eurasian J Vet Sci* **30(1):** 39-43.
4. Pozos RRA, Sainz GJM, Ortin A, Asin J, Climent M, Borderias L and De las Heras M. 2025. Histopathological and immunohistochemical study of neoplastic cell heterogeneity in early and advanced ovine pulmonary adenocarcinoma. *Animals* **15:** 2632.
5. Sasani F, Khaki F and Gharagouzloo MJ. 2017. Identification of atypic and classic, mucinous and nonmucinous forms of ovine pulmonary adenocarcinoma (OPA) and TTF1 marker expression. *Iran J Vet Med* **11(3):** 279-287.
6. Rosadio RH, Sharp JM, Lairmore MD, Dahlberg JE and De martin JC. 1988. Lesions and retroviruses associated with naturally occurring ovine pulmonary carcinoma (Sheep Pulmonary Adenomatosis). *Vet. Pathol* 2558-66.
7. Ozkan C, Yildirim S, Huyut Z and Ozbek M. 2020. Selected tumour biomarker levels in sheep with pulmonary adenomatosis. *J Vet Res* **64:** 39-44.
8. Quintas H, Pires I, Garces A, Prada J, Silva F and Alegria N. 2021.The diagnostic challenges of ovine pulmonary adenocarcinoma. *Ruminants* **1:** 58–71.
9. Minguijon E, Gonzalez L, De Las Heras M, Gomez N, Garcia Goti, M, Juste RA and Moreno B. 2013. Pathological and aetiological studies in sheep exhibiting extra-thoracic metastasis of ovine pulmonary Adenocarcinoma (Jaagsiekte). *J Comp Pathol* **148:** 139-147.

Indian J. Vet. Pathol., 50(3) : 262-266, 2026: DOI: https://doi.org/10.56093/150sym08

CASE REPORT

Concomitant occurrence of hepatocellular carcinoma and benign anthracotic lymphadenopathy in a German Shepherd dog

R. Madheswaran* and S. Mahalakshmi[1]
Department of Veterinary Pathology, Veterinary College and Research Institute, Tamil Nadu Veterinary and Animal Sciences University, Namakkal - 637 002, Tamil Nadu, India.
[1]Veterinary Dispensary, Animal Husbandry Department, Padi, Chennai – 600 101

***Address of correspondence**
Dr. R. Madheswaran, Associate Professor; E-mail: rmadheswaran2003@gmail.com
ORCID Id: 0000-0002-8113-6465

Received: 9.3.26; Accepted: 1.4.26

ABSTRACT

A nine-year-old male German Shepherd dog was presented with anorexia, lethargy and progressive weight loss. Clinical examination revealed emaciation, depression and dyspnoea. Haematological analysis showed leucocytosis and neutrophilia. The dog died following unsuccessful treatment and was submitted for necropsy. Gross examination revealed multiple tumour nodules in all liver lobes, lungs and lymph nodes (LN). The mesenteric lymph node (MSLN) appeared whitish-pink, whereas the mediastinal lymph node (MDSLN) showed black pigmentation on a greyish-white background. Cytology of hepatic nodules revealed clusters of neoplastic hepatocytes. Histopathology showed solid sheets of neoplastic cells consistent with hepatocellular carcinoma (HCC) with compression and invasion of adjacent hepatic parenchyma. Metastatic neoplastic cells were observed in the lungs and LNs. Additionally, the MDSLN showed macrophages containing black pigments consistent with benign anthracotic lymphadenopathy (BAL). Immunoreactivity of arginase-1 showed marked expression in the neoplastic cells. Hep-Par-1 showed minimal expression in neoplastic cells and strong expression in the normal hepatocytes. Mild expression of glypican-3 and AFP were noticed in the neoplastic cells. Both the MSLN and MDSLN showed strong expression of CD3 and moderate expression of CD20 in the lymphoid cells. Gross, cytological, histopathological and immunohistochemical findings were consistent in the diagnosis of HCC coexist with BAL in a dog.

Key words: BAL, Dog, HCC, Histopathology, Immunohistochemistry

Liver cancer in canines is rare, but a significant tumour, accounting for 0.6-1.3% of all neoplasms and primarily affecting dogs over 10 years of age[1,2]. Primary liver tumours include hepatocellular adenoma, hepatocellular carcinoma (HCC), cholangiocellular carcinoma and neuroendocrine carcinoma. Among these, HCC is the most prevalent cancer in both humans and animals[1,3]. The other less common hepatic tumours are bile duct carcinoma, sarcoma, lymphoma, malignant histiocytosis and mast cell tumours[3]. HCC in dogs usually occurs in solitary or massive, nodular and diffuse forms and mostly metastasizes within the liver by local infiltration or to extra-hepatic organs like lungs and local LNs[4].

Anthracosis refers to the deposition of carbon particles following repeated inhalation of biomass smoke, coal dust, cigarette smoke and environmental air pollutants[5,6]. It predominantly affects the lung parenchyma and airways, may also extend to extra-pulmonary sites including MDSLN and axillary LN[5,6]. Enlargement of the MDSLN is an important diagnostic finding that may arise from aetiologies like tuberculosis[7], sarcoidosis[6] and malignancies[8]. Among the various causes, accumulation of carbon particles within lymphoid tissues, resulting in anthracotic lymphadenopathy, is rarely studied in animals. Benign anthracotic lymphadenopathy (BAL) in humans may occur as a primary finding or in association with inflammatory conditions and malignancies[9,10], whereas comparable observations in veterinary practice are meager. Therefore, the present report describes a unique case of HCC associated with BAL in German Shepherd dog.

A nine-year-old male German Shepherd dog was presented to the small animal clinic for treatment with a history of anorexia, lethargy and weight loss.

How to cite this article : Madheswaran, R. and Mahalakshmi, S. 2026. Concomitant occurrence of hepatocellular carcinoma and benign anthracotic lymphadenopathy in a German Shepherd dog. Indian J. Vet. Pathol., 50(3) : 262-266.

The dog weighed about 23.7 kg and appeared emaciated, dull and depressed. Clinical examination revealed difficulty in breathing and congested visible mucous membranes. Haematological parameters, including total erythrocyte count ($5.38x10^6$/µL), haemoglobin (10.5 g/dL), packed cell volume (36.4%) and platelets ($352x10^3$/µL) were within the normal limits. A significant elevation in total leucocyte count ($33.9x10^3$/µl) and neutrophils (78%) with unaltered eosinophils (7%), basophils (0), lymphocytes (11%) and monocytes (4%) was noticed.

Serum biochemical values such as total protein (6.69 g/dL), albumin (2.50 g/dL), blood urea nitrogen (19.81 mg/dL), creatinine (1.44 mg/dL), calcium (7.44 mg/dL) and phosphorus (5.37 mg/dL) did not show any alterations. The dog was treated for five days, but died following unsuccessful treatment and was subsequently submitted for post mortem examination.

At necropsy, numerous nodules of varying sizes (3-24 mm) were noticed in all liver lobes (Fig. 1). The liver along with nodules weighed about 185 g. The cut surface of the nodules appeared grayish-white in colour. Cytology of hepatic nodules revealed a cluster of neoplastic hepatocytes with features of malignancy like anisocytosis, anisokaryosis and increased nuclear to cytoplasmic ratio (Fig. 2). Metastatic tumour nodules were also noticed in the lungs, MSLN and MDSLN. The MSLN appeared hard and whitish-pink in colour, whereas, MDSLN appeared in shades of black against a greyish-white background. Representative tissue pieces from liver, lungs and lymph nodes were collected, fixed in 10% neutral buffered formalin and processed for histopathology.

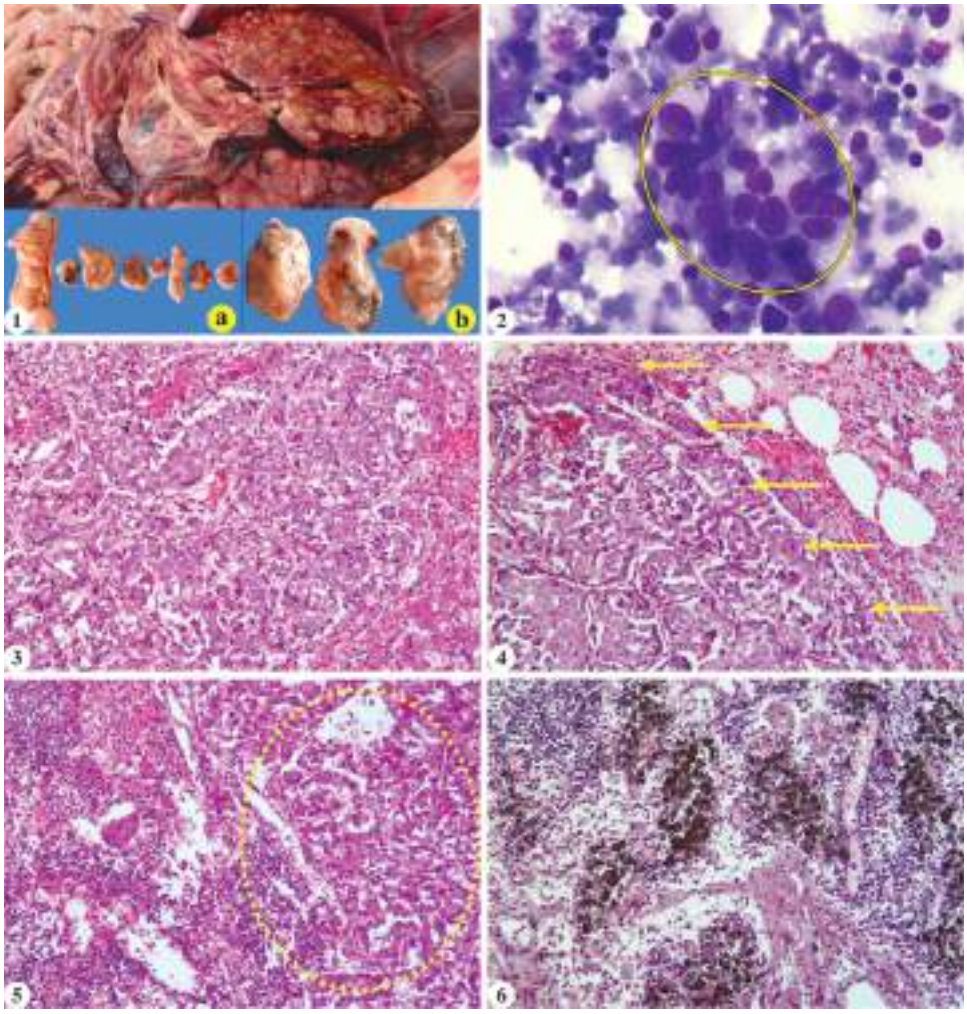

Fig. 1. German Shepherd dog: Liver showing numerous nodules of varying sizes in the surface of all lobes. a). Mesenteric lymph node appearing whitish-pink in colour. b). Mediastinal lymph node showing shades of black in greyish-white background; **Fig. 2**. Cytology of hepatic nodules showing a cluster of neoplastic cells with anisocytosis, anisokaryosis and increased nuclear to cytoplasmic ratios. Wright's-Giemsa x1000; **Fig. 3**. Hepatocellular carcinoma showing solid sheets of neoplastic cells arranged in trabecular and acinar patterns surrounded by collagenous stroma and angiogenesis. H&E x100; **Fig. 4**. Lung showing solid sheets of neoplastic cells occupying most of the alveoli (arrows). H&E x100; **Fig. 5**. Mesenteric lymph node showing the sheets of neoplastic cells (circle) replacing the lymphoid cells. H&E x100; **Fig. 6**. Mediastinal lymph node showing the deposition of carbon particles in the cytoplasm of macrophages consistent with anthracotic lymphadenopathy. H&E x100.

Microscopically, the hepatic nodules showed solid sheets of neoplastic cells surrounded by fine fibrous stromal tissues. The neoplastic cells arranged in trabecular and acinar patterns were surrounded with collagenous stroma and angiogenesis (Fig. 3). The neoplastic cells were round to polygonal in shape with eosinophilic cytoplasm, vesiculated nuclei and prominent nucleoli. High mitotic activity (15-20 mitoses per 10 high-power fields) and moderate degrees of anisocytosis and anisokaryosis were noticed. Hepatic parenchyma around the tumour nodules were invaded by neoplastic cells. The invaded areas showed necrosis with infiltration of lymphocytes and a few plasma cells. The metastatic neoplastic cells observed in lungs (Fig. 4), MSLN (Fig. 5) and MDSLN also revealed features similar to those noticed in hepatic neoplastic cells. In addition, MDSLN revealed deposition of black pigments in the cytoplasm of macrophages consistent with benign anthracotic lymphadenopathy (BAL) (Fig. 6).

A few paraffin-embedded tissue sections were subjected to immunohistochemical (IHC) staining. The sections were incubated with primary antibodies (Table 1) followed by a secondary antibody using the PolyExcel HRP/DAB detection system (M/s

Table 1. The details of primary antibodies used for immunohistochemistry.

S. No.	Primary antibody	Host	Clone	Dilution	Location of expression
1.	Arginase-1	Mouse	Monoclonal(ARG1)	1:25	Cytoplasmic
2.	Hep-par-1	Mouse	Monoclonal(EP265)	1:50	Cytoplasmic
3.	Glypican-3	Mouse	Monoclonal(GPC3)	1:50	Cytoplasmic
4.	Alpha fetoprotein (AFP)	Rabbit	Monoclonal(EP209)	1:50	Cytoplasmic
5.	CD3	Rabbit	Polyclonal(PP160)	1:25	Nuclear, Membranous
6.	CD20	Mouse	Monoclonal(L26)	1:50	Nuclear, Membranous

PathnSitu Biotechnologies, Hyderabad, India). Slides were counter stained with Mayer's haematoxylin. Immunoreactivity in tumour tissues showed marked cytoplasmic expression of arginase-1 in neoplastic cells and mild expression in normal hepatic cells and stromal tissues (Fig. 7). Hep-Par-1 showed minimal cytoplasmic expression in neoplastic cells, strong expression in normal hepatocytes and mild expression in stromal tissues (Fig. 8). Glypican-3 revealed mild cytoplasmic expression in neoplastic cells, minimal expression in normal hepatic cells and moderate expression in stromal tissues (Fig. 9). AFP showed mild cytoplasmic expression in neoplastic cells and minimal expression in normal hepatic cells and stromal tissues (Fig. 10). The metastatic neoplastic cells in the lungs, MSLN and MDSLN exhibited IHC expression patterns comparable to those of the hepatic neoplastic cells for Arginase-1, Hep-Par-1, Glypican-3 and AFP.

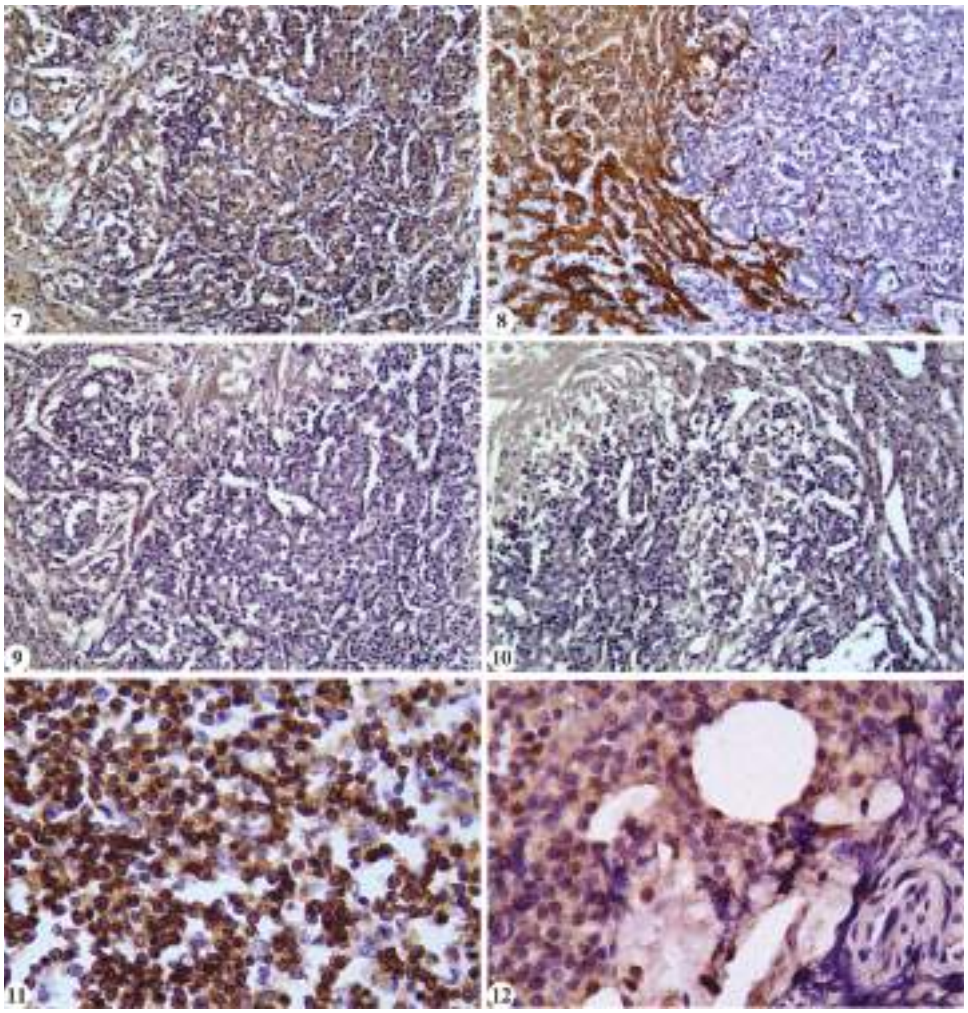

Fig. 7. Tumour section showing marked cytoplasmic expression to arginase-1 in the neoplastic cells. (IHC, Arginase-1 x100); **Fig. 8**. Tumour section showing minimal cytoplasmic expression in neoplastic cells and strong expression in normal hepatic cells to Hep-Par-1. (IHC, Hep-Par-1 x100); **Fig. 9**. Tumour section showing mild cytoplasmic expression to glypican-3 in the neoplastic cells. (IHC, Glypican-3 x100); **Fig. 10**. Tumour section showing mild cytoplasmic expression to AFP in the neoplastic cells. (IHC, AFP x100); **Fig. 11**. Mesenteric lymph node showing strong nuclear and membranous expression to CD3 in the lymphoid cells. (IHC, CD3 x400); **Fig. 12**. Mesenteric lymph node showing moderate nuclear and membranous expression to CD20 in the lymphoid cells. (IHC, CD20 x400).

Additionally, both MSLN and MDSLN exhibited strong nuclear and membranous immunoreactivity for CD3 in lymphoid cells (Fig. 11), indicating a predominance of T-lymphocytes, whereas CD20 expression was moderate with similar nuclear and membranous localization (Fig. 12), denoting a comparatively lower proportion of B-lymphocytes.

A rare case of HCC with BAL was diagnosed in male German Shepherd dog. The clinical signs recorded in this case could be attributed to

paraneoplastic syndromes that might be the reason for death of the dog[4]. Blood parameters revealed leucocytosis and neutrophilia in this case, similar to the previous workers[2,4], who also recorded anaemia and thrombocytosis in dogs affected with hepatic tumours. Serum biochemical values of this dog did not show any alterations. However, increased levels of total bilirubin, total protein, alanine transaminase, aspartate transaminase, alkaline phosphatase and lactate dehydrogenase were reported in dogs with liver tumours[2,4].

Grossly, the entire surface of all liver lobes showed numerous nodules, similar to the observations of previous workers, who also noticed higher frequency of tumour nodules in the left lateral lobe[4,11]. Cytological features of this case concur with the findings of earlier investigators[12]. Histological examination of tumour nodules showed features of HCC that are in agreement with the findings of previous workers[1,2,4]. HCC metastasis to lungs, MSLN and MDSLN concur with the findings of previous workers[2,4,13] who reported frequent metastasis to peritoneum along with these organs. The metastatic MDSLN also revealed the presence of anthracotic lymphadenopathy in the present case. Earlier reports are available on mediastinal lymphadenopathy due to metastasis of HCC and anthracosis in humans[5,6,9,10,14], whereas similar reports are lacking in dogs.

Immunoreactivity of arginase-1 showed marked expression in neoplastic cells in this case, which is in agreement with the observations of previous researchers in humans and animals[15,16,17]. Arginase-1 has been reported to exhibit 100% sensitivity in well-differentiated HCC in humans[15], with immunoexpression characteristically observed in the cytoplasm, along with variable nuclear and membranous localization within neoplastic cells[16]. Hep-par-1 showed minimal expression in neoplastic cells and strong expression in normal hepatic cells, which is in agreement with the findings of previous workers[1,15,16,17]. Hep-Par-1 has been documented to exhibit diminished cytoplasmic immunoreactivity along with relatively lower diagnostic sensitivity in well-differentiated HCC in humans[15,16]. Mild expression of glypican-3 and AFP in this study concurs with the findings of earlier workers[2,15,16].

In the present study, both the MSLN and MDSLN demonstrated strong CD3 expression and moderate CD20 expression in lymphoid cells, which is in agreement with previous workers[18]. This immunophenotypic pattern suggests a predominance of T-cells with a comparatively lesser proportion of B-cells, indicative of active lymphoid cell turnover, which may be associated with conditions such as anthracosis, inflammation or malignancy.

The study results revealed that the primary tumour originated from liver which metastasized to lungs and regional LNs. The MDSLN revealed mixed population of metastatic neoplastic cells and carbon particles laden macrophages. Considering the rarity of co-occurrence, the present case is reported to highlight the diagnostic challenges and clinical significance of concurrent HCC and BAL in dogs.

ACKNOWLEDGEMENTS

The authors are thankful to Tamil Nadu Veterinary and Animal Sciences University, Chennai for providing necessary facilities to carry out this work.

Financial support and sponsorship: None

Conflicts of Interest: None

Use of Artificial Intelligence (AI)-Assisted Technology for manuscript preparation: The authors confirm that there was no use of AI-assisted technology for assisting in the writing of the manuscript and no images were manipulated using AI.

REFERENCES

1. Tsuji Y, Kuramochi M, Izawa T, Akiyoshi H, Yamate J and Kuwamura M. 2019. Hepatic myoepithelial carcinoma in a dog: Immunohistochemical comparison with other canine hepatic carcinomas. *Vet Pathol* **56**:889-94.
2. Gibson EA, Goldman RE and Culp WTN. 2022. Comparative oncology: Management of hepatic neoplasia in humans and dogs. *Vet Sci* **9**:489.
3. Weiss DJ and Moritz A. 2002. Liver cytology. *Vet Clin North Am Small Anim Pract* **32**:1267-91.
4. Patnaik AK, Hurvitz AI, Lieberman PH and Johnson GF. 1981. Canine hepatocellular carcinoma. *Vet Pathol* **18**:427-38.
5. Haidar M, Bannoura S, Halal A, Ghanem AA, Dergham MY, Barakat A, Jreige Mand Shabb N. 2017. A case report of false positive FDG-PET/CT mediastinal lymph node in oesophageal adenocarcinoma revealed to be an anthracotic and anthraco-silicotic spindle cell pseudotumor (AASCP). *J Nuc Med Rad Ther* **8**:355.
6. Giri S, Kumar L, Mane K, Uppin MS, Bhrugumalla S and Sundaram S. 2024. 18F-Fluorodeoxyglucose-avid benign anthracotic mediastinal lymphadenitis mimicking metastatic lymphadenopathy. *Cureus* **16**:e59614.
7. Navani N, Molyneaux PL, Breen RA, Connell DW, Jepson A, Nankivell M, Brown JM, Morris-Jones S, Ng B, Wickremasinghe M, Lalvani A, Rintoul RC, Santis G, Kon OM and Janes SM. 2011. Utility of endobronchial ultrasound-guided transbronchial needle aspiration in patients with tuberculous intrathoracic lymphadenopathy: A multicentre study. *Thorax* **66**:889-93.
8. Onitilo AA, Engel JM, Tanimu SB and Nguyen TC. 2010. Anthracosis and large mediastinal mass in a patient with healed pulmonary tuberculosis. *Clin Med Res* **8**:99-103.
9. Hewitt RJ, Wright C, Adeboyeku D, Ornadel D, Berry M, Wickremasinghe M, Wright A, Sykes A and Kon OM. 2013. Primary nodal anthracosis identified by EBUS-TBNA as a cause of FDG PET/CT positive mediastinal lymphadenopathy. *Respir Med Case Rep* **10**:48-52.
10. Erol S, Anar C, Erer OF, Aydogdu Z and Aktogu S. 2018. Does anthracosis reported in endobronchial ultrasound-guided

transbronchial needle aspiration exclude metastasis? *Eurasian J Pulmonol* **20**:12-16.
11. Kinsey JR, Gilson SD, Hauptman J, Mehler SJ and May LR. 2015. Factors associated with long-term survival in dogs undergoing liver lobectomy as treatment for liver tumors. *Can Vet J* **56**:598-604.
12. Masserdotti C and Drigo M. 2012. Retrospective study of cytologic features of well-differentiated hepatocellular carcinoma in dogs. *Vet Clin Pathol* **41**:382-390.
13. Liptak JM, Dernell WS and Withrow SJ. 2004. Liver tumors in cats and dogs. *Compendium* **30**:50-57.
14. Ivanick NM, Shrestha P, Podolsky MJ, Walavalkar V, Lucas CH, Gesthalter YB and Seeley EJ. 2021. A retrospective observational study of benign anthracotic lymphadenitis and its association with PET avid lymph nodes in patients undergoing cancer evaluation. *J Thorac Dis* **13**:4228-4235.
15. Nguyen T, Phillips D, Jain D, Torbenson M, Wu TT, Yeh MM and Kakar S. 2015. Comparison of 5 immunohistochemical markers of hepatocellular differentiation for the diagnosis of hepatocellular carcinoma. *Arch Pathol Lab Med* **139**:1028-1034.
16. Takahashi Y, Dungubat E, Kusano H, Ganbat D, Tomita Y, Odgerel S and Fukusato T. 2021. Application of immunohistochemistry in the pathological diagnosis of liver tumors. *Intl J Mol Sci* **22**:5780.
17. Hughes K, Radakovic M, Gorman F, Malinowska B and Cullen JM. 2013. Immunohistochemical characterization of clear cell variant of hepatocellular carcinoma in a sheep. *J Comp Pathol* **204**:47-50.
18. Meuten DJ. 2017. Tumors in domestic animals: Tumors of the hemolymphatic system. 5thedn. Wiley Blackwell, Ames, Iowa, USA. pp. 203-321.

Indian J. Vet. Pathol., 50(3) : 267-270, 2026: DOI: https://doi.org/10.56093/qyerew83

CASE REPORT

Subcutaneous filariasis: Cytopathology of *Dirofilaria repens* associated neoplastic alterations in a Chippiparai dog

N. Babu Prasath*, R. Thangathurai[1], V. Kumar[1], M. Madheena Begum[2] and M. Shiju Simon[3]
Department of Veterinary Pathology, Veterinary College and Research Institute,
Tamil Nadu Veterinary and Animal Sciences University, Orathanadu,
[1]Department of Veterinary Pathology, Veterinary College and Research Institute, Tirunelveli
[2]Department of Clinics, Madras Veterinary College
[3]Veterinary Clinical Complex, Veterinary College and Research Institute, Tirunelveli

***Address of correspondence**
Dr. N. Babu Prasath; E-mail: vetdrprasad@gmail.com
ORCID Id: 0000-0002-8219-9265

Received: 7.4.26; Accepted: 4.5.26

ABSTRACT

A Chippiparai female dog of five years old was presented with nodular swellings in neck and leg at Veterinary Clinical Complex, Veterinary College and Research Institute, Tirunelveli. Grossly, slightly raised, firm masses were found subcutaneously over the neck, ear base, shoulder and leg. Fine-needle aspiration biopsy was performed from individual masses and examined microscopically. Cytological smears were composed of bloody background with clusters of epithelial cells and multiple filiform-shaped microfilaria. Morphology of microfilaria were identified as L1 of *Dirofilaria repens* whereas cellular clusters were identified as sebaceous adenoma. The present study records the incidence of subcutaneous filariasis in a Chippiparai dog with neoplastic changes in associated tissues.

Keywords: *Dirofilaria repens*, Dog, Microfilaria, Neoplasm, Subcutaneous nodule

Filariasis is a vector-borne disease caused by spirurid nematode of genus *Dirofilaria* spp. under the family *Onchocercidae*[1]. It is composed of five nematode species includes, *D. immitis*, *D. repens*, *D. tenuis*, *D. ursi* and *D. striata* affecting dogs, raccoons, bears and wild felids and rarely humans[2]. Culicine mosquitoes are the vectors, transmitting the disease causing microfilaria between the hosts. Among these, *D. immitis* is a most common filarid pathogen in dogs occupying heart/pulmonary arteries and causing the 'heartworm disease'[3]. Meanwhile, *D. repens* (Railliet & Henry, 1911) is the second most common filarid nematode causing subcutaneous nodules in dogs and occasionally in human beings. The nodular lesions induced by *D. repens* may resemble neoplastic lesions[4]. Evidence of inflammatory cells in cytology and histopathology of subcutaneous nodules indicates as inflammatory nodule by *D. repens*[4,5]. Conversely, the present study describes the subcutaneous dirofilariais by *D. repens* that was associated with sebaceous adenoma in Chippiparai dog.

A five year-old female Chippiparai dog was presented to Veterinary Clinical Complex, Veterinary College and Research Institute, Tirunelveli with the history of swelling over the face, neck and legs since two weeks. On physical examination the animal was dull and had slightly firm, wart-like, raised subcutaneous masses over the left ventral neck, base of the ear and the shoulder and leg region measuring 1x1 to 1.5 cm. Whole blood was collected and analyzed for routine hematology using an automated hematology analyzer Mindray VetBC 2800 cell counter. Fine needle aspiration biopsy (FNAB) was collected from masses of different location and processed for standard Leishman's staining protocol. Stained slides were examined under Nikon ES 200 microscope and images were analysed with VImage software.

Cytological examination of fine-needle aspiration biopsy (FNAB) smears revealed a background of smudged erythrocytes with clusters of epithelial cells and numerous microfilariae.

Epithelial cell clusters revealed nearly uniform cells exhibiting clear, complete cohesion. Cells were occasionally arranged as rosette (acini-like) pattern (Fig. 1). Cells had abundant cytoplasm containing discrete fine and coarse vacuoles. Cytoplasmic vacuoles were rarely single and distinct (Fig. 2) and mostly multiple, fine indistinct (foamy) structures (Fig. 3) contributing high cytoplasmic to nuclear ratio. Nuclei were large, vesicular and composed of course chromatin and inconspicuous

How to cite this article : Prasath, N.B., Thangathurai, R., Kumar, V., Begum, M.M. and Simon, M.S. 2026. Subcutaneous filariasis: Cytopathology of Dirofilaria repens associated neoplastic alterations in a Chippiparai dog. Indian J. Vet. Pathol., 50(3) : 267-270.

nucleolus (Fig. 4). Rarely, the cells were enlarged, showing coarse cytoplasmic vacuolation (Fig. 5) and binucleation (Fig. 6). Multinucleated giant cells were also observed. The cellular characteristics are suggestive of sebaceous adenoma.

The epithelial clusters were intermingled with numerous filiform microfilaria (Fig. 7). Microfilaria were elongated, long and slender and had tapering end. They were unsheathed and showed distinct transverse cuticular striations. The body contained somatic nuclei that extended along the entire length, except at the tail tip. Cephalic end of the microfilaria was blunt and rounded. The cephalic end was blunt and rounded, with a short, clear cephalic space containing two to three prominent nuclei, which were anterior to and slightly separated from the first somatic nuclei (Fig. 8). The anterior region showed a distinct nerve ring and excretory pore, while the posterior region contained genital cells and an anal pore (Fig. 9). Body tapers and slightly curved like-a-hook (Fig. 10), ends sharply with a whip-like tail without nucleus (anucleate tail tip). The measurement of microfilaria was showed an average length of 360 μm (range 354–372 μm) and an average diameter of 8.4 μm (range 7.2–9.2 μm). The morphology and morphometric analysis of microfilaria were consistent with *D. repens*[6].

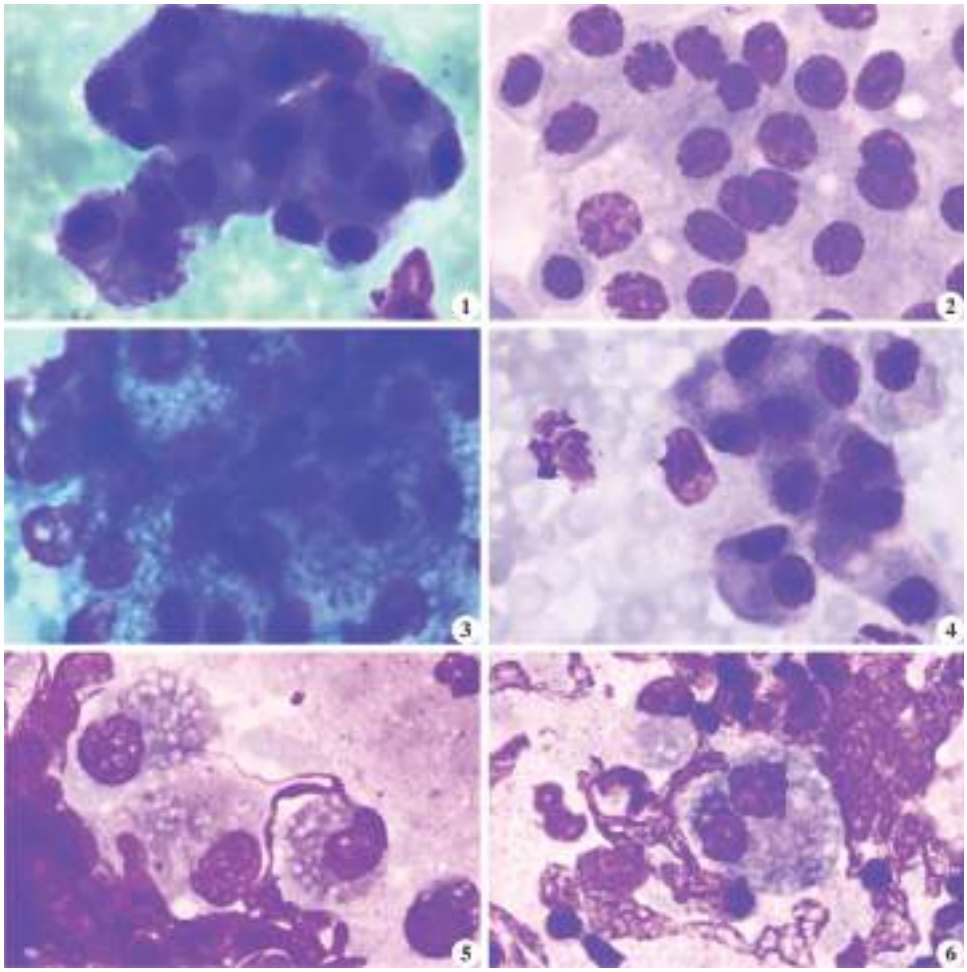

Subcutaneous filariasis and associated neoplastic alteration in Chippiparai dog. Fig. 1. Epithelial cell cluster with acinar arrangements – Sebaceous adenoma, Leishman stain x100; **Fig. 2.** Epithelial cell cluster with cytoplasmic vacuolation - Sebaceous adenoma, Leishman stain x400; **Fig. 3.** Epithelial cell cluster with fine cytoplasmic vacuolation – Sebaceous adenoma, Leishman stain x400; **Fig. 4.** Epithelial cell cluster with binucleation – Sebaceous adenoma, Leishman stain x100; **Fig. 5.** Individual cells with foamy cytoplasmic vacuolation – Sebaceous adenoma, Leishman stain x400; **Fig. 6.** Giant cell with binucleation and foamy cytoplasmic vacuolation – Sebaceous adenoma, Leishman stain x400.

Filariasis is a mosquito-borne disease of carnivores[7]. *D. immitis* is the most common species infecting dogs, followed by *D. repens*. *D. repens* infects dogs, cats, and occasionally humans[5]. Infection occurs when female mosquitoes transmit infective third-stage (L3) larvae to the host. Migratory L1 larvae mature in the subcutaneous tissue and initiate various clinical conditions such as skin nodules, pruritus, alopecia, itching, and asthenia[4]. These parasites often migrate within the subcutaneous tissue, resulting in soft nodular swellings of variable inflammatory response throughout the body[8]. Rarely, they have been reported to induce inflammatory and painful nodules in distant areas such as the scrotum[9]. Occasionally, dead worms in the subcutaneous tissue may trigger a granulomatous reaction with fibrous encapsulation. Furthermore, *D. repens* has been reported to localize in the ocular conjunctiva, body cavity and mesentery, leading to inflammatory exudation[10]. Some of these lesions may develop into abscesses[1].

Human dirofilariasis caused by *D. repens* has been reported in dog-mosquito endemic areas due to the bite of infected mosquitoes[11]. After deposition, wandering subcutaneous microfilariae mature and form nodules in the upper body regions, subconjunctival tissues of the eyes and rarely in the lungs, omentum, epididymis, spermatic cord and breast[11,12].

Dirofilarial reactive nodules in the subcutaneous tissue or other organs often

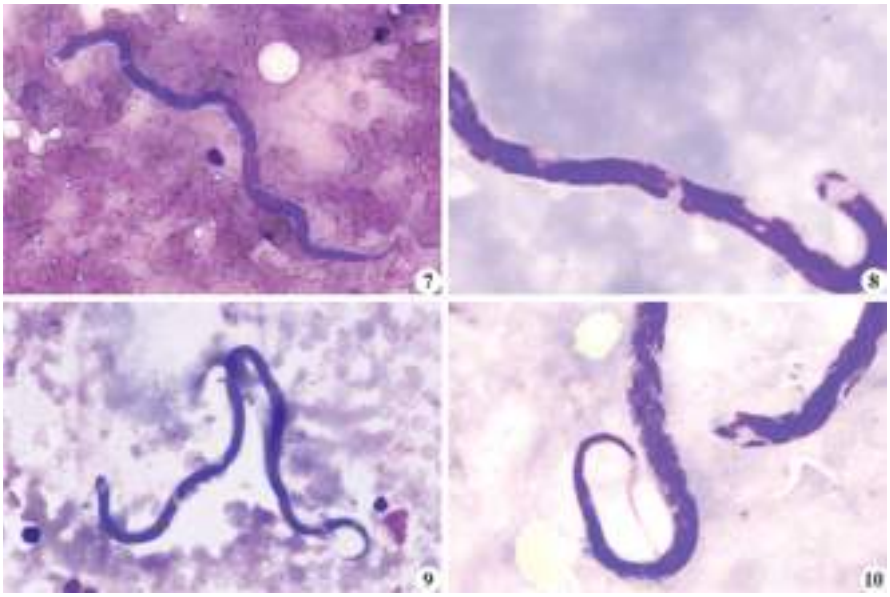

Subcutaneous filariasis and associated neoplastic alteration in Chippiparai dog. Fig. 7. Filiform microfilaria of *D. repens*, Leishman stain x100; **Fig. 8.** Blunt, round cephalic end with two prominent nuclei – *D. repens*, Leishman stain x400; **Fig. 9.** Microfilaria showing nerve rings, excretory pore and anal pore – *D. repens*, Leishman stain x100; **Fig. 10.** Hook-like tail and anucleate tail tip – *D. repens*, Leishman stain x400.

appear ill-defined, raising suspicion of malignancy such as incipient sarcoma or carcinoma[12,13]. In some instances, they mimic benign neoplastic lesions and are frequently confused with cutaneous epidermoid cysts, fibromas[14], melanoma[15], or pleural carcinomatosis[8]. Confirmation is usually based on cytology and histopathology. The presence of neutrophils, eosinophils, and scattered macrophages along with entire or fragmented microfilariae in cytology is regarded as indicative of inflammatory nodules[16]. Affected individuals may show elevated leukocyte counts, particularly eosinophils[1,9,17]. In a human case, eosinophils accounted for more than 48% of the differential leukocyte count[18]. However, eosinophilia may be mild[8] or even absent in some documented cases[5]. Histopathological analysis of these lesions has revealed multifocal purulent dermatitis, panniculitis, hyperpigmentation, and hyperkeratosis[4]. Eosinophilic necrotizing granulomatous or pyogranulomatous inflammation is the predominant histological lesion in most cases[5,19].

To date, studies on subcutaneous nodular masses in dogs and humans have suggested that these lesions represent host inflammatory reactions composed of inflammatory cells and exudates, as evidenced in cytological and histopathological findings[18]. The pathological changes are mostly associated with the migration of microfilariae and adult *D. repens*. The presence of the endosymbiotic bacterium *Wolbachia pipientis*, located in the hypodermal cords and germline of *D. repens*, has also been proposed to contribute to inflammatory tissue reactions by enhancing chemo-attraction through the release of the pro-inflammatory cytokine IL-8 at sites of parasitic migration[20].

The findings of the present study differ from the typical description of host inflammatory reactions. The smears revealed well-defined epithelial cell morphology with relatively uniform cellular clusters, abundant cytoplasm with distinct vacuolation, large nuclei, and rare mitotic figures. Additionally, some cellular groups exhibiting pleomorphism, clear and irregular cytoplasmic vacuolations, and occasional binucleation. Cytological evaluation of the biopsied masses was suggestive of sebaceous adenoma. Furthermore, the scarcity or absence of inflammatory cells in the biopsy specimens, along with evidence of a normal haemogram, suggests that the tissue masses were non-inflammatory in nature.

The role of microfilariae as the primary cause of sebaceous adenoma in the present Chippiparai dog remains speculative. However, the presence of multiple microfilariae in and around the biopsy cellular clusters suggests that the neoplastic changes might have resulted from irritation caused by migrating microfilariae and/or secretory products of adult *D. repens*. Although this remains hypothetical, associations between filarial nematodes and neoplastic changes have previously been reported with lymphoma[21], ovarian cystadenoma[22], and plasma cell myeloma[23] in humans. In most cases, microfilariae were incidentally detected during cytological examination[10,24]. Although often considered a chance association, some authors have suggested that microfilariae may play a role in tumorigenesis. In light of these reports, the authors speculate that the neoplastic changes observed in the present study may be associated with microfilarial infection. However, this hypothesis requires confirmation through excisional biopsy and detailed histopathological examination of the lesions. A limitation of the present study is that histopathology of the nodules was not performed, as the diagnosis was based only on FNAB and treatment was directed toward filariasis. Surgical removal of the subcutaneous masses was not undertaken because the patient was not presented for further follow-up.

The present study reports the microfilariasis of *D. repens* in Chippiparai dog causing subcutaneous nodules at various part of the body. Cytological evidence of

neoplastic alterations in subcutaneous nodules, along with the presence of microfilariae, raises suspicion that *D. repens* may be associated with tumorigenesis at the site of localization.

ACKNOWLEDGEMENT

We thank the Dean, Veterinary College and research Institute, Tirunelveli and Tamil Nadu Veterinary and Animal Sciences University for the facilities provided.

Financial support & sponsorship: None

Conflicts of Interest: None

Use of Artificial Intelligence (AI)-Assisted Technology for manuscript preparation: The authors confirm that there was no use of AI-assisted technology for assisting in the writing of the manuscript and no images were manipulated using AI

REFERENCES

1. Schatz C, Fubl M, Caf Y, Schmitz K, Kresse D, Ludwig W, Walochnik J, Knabl L. 2025. A rare case report of a human *Dirofilaria repens* infection. *Microorganisms* **13**: 476.
2. Adebayo OO, Akande FA, Adenubi OT. 2020. Canine dirofilariasis: A case report and review of the literature. *Folia Veterinaria* **64**(3): 75-81.
3. Savic S, Stosic MZ, Marcic D, Hernandez I, Potkonjak A, Otasevic S, Ruzic M, Morchón R. 2020. Seroepidemiological study of canine and human dirofilariasis in the endemic region of Northern Serbia. *Front Vet Sci* **7:** 571.
4. Albanese F, Abramo F, Braglia C, Caporali C, Venco L, Vercelli A, Ghibaudo G, Leone F, Carrani F, Giannelli A, Otranto D. 2013. Nodular lesions due to infestation by *Dirofilaria repens* in dogs from Italy. *Vet Dermatol* **24**(2): 255-e56.
5. Chisthi MM and Reghukumar A. 2015. Dirofilarial worms inside cutaneous nodules: A report with review of literature. *Int J Res Dermatol* **1**: 24-27.
6. Liotta JL, Sandhu GK, Rishniw M, Bowman DD. 2013. Differentiation of the Microfilariae of *Dirofilaria immitis* and *Dirofilaria repens* in stained blood films. *J Parasitol* **99**(3): 421-425.
7. Capelli G, Genchi C, Baneth G, Bourdeau P, Brianti E, Cardoso L, Danesi P, Fuehrer HP, Giannelli A, Ionica AM, Maia C. 2018. Recent advances on *Dirofilaria repens* in dogs and humans in Europe. *Parasit Vectors* **11**(1): 663.
8. Biasizzo H, Soba B, Ilovski F, Harlander M, Lukin M, Blatnik O, Turel M, Srpcic M, Kern I, Beovic B. 2022. Severe and rare case of human *Dirofilaria repens* infection with pleural and subcutaneous manifestations, Slovenia. *Emerg Infect Dis* **28**(12): 2504.
9. Barlozzari G, Felice T, Salvato L, Conti R, De Liberato C, Furzi F, Gabrielli S, Scarpulla M. 2021. Usual or unusual presentations of *Dirofilaria repens* in two sibling dogs: a case report. *Parasitol Res* **120**: 109-115.
10. Pazdzior-Czapula K, Otrocka-Domagała I, Myrdek P, Mikiewicz M, Gesek M. 2018. *Dirofilaria repens* - An etiological factor or an incidental finding in cytologic and histopathologic biopsies from dogs. *Vet Clin Pathol* **47**(2): 307-311.
11. Pampiglione S, Rivasi F, Angeli G, Boldorini R, Incensati RM, Pastormerlo M, Pavesi M, Ramponi A. 2001. Dirofilariasis due to *Dirofilaria repens* in Italy, an emergent zoonosis: report of 60 new cases. *Histopathol* **38**: 344-354.
12. Bezic J, Vrbicic B, Guberina P, Alfier V, Projic P, Marovic Z. 2006. DIAGNOSIS: Subcutaneous breast nodule due to *Dirofilaria repens* infestation. *Annals of Saudi Medicine* **26**(5): 414-416.
13. Frouge C, Vanel D, Tristant H. 1992. Dirofilariasis of the breast mimicking carcinoma on mammography. *Am J Roentgenol* **159**: 220-221.
14. Manzocchi S, Lendner M, Piseddu E, Sebastiani V, Morabito S, Daugschies A, Pantchev N. 2017. Nodular presentation of *Dirofilaria repens* infection in a cat mimicking a fibrosarcoma. *Vet Clin Pathol* **46**(1):158-163.
15. Oliva A, Gabrielli S, Pernazza A, Pagini A, Daralioti T, Mantovani S, Mattiucci S, D' Amati G, Mastroianni CM. 2019. *Dirofilaria repens* infection mimicking lung melanoma metastasis. Open Forum Infect Dis 6(3): ofz049.
16. Dzimira, S and Przemyslaw P. 2020. Cytological diagnostics of subcutaneous dirofilariasis imitating proliferative lesions in dogs. *Veterinarni Medicina* **65**(12): 537-542.
17. Wysmołek ME, Dobrzynski A, Długosz E, Czopowicz M, Wisniewski M, Jurka P, Klockiewicz M. 2020. Hematological and biochemical changes in dogs naturally infected with *Dirofilaria repens*. *Front Vet Sci* **7**: 590.
18. Pupic-Bakrac, A, Pupic-Bakrac, J, Beck, A, Jurkovic, D, Polkinghorne A, Beck, R. 2021. *Dirofilaria repens* microfilaremia in humans: Case description and literature review. *One Health* **13**: 100306.
19. Giudice E, Di Pietro S, Gaglio G, Di Giacomo L, Bazzano M, Mazzullo G. 2014. Adult of *Dirofilaria repens* in a dog with recurrent multiple subcutaneous nodular lesions. *Parasitol Res* **113**: 711-716.
20. Bazzocchi C, Genchi C, Paltrinieri S, Lecchi C, Mortarino M, Bandi C. 2003. Immunological role of the endosymbionts of *Dirofilaria immitis*: the Wolbachia surface protein activates canine neutrophils with production of IL-8. *Vet Parasitol* **117**: 73-83.
21. Jamal I, Raman RB, Choudhary VN. 2020. Chronic lymphocytic leukaemia with microfilaria: A rare coincidence with review of literature. *Indian J Pathol Oncol* **7**(3): 483-485.
22. Vasantham V, Yadav SK, Sarin N, Singh S, Pruthi SK. 2020. Incidental detection of microfilaria in cyst fluid of mucinous cystadenocarcinoma of ovary: A rare case report. *Int J Surg Case Rep* **70**: 56-59.
23. Kolte S and Mane P. 2015. Microfilaria of *Wuchereria bancrofti* in plasma cell myeloma: A case report. *J Vector Borne Dis* **52**(4): 342-343.
24. Gupta S, Sodhani P, Jain S, Kumar N. 2001. Microfilariae in association with neoplastic lesions: Report of five cases. *Cytopathology* **12**(2):120-126.

Indian J. Vet. Pathol., 50(3) : 271-274, 2026: DOI: https://doi.org/10.56093/7jwd2g49

CASE REPORT

Papillary cystic uterine adenocarcinoma in a New Zealand rabbit: Histopathology of a hidden reproductive threat

Gopinathan Alagappan*, Thangapandiyan Maruthai[1], Tamileniyan Elangovan[2] and Tensingh Gnanaraj Paulpandi[3]

Tamil Nadu Veterinary and Animal Sciences University

[1]Professor, Poultry Disease Diagnosis and Surveillance Laboratory, Veterinary College and Research Institute Campus Namakkal

[2]PG Scholar, Department of Veterinary Medicine, Veterinary College and Research Institute, Orathanadu, Thanjavur

[3]Professor and Head, Post Graduate Research Institute in Animal Sciences (PGRIAS)

***Address of correspondence**

Prof. Gopinathan Alagappan, Section Head, Rabbit Breeding Unit, Post Graduate Research Institute in Animal Sciences (PGRIAS), Kattupakkam; Email: gopiabg@gmail.com

ORCID Id: 000-0001-7789-5971

Received: 16.2.26; Accepted: 23.4.26

ABSTRACT

A 5-year-old female New Zealand White rabbit weighing 2.4 kg was presented with a history of repeated infertility following three unsuccessful matings and progressive abdominal distension. Owing to chronic infertility and clinical deterioration, the animal was euthanised and subjected to post-mortem examination. Necropsy revealed marked enlargement of both uterine horns and the uterine body with multiple firm, irregular masses and absence of fetuses. Histopathological examination showed an endometrial neoplasm infiltrating the myometrium, composed of papillary, tubular and cystic arrangements of epithelial cells supported by fibrovascular stroma. The neoplastic cells exhibited moderate pleomorphism with low mitotic activity and no metastatic lesions were observed in other organs. Immunohistochemically, the tumor cells showed strong cytoplasmic positivity for cytokeratin-7 and moderate apical to cytoplasmic expression of epithelial membrane antigen. Based on histomorphological features, the tumour was diagnosed as papillary and cystic adenocarcinoma of the uterus.

Key words: Adenocarcinoma, Histopathology, Rabbit, Tumor, Uterus

How to cite this article: Alagappan, G., Maruthai, T., Elangovan, T., and Paulpandi, T.G.. 2026. Papillary cystic uterine adenocarcinoma in a New Zealand rabbit: histopathology of a hidden reproductive threat. Indian J. Vet. Pathol., 50(3) : 271-274.

Rabbit farming focuses on the production and management of domestic rabbits (*Oryctolagus cuniculus*) for meat, fur, wool, research and companion animals. Rabbits are best known for their prolificacy, high fecundity, short generation interval, energy efficiency, and efficient feed conversion, traits that have made them valuable livestock and research subjects worldwide[1]. Despite these production advantages, rabbits are susceptible to a wide array of illnesses and reproductive pathologies that can adversely affect health, productivity and welfare[2]. Reproductive disorders further compound health and productivity concerns in female rabbits. Genital infections such as metritis, endometritis and pyometra are common and can lead to infertility or death if untreated; these conditions are frequently observed in commercial and small-scale rabbit operations alike cuniculture. Symptomatic reproductive infections are associated with chronic infertility, inflammation of the reproductive tract and obstetrical complications, thereby reducing reproductive efficiency in doe[3].

Uterine neoplasia is a major health concern in female rabbits (*Oryctolagus cuniculus*) with uterine adenocarcinoma being the less common tumour affecting the female reproductive tract. Multiple retrospective studies and clinical reports have documented the high prevalence of this malignancy in intact female rabbits, particularly as animals age. Uterine adenocarcinoma arises from the endometrial epithelium and represents the predominant form of reproductive neoplasia in this species[4]. The high prevalence of neoplasia unique among common domestic species; other animals such as guinea pigs and rodents may develop uterine lesions but tend to have a greater proportion of benign pathology compared to rabbits. In a comparative study of reproductive tract tumours in small pet mammals, endometrial adenocarcinoma predominated in rabbits, while benign lesions were more common in species like guinea pigs[5]. Clinically, affected rabbits may present with non-specific signs such as hematuria, serosanguinous vaginal discharge, abdominal distension, anorexia or depression; in many cases, abdominal palpation reveals enlarged or irregular uterine masses[6]. These tumours tend to be slow-growing but locally invasive with metastatic spread commonly occurring within 12 to 24 months after

onset of clinical signs. The lungs are the most frequently reported site of metastasis, followed by liver, bone and other visceral organs[7]. Histologically, adenocarcinomas of the rabbit uterus demonstrate diverse growth patterns, including tubular, solid and papillary variants, the latter characterized by fibrovascular cores lined by neoplastic epithelial cells projecting into glandular lumina[8] and this report describes a case of uterine papillary cystic adenocarcinoma and also elaborates the histopathology of uterine adenocarcinoma in a New Zealand White rabbit.

A 5-year-old female New Zealand White rabbit weighing 2.4 kg from the Rabbit Breeding Unit at the Post Graduate Research Institute in Animal Sciences (PGRIAS), Kattupakkam showed signs of of repeated infertility. The doe had been naturally mated on three separate occasions, each mating occurring at one-month intervals. Pregnancy diagnosis was performed following each mating and all examinations revealed negative results. On the day of clinical presentation, the rabbit was approximately 15 days beyond the expected gestation period. Despite the absence of confirmed pregnancy, the animal exhibited persistent abdominal enlargement. In view of the chronic infertility and progressive abdominal distension, the animal was humanely euthanised following standard ethical procedures.

On necropsy, multiple pale-red hard, sacular masses were observed on both uterine horns (Fig.1) and no fetuses were present in the uterine horns. Representative tissue samples were collected from different regions of the mass and fixed in 10% neutral buffered formalin for histopathological evaluation. Tissues were processed using the standard paraffin-embedding technique. Sections of 5 µm thickness were prepared and stained with haematoxylin and eosin (H & E)[9] for microscopic examination. Immunohistochemical staining for Cytokeratin (CK-7) and epithelial membrane antigen (EMA) was performed as per recommendation of the manufacturer (PathnSitu, USA) using super sensitive labeled poly horse radish peroxidase (HRP) polymer method. Paraffin-embedded uterine tumor tissues sectioned at 3–5 µm thickness and mounted on poly-L-lysine–coated slides. Sections were dried, deparaffinized in xylene, and rehydrated through graded alcohol to distilled water. Antigen retrieval was performed using heat-induced epitope retrieval (HIER) in citrate buffer (pH 6.0) in a microwave/pressure cooker for 10–20 minutes. Slides were allowed to cool at room temperature. Endogenous peroxidase activity was blocked using 3% hydrogen peroxide for 10 minutes. Non-specific binding was minimized using a protein blocking. Sections were incubated with primary antibodies, CK& and EMA. Incubation was carried out for 1 hour at room temperature. After washing with PBS, slides were treated with HRP-conjugated secondary antibody and visualized using DAB (3,3′-diaminobenzidine) chromogen, producing a brown reaction product. Sections were counterstained with hematoxylin, dehydrated, cleared, and mounted.

Histopathological examination of the tumour

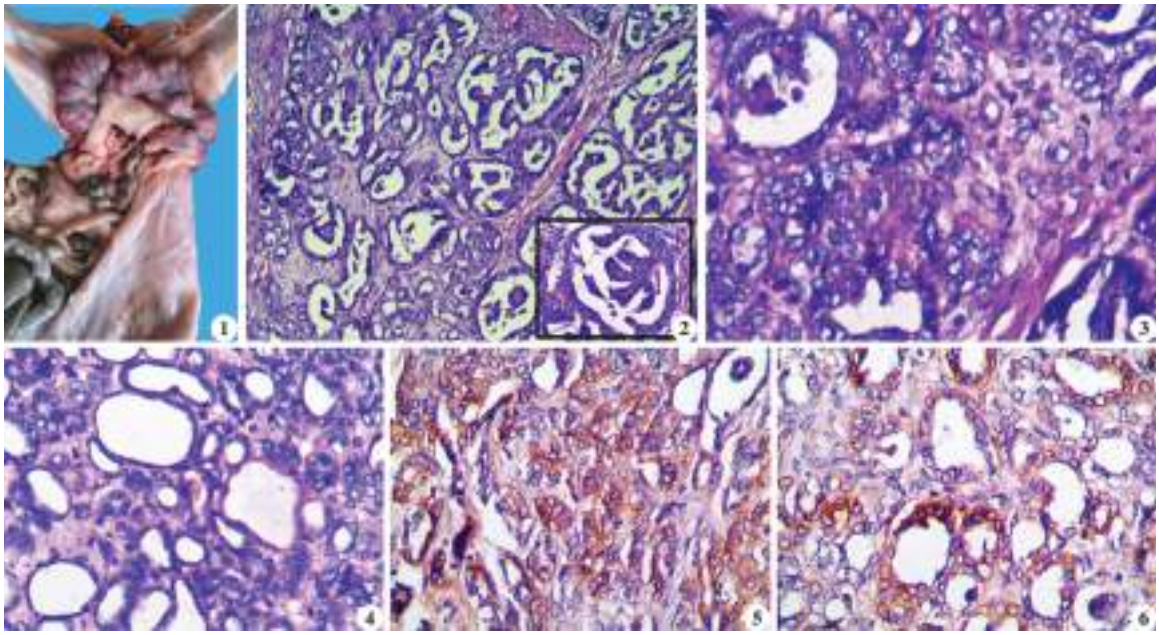

Fig.1. Uterus with multiple hard spherical masses; **Fig. 2**. Uterus: Papillary adenocarcinoma. H&E x 100. Inset: Papillary projections; **Fig. 3.** Uterus Papillary Adenocarcinoma - Moderate anisocytosis and anisokaryosis. H&E x 400; **Fig. 4.** Uterus: Papillary cystadenocarcinoma- Multiple thin walled cysts with flattened epithelium. H&E x 400; **Fig. 5.** Cytokeratin 7 - Strong diffuse cytoplasmic expression. IHC, DAB Brown x 400; **Fig. 6.** EMA - Moderate expressions of mixed apical and cytoplasmic staining. IHC, DAB Brown x 400

mass revealed an expansile neoplasm arising from the endometrium with marked infiltration into the underlying myometrium. The neoplastic cells were predominantly arranged in well-defined tubular structures and complex papillary projections, which extended into the uterine lumen (Fig. 2) as well as into the endometrial glandular architecture. These papillary fronds were supported by a delicate fibrovascular stroma imparting a characteristic papillary appearance to the tumour. The neoplasm was composed of polygonal to columnar or cuboidal epithelial cells exhibiting moderate pleomorphism. The cells showed moderate anisocytosis and anisokaryosis (Fig. 3), with hyperchromatic nuclei and indistinct cell borders. Mitotic activity was low to moderate, with one to two mitotic figures. In certain regions, the tumour exhibited moderate to severe cystic degeneration characterized by variably sized cystic spaces lined by flattened to attenuated epithelial cells (Fig. 4). These cystic areas were interspersed within the neoplastic tissue and contributed to the heterogeneous histomorphology of the mass. Microscopic evaluation of the lungs and other major visceral organs did not reveal any evidence of metastatic spread. The neoplastic glandular epithelial cells showed diffuse strong cytoplasmic positivity for CK-**7** (Fig. 5) and EMA showed moderate expressions of mixed apical and cytoplasmic staining pattern in moderately differentiated areas (Fig. 6). Based on the histopathological and immunohistochemical features observed, the neoplasm was diagnosed as uterine papillary cystic adenocarcinoma.

Uterine adenocarcinoma is one of the most frequently diagnosed malignancies in domestic rabbits and is widely recognised as uncommon reproductive neoplasm in this species. In contrast to many other domestic mammals where uterine adenocarcinoma is rare, intact female rabbits demonstrate a markedly higher predisposition to this tumour type, particularly as age advances[10]. Several retrospective studies have demonstrated that uterine adenocarcinoma is highly prevalent in older rabbits. Large pathological surveys of the genital tract indicate that uterine tumours are the most common uterine disorder in pet rabbits, with adenocarcinoma being the predominant neoplasm[4]. Prospective studies have reported that approximately 40 % of rabbits over three years of age are affected by malignant uterine neoplasia, while clinical case series have documented an incidence ranging from 43 % to more than 50 % among rabbits presented with suspected uterine disease often in association with cystic endometrial hyperplasia[2]. Breed predispositions have been suggested, with New Zealand White, Dutch, and California breeds frequently represented in studies reporting high prevalence, although statistical breed predisposition is variable across datasets[11,10].

The exact pathogenesis of uterine adenocarcinoma in rabbits remains unclear; however, several biological and environmental factors have been proposed. Persistent unopposed estrogen stimulation related to the induced ovulatory nature of rabbits[12] and frequent pseudopregnancies known to be considered as major predisposing factor, promoting prolonged endometrial proliferation and neoplastic transformation. Histological alterations such as endometrial hyperplasia, glandular epithelial atrophy and increased stromal collagen deposition are commonly observed preceding lesions, supporting a progressive transition from hyperplasia to adenocarcinoma[13]. Additionally, immunohistochemical studies have demonstrated overexpression of cyclooxygenase-2 (COX-2) in tumour tissues suggesting its role in tumour development and progression[8]. In the present study, CK7 showed strong diffuse cytoplasmic positivity, consistent with its expression in endometrial glandular epithelium and CK7 is a reliable marker of Müllerian-derived epithelial tumors[14]. EMA (MUC1) expression demonstrated a grade-dependent staining pattern, similar observations have been reported in endometrial adenocarcinomas across species[15].

Although inherited susceptibility has been suggested in certain breeds, definitive genetic determinants have not yet been identified. The reproductive history of rabbits with uterine adenocarcinoma frequently reveals disturbances such as diminished fertility, reduced litter size, stillbirths and failed pregnancies preceding tumour detection. The chronic infertility and repeated negative pregnancy diagnoses described in this case align with accounts from clinical studies of reproductive disruption preceding histologically confirmed adenocarcinoma. Uterine adenocarcinoma is an uncommon neoplasm in intact female rabbits, particularly in older does and often manifests as chronic infertility and progressive abdominal distension. Definitive diagnosis relies on histopathological examination, as clinical signs may remain subtle until the disease reaches an advanced stage. In the present case, papillary and cystic adenocarcinoma with myometrial invasion was identified without evidence of metastasis. From a farm management perspective, this condition leads to repeated breeding failures and reduced reproductive efficiency, resulting in increased feed, labour and housing costs. Delayed diagnosis frequently necessitates culling or euthanasia, causing direct economic losses and loss of valuable breeding stock. Therefore, routine reproductive health monitoring, timely culling of affected does and preventive measures such as ovariohysterectomy in non-breeding animals are essential to improve productivity, animal welfare and the economic sustainability of rabbit farming systems.

Financial support & sponsorship: None

Conflicts of Interest: None

Use of Artificial Intelligence (AI) Assisted technology for manuscript preparation: The authors confirm that there was no use of AI – Assisted Technology for assisting in the writing of the manuscript and no images were manipulated using AI

REFERENCES

1. Bharathy N, Sivakumar K, Vasanthakumar P, Sakthivadivu R. 2022. Rabbit farming in India: an overview. *Agric Rev* **43(2):**218–224 https://doi.org/10.18805/ag.R-230
2. Mäkitaipale J, Airas N, Engblom S, Lindén J. 2019. Prospective survey of neoplastic and non-neoplastic uterine disorders in 116 domestic rabbits (*Oryctolagus cuniculus*). *J Exot Pet Med* **30:**1–7.
3. da Silva BZ, Moure A, Schmidt VRQ, Capriolli G, Bandeira LB, Valandro MA, Gorczak R. 2022. Cystic endometrial hyperplasia in a domestic rabbit (*Oryctolagus cuniculus domesticus*). *Acta Sci Vet* 50:1–6. https://doi.org/10.22456/1679-9216.119718
4. Bertram CA, Müller K, Klopfleisch R. 2018. Genital tract pathology in female pet rabbits (*Oryctolagus cuniculus*): a retrospective study of 854 necropsy examinations and 152 biopsy samples. *J Comp Pathol* **164:** 17–26. https://doi.org/10.1016/j.jcpa.2018.08.003
5. Paździor-Czapula K, Mikiewicz M, Fiedorowicz J, Otrocka-Domagała I. 2024. Mammary and reproductive tract tumours and tumour-like lesions of 286 small pet mammals: a retrospective study. *J Comp Pathol* **213:**46–58. https://doi.org/10.1016/j.jcpa.2024.07.002
6. Künzel F, Grinninger P, Shibly S, Hassan J, Tichy A, Berghold P, Fuchs-Baumgartinger A. 2015. Uterine disorders in 50 pet rabbits. *J Am Anim Hosp Assoc* **51(1):**8–14. https://doi.org/10.5326/JAAHA-MS-5812
7. Walter B, Poth T, Böhmer E, Braun J, Matis U. 2010. Uterine disorders in 59 rabbits. *Vet Rec* **166:**230–233.
8. Vaccaro E, Navas L, Ercolano M, Piegari G, Di Napoli E, Papparella S, Inverso D, Brunetti B, Paciello O, Russo V. 2024. Immunohistochemical investigation of cyclooxygenase-2 expression in rabbit uterine adenocarcinoma and the potential use of COX-2 inhibitors in cancer therapy. *Animals* **14(22):**3169. https://doi.org/10.3390/ani14223169
9. Bancroft JD, Layton C. 2019. The hematoxylins and eosin. In: Suvarna SK, Layton C, Bancroft JD eds. Theory and practice of histological techniques. 8th edn. Elsevier, UK.
10. Quesenberry KE, Carpenter JW. 2003. Ferrets, rabbits and rodents: clinical medicine and surgery. St Louis: Saunders.
11. Moulton JE. 1978. Tumors in domestic animals (2nd edn). Berkeley: Univ Calif Press.
12. Chen S, Quesenberry KE. 2006. Rabbits. In: *Saunders manual of small animal practice* 1858–1880. https://doi.org/10.1016/B0-72-160422-6/50178-9
13. Elsinghorst TA, Timmermans HJ, Hendriks HG. 1984. Comparative pathology of endometrial carcinoma. *Vet Q* **6(4):**200–208. https://doi.org/10.1080/01652176.1984.9693937
14. Kim SH, Kwon HJ, Song KH. 2025. A case of uterine adenocarcinoma in companion rabbit. *J Prev Vet Med* **49(4):**274–276.
15. Walter B, Poth T, Böhmer E, Braun J, Matis U. 2010. Uterine disorders in 59 rabbits. *Vet Rec* **166:** 230–233.

Indian J. Vet. Pathol., 50(3) : 275-277, 2026: DOI: https://doi.org/10.56093/d5trwy62

CASE REPORT

Pathomorphology of *Trichosomoides crassicauda* in a Wistar rat

Monisha D.C.*, Gopal K., Karthick M., Srinivasan P. and Velusamy R.[1]
Department of Veterinary Pathology, Veterinary College and Research Institute, Namakkal-2, TANUVAS, Tamil Nadu
[1]Department of Veterinary Parasitology

***Address of correspondence**
Dr. Monisha D.C., Ph.D. Scholar; E-mail: dcmonishadpi@gmail.com
ORCID Id: 009-0003-1360-054X , 0000-0002-8747-9776

Received: 18.3.26; Accepted: 29.4..26

ABSTRACT

Trichosomoides crassicauda is a nematode parasite inhabiting the urinary bladder of wild and laboratory rats. Its unique feature is the presence of the male worm permanently embedded within the uterus of the female worm. On gross examination, no specific lesions could be detected in the urinary bladder. Histopathological examination of urinary bladder revealed epithelial hyperplasia, mucosal thickening and multiple cut sections of parasite. Within the lumen and mucosa well-developed eggs and female parasites were embedded in the epithelium of urinary bladder with no inflammatory reaction around the parasite. Based on the gross examination and histopathological findings, the case was identified as incidence of *Trichosomoides crassicauda* in rat.

Keywords: Nematode, Urinary bladder, Embryonated eggs, Epithelial hyperplasia

INTRODUCTION

Rats are widely used as laboratory animals and are known to harbour several parasitic organisms. *Trichosomoides crassicauda* is a helminth that inhabits the urinary bladder of rats. It is a slender, hair like nematode generally considered non-pathogenic and these parasites have been documented in both laboratory and in Wistar rats[1], Long-Evans rat[2] and Albino rats[3,4]. In addition to urinary bladder, the parasite has been noticed in other organs such as uterus, kidney and lungs[4]. *T. crassicauda* exhibits sexual dimorphism; The female worm measuring about 8-15 mm is typically found free in the lumen of the bladder and resides in the urinary bladder while male worm is very short (1-2 mm) and located within the uterus of the female this intrauterine localization of the male parasites helps in identifying the species[5,6].

The male worm resides within the uterus or vagina of the adult female rats and this parasite has direct life cycle and transmission occurs through ingestion of embryonated eggs contaminated with feed and water which are excreted through the urine of infected rats. After ingestion, the larva hatch in the stomach and migrate to the lungs through the body cavities or via the bloodstream. Subsequently, the larvae reach the kidneys through the blood stream and eventually migrate to the urinary bladder through the ureters[7]. Because of the larval migration, it induces granuloma formation and it produces granulomatous lesions in the urinary bladder[6]. This report documents the incidental findings of *T. crassicauda* in a Wistar rat.

MATERIALS AND METHODS

Rat tissues from sub-acute toxicological study were submitted to Regional Histopathology Laboratory for Animal Disease Diagnosis, Department of Veterinary Pathology, Veterinary College and Research Institute, Namakkal for histopathological examination. The formalin fixed rat tissue samples were processed, embedded and cut into 4 µm thickness and stained with Haematoxylin and Eosin (H & E) for histopathological examination[8].

How to cite this article : Monisha, D.C., Gopal, K., Karthick, M., Srinivasan, P. and Velusamy, R. 2026. Pathomorphology of Trichosomoides crassicauda in a Wistar rats. Indian J. Vet. Pathol., 50(3) : 275-277.

RESULTS

The gross pathological examinations revealed no specific lesions in the urinary bladder. However, there were much pronounced histopathological lesions noticed in the urinary bladder. The histopathological examination of urinary bladder revealed presence of female worms in the lumen of the urinary bladder (Fig. 1), female worm embedded in the mucosa with gravid uterine segments in the urinary bladder (Fig. 2). Epithelial hyperplasia, mucosal thickening with no inflammatory reaction around the parasite were observed (Fig. 3). Hyperparasite of the male worm noticed in the uterus of the female worm (Fig. 4) embedded in the mucosa.

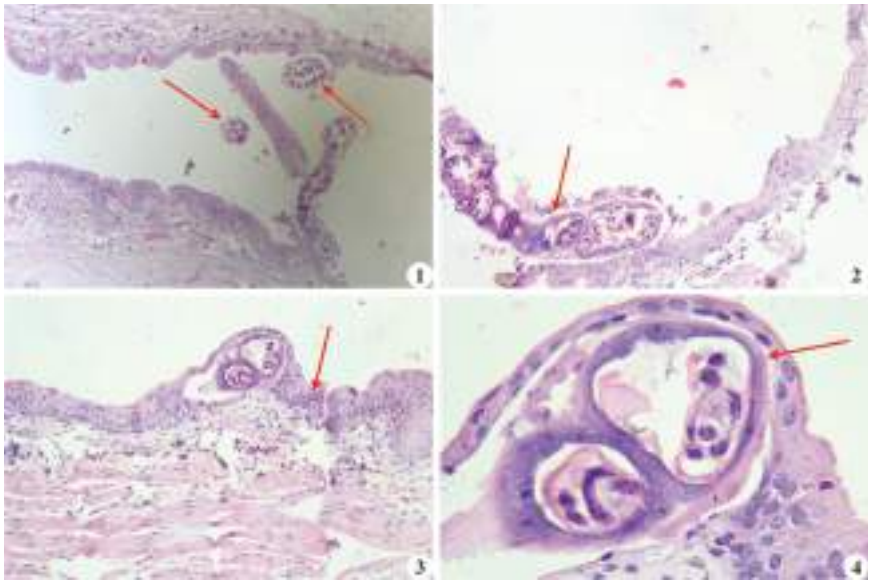

Fig. 1. Sections of female worms (red arrows) present freely in the lumen of urinary bladder (H&E x 40); **Fig. 2.** Urinary bladder revealing adult female worm embedded in the mucosa with gravid uterine portions distended with numerous eggs (H&E x 100); **Fig. 3.** Female worm completely embedded into the transitional epithelium of the urinary bladder with no inflammatory reactions (H&E x 100); **Fig. 4.** Urinary bladder revealing male parasite in the uterus of female adult worm **(**H&E x 400)

DISCUSSION

Experimental studies in various fields of biological and medical sciences mostly rely on laboratory animals. Among these, rats are the second most widely used experimental animals worldwide. On account of this, rats serve as valuable animal models in multiple areas of biomedical research *viz.*, pharmacology, cancer research, toxicology and immunology[9]. However, the possible interactions between laboratory animals and pathogens often occur without any apparent clinical signs, which may influence the experimental outcomes and thereby, compromising the reliability of the results obtained[6]. In the present study the rat was utilized as an animal model for sub-acute toxicological investigations and the presence of this parasite in the urinary bladder was observed as an incidental finding.

Parasites are recognized as the most frequently encountered pathological agents macroscopically[10]. However, in the present study, there was no adult worms noticed in the urinary bladder, the impact of *T. crassicauda* on the urinary bladder was assessed only by histopathological examination.

The presence of the nematodes within the urinary bladder has been related with the pathological conditions such as cystitis, urolithiasis, epithelial metaplasia and neoplastic alterations [2,11]. However, in the present study there was no such apparent clinical signs and also no inflammatory reaction noticed which is in accordance with the earlier reports of author[3,4]. This might be due to the low pathogenicity of the parasite and its localized habitat within the urinary bladder and the host capacity for physiological adaptation. In addition, the parasitic infection causes mild or no inflammatory responses that are insufficient to produce overt clinical signs.

The nematodes alter the structural integrity of the epithelium lining the bladder by penetrating the glycosaminoglycans layer and localizing within the mucosal tissue. Thereby, the invasion of the parasite is associated with the mild inflammatory response and minimal histopathological alterations[3]. The histopathological examination of urinary bladder revealed presence of female worms in the lumen of the urinary bladder and in multiple areas completely embedded into the transitional epithelium, epithelial hyperplasia, mucosal thickening with no inflammatory reaction around the parasite and hyperparasite of the male worm noticed in the uterus of the female worm. These histopathological lesions were very well correlated with earlier findings of the authors[1,3,4,6].

The hyperplasia of the bladder epithelium provides viable environment for the adult *T. crassicauda* parasite, thereby limiting the effective immune response in the host during the life cycle of the parasite[7]. The maturation of the worm is associated with the irritation of the urinary bladder resulting in the degenerative changes in the epithelium lining the bladder[4] and this finding is in contrast with the present report. There was no much degenerative change in the bladder mucosa. This might be due to the host physiological adaptation to the parasite.

CONCLUSION

T. crassicauda is a common bladder nematode in rats. Usually, it is subclinical, but it may cause urinary pathology. Diagnosis is mainly by examination of urine and histopathology. The presence of this parasite in rats is of considerable veterinary and experimental relevance due to its potential in affecting animal health and experimental research outcomes.

Financial support and sponsorship: None

Conflict of Interest: None

Use of Artificial Intelligence for manuscript preparation: The author confirms that there was no use of AI-assisted technology for assisting in the writing of the manuscript and no images were manipulated using AI.

REFERENCE

1. Bahrami S, Rezaei A and Alborzi AR. 2014.Trichosomoides crassicauda infection in wistar rats. *Arch Razi Inst* **69**(1): 63-67.
2. Paul SK, Sarker RD, Rahman MM, Biswas B, Dash P and Mondal D. 2025. *Trichosomoides crassicauda* infection in laboratory Long-Evans rats. *Bang Vet* **42(1):** 38-43.
3. Sikora VV, Lyndin MS, Hyriavenko NI, Moskalenko RA, Lyndina YM, Sikora KO and Romaniuk AM. 2021. Morphological peculiarities of parasitic *Trichosomoides crassicauda* infection in rat urinary bladder. *Mac Vet Rev* **44(2):** 159-167.
4. Gokalp Ozkorkmaz E. 2011. Microscopic investigations in a diabetic rat urinary bladder infected with *Trichosomoides crassicauda*. *J Electron Microsc* **60(4):** 261-265.
5. Soulsby EJL. 1982. *Helminths, Arthropods and Protozoa of Domesticated Animals.* 7th edn. Bailliere Tindall, London. **pp. 705–707.**
6. Najafi F, Taghavi Ghadikolai M, Naddaf SR, Hasanpour H, Mobedi I and Mowlavi G. 2017. *Trichosomoides crassicauda* infection in laboratory rats with histopathological description in the bladder tissue. *J Med Microbiol Infec Dis* **5(1):** 31-34.
7. Antonakopoulos GN, Turton J, Whitfield P and Newman J. 1991. Host-parasite interface of the urinary bladder-inhabiting nematode *Trichosomoides crassicauda* changes induced in the urothelium of infected rats. *Int J Parasitol* **21(2):** 187-193.
8. Bancroft JD and Gamble M. 2012. Theory and practice of histological techniques. Edinburgh. Churchill Livingstone, London. 7th edn Pp: 105-125.
9. Perec-Matysiak A, Okulewicz A, Hildebrand J and Zaleśny G. 2006. Helminth parasites of laboratory mice and rats. *Wiad Parazytol* **52(2):** 99-102.
10. Iliev PT, Georgiev GZ, Kirkova ZT and Chakarova BG. 2017. A survey of helminth infections in the black rat from Stara Zagora district, Bulgaria. *Mac Vet Rev* **40(2):** 177-182.
11. Serakides R, Ribeiro AFC, Silva CM, Santos RL, Nunes VA and Nascimento EF. 2001. Proliferative and inflammatory changes in the urinary bladder of female rats naturally infected with *Trichosomoides crassicauda*: Report of 48 cases. *Arq Bras Med Vet Zoot* **53:**1-5.

Indian J. Vet. Pathol., 50(3) : 278-279, 2026: DOI: https://doi.org/10.56093/kzrc2x85

CASE REPORT

An unusual case of cavernous haemangioma in indigenous chicken

D.C. Monisha, K. Gopal*, K. Sowmya and A. Arulmozhi
Department of Veterinary Pathology, Veterinary College and Research Institute, Namakkal
Tamil Nadu Veterinary and Animal Sciences University, Chennai, Tamil Nadu

***Address of correspondence**
Dr. K. Gopal; E-mail: drvetpal@gmail.com
ORCID Id: 009-0003-1360-054X, 0000-0002-8747-9776

Received: 17.3.26; Accepted: 8.4.26

ABSTRACT

Vascular tumours are seldom found in birds. An adult 35 weeks old indigenous chicken was brought for postmortem examination with the history of sudden death. On postmortem examination, multiple tiny reddish nodules were noticed on liver. Histopathological examination revealed wide blood-filled vascular structure densely packed with nucleated erythrocytes compressing liver parenchyma. Based on gross and histopathology, the case was diagnosed as cavernous haemangioma.

Keywords: Chicken, Liver, Haemangioma, Nucleated erythrocytes

How to cite this article : Monisha, D.C., Gopal, K., Sowmya, K. and Arulmozhi, A. 2026. An unusual case of cavernous haemangioma in indigenous chicken. Indian J. Vet. Pathol., 50(3) : 278-279.

Haemangioma is a benign tumour arising from blood vessels and usually composed of tiny blood vessels and vascular endothelial cells. These tumours include cavernous haemangioma, capillary haemangioma, haemangio-endothelioma and haemangio-endotheliosarcoma frequently seen in humans and mammals[1]. Cutaneous haemangiomas usually start as red spots with increased endothelial proliferation, later formed new capillaries and eventually progress into cavernous forms, which are characterized by dilated blood vessels filled with erythrocytes[2]. Most avian haemangiomas tend to rupture easily, often leading to fatal bleeding, but their mode of induction is unclear[3].

Cavernous haemangiomas are most prevalent in avian species and primarily affecting broilers. These tumours are seldom found in internal organs of birds but there are few reports of haemangioma in liver of quail[4], Amazona farinose parrot[5], spleen of budgerigar[1] and liver of layer chicken[6]. The present case reports the very common findings of cavernous haemangioma in an indigenous chicken.

An adult 35 weeks old indigenous chicken was brought to Department of Veterinary Pathology, Veterinary College and Research Institute, Namakkal for postmortem examination. As described by the owner, the bird showed clinical signs like debility, dullness and depression, reduced feed intake and died shortly. Detailed post mortem was carried out and samples were collected in 10 % formalin. Paraffin embedded tissue sections were cut into 4µm thickness and were stained with Haematoxylin and Eosin staining[7].

The dead bird was markedly emaciated and dehydrated. External examination revealed ruffled feathers, an enlarged abdomen and feather loss over abdomen and inner thighs. Internally, multiple tiny reddish nodules were appreciable on the liver (Fig.1). The nodules were variable in size and were scattered distinctly on the entire liver parenchyma (Fig.2) On incision, they were found to extend deep into the parenchyma. The nodules appeared reddish brown in colour, soft in consistency and exuded red tinged fluid on incision. Microscopically, variable sized vascular structures

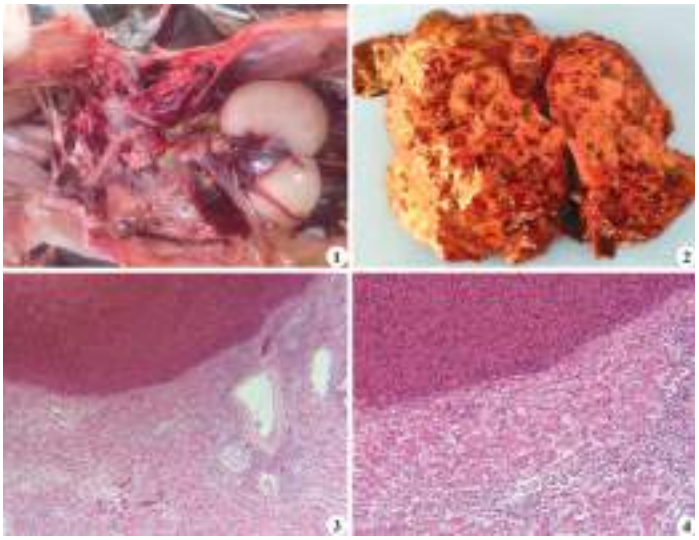

Fig. 1. The emaciated bird showing reddish brown nodules on liver; **Fig. 2.** Gross picture of liver showing multiple tiny reddish-brown nodules on the parenchyma; **Fig. 3.** Liver – A wide blood-filled vascular structure and compression of parenchyma. (H&E x40); **Fig. 4.** Liver – hepatic parenchyma replaced by numerous capillary structures filled with nucleated erythrocytes and compression of adajenct hepatocytes (H&E x400)

were observed in liver parenchyma and these structures densely packed with nucleated erythrocytes (Fig.3) compressing the liver parenchyma that leads to loss of normal hepatic architecture. The hepatic architecture is completely replaced by numerous capillary structures filled with nucleated erythrocytes and compression of adjacent hepatocytes (Fig.4). The tumour exhibited the appearance of a cavernous haemangioma. The vascular endothelial cells were hyper chromatic, with round to spindle shaped nucleus and indistinct cytoplasmic boundaries and mitotic figures were not evident.

The incidence of cavernous haemangioma in avian species was reported above five weeks of age[1]. In the current case, the bird was 35 weeks old. These tumours in birds are usually multifocal, and most of the affected birds had more than one tumour. The skin is the most frequently affected site (85% of the hens), followed by muscle and extremities involvement (61%), then liver (31%) and other organs[8]. In this case, the tumours were identified in liver and there were no appreciable lesions in the skin. Grossly, the tumour appeared as tiny reddish mass with varying diameter. Upon incision, the tumour masses were found to be deeply embedded in the liver parenchyma. This is correlated with the previous findings of [2,8].

The histopathological study revealed that the liver had an excessively irregular appearance and the hepatic parenchyma lost its typical architecture with hepatic triads being absent[6]. Liver showed widened blood-filled vascular structures, lined with plumpy endothelial cells. These findings are consistent with reports of [8,9] except for the presence of solid cell mass and intra vascular papillary endothelial proliferation. In electron microscopy, cutaneous haemangioma primarily composed of undifferentiated mesenchymal cells with an alveolar structure[9].

Avian Leucosis Virus subtypeJ (ALV-J) is commonly responsible for development of haemangiomas in most of the spontaneous cases[10,11]. Hens affected with ALV-J-induced haemangiomas often die suddenly due to massive haemorrhages or anaemia[3]. This is in accordance with the current case where the bird experienced sudden death although the haemangioma did not rupture. The LTR and env genes are associated with both pathogenic as well as biological characteristics of ALV-J[12]. However, ALV-J induces oncogenesis by insertional mutagenesis and integrations in the MET oncogene can drive the over expression of MET and contribute to the development of haemangiomas[13]. The exact molecular mechanism is not fully understood.

Bases on the gross and histopathological examination, the current case was diagnosed as cavernous haemangioma in indigenous chicken.

ACKNOWLEDGEMENT

The author extends their deep gratitude to the Head and Staff of the Department of Veterinary Pathology, Veterinary College and Research Institute, Namakkal necessary to carry out this case report.

Financial support and sponsorship: None

Conflict of Interest: None

Use of Artificial Intelligence for manuscript preparation: The author confirms that there was no use of AI-assisted technology for assisting in the writing of the manuscript and no images were manipulated using AI.

REFERENCES

1. Fadly AM, Nair V and Reece RL. 2008. Neoplastic diseases in: Saif Y.M, Fadly A.M, Glisson J.R, McDougald L.R, Nolan L.K, Swayne D.E, editors. Diseases of poultry, 12th edition. Iowa: Blackwell Publishing. pp. 449-616.
2. Sola SC, Borello B and Castagnaro M. 1997. Occurrence of cutaneous haemangiomas in chickens: morphological aspects. *Avian Pathol.,* **26(3):** 501-510.
3. Zhang H, Liu Q, Liu J, Zhang L, Liu G, Qiu B and Cheng Z. 2009. Hemangioma and myelocytomas induced by avian leukosis virus subgroup J in commercial layer flocks. *Israel J. Vet. Med.,* **64:** 39-44.
4. Reece RL. 1992. Observations on naturally occurring neoplasms in birds in the state of Victoria, Australia. *Avian Pathol*., **21:** 3-32.
5. Rossi G. 1998. A poorly differentiated hepatic haemangiosarcoma in an Amazona farinose parrot. *Avian Pathol.,* **27:** 427-430.
6. Rajkhowa TK and Arya RS. 2016. Concurrent occurrence of haemangioma and hepatocellular carcinoma in layer chicken – A case report. *Indian J. Vet. Pathol.,* **40(1):** 96-98.
7. Bancroft JD and Gamble M. 2012. Theory and practice of histological techniques. Edinburgh. Churchill Livingstone, London. 7th edn Pp: 105-125.
8. Soffer D, Resnick-Roguel N, Eldor A and Kotler M. 1990. Multifocal vascular tumors in fowl induced by a newly isolated retrovirus. *Cancer Res*., **50:** 4787 – 4793.
9. Masegi T, Inoue Y, Yanai T and Ueda K. 1993. An ultrastructural study of cutaneous hemangioma in two chickens. *J. Vet. Med. Sci.,* **55:** 185–188.
10. Zhang HN, Lai HZ, Qi Y, Zhang XT, Ning ZY, Luo KJ, Xin CA, Cao WS and Liao M. 2011. An ALV-J isolate is responsible for spontaneous haemangiomas in layer chickens in China. *Avian Pathol.,* **40(3):** 261-267.
11. Meng F, Li Q, Zhang Y, Cui Z, Chang S and Zhao P. 2018. Isolation and characterization of subgroup J Avian Leukosis virus associated with hemangioma in commercial Hy-Line chickens. *Poul. Sci.,* **97(8):** 2667-2674.
12. Burstein H, Resnick-Roguel N, Hamburger J, Arad G, Malkinson M and Kotler M. 1990. Unique sequences in the envgene of avian hemangioma retrovirus are responsible for cytotoxicity and endothelial cell perturbation. *Virol.,* **179:** 512-516
13. Justice J, Malhotra S, Ruano M, Li Y, Zavala G, Lee N, Morgan R and Beemon K. 2015. The MET gene is a common integration target in avian leukosis virus subgroup J-induced chicken hemangiomas. *J. Virol.*, **89:** 4712–4719.

Indian J. Vet. Pathol., 50(3) : 280-283, 2026: DOI: https://doi.org/10.56093/pgd7t797

CASE REPORT

Pulmonary tuberculosis in a captive giraffe *(Giraffa camelopardalis)*

Kaushal Kumar, Vishal K. Sinha*, Deepak Kumar, Imran Ali, Bikram Kumar[1] and Kushagra Anand
Department of Veterinary Pathology, Bihar Veterinary College, Bihar Animal Sciences University, Patna, Bihar, India
[1]Veterinary Officer, Sanjay Gandhi Biological Park, Patna, Bihar, India

***Address of correspondence**
Dr. Vishal K. Sinha; E-mail: vishalbvc17@gmail.com
ORCID Id: 0009-0008-8765-1485

Received: 8.4.26; Accepted: 30.4.26

ABSTRACT

This study reports gross and histopathological findings in a 16-year-old pregnant female giraffe (≈13 months gestation) that died of systemic tuberculosis. Ante-mortem signs included anorexia, lethargy, weight loss, and weakness, which worsened despite supportive care. Postmortem examination revealed markedly enlarged, firm lungs studded with multiple grayish-white nodules throughout the parenchyma. Cut sections of lungs showed caseous, gritty areas consistent with chronic granulomatous inflammation. The heart was mildly enlarged with pale streaks and focal discoloration, suggesting degenerative and inflammatory changes. Histopathology of the lungs demonstrated classical granulomas with central caseous necrosis surrounded by epithelioid macrophages, Langhans-type multinucleated giant cells, lymphocytes and fibrous tissue, confirming tuberculosis. Adjacent lung tissue showed congestion and inflammatory infiltration. Cardiac sections revealed myocardial fibre degeneration, interstitial edema and mononuclear cell infiltration, consistent with myocarditis. Based on these findings, a diagnosis of disseminated tuberculosis with myocardial involvement was established. The occurrence in an advanced pregnant animal suggests that physiological stress and immunomodulation may have contributed to disease progression. This study highlights the importance of thorough necropsy and histopathological evaluation in detecting infectious diseases in wild species and emphasizes the potential for multisystem involvement in tuberculosis, complicating clinical presentation and outcomes.

Keywords: Giraffe, Granulomatous inflammation, Histopathology, Myocarditis, Tuberculosis

INTRODUCTION

Tuberculosis (TB) is a chronic granulomatous infectious disease caused by members of the *Mycobacterium tuberculosis* complex, affecting a wide range of domestic and wild animals, including large ruminants and exotic species such as giraffes[1,2]. It represents a significant zoonotic and wildlife health concern due to its persistence in the environment, wide host range and potential for interspecies transmission at the human–animal interface[3,4]. In wild herbivores, the disease typically progresses insidiously with vague clinical signs such as anorexia, weight loss and lethargy, often leading to delayed diagnosis and detection only during postmortem examination[5,6].

Giraffe (*Giraffa camelopardalis*), although generally considered relatively resistant to infectious diseases, have been reported to develop tuberculosis, particularly under captive conditions where factors such as stress, overcrowding and prolonged exposure to infected animals may predispose them to infection[2,7]. The primary route of transmission is aerosol, with the lungs being the principal site of infection; however, hematogenous and lymphatic dissemination may occur in advanced stages leading to multisystemic involvement[1,4]. Physiological stressors such as pregnancy and compromised immunity may further exacerbate disease progression and severity[6,8].

Gross pathological findings in tuberculosis are typically characterized by multiple nodular lesions (tubercles) in the lungs and associated lymph nodes, which may show caseation and calcification in chronic stages of infection[5,9]. In disseminated forms, lesions may extend to extrapulmonary organs including liver, spleen and occasionally the heart, indicating systemic spread[3,6]. Cardiac involvement, although rare, has been documented and may manifest as myocarditis due to inflammatory infiltration and myocardial degeneration [4,10].

How to cite this article : Kumar, K., Sinha, V.K., Kumar, D., Ali, I., Kumar, B. and Anand, K. 2026. Pulmonary tuberculosis in a captive giraffe *(Giraffa camelopardalis)*. Indian J. Vet. Pathol., 50(3) : 280-283.

Histopathologically, tuberculosis is characterized by the formation of granulomas consisting of a central area of caseous necrosis surrounded by epithelioid macrophages, Langhans-type multinucleated giant cells, lymphocytes and fibrous connective tissue encapsulation[1,5]. These granulomatous lesions represent a host immune response aimed at containing the infection but may also contribute to progressive tissue destruction and organ dysfunction. Histopathological examination thus remains the gold standard for definitive diagnosis, particularly in wildlife species where antemortem diagnostic approaches are limited[2,7].

The epidemiology of tuberculosis in wildlife is influenced by multiple factors including environmental conditions, population density, management practices and interaction with domestic animals or humans[3,8]. Despite its recognized importance, reports of tuberculosis in giraffes remain scarce, especially in the Indian context, with limited studies documenting detailed pathological and systemic involvement.

The present study was therefore undertaken to investigate the gross and histopathological alterations associated with tuberculosis in a pregnant giraffe, with special emphasis on pulmonary granulomatous lesions and cardiac involvement. The findings are expected to contribute to a better understanding of the pathological manifestations and systemic impact of tuberculosis in exotic wildlife species, thereby aiding in improved diagnosis and disease management strategies.

MATERIALS & METHODS

The present study was conducted on a deceased 16-year-old female giraffe (*Giraffa camelopardalis*), approximately 13 months pregnant, maintained under captive conditions at Sanjay Gandhi Biological Park, Patna. The animal died following a history of progressive anorexia, lethargy, weight loss, and general debility. Detailed anamnesis regarding clinical signs, duration of illness and management conditions was recorded from the caretakers prior to necropsy. During postmortem examination, the animal was in lateral recumbency showing an intact external body with apparent abdominal distension (Fig. 1).

A systematic and thorough postmortem examination was performed following standard necropsy procedures[11]. External examination included assessment of body condition, mucous membranes and any visible lesions. Internal examination revealed gross pathological alterations in various organs, with particular emphasis on the respiratory and cardiovascular systems. The lungs were carefully examined for size, consistency, colour and presence of nodular lesions while the heart was evaluated for any changes in size, shape and myocardial appearance. Representative tissue samples from lungs and heart were collected for further laboratory investigation.

For histopathological examination, tissue samples were immediately fixed in 10% neutral buffered formalin for 24–48 hours. Fixed tissues were processed using standard paraffin embedding techniques. Sections of 4–5 µm thickness were prepared using a microtome and stained with Haematoxylin and Eosin (H&E) for microscopic evaluation[12]. The stained sections were examined under a light microscope to identify characteristic pathological changes, particularly granulomatous lesions in the lungs and inflammatory changes in cardiac tissue.

Based on gross and histopathological findings, a presumptive diagnosis of tuberculosis was made; however, in the absence of Ziehl–Neelsen staining or molecular confirmation, the diagnosis remains morphological. All procedures were conducted in accordance with standard ethical guidelines for postmortem examination.

RESULTS & DISCUSSIONS

Gross postmortem examination of the giraffe revealed severe pathological alterations predominantly in the respiratory system. The lungs were markedly enlarged, heavy and firm in consistency, and extensively studded with numerous, variably sized grayish-white nodules distributed throughout all lobes. On cut section of both lungs, these nodules exhibited caseous and gritty material, indicative of chronic granulomatous inflammation (Fig. 2 & Fig. 3). In some areas, coalescing lesions formed larger consolidated patches suggestive of advanced disease. Similar gross findings of multiple caseating tubercles in the lungs have been widely reported in tuberculosis of domestic and wild animals[5,9].

Fig.1. Gross photograph of a giraffe in lateral recumbency during postmortem examination showing an intact external body with apparent abdominal distension; **Fig.2.** Cut surface of the right lung showing numerous coalescing grayish-white nodules with central caseous necrosis; **Fig.3.** Cut surface of the left lung showing multiple disseminated grayish-white nodular lesions with caseous material; **Fig.4.** Gross view of lungs with heart showing congestion, multiple nodular lesions and cardiac enlargement

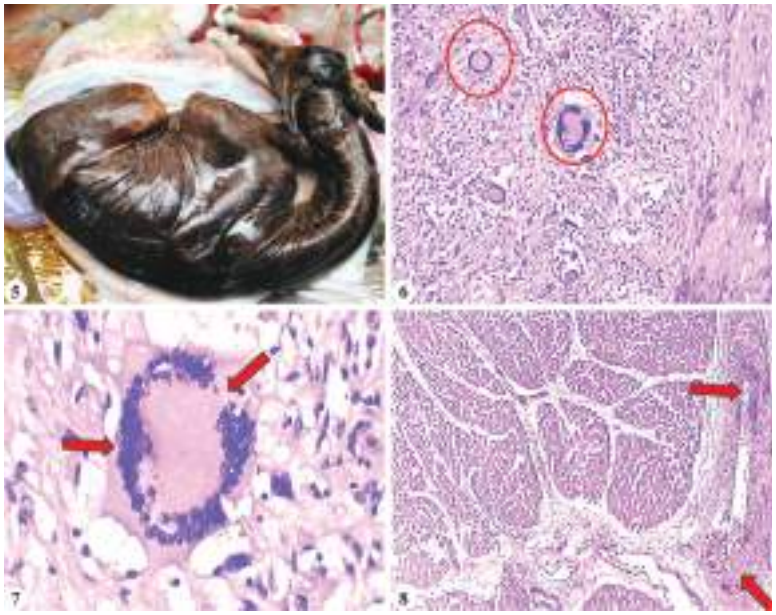

Fig.5. Gross photograph of a near-term giraffe foetus recovered during post-mortem examination, showing a well-developed foetus with intact foetal membranes following intrauterine death; **Fig.6.** Histological section of lung of giraffe showing granulomatous inflammation with central caseous necrosis surrounded by epithelioid cells and Langhans giant cells (H&E, 100x); **Fig.7.** Histological section of lung of giraffe showing a higher magnification view of granulomatous lesion with prominent central caseous necrosis and a surrounding rim of epithelioid macrophages and Langhans giant cells (H&E, 400x); **Fig.8.** Histological section of heart of giraffe showing myocardial fibre degeneration with interstitial edema and mononuclear inflammatory cell infiltration (H&E, 100x).

The tracheobronchial lymph nodes were also enlarged and exhibited caseation, supporting systemic dissemination.

The heart appeared mildly enlarged with congestion (Fig. 4). These alterations were indicative of underlying degenerative and inflammatory processes. Although cardiac involvement in tuberculosis is relatively uncommon, comparable myocardial lesions associated with disseminated tuberculosis have been reported previously[3,4]. No significant gross lesions were observed in other visceral organs, apart from mild congestion. Additionally, a near-term, well-developed foetus enclosed within intact foetal membranes was recovered from the uterus, suggestive of intrauterine death (Fig. 5).

Histopathological examination of lung sections (H&E, 100x and 400x) revealed classical granulomatous lesions characterized by central caseous necrosis surrounded by epithelioid macrophages, numerous Langhans-type multinucleated giant cells and a peripheral rim of lymphocytes and fibrous connective tissue encapsulation (Fig. 6 & 7). Adjacent pulmonary parenchyma showed congestion, edema and infiltration of inflammatory cells. These findings are consistent with the typical histomorphological features of tuberculosis as described in earlier studies[1,10].

Microscopic examination of cardiac tissue (H&E, 100x) revealed myocardial fibre degeneration, interstitial edema and infiltration of mononuclear inflammatory cells, confirming myocarditis (Fig. 8). The presence of inflammatory infiltration in the myocardium suggests possible hematogenous spread of infection, which has been reported in advanced or disseminated tuberculosis[2,7].

The observed lesions clearly indicate a disseminated form of tuberculosis with primary pulmonary involvement and secondary cardiac changes. The chronic granulomatous inflammation observed in the lungs reflects a well-established host immune response attempting to contain the infection; however, progressive caseation and tissue destruction ultimately compromise organ function[1,6]. The presence of myocarditis further suggests systemic spread and increased disease severity.

The occurrence of tuberculosis in an advanced pregnant giraffe highlights the possible role of physiological stress and immunomodulation during pregnancy, which may predispose to disease progression and dissemination. Similar observations have been made in other species where immunosuppression contributes to reactivation or exacerbation of latent infections[8].

The findings of the present study are in accordance with previous reports describing tuberculosis as a chronic, multisystemic disease with predominant pulmonary lesions and occasional extrapulmonary involvement in wildlife species[3,9]. The absence of antemortem diagnosis and the reliance on postmortem and histopathology emphasize the challenges associated with early detection in exotic animals.

Overall, the study underscores the importance of detailed necropsy and histopathological evaluation in identifying lesions suggestive of tuberculosis in wild and captive animals. However, in the absence of Ziehl–Neelsen staining or molecular confirmation, the diagnosis remains presumptive, as other granulomatous diseases may produce similar lesions. The findings highlight potential systemic involvement, including cardiac lesions and emphasize the need for confirmatory diagnostics, improved surveillance, management and biosecurity in captive wildlife populations.

CONCLUSION

Tuberculosis in giraffe is a significant

infectious disease, particularly under stress conditions such as captivity and advanced pregnancy, due to its chronic, progressive and multisystemic nature. The present study highlights pulmonary granulomatous lesions with concurrent myocardial involvement, indicating systemic dissemination. As antemortem signs are often nonspecific, accurate diagnosis relies on postmortem and histopathological evaluation, underscoring the need for routine monitoring and strict biosecurity in captive populations

ACKNOWLEDGEMENTS

The authors express their gratitude to the Honourable Vice Chancellor, Bihar Animal Sciences University, Patna, and the Dean of Bihar Veterinary College, Bihar Animal Sciences University, Patna, along with Director, Sanjay Gandhi Biological Park, Patna, for providing the necessary facilities to carry out this work.

Financial support & sponsorship: None

Conflicts of Interest: None

Use of Artificial Intelligence (AI)- Assisted Technology for manuscript preparation: The authors confirm that there was no use of AI- assisted technology for assisting in the writing of the manuscript and no images were manipulated using AI.

REFERENCES

1. Flynn JL and Chan J. 2001. Immunology of Tuberculosis. *Ann Rev Immuno.* **19:** 93-129. https://doi.org/10.1146/annurev.immunol.19.1.93
2. Thoen C, LoBue P and de Kantor I. 2006. The Importance of Mycobacterium bovis as a Zoonosis. *Vet. Microbiol.* **112:** 339-345. https://doi.org/10.1016/j.vetmic.2005.11.047
3. Michel AL, Müller B and van Helden PD. 2010. Mycobacterium bovis at the animal-human interface: a problem, or not? *Vet. Microbiol.* **140(3-4):** 371-81.
4. O'Reilly LM and Daborn CJ. 1995. The epidemiology of Mycobacterium bovis infections in animals and man. *Tuber Lung Dis.* **76(Suppl 1):** 1-46.
5. Palmer MV. 2013. Mycobacterium bovis: Characteristics of wildlife reservoir hosts. *Transbound Emerg Dis.* **60 (Suppl 1):** 1-13.
6. Khairullah AR, Moses IB, Kusala MKJ, Tyasningsih W, Ayuti SR, Rantam FA, Fauziah I, Silaen OSM, Puspitasari Y, Aryaloka S, Raharjo HM, Hasib A, Yanestria SM and Nurhidayah N. 2024. Unveiling insights into bovine tuberculosis: A comprehensive review. *Open Vet J.* **14(6):** 1330-1344.
7. Olea-Popelka F, Muwonge A, Perera A, Dean AS, Mumford E, Erlacher-Vindel E, Forcella S, Silk BJ, Ditiu L, El Idrissi A, Raviglione M, Cosivi O, LoBue P and Fujiwara PI. 2016. Zoonotic tuberculosis in human beings caused by Mycobacterium bovis - a call for action. *Lancet Infect. Dis.* Advance online publication. https://doi.org/10.1016/S1473-3099(16)30139-6
8. Renwick AR, White PCL and Bengis RG. 2007. Bovine Tuberculosis in Southern African Wildlife: A Multi-Species Host-Pathogen System. *Epidemiol. Infect.* **135(4):** 529-540.
9. Cassidy JP. 2006. The pathogenesis and pathology of bovine tuberculosis with insights from studies of tuberculosis in humans and laboratory animal models. *Vet Microbiol.* **112 (2-4):** 151-61.
10. Corner LAL. 2006. The Role of Wild Animal Populations in the Epidemiology of Tuberculosis in Domestic Animals: How to Assess the Risk. *Vet Microbiol.* **112:** 303-312. http://dx.doi.org/10.1016/j.vetmic.2005.11.015
11. Maxie MG. (Ed.) 2015. *Jubb, Kennedy & Palmer's Pathology of Domestic Animals,* 6th edition. Elsevier.
12. Luna LG (Ed.) 1968. *Manual of histologic staining methods of the Armed Forces Institute of Pathology* 3rd edition McGraw-Hill, New York. https://lib.ugent.be/catalog/rug01:000229104

Title of Thesis	:	Evaluation of antitumor efficacy of nanocurcumin on dalton's ascites lymphoma using *in vitro* and *in vivo* studies
Name of the Student	:	**P. Krishnaveni**
Name of the Guide	:	Dr. M. Thangapandiyan
Degree/Year	:	MVSc/2022
Name of the University	:	Tamil Nadu Veterinary and Animal Sciences university, Chennai, Tamil Nadu - 600 051

The present study was conducted to evaluate the antitumor effect of curcumin and nanocurcumin on Dalton's Ascites Lymphoma bearing mice in 102 male BALB/c mice for 6-8 weeks. The effect of curcumin and nanocurcumin was compared with that of methotrexate. Two experimental models are considered in this study which comprises of ascites model and a solid tumor model. *In silico* interaction studies between curcumin and various protein targets involved in cancer pathways like Nf-kBp50 and p65 subunit, MMP9, Cyclin D1 and Bax revealed that they interact with high dock score and relative binding energy. Synthesis and characterization of nanoparticles were carried out. The 12 mg of CUR-SLN with mean particle size of 91.1+ 7.5nm, PDI of 0.367 and zeta potential of -37.6mv was synthesized. The CUR-SLN showed common peak with blank solid lipid nanoparticles at 3355cm-1. and with curcumin at 2966 cm-1 and 2879 cm-1 in FTIR. The absence of peak at 3400-3200 cm-1 in curcumin indicated the formation of CUR-SLN. Scanning electron microscopy revealed that CURSLN have smooth surface whereas curcumin had rough surface. *In vitro* cytotoxicity studies in different DAL, A72 and HT29 cell lines revealed better antiproliferative effect of nanocurcumin than curcumin as IC50 value of nanocurcumin was found lower than curcumin. Induction of tumor increased the bodyweight, tumor volume and weight. Administration of methotrexate, curcumin and nanocurcumin showed a significant reduction in bodyweight, tumor weight. Hematobiochemical parameters were altered in the DAL induced mice which was restored towards the normal range in the treatment group. Liver antioxidant and lipid peroxidation parameter also found altered in the tumor control mice. The levels of GSH, GPx and SOD found decreased in the tumor bearing mice, whereas the MDA levels was found to be elevated. Treatment groups restored the values towards the normal range. In the ascites model, there was a greater distension of the abdomen with increased vascularity of the peritoneum which was found decreased in the treatment group. In solid tumor model DAL cells inoculated area showed red to brown spherical mass with varied size in which the size of the tumor got reduced in the treatment group.

AO/PI staining of tumor cells from different groups revealed majority of live cells in the tumor control group whereas the treatment group showed increased percentage of apoptotic cells. Histopathology of the peritoneal layer showed an increased infiltration of the tumor cells even in to the underlying muscle layer along with increased vascularity and found decreased in treatment groups. In solid tumor model presence of solid sheets of lymphoblast cells infiltrated deep in to the muscle layer was noticed. Increased neovascularization also was evident. Large areas of necrosis and apoptotic features along with less invasion in to the underlying muscles were present in the treatment group.

Immunocytochemistry and immunohistochemistry revealed an increased expression of Bax and Caspase 8 and decreased expression of Bcl2, PCNA, Cyclin D1, CD31, MMP9 and COX 2 in the treatment group as compared to tumor control group. TUNEL assay revealed the presence of more apoptotic cells in the treatment group as compared to the normal control group. Immunofluorescence staining revealed the nuclear localization of Nf-kB in tumor control and cytoplasmic localization in the treatment group. Also, it confirmed increased expression of caspase 8 in the treatment group as compared to the tumor control group. Real time PCR analysis showed the upregulation of Caspase8 and 9 and p53 gene expression and down regulation of Nf-kB and Bcl2. There was downregulation of miR181a, pre-miR182 and miR155 in the treatment group as compared to control group.

Curcumin and nanocurcumin were also found to increase the mean survival time and percentage increase in lifespan in tumor induced mice. To conclude, Nanocurcumin @ 50mg/kg body weight was found to exhibit chemopreventive property by inhibition of cell proliferation, induction of apoptosis and regulation of miRNA involved in carcinogenesis.

Title of Thesis	:	Pathology of experimentally induced aflatoxicosis and its amelioration by *Emblica officinalis* in broiler chicken
Name of the Student	:	**Kundarapu Sowmya**
Name of the Guide	:	Dr. K. Gopal
Degree/Year	:	MVSc/2025
Name of the University	:	Tamil Nadu Veterinary and Animal Sciences University

The poultry industry is a major source of animal protein and livelihood, but its productivity is often hindered by feed contamination with aflatoxins produced by aspergillus species. Aflatoxicosis causes poor growth, immunosuppression and mortality in birds. Growing concern over chemical additives has increased the use of herbal alternatives with proven antioxidant and immunomodulatory properties.

The present study was undertaken to investigate the toxic effects of aflatoxin on various organs and evaluating the protective efficacy of Emblicaofficinalis through hematological, biochemical, antioxidant, histopathological and immunohistochemical analyses.AF was produced in maize by inoculating it with Aspergillus flavus and the phytochemical analysis of E. officinalis revealed the presence of rich phytochemicals with potent antioxidant properties.

An experimental trial was conducted using hundred day-old broiler chicks which were randomly divided into five groups with two replicates of ten birds each. Group I acted as control and received basal diet; Group II received AF (1 ppm); Group III received AF (1 ppm) along with commercial toxin binder, UTPP (Ultimate Toxin Prevention Program) (1g/kg), Group IV and V treated with AF (1 ppm) and two different doses (1g/kg, 2g/kg) of E. officinalis. The trial was carried out for 35 days, after which all the birds were sacrificed for detailed evaluation.

Haematological analysis revealed significant reduction in haemoglobin (Hb), packed cell volume (PCV), total erythrocyte count (TEC), lymphocyte count and elevation in heterophil count, while serum biochemical analysis showed hypoproteinaemia and increased alanine amino transferase (ALT), aspartate aminotransferase (AST) and blood urea nitrogen (BUN) values in aflatoxin fed birds. But these hematobiochemical parameters showed improvement in treatment groups. Marked hepatic and renal alterations were supported by increased lipid peroxidation and reduced antioxidant activities (catalase (CAT), superoxide dismutase (SOD), glutathione peroxidase (GPx) and reduced glutathione (GSH)). Aflatoxin fed birds showed increased weights of liver and spleen and reduced bursal weight. Commercial toxin binder as well as E. officinalis supplemented groups exhibited improvement in all these parameters, showing higher Hb, PCV and TEC values, normalization of serum biochemistry, reduced LPO and enhanced antioxidant profile comparable to control group. Aflatoxin residue analysis revealed reduced residues in liver and muscle of treated birds, confirming its detoxifying effect.

Grossly, the liver of aflatoxinfed birds (group II) appeared enlarged, friable and pale to yellowish in color, lymphoid organs like spleen was enlarged whereas the bursa was atrophied. Histopathological examination revealed ballooning degeneration, bile duct proliferation and periportal mononuclear cell infiltration in liver; mesangial cell proliferation, degeneration and desquamation of tubular epithelium in kidney; Endocardial haemorrhage, cardiac muscle degeneration and mononuclear cell infiltration in heart; Haemorrhages in lungs; Lymphoid depletion in spleen, thymus and bursa; Infiltration of mononuclear cells in the proventriculus; Decreased volume of zymogen granules in pancreas; Distortion of villi and goblet cell hyperplasia in intestine. These histopathological lesions in all the examined organs were moderate in AF+EO(1g/kg) group and mild in AF+UTPP, AF+EO(2g/kg) groups. Morphometric analysis of intestine in AF fed birds showed decreased villus length and increased crypt depth compared to control, whereas supplemented birds showed improved villus height and preserved mucosal integrity.

Immunohistochemical examination of lymphoid tissues revealed intense caspase-3 expression with reduced CD3 and PAX5 labelling, indicating apoptosis and immunosuppression. Supplemented groups showed reduced caspase-3 and enhanced CD3, PAX5 and Bcl-2 expression, demonstrating attenuation of apoptosis and restoration of lymphoid function.

The study concludes that the higher dose of E. officinalis (2g/kg) effectively ameliorated aflatoxin toxicity, followed by the commercial toxin binder and the lower dose of E. officinalis (1g/kg).

Tittle of Thesis : Pathomorphological studies on spleen and lymph nodes in buffaloes

Name of the Student : **T. Mounica**

Name of the Guide : Dr. P. Amaravathi

Degree/Year : MVSc/2026

Name of the University : Sri Venkateswara Veterinary University, Tirupati, Andhra Pradesh - 517502

The spleen and lymph nodes are important secondary lymphoid organs that are essential for immunological surveillance, filtration of blood and lymph, and initiation of immune responses. The present study was undertaken to investigate the naturally occurring pathomorphological alterations in spleen and lymph nodes of buffaloes. The present study involved the collection and examination of 50 spleens and 250 lymph nodes that included prescapular, prefemoral, hepatic, mesenteric and bronchial lymph nodes from 50 buffaloes. Degenerative changes, vascular disturbances, growth disturbances, necrosis and pigmentation were common in both spleen and lymph nodes. Inflammatory changes in spleen, calcification and tumors in lymph nodes were observed. Miscellaneous conditions had the highest occurrence in both spleen and lymph nodes. Gross lesions noticed in spleen were enlargement, congestion and increased white pulp. Cytology of spleen revealed neutrophils, eosinophils, mast cells, giant cells, amyloid, mott cells, macrophages, reactive lymphocytes, plasma cells, fibroblasts, large granular lymphocytes, megakaryocyte, nucleated RBC and bacterial rods. Histopathological examination of spleen showed amyloid, myxomatous degenerations, vascular disturbances like hyperemia, congestion,

hemorrhages and thrombus. Growth disturbances like atrophy, necrosis and inflammatory cell infiltration were observed. Pigmentations like hemosiderin and miscellaneous conditions showed characteristic features. In lymph nodes, enlargement, edema, congestion and pigmentation were the gross lesions noted. In lymph nodes E.coli, Salmonella, Pseudomonas and Klebsiella were isolated. In lymph node cytology, hyperplastic, dividing cells, hemosiderin, melanin, apoptosis, chromatolysis, fibroblasts, neutrophils, plasma cells, reactive lymphocytes, eosinophils, mast cells, macrophages, giant cells, mott cells and amyloid were observed. In lymph nodes, microscopically myxomatous, amyloidosis, hyaline degeneration, corpora amylacea were observed. Congestion, hemorrhages, edema, thrombus, hyperplasia of follicles, necrotic changes, hemosiderin, melanin, lipofuscin pigments, calcified areas, tumors and miscellaneous alterations were noticed. Immunohistochemical studies revealed immunopositive reaction with caspase-9 and BCL-2 in large lymphocytes. Positive reaction against VEGF and CD31 in necrotic and endothelial cells were noted. CD4 positivity and negative for CD20 confirmed the T-cell lymphoma, while strong immunopositive reaction for CD20 for B-cell lymphoma was observed. Mild positive with CD5 and absence of CD79a reaction for T-cell lymphoma were noticed in lymph nodes of buffaloes.

Tittle of Thesis : Pathomorphological studies and molecular detection of avian leukosis virus in chicken

Name of the Student : **Inchara. Y**

Name of the Guide : Dr. N. Sailaja

Degree/Year : MVSc/2026

Name of the University : Sri Venkateswara Veterinary University, Tirupati, Andhra Pradesh - 517502

Avian leukosis is a significant neoplastic disease of poultry causing economic losses due to reduced productivity and increased mortality. The disease persists in flocks mainly through vertical transmission, making control difficult. Field cases often go undiagnosed in early stages, allowing silent spread within the flocks. Gross and histopathological lesions provide important clues, but confirmation requires molecular detection. Identification of viral subgroups is essential to understand local epidemiology and transmission of disease. Limited data is available in the study area on circulating ALV subgroups. Therefore, this work was undertaken to provide baseline information for planning control strategies.In the present study, around 553 birds were suspected based on gross lesions, and 87 birds were confirmed as ALV infected by PCR detection. Among them, 83 birds showed multiple organ involvement with lesions in three or more organs. The most common clinical signs like emaciation in 36 (41.33%), anaemia 16(18.39%), and dehydration were observed in infected birds, though these were non-specific. On gross examination, the liver was the predominant organ affected, showing severe enlargement in all infected birds. Diffuse enlargement of spleen and kidneys was noted in 93.10% and 79.31% of cases, respectively. Nodular growths were recorded in liver (43.67%), spleen (25.23%), kidney (5.75%), heart (4.59%), lung (3.44%), ovary (1.44%), bursa of Fabricius (2.30%) and less frequently in, proventriculus, intestine, and caecal tonsils 1.44% each. Other lesions included were congestion of visceral organs, fatty changes in liver, pulmonary consolidation, and catarrhal enteritis. Cytological examination of tissue impression smears revealed varying degrees of cellularity across organs. High cellularity was observed in liver and spleen, while moderate and mild cellularity were noted in other organs. The infiltrated cells were fairly uniform in size, with scanty to moderate basophilic cytoplasm and increased nuclear to cytoplasmic ratio. Nuclear atypia, mitotic figures, and prominent nucleoli were observed. Occasional plasmacytoid cells, lymphoglandular bodies, and naked nuclei of lymphoblasts were seen. Degenerative changes in hepatocytes and renal tubular epithelial cells were noted alongside neoplastic cells. Histopathological examination revealed varying degrees of lymphoid infiltration in visceral organs. Severe and moderate infiltration predominated in the liver, while spleen and kidney showed mild to severe changes. Severe infiltration was predominant in bursa, whereas moderate infiltration was observed in lung, heart, proventriculus, ovary, and caecal tonsils. The pattern of infiltration was mainly diffuse in liver, spleen, lung, thymus, and bursa, while multifocal interstitial in kidney, myocardium, and other organs, leading to architectural distortion. Neoplastic cells were distributed in capsular, subcapsular, periportal, perivascular, and intravascular locations, including periglomerular areas in kidney and alveolar lumina in lung. Degenerative changes such as vacuolation, pyknosis, karyorrhexis, epithelial desquamation, and necrosis were evident. Vascular changes including congestion, haemorrhages, and thrombosis were observed. Intravascular neoplastic cells indicated haematogenous dissemination and metastasis. AgNOR count of 4.01 per cell suggested malignancy.PCR analysis of 50 samples revealed 7 positives, all identified as ALV subgroup E. The findings substantiate the prevalence of ALV with PCR as essential for confirmation and subgroup identification.

Title of the Thesis	:	Clinico-pathological and histopathological studies on peritoneal effusions and peritoneum in dogs
Name of the Student	:	**J. Hari Chandana**
Name of the Guide	:	Dr. A. Nasreen
Degree/Year	:	MVSc/2026
Name of the University	:	Sri Venkateswara Veterinary University, Tirupati, Andhra Pradesh - 517502

Peritoneal effusions in dogs represent a clinically significant manifestation of diverse pathological conditions ranging from localized inflammatory disorders to systemic, metabolic and neoplastic diseases. Diagnosis based on individual parameters often provides limited information, while pathological alterations of the peritoneum are frequently overlooked. Therefore, the present study was undertaken to evaluate peritoneal effusions along with associated peritoneal alterations in dogs through a combined clinicopathological approach to support accurate diagnosis.

A total of 50 dogs presented with abdominal distension, undergoing laparotomy or necropsy, were included in the study. Based on the approximate volume of peritoneal fluid, cases were classified into Group A (no significant effusion), Group B (<10 ml), Group C (10-100 ml) and Group D (>100 ml). Group A constituted the highest proportion (44%), followed by Group D (34%), Group C (14%) and Group B (8%). The cases included elective ovariohysterectomy, pyometra, parasitic infestations, uroabdomen, cardiac disorders, foreign body ingestion, diaphragmatic hernia, hepatomegaly, neoplasia and other systemic diseases.

Haematological evaluation revealed mild to moderate anaemia, particularly in Groups C and D, associated with chronic disease, parasitic infestations and systemic involvement. Leukocytosis with predominant neutrophilia was commonly observed in inflammatory, infectious and neoplastic conditions, while eosinophilia was associated with parasitic infestations. Serum biochemical analysis revealed significant alterations indicating hepatic, renal and metabolic involvement, especially in Groups C and D. Decreased total protein and albumin levels suggested hypoproteinemia contributing to fluid accumulation. Elevated ALT, AST and ALP indicated hepatic dysfunction, whereas increased BUN and creatinine reflected renal involvement. Alterations in glucose, lipid profile and LDH levels indicated metabolic disturbances and tissue damage.

Radiography aided in detecting moderate to severe effusions through loss of serosal detail and ground-glass appearance, whereas ultrasonography was more sensitive in detecting fluid accumulation and associated lesions. Peritoneal fluid analysis revealed transudates in Group B, modified transudates in Group C and exudative or haemorrhagic effusions in Group D. Protein concentration, cellularity and biochemical constituents varied according to the nature of the effusion. Elevated peritoneal fluid creatinine compared to serum was characteristic of uroabdomen, and serum-ascites albumin gradient aided in differentiating portal hypertensive from non-portal causes.

The total nucleated cell count and specific gravity increased with severity of effusion. Cytological examination revealed reactive mesothelial cells as the predominant cell type. Inflammatory conditions showed increased neutrophils and macrophages, whereas neoplastic effusions exhibited marked cellular atypia. Mesothelioma demonstrated pleomorphic clustered mesothelial cells, while myxosarcoma showed spindle to stellate cells within a myxoid background.

Gross examination of the peritoneum ranged from normal smooth surfaces in Group A to congestion, thickening, fibrin deposition, adhesions and nodular haemorrhagic lesions in severe and neoplastic conditions. Histopathological changes progressed from mild congestion and mesothelial hyperplasia to fibroplasia, inflammatory infiltration, fibrosis and haemorrhage. Mesothelioma exhibited tubulopapillary proliferation of pleomorphic mesothelial cells, whereas myxosarcoma showed abundant myxoid matrix with spindle-shaped cells. Alcian blue and Van Gieson stains highlighted acidic mucopolysaccharides and collagen deposition, respectively. Immunohistochemistry confirmed mesothelioma through cytokeratin, vimentin and calretinin expression, while myxosarcoma showed strong vimentin positivity and CD31 negativity. Overall, the study demonstrated that peritoneal effusions in dogs are associated with diverse clinicopathological, biochemical, cytological and histopathological alterations, emphasizing the value of an integrated diagnostic approach for accurate diagnosis and effective clinical management.

Title of Thesis	:	Incidence of respiratory diseases in chicken with special reference to viral etiology
Name of the Student	:	**Sangamoni Pavan Kumar**
Name of the Guide	:	Dr. Swathi Bora
Degree/Year	:	MVSc/2026
Name of the University	:	P.V. Narsimha Rao Telangana Veterinary University, Hyderabad

Respiratory viral diseases represent a major constraint to commercial poultry production due to their high morbidity, mortality, and associated economic losses. The present investigation was undertaken to determine the incidence, seasonal distribution, pathological alterations, and molecular prevalence of major viral respiratory pathogens in chickens from different locations in and around Hyderabad. A total of 439 birds from 32 commercial poultry flocks were examined during the period from June to November 2025. Among these, 262 birds showed gross lesions suggestive of respiratory disease, and 104 cases (23.69%) were confirmed as viral respiratory infections by PCR.

Location-wise analysis revealed considerable variation in incidence with the highest occurrence recorded in Keshampet (34.32%), followed by Rajendranagar (27.65%) and Shadnagar (23.72), while the lowest incidence was observed in Bibinagar (16.70%). Flock level molecular screening demonstrated Newcastle disease virus (NDV) as predominant pathogen, detected in 40.63% of flocks, followed by infectious bronchitis virus (IBV) in 25% and Fowl adenovirus (FAdV) in 12.5% of flocks. Seasonal analysis indicated a significantly higher incidence during the winter months (30.18%) compared to the rainy season (20%), with NDV detected consistently throughout the study period.

Clinically affected birds exhibited respiratory distress, nasal and ocular discharge, diarrhoea, neurological signs, and abnormalities in egg production. Gross pathological findings varied with the viral aetiology and included congested and oedematous lungs, haemorrhagic tracheitis, thickened air sacs, renal alterations, and hepatic lesions.

Disease-wise histopathological examination of respiratory tissues revealed distinct lesions corresponding to individual viral infections. NDV-infected birds showed tracheal epithelial hyperplasia, deciliation, necrosis, submucosal oedema, vascular congestion, and mononuclear cell infiltration, while lungs exhibited congestion, interstitial oedema, heterophilic plugs, and parabronchial epithelial thickening. IBV infection was characterized by severe tracheal epithelial damage with ciliary loss, goblet cell depletion, epithelial sloughing, submucosal oedema, and prominent lymphoid aggregation. Pulmonary lesions in IBV included inter-alveolar septal thickening, congestion, haemorrhages, and mixed inflammatory cell infiltration.

FAdV infected birds showed mild to severe tracheal deciliation and epithelial desquamation with pulmonary congestion and focal haemorrhages. A characteristic feature of FAdV infection was hepatic degeneration and necrosis with prominent intranuclear inclusion bodies. Overall, disease-specific histopathological patterns correlated well with molecular findings, supporting the diagnostic value of histopathology in viral respiratory diseases of poultry.

Molecular detection by RT-PCR and PCR confirmed NDV as the most prevalent virus (62.50%), followed by IBV (22.12%) and FAdV (15.38%). The study highlights the continued predominance of NDV and the significant contribution of IBV and FAdV to respiratory disease complexes in poultry, emphasizing the need for integrated pathological and molecular surveillance to strengthen control and prevention strategies.

OBITUARY

Dr Prem Prakash Gupta

F.R.V.C.S., FNAVS (India)

With profound grief and deep sorrow, the Indian Association of Veterinary Pathologists (IAVP) mourn the sad demise of Dr Prem Prakash Gupta, one of the most distinguished, eminent and highly decorated Veterinary Pathologists of his generation, who passed away on 16th August 2026, leaving behind a rich and enduring legacy in Veterinary Pathology, veterinary education and scientific research.

Dr Prem Prakash Gupta, born on 16 July 1941 at Moradabad, India, Dr Gupta pursued an outstanding academic career, obtaining (1955-72) his B.Sc., B.V.Sc. & A.H., M.V.Sc. and Ph.D. degrees from premier institutions in India, including Meerut College, the U.P. College of Veterinary Science and Animal Husbandry, Mathura and the All-India Institute of Medical Sciences, New Delhi. He further enriched his professional expertise through advanced training at the Royal College of Veterinary Science, Uppsala, Sweden, where he was awarded the F.R.V.C.S. in 1980.

Dr Gupta served the Indian Council of Medical Research, New Delhi, as a Research Officer (1968-73) and joined Punjab Agricultural University (PAU), Ludhiana in 1973, where he served with distinction as Associate Professor and Professor of Veterinary Pathology till 1983. He subsequently served as Head, Department of Veterinary Pathology (1983-2000), and as Additional Director of Research (Veterinary and Animal Sciences) and retired from university service in July 2001 after an illustrious academic career spanning several decades.

As a scientist, Dr Gupta made seminal contributions to the understanding of cardiovascular, respiratory, genital, mycoplasmal and mycotic diseases in animals. His research significantly enriched veterinary disease pathology and contributed to the advancement of veterinary science in India. As a teacher, he inspired generations of veterinary students and postgraduate scholars through his profound knowledge, clarity of thought and commitment to academic excellence. His exceptional contributions were recognized through numerous prestigious national and international awards and honours, including the Science Pioneer Prize of the Egyptian Veterinary Association, ICAR Team Research Award, ICAR Best Teacher Award, Smt. Pushpa Sriramachari Award for outstanding research in cardio-vascular diseases of ICMR, Meritorious Teacher Award of PAU, ICAR Outstanding Teacher Award, Drs N.C. Jain and J.L. Vegad Award, ICAR Rafi Ahmed Kidwai Award, IAVP Lifetime Achievement Award, Dr P. Bhattacharya Memorial Award, Distinguished Service Awards (Heart Care Foundation of India, ICAR & MIEF), and the Glory of India Award. He was Fellow of the National Academy of Veterinary Sciences (India) and acted as Member of the Governing Council of the National Academy of Veterinary Sciences and Fellow of several professional and academic organizations. Beyond his scientific accomplishments, Dr Gupta was admired for his warm, generous, jovial and ever-helpful personality. He was a mentor in the truest sense of the word and extended his guidance and encouragement generously to students, young scientists and colleagues. His presence at meetings and conferences of the Indian Association of Veterinary Pathologists was always marked by warmth, affection, camaraderie and intellectual inspiration. To many members of the veterinary fraternity, he was not only a respected senior scientist but also a cherished teacher, mentor and friend.

Dr P.P. Gupta was also a visionary founder member of the Indian College of Veterinary Pathologists (ICVP), established in 2008. His foresight and commitment played an important role in shaping professional standards, training and board certification in Veterinary Pathology in India. His contribution to the development and professionalization of Veterinary Pathology will remain an important part of the history of discipline in the country. In recognition of his monumental contributions to Veterinary Pathology and his enduring legacy, the Indian Association of Veterinary Pathologists established the prestigious "Dr P.P. Gupta Oration Award" in his honor. This distinction stands as a lasting tribute to his exceptional contributions to the profession and will continue to inspire future generations of Veterinary Pathologists. Dr Prem Prakash Gupta was a teacher by heart, a researcher by passion, a mentor by nature and a friend to many. His remarkable legacy extends far beyond his publications, awards and academic positions. It lives on in the students he taught, the researchers he guided, the colleagues he inspired and the institutions and professional organizations he helped strengthen. His passing is an irreparable loss to the veterinary fraternity, the academic and scientific community and to all those who had the privilege of knowing and learning from him. His contributions to Punjab Agricultural University, the Indian Association of Veterinary Pathologists, the Indian College of Veterinary Pathologists, the National Academy of Veterinary Sciences and the broader veterinary profession shall be remembered with immense respect, gratitude and affection. On behalf of the Indian Association of Veterinary Pathologists (IAVP), we convey our heartfelt and deepest condolences to the bereaved family, relatives, colleagues, students, disciples and countless admirers of Dr Prem Prakash Gupta.

SUPERANNUATION

Prof. (Dr) Madhurendu Kumar Gupta
University Professor cum Chief Scientist and Chairman,
Department of Veterinary Pathology, RVC, BAU, Ranchi

Professor Madhurendu Kumar Gupta was born on May 2nd, 1961 in Patna, Bihar. He completed his BVSc & AH in 1983, MVSc in 1986, and PhD in 1995 from Ranchi Veterinary College, Birsa Agricultural University, Ranchi, Jharkhand. He started his career as Assistant Professor in the Department of Veterinary Pathology, Ranchi Veterinary College, BAU, Ranchi Jharkhand in 1989. He had been in Academia for 37 years in continuation. He also served as DRI cum Dean PGs, BAU, from 2021 to 2026 and Dean College of Veterinary Science & AH, BAU, Ranchi, Jharkhand from 2025 to 2026. He has guided six MVSc students and 2 PhD students as a Major Guide and published more than 80 research articles in national and international journals. He has attended 4 summer schools, 12 conferences/ symposiums, 15 seminars and two workshops. Realizing the importance of clinical pathology in disease diagnosis, he popularized the veterinary clinical pathology in Jharkhand amongst the veterinary practitioners and created awareness amongst the farmers and pet owners about the benefit of clinical examination for the early and accurate disease diagnosis. He is Diplomate of ICVP and Fellow (IAVP).

Dr. Gupta contribution in diagnosis and control of haemoprotozoan (theileriosis, babesiosis, trypanosomiasis), and haemorickettsial (anaplasmosis) diseases has made significant impact in the therapeutic approach against these very economically important diseases of cattle. Apart from clinical pathology, he has significant interest in poultry pathology, toxicopathology, oncology, and transboundary diseases like African swine fever, Lumpy skin disease, EEHV in elephants, the incidence of all of which was reported for the first time from Jharkhand. The Ranchi strain of LSD virus has been successfully used for the preparation of commercial vaccine against LSD. He acted as a principal investigator, he handled FMD network unit and collaboration center of AICRP on FMD, in CVSc&AH, BAU, Ranchi since 2022 to 2026. In that he was actively engaged in Sero surveillance and Sero monitoring of FMD for seroprevalence study in Jharkhand and analysis of protective antibody titre in both prevaccinated and post vaccinated cattle of Jharkhand against FMD. He worked as a Co-pI in ICAR Outreach Program on monitoring of drug residues and environmental pollution as well as AICRP on poultry and livestock product safety. As a consultant, he has played crucial role in the control of wildlife diseases in Jharkhand for last 40 years. He was also involved in developing Web Enabled Access of Agriculture and Animal Husbandry information through PC and mobile devices for giving consultancy to the farmers through ITK for which he as a member of team was given "The Manthan Award, South Asia 2011" and SKOCH order of the Merit award, New Delhi for qualification in the India's best governance project. He is recipient of IAVP President Appreciation Award for 2019.

Prof. MK Gupta superannuated on 31st May 2026 as University Professor cum Chief Scientist and Chairman, Department of Veterinary Pathology, RVC, BAU, Ranchi. The Indian Association of Veterinary Pathologists wishes him a healthy, peaceful, and fulfilling post-retirement life.

SUPERANNUATION

Dr. Arvind D. Ingle

Scientific Officer 'H' & Officer-in–Charge, Laboratory Animal Facility and Histopathology
at Tata Memorial Center, Advanced Center for Treatment,
Research and Education in Cancer, Kharghar, Navi Mumbai

Dr. Arvind D. Ingle, Scientific Officer 'H' & Officer-in–Charge, Laboratory Animal Facility and Histopathology at Tata Memorial Center, Advanced Center for Treatment, Research and Education in Cancer, Kharghar, Navi Mumbai - 410 210, MS, India born on June 02, 1966.

He graduated from Nagpur Veterinary College, Nagpur in 1989, MVSc., from Post Graduate Institute, Dr. Punjabrao Deshmukh Krishi Vidyapeeth, Akola in 1992 and Ph.D from Kuvempu University, Karnataka in 2012. He has done number of certificate courses viz; Certificate Course in Laboratory Animal Science, National Centre for Laboratory Animal Science, National Institute of Nutrition, Indian Council of Medical Research, Hyderabad in 1994 and certificate Course in Laboratory Animal Science (Meet FELASA 'C' Certificate), jointly conducted by CCSEA, NIAW, LASA India and TANUVAS, Chennai, 2013. He is Diplomate ICVP (2010) and Diplomate ICLAM (2021). He was awarded Fellow NAVS (I) in 2013, FIAVP in 2019 and FLASA, India in 2024.

Dr. Ingle has worked on a project "*Generation and Characterization of Knock-out mice for Ulip gene*" in the Lab. of Dr. Carol Thiele, Cell and Molecular Biology Section, Paediatric Oncology Branch, National Cancer Institute, NIH, Bethesda, Maryland, USA under the Fogarty International Fellowship during 99-2000. He has delivered more than 150 guest lectures in various National and International Conferences.

Dr Arvind has organized more than 15 National Meetings, conferences and workshops. He is served as Member, Inspection team (CDCSO, DGHS, Govt. of India) for inspection of a Drug Manufacturing company in Mumbai, 2016., GLP Inspector (Fellow), NCGMA, DST, Govt. of India, 2022, Governing Board Member, ICLAS, 20120-26, **Chairman, Education and Training Committee, ICLAS, 2020-26,** Site visitor, AAALAC International, USA, 2010-25, DBT Nominee on IBSC's of two organizations and Central Committee Member, CCSEA, Ministry of Fisheries, Animal Husbandry and Dairying, Government of India, New Delhi, 2025-27. He is recipient of more than 30 national and international honours and awards.

Dr. Ingle conducted 2 certificate courses in 2013 of 6 months and one month duration. He has published around 39 comparative pathology work, 46 collaborative research work, 3 xenograft establishment work, 5 embryo cryopreservation work, 5 lab mouse papilloma discovery work and 10 lab animal quality control work. He has written 1 book and 3 book chapters.

He superannuated from his active service on 30-6-2026. The Indian Association of Veterinary Pathologists wishes him a healthy, peaceful, and fulfilling post-retirement life.